The Prediction and the Exploitation of the Thermodynamic Properties of Non Ozone Depleting Refrigerants

Colm Domhnall Fitzgerald

Doctor of Philosophy

University of Edinburgh

June 1997

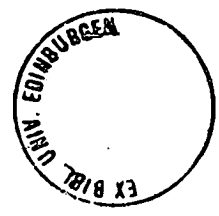

Declaration

The work described in this thesis is the original work of the author and was carried out without the assistance of others, except where explicit credit is given in the text. It has not been submitted, in whole or in part, for any other degree at any University.

Acknowledgements

Ba mhaith liom buíochas a thabairt le gach duine anseo. Ni dhóigh liom go ndeánfádh mé an obair seo gan sibh.

The final submission of this thesis will no inspire a certain amount of incredulity among friends, family and acquaintances. There are a number of people and organisations whom I would like express considerable gratitude without whom this probably not have happened:

- Dr. Colin Pritchard for supervising the project, furnishing valuable advice and arranging new employment when the original grant had long since become a financial fiction.
- I.C.I. Chemicals & Polymers and the Engineering and Physical Sciences Research Council for providing the financial backing for the project.
- My parents, family and relations for encouraging me to do this.
- Dr. Dick Powell, Tom Murphy and Bob Low at I.C.I. Chemicals & Polymers for providing invaluable advice.
- Mr. Matthew Rea for assisting me with innumerable problems and guiding me through the witchcraft of electronics.
- Mr. Rab Kilgour, Bobby Hogg, Kenny Fee and Tommy Murray for the many occasions they rendered technical assistance to a mechanical imbecile.
- John Currie for volunteering to proof read this thesis without any degree of compulsion whatsoever.
- Adam Harvey, Rory McKinnel, Eoin McCarthy, Jonathan Dempsey and other postgraduates for furnishing their friendship and making life more tolerable.
- Keith Manning, Paul O'Leary, Pat Griffin, Trevor Sheahan, Ciarán Kelliher, Sheila O'Keeffe, Alan Power, Kieran Hannon and many other Cork based friends for maintaining their friendship throughout the years.

Go n-éirí an bothár libh go léir.

Abstract

The use of mixtures of refrigerants in refrigeration cycles can lead to improvements in cycle efficiency. The majority of refrigerant working fluids have been pure fluids. With pure refrigerants temperature profiles between the working fluid and the heat source and sink fluids may not be well matched. Mixtures of refrigerants boil and condense across a temperature range. This property can be used to reduce the mean temperature differences in the heat exchangers, and to improve the matching of the temperature profiles. This leads to higher coefficients of performance (COP). In this thesis, the improvement in refrigeration COP due to mixtures of refrigerants is investigated. Ratification of the Montreal protocol led to the phasing out of chlorofluorocarbon (CFC) refrigerants. Hydrofluorocarbon (HFC) refrigerants are the leading candidates to replace CFCs. Mixtures of HFC refrigerants are examined. An existing pilot plant refrigeration cycle was adapted and modified for use with HFC refrigerants. A binary mixture of difluoromethane (R32) and 1,1,1,2-tetrafluoroethane (R134a) is examined experimentally.

The phasing out of CFC refrigerants means that there exists a need for methods which can predict accurately the thermodynamic properties of a proposed replacement refrigerant, from sparse amounts of data. The Cubic Chain-of-Rotators (CCOR) equation of state requires relatively little knowledge of the fluid it describes. CCOR predictions of pure and mixed HFC thermodynamic properties, were compared with published experimental data. Comparisons were also made with the more complex Carnahan-Starling-DeSantis (CSD) equation. The CCOR equation predicted saturated and superheated vapour pressure with satisfactory accuracy. Liquid density was not predicted with the same precision. Vapour density was described no worse than the CSD equation. CCOR description of binary vapour-liquid equilibrium (VLE) was superior to that of the CSD equation. Prediction of VLE data was improved by using optimal interaction constants. It was shown that if an optimal set of interaction constants was located for each experimental data point for bubble point VLE data, the interaction constants exhibited a regular dependence upon temperature and composition. The CCOR equation can be used to provide approximate preliminary thermodynamic data for a new refrigerant, for which little data exists.

A simulation model of a refrigeration cycle was developed, based upon the CCOR equation. Six binary HFC mixtures were modelled. The COPs of the mixtures were compared to pure fluid COPs. Improvements in mixture COP were in the range 0.0-14.5%, depending on composition and conditions. Improvements in the UA values of the heat exchangers led to a larger mixture COP enhancement. Increased compressor polytropic efficiency had no significant effect upon mixture COP enhancement. Mixtures outperformed pure fluids when the evaporator heat source fluid temperature change was increased. Mixtures performed better than pure fluids, under conditions of higher pressure drop and decreased heat sink flow rate. Liquid-suction heat exchange affected mixtures, which performed poorly in the basic cycle, more than those that performed relatively well.

Contents

List of Tables

List of Figures

Chapter 1

Introduction

Refrigeration cycles are an integral part of modern daily life. They provide the cooling of food, beverages and pharmaceuticals necessary for our current way of life. Homes, places of work and modes of transport are made more comfortable in countries with hot inhospitable climates. They also manifest themselves in heat pumps to provide heat in domestic and industrial settings. The modern tendency towards urbanisation in industrialised countries means that we are more dependent upon refrigeration. As developing countries strive to become more industrialised, refrigeration will play an important part in the improvement of living conditions. As an indication of the importance of refrigeration, the annual investment in refrigeration equipment was estimated to be 100 billion dollars in 1990. The values of the products being treated was assessed at 10 times that figure [*Mattarolo 1990*]. The application of refrigeration requires energy. Serious concerns exist about the possibility that anthropogenic gases and combustion products, emanating from processes that provide energy, could affect the global climate in a dramatic fashion. It has also been strongly suspected that certain commonly used refrigerants are depleting the protective ozone layer in the atmosphere. As a result, replacement of these with more benign refrigerants is well advanced. Opportunities exist to improve the efficiency of equipment which employ refrigeration cycles and reduce the consequences for the environment.

1.1 Refrigeration

The word "refrigeration" implies the maintenance of a temperature below that of the surroundings. This is normally accomplished by evaporation of a liquid in a steady state continuous flow process. Heat is removed from a cold body (called the *heat source*), which results in a reduction in temperature, and is transferred to a hotter body (the *heat sink*). Essentially this is what a refrigeration process (or a refrigeration cycle as it is more commonly referred to) does. In order to effect this transfer of heat, work must be expended by the device transferring the heat. This is a consequence of the Second Law of Thermodynamics, which says that it is impossible to construct a system which will operate in a cycle and transfer heat from a cooler body to a hotter one, without work being done on the system by the surroundings. The energy flows in a refrigeration cycle are shown diagrammatically in Figure 1.1.

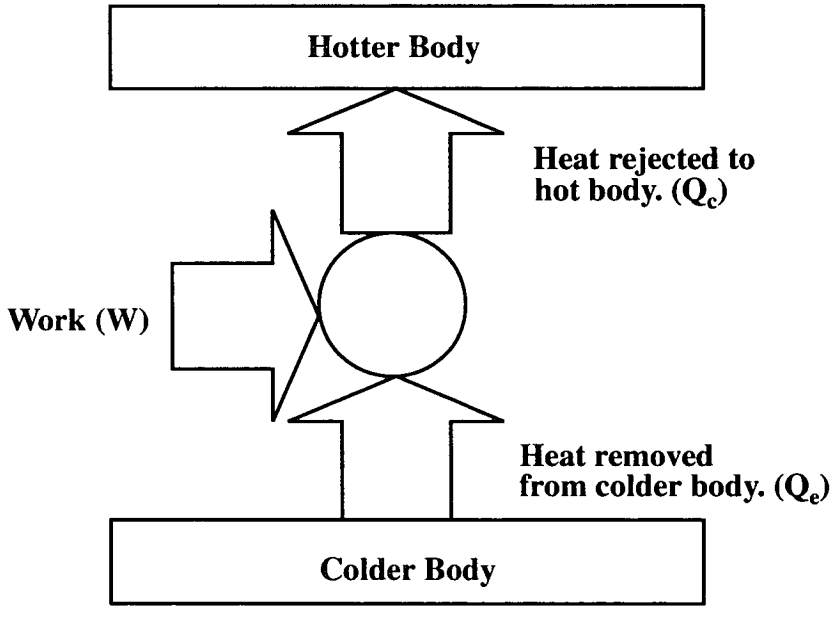

Figure 1.1: Energy flows in a refrigeration cycle

In refrigeration the body from which heat is taken is smaller than the body to which the heat is rejected resulting in a desirably significant reduction in temperature. A heat pump uses the same mechanism and principles. However, in this case the focus is on the body receiving the heat which experiences a significant increase in temperature e.g. heating of water or of a room. If the First Law is applied then by inspection the heat rejected to the hotter body is equal to the work added and the heat removed from the colder body i.e.

$$W + Q_e = Q_c \qquad \text{(Eq 1.1)}$$

The criterion of performance, expressed as a ratio of input to output, depends on what is viewed as the output. In refrigeration we endeavour to extract the most amount of heat (Q_e) from the cold reservoir for a given expenditure of work. Therefore the *coefficient of performance* of a refrigerator is defined as:

$$COP_{ref} = \frac{Q_e}{W} \qquad \text{(Eq 1.2)}$$

In a heat pump one is concerned with the amount of heat that can be transferred to the hot body; Q_c. Thus the heating COP is defined by:

$$COP_{hp} = \frac{Q_c}{W} \qquad \text{(Eq 1.3)}$$

Throughout this thesis the former convention (i.e refrigeration COP) is used, unless otherwise explicitly stated. The majority of refrigeration, heat pump and air conditioning cycles use the *vapour compression* cycle as their basis of operation. A liquid *working fluid* evaporating at constant pressure provides the means of for heat absorption. Likewise condensation of the vapour after compression to a higher pressure, provides for the rejection of heat (Section 2.1.1 on page 16). Until recently the majority of refrigerant working fluids were chlorofluorocarbons (CFCs). These

compounds comprise different molecular combinations of carbon, chlorine and chlorine. A large amount of knowledge and experience of these refrigerants had been built up, to the extent that standardised refrigeration equipment was available. The performance and thermodynamic behaviour of CFCs was well known to the refrigeration industry. The 1991 assessment of the Montreal Protocol [*U.N.E.P. 1991*] demonstrates the dominance of CFCs in the refrigeration industry. Concerns about the environmental suitability of CFCs led to a scheduled phasing out of their production. These concerns focused on the ability of CFCs to deplete atmospheric ozone.

1.2 Refrigerants and Climate Change

Currently there is much debate regarding ozone depletion in the upper atmosphere and "The Greenhouse Effect" and their consequences. In this section a very brief discussion is given on these topics and their consequences for refrigerants and refrigeration.

1.2.1 Ozone Layer Depletion

Ozone (O_3) is found at all altitudes in the atmosphere. Ninety percent of ozone is found between altitudes of 15km and 60km (i.e. in the stratosphere). Ozone is a primary absorber of ultra violet and visible radiation in the atmosphere. It prevents potentially harmful amounts of UV light from reaching the earth's surface. In 1974 Molina et al. [*1974*] hypothesised that chlorine from CFCs could efficiently destroy stratospheric ozone. Since then, considerable effort and resources have gone into measuring ozone concentrations in the atmosphere. At first in the mid 1980s it was not very clear whether there was in fact any significant ozone depletion. Ozone levels naturally vary considerably from season to season. NASA reported a 3% loss of total ozone over the period 1979-1984 [*Embler et al. 1986*]. Some scientists considered

this within the scope of natural variability and did not think there was any cause for alarm. However, since then the issue has become a little more clear. There has been a reasonably well defined drop in ozone levels. Satellite data indicated a 2.9% decrease in total ozone during the summer and a 5.6% decrease during the winter in the Northern Hemisphere at mid-latitudes since 1979 [*Wuebbles 1992*]. Today there is a substantial agreement among scientists that chlorine from CFCs causes ozone depletion. However there is not total unanimity and some dissenting voices remain [*Singer 1994*]. The reader is referred to two excellent summaries of the issues pertaining to ozone depletion and the greenhouse effect. These are presented by Embler et al. [*1986*] and by Wuebbles et al. [*1992*]. The former deals with the science and socioeconomic consequences of climate change, although it is somewhat out of date. Wuebbles presents a more up to date synopsis.

1.2.2 The Montreal Protocol and its Provisions

Throughout the early and mid 1980s the balance of opinion in the scientific community shifted towards the belief that CFCs were likely to be culpable for ozone depletion. On September 19, 1987, 24 countries met in Montreal and signed the "*Protocol on Substances that Deplete the Ozone Layer*". The protocol called on the ratifying states to phase out and eliminate the production and trade of CFCs. Specifically it limited production of specified CFCs to 20% of 1986 levels by July 1st 1993 and a further 50% cut by 1998 [*Lucas 1993*]. The restrictions were placed on production and not on use. HCFCs and Halons were not considered at this stage. The protocol provided for revisions and updates of the timetables. An earlier phase-out date, set at the year 2000, was adopted for developing countries. More substances became controlled and a target date for the phasing-out of HCFCs was set between 2020 and 2040 [*Lucas 1993*]. As a result of ever decreasing values of reported ozone in the early 1990s [*Kiernan 1993*], [*Gleason et al. 1993*], an accelerated phase-out of CFCs was adopted at the Copenhagen summit in November 1993. By then the

original treaty had been amended so that CFCs were to be phased out by January 1st 1996 [*Reed 1993*]. The timetable on the phasing out of HCFCs was more gradual. These were to be completely eliminated by 2030. At the time of writing all of the major manufacturers of CFCs in the developed world have ceased production.

1.2.3 Hydrofluorocarbon Replacement Refrigerants

As a result of the restrictions imposed on CFCs, replacement refrigerants had to be found. When a particular substance is being considered as a refrigerant working fluid it must satisfy a number of criteria. Potential refrigerants must be safe to use, thermodynamically suitable for the cycle in question and must not degrade the environment. McLinden et al. [*1986*] undertook a molecular based study to examine potential replacements and to screen out substances that possessed undesirable properties. Their search pointed to the chlorofluorocarbon families as a starting point in the search for new refrigerants. They concluded that research and development should be concentrated on environmentally acceptable members of the CFC family. This would lead to the least disruption and expense for the refrigeration industry, while at the same time conforming to refrigerant restrictions. They also found that the number of suitable replacement refrigerants meeting all or most of the criteria is very low. At the moment, the leading long term replacement candidates are Hydrofluorcarbons (HFCs). These are made up of carbon, hydrogen and fluorine. These substances do not contain any chlorine and hence do not deplete ozone. Like CFCs they are very stable and inert. They possess similar, although not identical, thermodynamic properties to CFCs. HFCs satisfy most if not all of the requirements of a refrigerant. Currently R134a (1,1,1,2-tetrafluoroethane) is the leading replacement refrigerant for R12, which was commonly used in domestic refrigerators. R22 and R502, used in supermarket and commercial refrigerators are being replaced by a wide variety of refrigerant mixtures. In 1993, Pearson [*1993*] presented a list of 29 interim and long term replacement blends for R22 and R502. These included

various blends of the HFC refrigerants R134a, R32 (difluoromethane) and R125 (pentafluoroethane). As time goes on, the number of replacements will reduce as the refrigeration market favours certain blends over competing mixtures.

1.2.4 The Greenhouse Effect

Carbon dioxide (and other gases) absorb infrared light reflected from the earth's surface, raising the earth's temperature by about 35 degrees C. Since the industrial revolution there has been a large increase in the CO_2 concentration in the earth's atmosphere. This has been attributed to anthropogenic production of CO_2, from the burning of fossil fuels. This has led to fears that the global average temperature could rise by a few degrees C because of increased levels of CO_2 in the atmosphere. The global average temperature has risen by 0.5 degrees over the last century [*Embler et al. 1986*]. It has been postulated that if this continues unchecked, it may lead to desertification of food producing areas, an increase in sea level and more extreme effects of storms on coastal areas. Currently, there is much debate about the likelihood and consequences of the greenhouse effect. The reader is directed to other references for more detailed information [*Embler et al.1986*] [*Wuebbles1992*] [*Kerr 1995*].

CFC refrigerants also have an effect upon global warming. CFCs and HCFCs are greenhouse gases. In fact they are far more powerful greenhouse gases than CO_2 Despite their small atmospheric concentrations, it is believed that CFCs make a significant contribution to the greenhouse effect. It has been estimated that CFCs are responsible for 24% of the increase in radiative forcing that has occurred from 1980 to 1990 [*Wuebbles 1992*]. (Radiative forcing is the surface temperature change caused by the presence of a substance in the atmosphere). When considering the contribution of a CFC, or any other refrigerant for that matter, to the greenhouse effect as a whole, it is necessary to consider the application of the refrigerant. Refrigerators, heat pumps, and air conditioners are normally powered by electricity. If fossil fuel is used

to generate this electricity, a certain amount of CO_2 is released to the atmosphere. The refrigerant has a direct effect on global warming when it is released, and an indirect effect which depends on the efficiency of the installation and the method used to generate and transport the electricity. For a domestic refrigerator, 99% of its contribution to the greenhouse effect emanates from the power needed to run it [*Lucas 1993*]. Use of more efficient refrigeration equipment can reduce the indirect contribution of refrigerants to the greenhouse effect.

1.2.5 Countering the Greenhouse Effect

Alleviating the greenhouse effect will prove to be a more intractable problem than reversing ozone depletion. Today we are highly dependent upon fossil fuels to provide our energy needs and maintain our current quality of life. A study of alternative energy options was undertaken by the Oak Ridge National Laboratory in 1989 [*Fulkerson et al. 1989*]. They examined various energy technologies that could potentially help to reduce CO_2 emissions and where research and development efforts should be focused. They concluded that there is no clear superior energy technology that could replace fossil fuels in the short to mid term. Although alternative energy sources such as biomass, wind energy and nuclear power will become more common, none are yet ready to replace fossil fuels on the scale necessary to reduce CO_2 emissions. The report also concluded that technical improvements in energy efficiency could result in large economic improvements. Increasing research and development into efficiency is the best near to mid term strategy for reducing the growth of CO_2 emissions. The authors of this report noted that experience over previous 12-15 years suggests that increased energy efficiency improvements can bring favourable impact on energy use. Over the period 1972-1986 the amount of energy used by OECD countries has remained more or less constant. However, GDP has increased by about one third over this period. Whilst some of this was due to structural changes, much of the improvement can be attributed to improved energy

use. Using finite energy resources in a more efficient manner can reduce the consequences of the greenhouse effect and allow time for other forms of energy sources to be developed.

Improving the efficiencies of refrigeration equipment is one particular aspect of improving energy use. The use of more efficient refrigeration equipment reduces the indirect effect that refrigeration unit has upon global warming. Although only a small part of the total drive to obtain better energy use, increasing the performance of refrigeration cycles can play an important part in alleviating the greenhouse effect.

1.2.6 Refrigerant Mixtures

In their survey of fluids likely to replace CFCs, McLinden et al.[*19 86*] pointed out that no one single replacement may satisfactorily meet all the necessary requirements of a refrigerant. The use of mixtures of refrigerants may help to override this problem. One advantage of using mixtures of refrigerants, is that under certain circumstances, they may exhibit better performance than pure components. With pure working fluids, large temperature differences between the refrigerant and heat source and sink temperatures may exist, especially if the sink and source fluids undergo a large temperature change. A liquid composed of two mutually soluble components boils across a temperature range rather than at a fixed temperature. If such a mixture were used as a working fluid, it would be possible to 'match' the change in temperature in the condensation and evaporation stages of the vapour compression cycle with the temperature changes in the heat sink and source fluids. This can lead to improved cycle COPs. (This is further described in Chapter 2, Section 2.2 on page 18). It would be advantageous to quantify the benefits to refrigeration COP through the application of refrigerant mixtures. Determination of how well mixtures outperform, or indeed are inferior to, pure refrigerants would give refrigeration engineers a larger body of

knowledge from which to base a decision on the choice of working fluid for a given application.

1.3 Aims of Research and other such mindnumbingly boring topics which nobody in their right mind would do

1.3.1 Experimental Determination of COP Benefits of HFC Refrigerant Mixtures

Until recently most vapour compression cycles employed a pure, single component working fluid. Many refrigerant applications require the heat sink and source fluids to go through a quantifiable temperature change. By matching these temperature changes with the change in temperature experienced by a mixed refrigerant working fluid when it undergoes a phase change, it is theoretically possible to increase the COP of a cycle. System pressures and pressure ratios may also be reduced. The use of non-azeotropic refrigerant mixtures can lead to improved energy performance in a vapour compression cycle, depending on the application. There would be little point in investigating the behaviour of CFC mixtures since they will be phased out. It would be more beneficial path to investigate mixtures of non-ozone depleting HFCs since these are the leading candidates to replace CFCs. By constructing and operating a cycle with HFC mixtures, sufficient information should be gathered to ascertain if HFC mixtures can lead to improved cycle efficiency. Data on the performance of pure HFCs would also be gathered and analysed. Since a two fluid cycle already existed within the department, constructed by Low (Section 1.4), it was intended that this cycle be reused to examine the possibility of energy use improvements using mixtures. This required that the system be modified and redesigned to accommodate the thermodynamic properties of HFCs, especially higher vapour pressures. This project received the financial backing of I.C.I. Chemicals and Polymers Ltd. and the

Engineering and Physical Sciences Research Council. In discussions with I.C.I., it was decided that instead of using a convection flow evaporator, as used by Low, a pool boiling evaporator should be used. It was intended to examine how the COP, and other cycle parameters, varied with composition of the working fluid. In the last number of years the use of refrigerant mixtures has received increased attention and is covered in the literature review (Chapter 2, Section 2.3 on page 20).

1.3.2 Simulation of a Refrigeration Cycle to Quantify COP Improvements of HFC Refrigerant Mixtures

A refrigeration cycle will be simulated by a computer model. This allows a greater number of mixtures and parameters to be examined than that achievable through experimental techniques. A simulation model is much more flexible and many more parameters and mixtures can be examined than by experimental analysis. The benefits to the COP of a number of HFC binary mixtures will be investigated. Cycle parameters will be varied to examine their effect upon mixture COP.

1.3.2.1 Subsidiary Aim: Prediction of HFC Refrigerant Thermodynamic Properties From Sparse Data

Currently HFC refrigerant such as R134a, R32, R125 and various mixtures of these are the leading candidates to replace CFC refrigerants. Replacement refrigerant must have suitable thermodynamic properties for the application in question.The thermodynamic properties of a refrigerant determine the COP of the cycle. In a vapour compression cycle the operating pressures within the cycle depend on the vapour pressure of the refrigerant. Enthalpy values need to be accurately predicted so that the energy transfers in the cycle can be determined. The working fluid is often saturated and hence saturation data for the refrigerant must be supplied. McLinden et al. [*1986*] identified the thermodynamic properties needed to assess a refrigerant.

They categorised the properties needed in order of importance. The first group consisted of the molecular structure and normal boiling point. These are the most basic requirements. The second group of properties needed, included the critical points, vapour pressure, saturated liquid density and PVT data. Transport properties such as viscosity and thermal conductivity data, needed for equipment design, were categorised in the third group. The fourth and fifth groups consisted of a more complete description of the fluids.

Scientists and engineers often use an *equation of state* to determine the thermodynamic properties of a fluid. This is a mathematical relationship which describes the temperature, volume and pressure behaviour of a fluid in one equation. They can also be viewed as storing a huge amount of experimental data in one short concise equation. They vary from simple to highly complex equations with many parameters. Most equations of state require coefficients calculated from experimental data, usually from the second group thermodynamic properties identified by McLinden and Didion. In embarking on the process of replacing an existing refrigerant it may be necessary to screen as wide a range of potential fluids. The required thermodynamic data needed to assess a potential fluid's suitability as a refrigerant may not exist, or only a sparse amount of data may be available. In this case vapour pressure, density, PVT behaviour, etc. would have to be experimentally measured. At the initial stages this may not be feasible for a large number of potential replacement refrigerants. A need exists for a method which can provide accurate thermodynamic data from a minimal amount of data on the fluid. Accurate determination of the thermodynamic properties of a fluid from sparse data would enable those fluids with the most suitable thermodynamic properties for replacement of CFCs (or other refrigerants) to be identified quickly and with a minimum of effort. As mixtures become increasingly common, methods for accurate prediction of mixture properties will have to be implemented. There is an inevitable trade-off between accuracy and the amount data needed by a particular method to determine thermodynamic properties. Equations which use extensive amounts of experimental

data are likely to be more accurate than those which use a minimum of data. Once a fluid has been established as a likely replacement candidate, then its properties will be experimentally investigated and high accuracy correlations or equations of state developed especially. At the initial stages, it is advantageous to be able to determine a refrigerant's thermodynamic properties from a minimum of data.

As part of the simulation of the refrigeration cycle, methods which can calculate the thermodynamic properties of refrigerants from sparse data will be examined. They may then be used to determine the COP (and other cycle parameters) of proposed refrigerants. Specifically, the Cubic Chain-of-Rotators equation of state will be examined to see how well it can predict the thermodynamic properties of non ozone depleting refrigerants. This equation of state requires a comparatively small amount of information about the fluid it describes. It only requires the critical temperature, critical pressure and acentric factor to determine properties such as vapour pressure, enthalpy etc. The predicted properties of pure and mixed HFCs will be compared to published experimental data. The predictions will also be compared to a method commonly used to determine refrigerant thermodynamic properties. By comparing the calculated value with published data in the literature the suitability of this equations may be gauged.

1.4 Robert E. Low's Research

In 1991 Robert E.Low successfully submitted a doctoral thesis [*Low 1991*] entitled "A Variable Capacity Heat Pump for Renewable Energy Recovery". He investigated whether it was possible to construct a heat pump which could produce a constant heat output with a variable work input. The heat pump was designed to be coupled with a renewable energy source. These often produce highly variable work loads. Often in a heat pump system, the heat source fluid requires a constant heat load. Low designed and constructed a heat pump utilising refrigerant mixtures within the Department of

Chemical Engineering at Edinburgh University. Other features of the system included dual condensers, refrigerant holding tanks and metering pumps. These were used to alter the composition of the circulating working fluid as the work input changed. Low employed CFC mixtures of R114/R113 in the heat pump system. Other significant research themes included the examination of the Cubic Chain-of- Rotators (CCOR) equation of state for its suitability in predicting the thermodynamic properties of pure CFCs and also for CFC mixtures. Comparison of experimental data and predicted data produced by the CCOR were made. An examination of the effects of binary interaction coefficients (k_{ij}), used to calculate equation of state parameters, was also conducted. The main conclusions of the work were:

- The principle of capacity self regulation was experimentally verified. The composition shifted in response to a change in the heat sink flowrate.
- The CCOR equation of state was found to be superior to other cubic equations of state for the predicting of liquid phase properties. It exhibited an underprediction for saturated vapour properties for reduced temperatures below 0.85. The prediction of saturated properties could be improved by the fitting of four parameters to reported experimental data. The equation was able to represent vapour liquid equilibrium of CFC mixtures, if two interaction constants were fitted to experimental data.

The research work conducted for this thesis, used the equipment and some of the computer software developed by Low. These were modified and adapted where necessary so that the objectives of this work could be achieved.

Chapter 2

Theory and Literature Review

The theory of applying non-azeotropic mixed refrigerants to improve COPs in refrigeration cycles is outlined in this chapter. A review of articles from the literature concerned with investigations into improving COP using refrigerant mixtures is presented. Investigating mixed refrigerants introduces the question on what basis pure and mixed cycles are compared. This is discussed in the literature review.

As a part of the research work for this thesis, a model of a refrigeration cycle was developed to quantify the how HFC mixtures can improve COP. The model and its results are discussed in Chapter 5. Thermodynamic data for the model was supplied by the Cubic Chain-of-Rotators equation of state. Before implementation of the model the ability of the CCOR equation to predict HFC thermodynamic properties was investigated. Comparisons were also drawn with the Carnahan-Starling-DeSantis equation of state. Consequently articles in the literature pertaining to the CCOR and CSD equations and the prediction of refrigerant thermodynamic properties in general are presented in this chapter.

2.1 Vapour Compression Cycles

The majority of refrigeration units, air conditioners and heat pumps are based upon the *vapour compression cycle*. The simplest form contains four pieces of equipment: compressor, condenser, expansion device and an evaporator (Figure 2.1). This cycle utilizes the latent heat of the working fluid to effect heat removal from the heat source and heat addition to the heat sink. Saturated vapour enters the compressor where the working fluid's pressure is increased. The vapour leaving the compressor will often be superheated in a real process. The high pressure vapour is desuperheated and condensed in the condenser, rejecting the heat to the high temperature heat sink. The liquid is then adiabatically expanded to the lower pressure, usually across a throttling valve. The throttling has the effect that some of the liquid is vaporised. The vapour-liquid mix is then fully vaporised in the evaporator which receives the heat from the heat source.

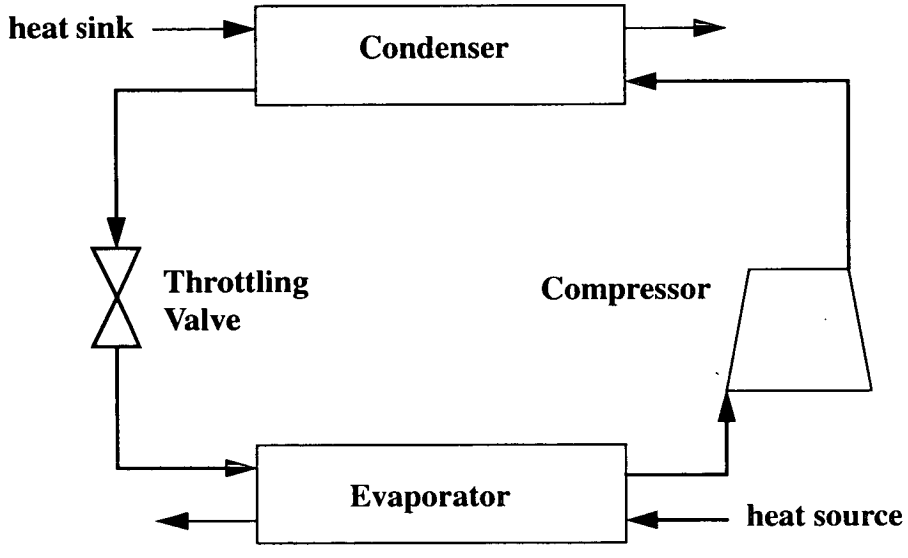

Figure 2.1: Vapour compression cycle schematic diagram

Vapour compression cycles come in many different configurations. Compressors may be positive displacement or centrifugal. The heat exchangers may be simple double pipe affairs or large shell and tube versions, depending on the duty and conditions. Some cycles may use more than one evaporator or condenser. The ideal cycle is sometimes referred to as the *Carnot Cycle*. This represents the highest thermodynamic efficiency which a real cycle can approach. The work required by a real cycle is always greater than the work required by a Carnot cycle, operating at the same conditions. The necessary power depends on individual component losses, operating conditions and refrigerant properties. Various thermodynamic parameters exist to describe the performance of a vapour compression cycle (e.g. COP).

2.2 Refrigeration Cycles Employing Mixed Working Fluids

In many refrigeration cycles the heat sink/source fluids undergo a finite and definite temperature change (Figure 2.3(a)). Many refrigeration cycles employ a pure fluid which evaporates and condenses at a constant temperature (assuming no pressure drop). In a vapour compression cycle employing a single component refrigerant there are energy penalties associated with the mismatch in temperatures. The condenser temperature must be higher than the maximum temperature of the heat sink fluid and the evaporator must operate at a temperature lower than the minimum temperature of the heat source fluid. When a non-azeotropic fluid (sometimes called *zeotropic*) mixture undergoes a phase change, at constant pressure, a change in temperature will occur unlike a pure substance which boils and condenses at a constant temperature. Figure 2.2 shows a binary fluid in a closed container boiling at constant pressure. At point 1 the mixture is just at the boiling point and the vapour will be richer in the more volatile component. When point 2 has been reached, about half of the liquid has evaporated, and the temperature is higher than point 1.

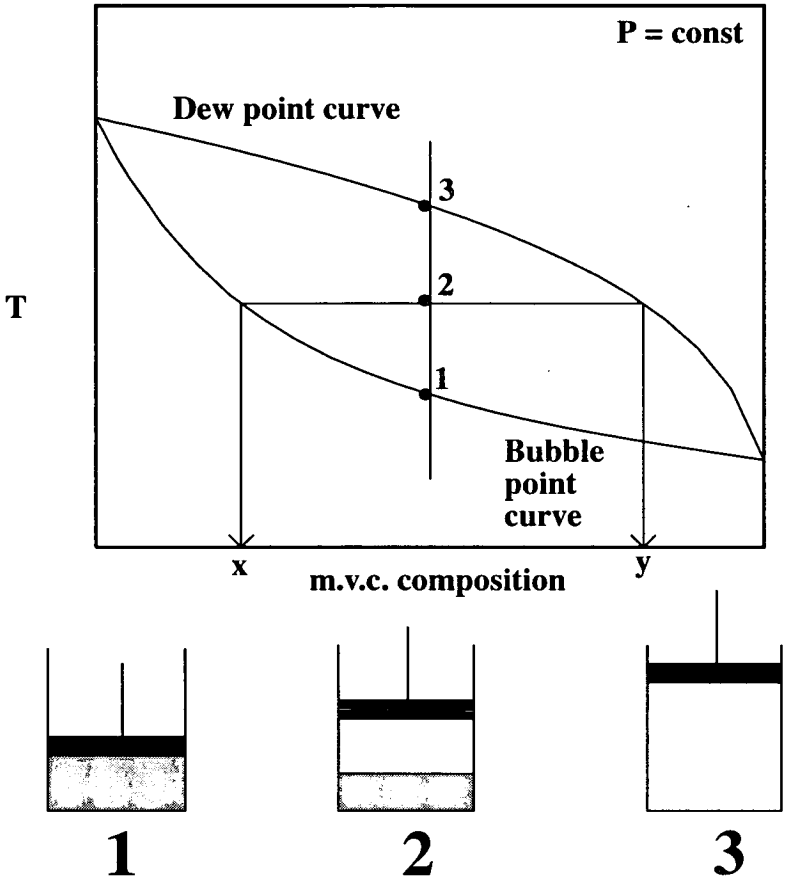

Figure 2.2: Phase diagram of a non-azeotropic mixture

At point 3 the mixture has reached the dew point and has completely evaporated. The evaporating fluid experiences an increase in temperature due to the difference in the volatilities of the components. A similar situation prevails for condensation. This change in temperature is referred to as the *gliding temperature difference* (GTD). The gliding temperature difference can be harnessed in a refrigeration cycle to increase the COP beyond what can be achieved by a pure working fluid.

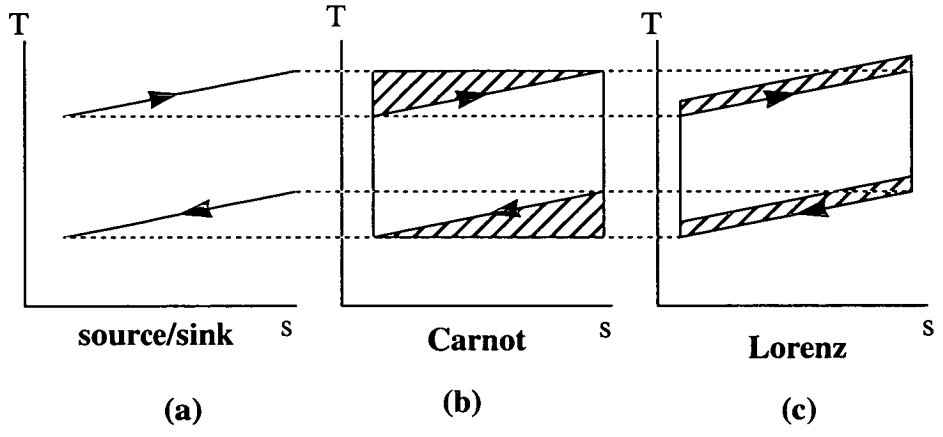

Figure 2.3: Temperature-entropy diagrams of pure and mixed cycles

Figure 2.3 shows the temperature profiles of a source and sink fluid in the evaporator and condenser on a temperature-entropy diagram. Also shown are the temperature-entropy diagram of a pure fluid (Carnot Cycle) and that of a mixed refrigerant (sometimes called a Lorenz cycle). The shaded areas in Figure 2.3(b) and Figure 2.3(c) represent the temperature differences between the refrigerant and the sink and source fluids. These differences represent inefficiencies or exergy losses. If the working fluid phase change is isothermal and the heat transfer fluids experience a large temperature change (Figure 2.3(b)) then the exergy loss will be relatively large. If the working fluid's temperature profile matches that of the sink/source fluids then the exergy loss will be reduced (Figure 2.3(c)). By using a non-azeotropic refrigerant mixture, one can use its non-isothermal phase change behaviour to achieve better temperature matching. Consequently the *average* refrigerant temperature in the condenser and evaporator is reduced. Less work must be supplied by the compressor to achieve the same duty. In summary, there is a potential for increased efficiency by applying a mixed refrigerant as a result of better temperature matching. The gain in efficiency will depend on the cycle configuration and the refrigerant mixture actually

used. The magnitude of such improvements can be found by experimental investigation and by accurate simulation.

2.3 Comparison of Pure and Mixed Refrigeration Cycles

Refrigerant mixtures were investigated as far back as the 1880s. However, it was not until the 1960s that engineers began to explore experimentally the possible benefits that could accrue from refrigerant mixtures. Much of this research was focused on heat pumps. In the early 1970s rising energy costs, due to the oil crisis led to increased research and more publications in the field. With the advent of cheaper and more powerful computing facilities a substantial part of research into refrigerant mixtures has been conducted using mathematical models. This has the obvious advantage of not having to construct or purchase experimental test apparatus (resulting in substantially reduced stress levels in researchers). The signing of the Montreal Protocol led to a further substantial increase in the volume of research dealing with refrigerant mixtures, the majority of which deals with proposing and testing of various non-ozone depleting refrigerant blends with a view towards replacing commonly used CFCs, rather than a systematic attempt to investigate the efficiency benefits of such mixtures. A summary of past research work, both experimental and theoretical, in the field of refrigerant mixtures is presented here. Before citing publications in the literature it is instructive to discuss how one compares mixed cycles to those using a pure working fluid.

Implicit in investigating the benefits of mixed refrigeration cycle is the problem of how a pure cycle is to be compared with a cycle employing a working fluid of more than one compound. There are several possible methods of comparison: equal condenser and evaporator inlet temperatures, equal heat loads and equal mean temperature differences. How one makes such a comparison is not as simple as one

would first assume. It is possible to select a basis of comparison which is unduly unfair to either a pure or mixed working fluid. The outcome of such an investigation can strongly depend upon the basis of comparison if care is not taken.

2.3.1 Comparison Method Described by McLinden and Radermacher

McLinden and Radermacher [*1987*] examined four different methods of comparing pure cycles with mixed ones. A computer model of a heat pump was developed (named CYCLE-7). A heat pump circuit employing R22/R114 and R22/R11 mixtures was modelled. The cycle was modelled with pure and mixed refrigerants so that comparisons could be drawn. The four methods of comparison are shown in Figure 2.4: (Case A) equal evaporator and condenser *inlet* temperatures; (Case B) equal evaporator and condenser *outlet* temperatures; (Case C) equal average temperatures for each phase change; and (Case D) a combination of the previous three. They found that the method of comparison greatly influences the result. Figure 2.5 shows the heating COP plotted against R22 composition for the R22/R114 mixture using the four methods of comparison outlined. Mixtures had higher heating COPs than pure, in Case A (equal inlet temperatures) and consequently there is a pronounced maximum in heating COP around a composition of 0.5 mole fraction R22.

From Figure 2.4 the average evaporator refrigerant temperature for mixtures is higher than that for pure fluids and the average mixture condenser temperature is less than that for pure fluids, hence the compressor pressure ratio is less for the mixture and less work is needed by the mixture to achieve the same condenser inlet and evaporator outlet temperatures. The direct opposite occurred when equal outlet temperatures was selected as the basis of comparison (Case B). The mixture condenser and evaporator average temperatures are higher and lower, respectively, than the pure fluid

temperatures which requires more compressor work. The remaining two methods showed no substantial variation in heating COP with composition.

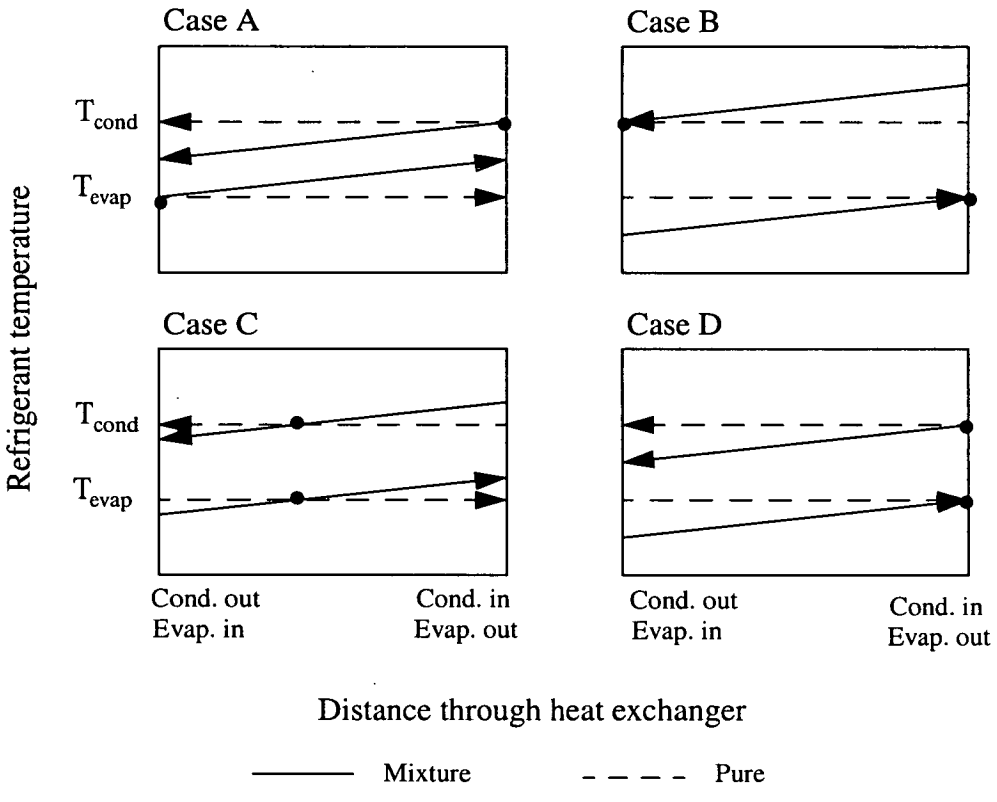

Figure 2.4: Specified refrigerant temperatures in comparing pure and mixed cycles

Rather than specifying refrigerant temperatures, McLinden and Radermacher recommended that a fair and meaningful comparison must include the application of the refrigeration cycle. The heat transfer fluid temperatures should be specified and a constant total heat transfer area per unit capacity should be maintained. They also concluded that keeping the log mean temperature difference constant is also a valid method of comparison. The refrigerant temperatures and pressures should be allowed

to vary so that a specified temperature change in the heat and sink source stream, and a specified heat load per heat transfer area can be achieved.

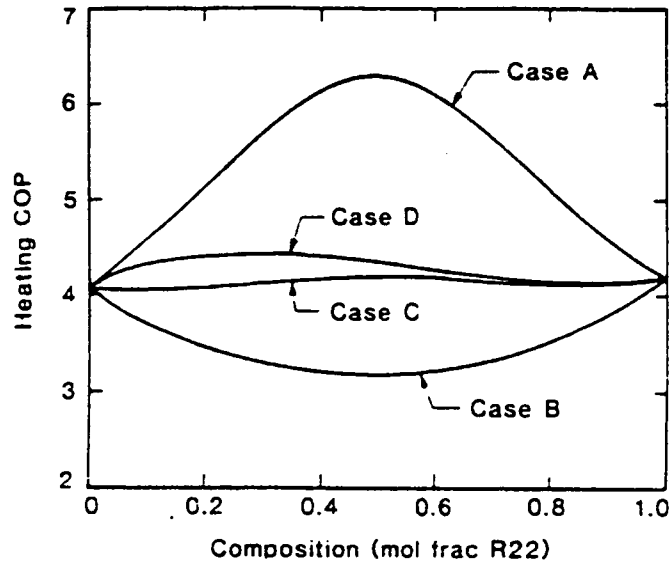

Figure 2.5: Heating COP-composition profiles for four methods of comparing pure and mixed cycles (Taken from McLinden et al. [*1987*])

Using the same mixtures (R22/R114 and R22/R11) they examined the variation in heating COP, evaporator and condenser gliding temperature differences and the percentage superheat in the total condenser heat load, for these two mixtures. The results are displayed in Figure 2.6 and Figure 2.7 as functions of R22 composition. They specified the heat sink and source fluid temperatures and a parameter they called UA_{tot}/Q_c, (set to a value of 0.36 K^{-1}) which is the total heat transfer area per unit heat capacity A_{tot} is the sum of both condenser and evaporator. For R22/R114 mixtures and a heat transfer fluid temperature (HTF) difference of 10 degrees C, there was no substantial improvement in heating COP. The COP stayed relatively constant because of a trade off between a well matched condenser GTD and a mismatched evaporator GTD (Figure 2.6). With a 25 degrees C change in HTF temperature there was a

pronounced maximum of heating COP at 0.6 mole fraction R22. However, the COP was lower than the 10 degrees C case across the whole composition range.

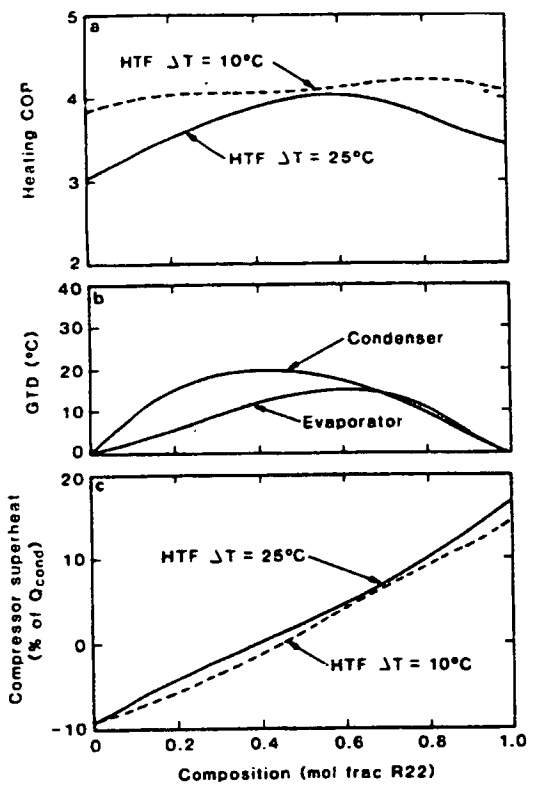

Figure 2.6: Heating COP, GTD and percentage superheat vs. R22 composition for R22/R114 (Taken from McLinden et al. [*1987*])

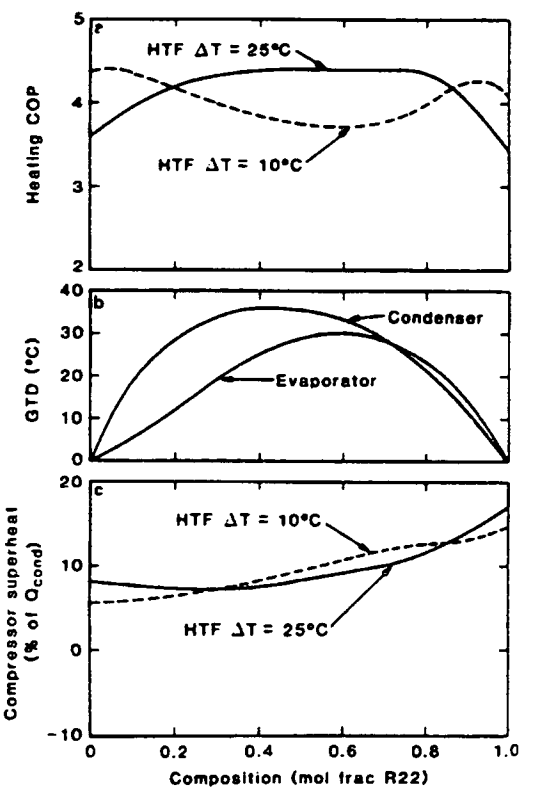

Figure 2.7: Heating COP, GTD and percentage superheat vs. R22 composition for R22/R11 (Taken from McLinden et al. [*1987*])

The same HTF and UA_{tot}/Q_c conditions were then applied to a R22/R11 mixture which has a larger glide than R22/R114. The 25 degrees C change exhibited a broad maximum between 0.4 and 0.75 mole fraction R22. In this case the HTF of the evaporator was well matched to the GTD of the mixture. In conclusion, they found that the better the matching between the GTD and the temperature change of the source and sink fluids, the more the COP will be improved.

2.3.2 Comparison of Högberg

Högberg et al. [*1993*] also carried out a simulation of a heat pump cycle and, using different comparison criteria, examined the variation of heating COP with composition. In this study, three different methods of comparison were used: equal minimum approach temperatures (method I), equal mean temperature differences (method II) and equal areas (method III). Two mixtures, R22/R142b and R22/R114, were examined across the full composition ranges. Source and sink temperature changes of 5 degrees C and 15 degrees C were selected. Method I showed the largest variation in COP with composition, depending on the application and the mixture. The COP-composition curves for methods II and III showed a similar shape. Both mixtures, and all three methods, showed maxima for the COP in the case of the 15 degrees C source/sink temperature change. They attributed the rise in COP to the fact that large HTF temperature changes allow a greater potential increase in evaporator working fluid temperature. In contrast, small changes in HTF temperature restrict an increase in evaporator dew point temperature. Figure 2.8 and Figure 2.9 show the temperature profiles in the condenser and evaporator. The dashed lines represent the sink and source fluids.

In Figure 2.8 the sink and source fluids experience a large change in temperature, while in Figure 2.9 they undergo a smaller change in temperature. The mean values of the sink and source temperatures are the same in both diagrams. Curves marked '1' represent the temperature profile of a mixed refrigerant. Those denoted with '2' represent a pure working fluid. From the diagrams, it can be seen that a cycle with large external (sink/source) glides has a greater potential for an increase in the evaporator dew point, and consequent reduction in pressure ratio and work input. When the evaporator dew point temperature is increased, there is an increase in the condenser temperature. The maximum increase in evaporator dew point temperature that can be achieved is the difference between the inlet temperature of the external fluid and the saturation temperature of a pure working fluid.

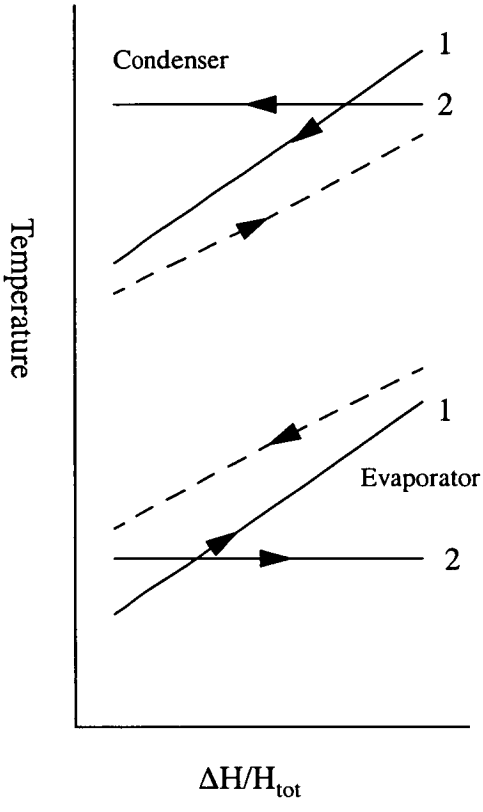

Figure 2.8: Temperature profiles in heat exchangers with large HTF temperature changes

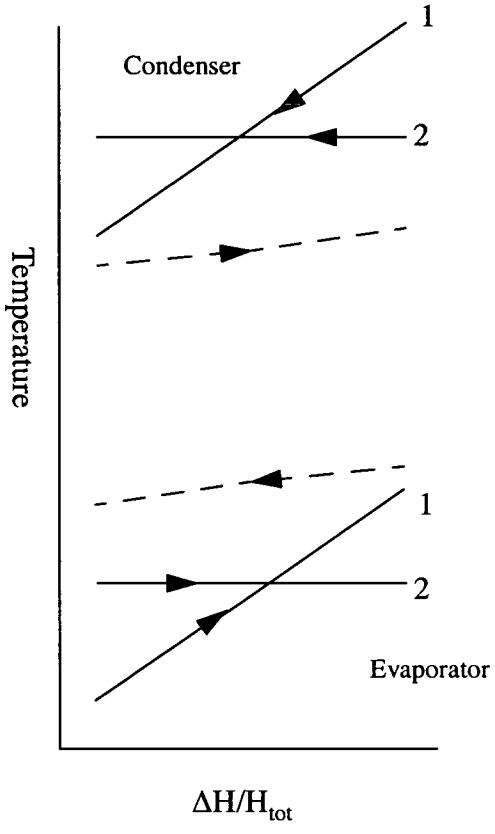

Figure 2.9: Temperature profiles in heat exchangers with small HTF temperature changes

With small source/sink glides the increase in condenser temperature is large relative to the evaporator temperature increase. In Figure 2.9 the potential for increase in the evaporator temperature is limited and the increase in the condenser dew point temperature is large relative to the increase in the evaporator. With large external glides (Figure 2.8) the increase in the evaporator dew point temperature is larger than the increase in the condenser temperature. Thus the possibility of increasing the heating COP are greater with larger external temperature glides.

Högberg recommended that making comparison between pure and mixed fluids on the basis of equal minimum approach temperatures (method I) be avoided since this means that comparisons will be made with different heat exchanger areas. If a mixture and a pure fluid have the same minimum approach temperature, then the mixture will have a lower log mean temperature difference and hence a larger area is needed to transfer the same amount of heat. Using equal mean temperature differences as a basis of comparison (method II), they concluded that this method can be used to compare the heating COPs of pure and mixed fluids for rough estimations of COP. They also noted that if equal mean temperature difference is to be used as a basis of comparison, it is important to determine the log mean temperature difference (LMTD) by numerical integration along the temperature profiles rather than relying on the end temperatures. They found that differences of up to 20% occurred between the two methods. If a completely rigorous comparison is to be made, taking into account effects such as pressure drop, mass transport resistance in heat transfer, the authors concluded that it is essential that method III (equal areas) be used.

2.4 Literature Review of Experimental Investigation of Mixed Cycles to Improve COP

A summary of articles published in the literature concerning experimental investigation into the use of mixed refrigerants is given in this section. Investigations using computer simulations are discussed in Section 2.5 on page 40. The most important results of each article and the basis of comparison which the author used in comparing pure and mixed cycles will be described. A tabular summary of all articles discussed is presented Section 2.6 on page 49.

2.4.1 Early Work

One of the earliest investigations into refrigerant mixtures was conducted by Carr [*1949*]. He pointed out that increased efficiency could come from better matching of the temperature profiles. The work required for an ethane/propane/butane cycle was calculated and compared to an ammonia cycle. Equal log mean temperature differences were used as a basis of comparison. The work requirement of the hydrocarbon working fluid was calculated to be 71% that of the ammonia cycle.

Haselden and Klimek [*1957-58*] experimentally examined various propane/n-butane mixtures. They varied the propane composition from 0% to 30% in increments of 5% (presumably wt.%). A simple cycle with an expansion precooler was used. An alcohol stream was cooled from 70°F to 45°F. The heat was rejected to a water stream, whose temperature increased from 80°F to 105°F. A 7% power saving was found with the 30/70 mix, compared to pure n-butane. The authors stated that better savings could have been achieved with more appropriate selection of heat transfer surface configuration. They also carried out some calculations comparing a cycle employing R12, ammonia and three hydrocarbon binary pairs. The 50/50 propane/butane mixture had a power requirement 50% less than that of R12. Although this pair needed 2.8 times the heat transfer surface area, compared to R12, they found that the increase in capital cost of the heat exchange surface would be offset by reduced compressor and motor size.

2.4.2 E.I. du Pont Nemours & Co., Delaware, U.S.A.

One of the first investigations involving CFC mixtures was conducted by McHarness and Chapman [*1961*] in the early 1960s. They carried out an extensive series of tests with combinations of R13B1, R12 and R22. A simple refrigeration cycle with a receiver after the condenser was used. The first series of tests involved pure refrigerants and two mixtures. The condenser refrigerant inlet temperature was kept

constant at 110°F while the evaporator inlet was set at -20°F, -10°F and 40°F. A wealth of data was presented in various tables allowing one to compare cycle parameters across the refrigerants tested. R22 had the highest COP at -20°F and 40°F. In a second series of tests the three binary combinations of R13B1, R12 and R22 were tested. As with the pure refrigerants the same evaporator and condenser conditions were specified. The compositions of each pair was varied in 25 wt.% increments. The R22/R12 pair showed a very slight maximum at 85% R22, at -20°F and -10°F. For the R13B1/R12 pair a 5% increase in actual COP was noted, at a composition 25% R13B1. The R13B1/R22 pair did not show any improvement in COP compared to the pure component COPs. Refrigeration capacity data was graphically presented to show the variation with composition The R13B1/R22 exhibited the highest capacity of the mixtures examined. The authors concluded that mixtures offers the engineer flexibility in selecting a capacity for a particular application.

2.4.3 Indian Institute of Technology, New Delhi, India

Arora [*1967*] outlined work he had carried out with R22/R114 mixtures. A refrigeration cycle was examined both theoretically and experimentally. Calculations were conducted on a cycle whose working fluid had an evaporation temperature of -15°C and a condensing temperature of 35°C. The condenser log mean temperature difference was specified as 4.33 degrees C. The R114 composition was varied from 0 wt.% to 20 wt.% in steps of 5%. Pure R114 was examined also. As the composition of R114 was increased, an increase in calculated COP occurred. At 20% R114 there was a 13.78% increase in power savings. The experiments yielded similar results. The evaporator temperature was varied from -25°C to 0°C and the R114 composition was varied from 0 to 30 wt.%. The power consumption showed a decrease with addition of R114. The COP (or cooling energy ratio as Arora refers to) showed a maximum at around 10% R114. The largest power saving achieved was 17% at a composition of

12% R114 and a temperature of -10°C. The specific volumetric capacity decreased with addition of R114.

2.4.4 VEB dkk Scharfenstein, Former G.D.R

The problem of removing heat at two different temperature levels in a domestic refrigerator provided the impetus for Lorenz and Meutzner [*1975*] to look at refrigerant mixtures. Increased cooling capacity at the lower temperature level, with pure R12, leads to large compressors and higher production and running costs. They concentrated on finding a mixture and a refrigerant circuit that could provided cooling at two temperature levels in an economical manner.

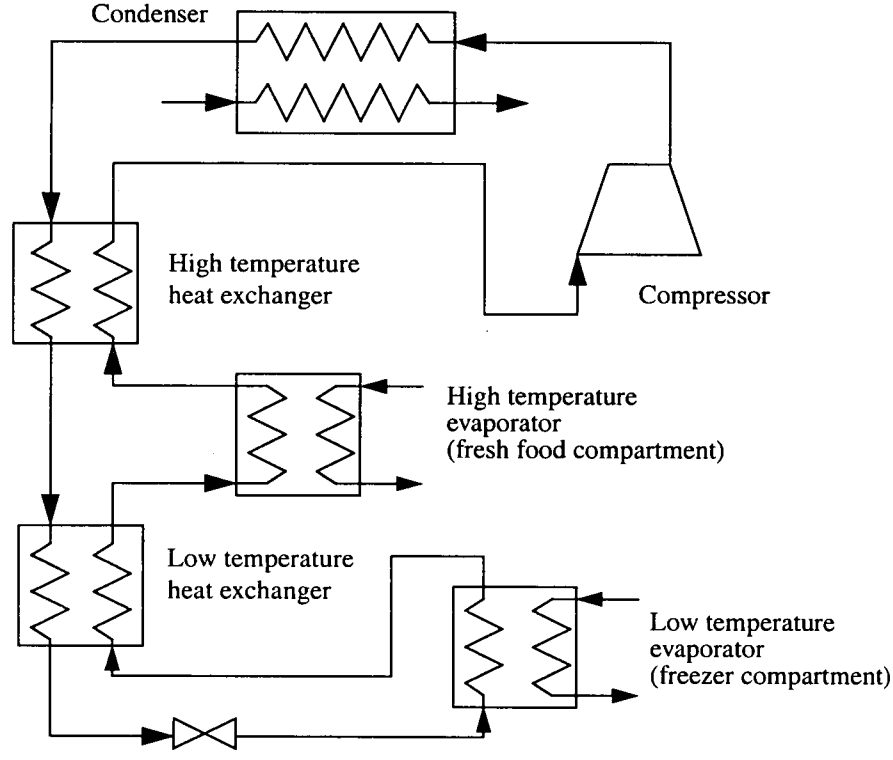

Figure 2.10: Lorenz Meutzner cycle

Preliminary tests with an R11/R12 mixture showed increased COP near the more volatile component (R11). A 50/50 wt.% R22/R11 mixture was then tested on a domestic refrigerating circuit which used two regenerative heat exchangers and two evaporators (i.e. a fresh food compartment and a freezer compartment, Figure 2.10). Liquid leaving the condenser is subcooled by vapour entering the compressor. The liquid is then further subcooled in the second regenerative heat exchanger. The heat is removed by a vapour liquid mix leaving the first evaporator. The circuit was operated at ambient temperatures of 32, 25, 16 and -10°C. Power savings of up to 20% compared to pure R12 were noted. The article did not detail at what ambient temperature this occurred. The circuit displayed excellent control performance. The cooling in the freezer compartment was found to be very stable and independent of the ambient temperature.

2.4.5 Patents

A number of patents relating to refrigerant mixtures have been granted. Most deal with mechanisms which regulate the load of a heat pump or refrigeration circuit at a constant evaporator or condenser temperature by changing the composition of the circulating working fluid. Etherington [*1958*] successfully patented a refrigeration cycle which incorporated a molecular sieve. This sieve preferentially absorbed R22 from an R22/R12 mixture. The sieve was placed in parallel with the compressor suction. The sieve acted as a storage buffer for R22. It releases or absorbs R22 as the cooling load varies. A number of cycles with a variable capacity have been patented by Vakil [*1979*] [*1981*] [*1983*]. These cycles consist of a mixed refrigerant working fluid being used in tandem with two or more accumulator tanks placed at strategic points in the refrigeration cycle. Each cycle is a variation of the other. As the required capacity changes, the composition of the circulating fluid changes so that a constant temperature in the evaporator is maintained.

2.4.6 Technical University of Hanover, Germany

Kruse [*1981*] experimentally examined the benefits of refrigerants on heat pump cycles. He noted that if heat pumps were to compete with conventional heating systems they must operate at as high a COP as possible and have good reliability. To meet these simultaneous demands he examined R22/R114 and R12/R114 mixtures. By correctly matching the temperature profiles, the heating COP could be increased. Reduced pressure levels would lead to longer life and greater reliability. In his experiments the maximum condenser refrigerant temperature was kept constant at 55°C and the evaporator minimum temperature was varied from -10°C to +5°C in steps of 5 degrees C. No indication of the external fluid temperature were given. The heating COP exhibited a maximum at 50% R22 with a COP approximately 25% higher than pure R22 alone. Increased addition of R114 to R22 lead to reduced pressure ratios and hence extended component life. Similar experiments were carried out with an R12/R114 mixture under slightly different condenser and evaporator conditions. This mixture showed a flatter heating COP vs. composition curve. The largest increase with this mixture was 15% at a composition of 60% R114. With the R22/R114 mixture another set of experiments was carried out under fixed condenser heat sink temperatures, namely water increasing from 45°C to 55°C. Three blends were examined as well as pure R22 and pure R12. The 79.1%/20.9% mixture showed the highest COP whilst R12 had the highest capacity. The addition of R114 to R22 led to a reduction in the heating capacity.

2.4.7 Electricitè de France, Direction des Etudes et Recherches, France

The first industrial examination of a non-azeotropic mixture was undertaken by Blaise and co-workers [*1989*]. Using a ternary refrigerant mixture, whose components the authors did not specify, experiments were carried out on a heat pump which warmed

water from 58°C to 68°C in a meat salting factory. Ammonia was used as the heat source. The results for the ternary mixture were compared to pure R12. No serious technical problems occurred. The same oil was used and there were no problems in charging. The heating capacity increased by about 20% while there was a very small increase in heating COP (≈1.5%) due to a small temperature change in the heat source. The compressor isentropic efficiency did not change substantially. The condenser heat transfer coefficient was slightly higher for the ternary mixture. A leak test was conducted to examine changes in composition. With a 30% leak in total working fluid there was a small change in the composition of the components but not significant enough to alter the performance of the cycle.

2.4.8 Department of Mechanical Engineering, Seoul National University, Korea

Kim et al. [*1994*] carried out an in-depth study of the mixture R22/R142b. An experimental program and a computer simulation were undertaken. In the experimental analysis a heat pump cooled a water stream from 25°C to 10°C and rejected the heat to another stream heating it from 23°C to 33°C. The compressor speed and global mixture composition were both varied separately. The speed of the compressor was varied by changing the frequency of the input voltage. The composition was varied from pure R22 to pure 142b in steps of 20 wt.% R22. The temperature and pressure of the refrigerant was recorded at 13 locations inside the evaporator. This allowed an average value of the refrigerant heat transfer coefficient to be calculated. The authors initially presented graphs of evaporator heat load, evaporator pressure loss and average evaporator heat transfer coefficient vs. the compressor mass flowrate. The heat load increased almost linearly with mass flowrate with R22 rich mixtures being represented in the higher mass flowrates. Pressure loss and average heat transfer coefficient increased with mass flowrate but not as regularly on linearly as the evaporative load.

The data was analysed by examining those experimental runs whose (evaporative) cooling load was close to 2kW. The dependence of COP, pressure ratio, average evaporator refrigerant heat transfer coefficient ($\bar{h}$) and *overall* evaporator heat transfer coefficient (U) on composition were examined. At a composition of 60 wt.% R22, a 10% enhancement of COP compared to the COP of R22 was reported. The GTD of a 50./50 mol.% R22/R142b mixture is 16.4 degrees C while the temperature change in the evaporator was 15 degrees C hence there was quite a good matching of the profiles. The pressure ratio was found to decrease with increased R22 composition. The refrigerant heat transfer coefficient for the mixtures was smaller than that of the pure refrigerants. The plot of $\bar{h}$ vs. R22 composition displayed a trough-like profile with its minimum value at 60 wt.% R22. The plot of U vs. composition also displayed a similar profile but with a much smaller decrease. The decrease was less since the water side coefficient hardly changed. The authors attributed the increase in mixture COP to the fact that the degree of superheating in the evaporator was less for mixtures. The mixtures had smaller heat transfer coefficients and therefore a larger area was needed for the phase-change. They also noted reduced subcooling in the condenser. They claimed that reduced superheating in the evaporator and reduced subcooling in the condenser led to smaller differences between the average condensing and evaporating temperatures and hence smaller compressor pressure ratios.

A 2kW cooling load was considered by the simulation, with the R22/R142b pair. A water stream was cooled from 25°C to 10°C and the heat was rejected to water, increasing its temperature from 25°C to 40°C. As a result of information garnered from the experiments UA values, the degree of superheating in the evaporator (DSH) and the degree of subcooling in the condenser (DSC) were specified as parabolic functions of the working fluid composition. The minima of these functions were located at the 50:50 composition (by mass). Four different cases were simulated. For each case, the parabolic functions set DSH and DSC for the pure fluids to 20 and 10 degrees C respectively. Each case differed in the respect that at the 50/50 mixture the

minimum value of DSH and DSC were increased from 0 degrees C (i.e. no superheat nor subcooling) to the values of the pure fluids, mentioned above. The composition was also varied from pure R22 to pure R142b for each case. COP was plotted as a function of composition for the four situations considered. When DSH and DSC were set to 0 for the 50/50 composition (case 1) the mixture COP exhibited a maximum increase of 20% compared to pure R22, at a composition of around 70 wt.% R22. The temperature change for both the sink and source was 15 degrees C which is close to the GTD of R22/R1422b (16.4 degrees C). Consequently there is a good match and an improvement in mixture COP. As DSH and DSC for the mixtures increased, the mixture enhancement of COP decreased. For Case 4, when DSH and DSC for the 50/50 composition were set to the values of the pure fluids, the COP-composition curve showed a trough-like profile with the 50/50 mixture displaying approximately a 19% decrease in COP. For the mixture R22/R142b the increase in DSH and DSC results in a divergence of average refrigerant temperature in the evaporator and condenser. This divergence leads to higher pressure ratios and reduced COPs. From these results, Kim et al. concluded that reduction in evaporator superheat and condenser subcooling with mixed refrigerants led to increased COPs. However Kim et al. should have pointed out that these results are only specific to the mixture R22/R142 since its GTD was similar to the temperature change of the heat source and sink. For a mixture whose GTD is around 3-5 degrees C then increased values of DSH and DSC may *improve* mixture COP since a better matching of temperature changes would occur as DSH and DSC were increased.

2.4.9 Institut für Verharens - und Kältetechnik, ETH Zürich, Switzerland

Another recent examination of refrigerant mixtures includes work conducted by Trepp et al. [*1992*]. The performance of various compositions of R22/R142b were compared to R22/R114 and R22/R12 mixtures. The dew point in the condenser was

fixed at 40°C and the start of vaporisation in the evaporator was set at 0, -5 and -10°C. The authors did acknowledge that ideally it would have been more meaningful to have equal external conditions. However, this can be very difficult to achieve with a fixed installation. (The author of this thesis can empathise with this attitude). Heat was removed from a water/glycol mix and rejected to a water sink. System parameters such as suction pressure and pressure ratio were plotted against composition for each mixture. For the R22/R142b mixture refrigeration capacity increased with increased R142b composition. The capacities were greater than that for R12. COPs for mixtures showed a small maximum at around 70% R22. It is interesting to note that the pressure ratio exhibited a minimum near the concentration range where the COP showed a maximum. Trepp concluded that, with appropriate matching of temperatures, power savings are possible and he proposed that mixtures or R22/ R142b with compositions of 50%-70% R22 could replace R12 in industrial use.

2.4.10 National Institute of Science and Technology (formerly National Bureau of Standards), U.S.A.

A considerable body of work has been published by N.I.S.T. on various aspects of mixtures of refrigerants. Extensive experimental and modelling work has been completed. Mulroy et al. [*1988*] examined two mixtures in an air conditioning unit; namely R22/R114 and R13/R12. Water was cooled from 26.7°C to 12.8°C in the evaporator and a further water stream was heated from 27.8°C to 47.2°C in the condenser. The capacity of the air conditioner was kept constant for each test run. Refrigerant pressures and temperatures and compressor speed were varied to meet the listed conditions. By inserting thermocouples in the wall of the evaporator the temperature profiles of the phase change could be determined and their effect on COP could be deduced. The best mixture was R22/R114 and its COP was found to be 32% higher COP than that for pure R22. The corresponding increase for R12/R13 was 16%. The authors found that the best improvement in COP occurred when the

refrigerant evaporator temperature glide closely matched that of the heat source and where the refrigerant profile exhibited a high degree of linearity. Large pressure drops and non linear temperature profiles in the heat exchangers can lead to pinch points which limit the refrigerant's ability to utilize the exchangers effectively.

The effects of a liquid suction heat exchanger (LSHX) were examined. The liquid from the condenser is subcooled by the vapour leaving the evaporator. This has the effect of reducing the vapour quality after expansion.

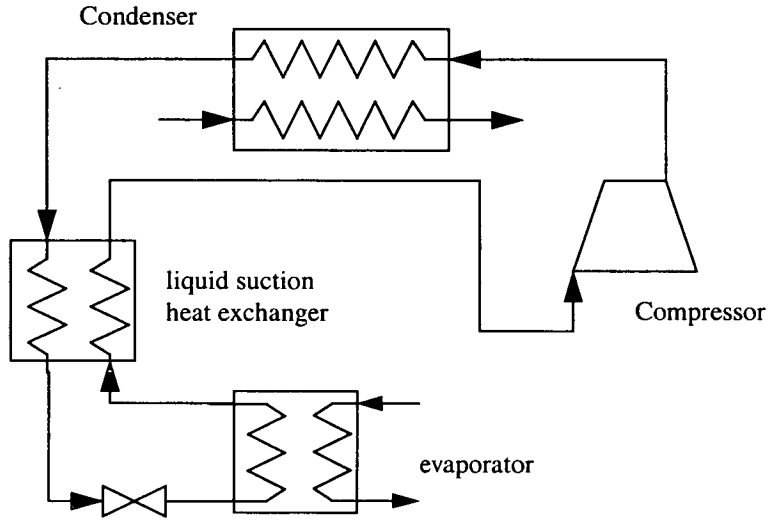

Figure 2.11: Refrigeration cycle with liquid-suction heat exchanger

The proportion of liquid available for evaporation is greater at the expense of an increased inlet temperature to the compressor and a consequent increased discharged temperature. Such an arrangement is shown in Figure 2.11. With the R13/R12 mix there was a dramatic improvement in COP; but there was little effect on the R22/R114 mix. The authors attributed this to the fact that subcooling of the condenser liquid did not lead to an increased evaporator pressure in the case of R22/R144.

Pannock et al. [*1992*] conducted a study on 15 different HFC mixtures using the CYCLE-11 computer model, developed by Domanski and McLinden (Section 2.5.3 on page 44). All possible binary combinations of R23, R32, R125, R134a, R143a and R152a were examined. Air was used in the heat source and sink streams. Specified inlet and outlet source and sink stream temperatures were kept constant. Each mixture was simulated at four different operating conditions at 5 wt.% intervals in composition. The COP and volumetric capacity were compared to those for R22. Only the pairs R32/R134a and R32/R152a showed a better performance than pure R22. On the basis of these results, these two mixtures were selected to be tested experimentally in a heat pump. The tests were conducted at the same capacity as R22 in order to draw meaningful conclusions. The compositions ranges were changed on the basis of giving the same volumetric capacity as R22. At low R32 compositions, and without an LSHX, the R32/R152a mixture exhibited the better performance. For mixtures consisting of at least 35% R32, then the R32/R134a has an equivalent if not better performance than R32/R152a. An LSHX improves the efficiency of the R32/ R134a much more than R32/R152a. COP improvements, compared to R22, varied from the same to an enhancement of 24% depending on the test. UA values for both these HFC mixtures were greater than those for R22, in the condenser. In the evaporator the UA values were similar. The authors concluded that the mixture R32/ R134a should be used in conjunction with an LSHX and with a R32 content no higher than 35%. This would have similar if not better performance than R22 and would reduce the flammability risk posed by R32.

The effect of temperature profiles on refrigeration cycle performance was studied both experimentally [*Mulroy et al. 1994*], and through a computer simulation [*Domanski et al. 1994b*]. They postulated that a non linear temperature profile of a binary fluid undergoing a phase change could be avoided by addition of a third component, whose boiling point was midway between the two components. If the profile in the evaporator or condenser is non-linear then a pinch point can occur. A mixture of R23/ R142b was used because it has a large temperature glide. R22 was selected as the

intermediate component. The experiments were carried on the same equipment as used previously by Mulroy et al. [*1988*]. The same test conditions were used. The tests indicated that adding R23 to R142b improved cooling COP by 28%. This occurred at an evaporator glide of 8 degrees C. A 22% enhancement of COP occurred when R142b was added to R22. This occurred at a glide of 12 degrees C. The ternary R23/R22/R142b mixture resulted in COPs 28% greater than pure R22. This had the highest COP of all of the tests. It is interesting to note that this occurred at a glide of 13.0 degrees which is quite close to the evaporator water temperature drop of 13.8 degrees C. Examination of the ternary mixture's temperature profile showed small temperature differences, good linear behaviour and well matched profiles. The authors demonstrated the need to have good linearity *as well as* good matching to improve efficiencies. The profile for an R23/R142b mixture exhibited a concave pattern. This resulted in a pinch in the middle of the evaporator which limits COP improvement. Although the pair R22/R142b displayed a linear profile, the glide was not large enough and this resulted in a pinch at the evaporator inlet. The benefits of adding a third component to improve the temperature profile were demonstrated.

The results of these experiments were compared against the refrigeration cycle simulation model CYCLE-11 developed by Domanski and McLinden ([*1992*], Section 2.5.3 on page 44). This model performs an analysis of a refrigeration cycle given the inlet and outlet temperatures of the external fluids. It models the heat exchangers by subdividing them into 128 areas of equal enthalpy change. The thermodynamic properties are calculated by the Carnahan-Starling-DeSantis (CSD) equation of state (Section 2.7.4 on page 62). The same external fluid temperatures as in the experimental trials were used. Predicted COP improvements occurred at temperature glides very similar to the results of the experiments. Calculated temperature profiles displayed patterns were in agreement with those determined by experiment. The concave pattern of the 4/96 wt.% R23/R142b was predicted by the model. The simulation also verified the linearisation of the temperature profile of R23/R142b by addition of R22.

Didion and Bivens [*1990*] published an excellent article on how refrigerant mixtures could provide solutions as alternatives to CFCs. They classified mixed refrigerants into three categories: azeotropes, near azeotropes and zeotropes. They pointed out that azeotropes have been used with success in the past but that there was a slim chance of finding new ones to meet all the given requirements, including the recent environmental criteria. Near azeotropes offer the same properties as azeotropes but with a much wider selection choice. Possibilities of refrigerant composition changing due to leaks were examined. They concluded that the problem of composition change was exaggerated. Zeotropes offered improvements in energy benefits. However the authors noted that they may require hardware changes since counterflow heat exchangers are needed. Growing concern with greenhouse warming, and the subsequent demands for greater energy efficiency means that zeotropes will be a part of the refrigeration industry in the future. A few years later in a similar article, Didion [*1994*] confirmed his forecast that zeotropes would be used by the refrigeration industry, although not necessarily indefinitely. The current multitude of transition fluids gives the industry experience with mixtures. If energy gains obtained through better matching of temperature glides were of sufficient significance, then production of zeotropic refrigeration equipment may occur. Further research into wide boiling zeotropes was recommended.

2.5 Simulation Studies

The proliferation of reasonably cheap, fast and powerful computing facilities meant that a large proportion of the research into mixtures of refrigerants could be done by modelling. Computer models have the advantage of flexibility. Many more parameters and conditions can be investigated in a much shorter time compared to an actual experimental program. The removal of the trauma of having to design, construct, troubleshoot and operate an experimental plant is also an added bonus, although

considerable time has to be invested in learning the necessary skills to adequately write a simulation program. There is also the question as to how accurate a particular model represents a real refrigeration cycle. In order to take account of all irreversibilities, models can become quite complex.

2.5.1 Department of Mechanical Engineering, University of Illinois, U.S.A.

Stoecker and Walukas [*1981*] published an analysis of refrigeration cycles charged with refrigerant mixtures. A simple cycle using an R12/R114 mixture was initially modelled. The cycle was then examined with a liquid suction heat exchanger and finally a two evaporator cycle as used by Lorenz and Meutzner [*1975*] was simulated. The authors outlined the difficulty in comparing data from pure and mixture cycles. They concluded that the refrigeration capacity would have to be kept constant as a basis for making comparisons. In their analysis the external fluid temperatures were specified as well as the cooling load. The condenser and evaporator UA values were also specified. This was in broad agreement with the method of comparison recommended by McLinden et al. [*1987*]. Simple correlations were used to calculate thermodynamic properties rather than an equation of state approach. Equilibrium was calculated on the basis of Raoult's Law. The composition of R114 was varied from 0 to 60% in 20% intervals. Results for the simple cycle showed a maximum decrease in power requirement of 7.2% at 40% R114. The addition of a liquid-suction heat exchanger lead to an 11.4% decrease in power consumption as compared to pure R12 at a 50% R114 composition. The two-evaporator cycle exhibited a decrease in power consumption of 12%. Although the model was not very rigorous, it demonstrated that efficiency gains could be made with mixtures.

2.5.2 Department of Mechanical Engineering, University of Maryland, U.S.A.

A model of a single evaporator refrigerator cycle (called SERCLE) was developed by Jung and Radermacher [*1991a*]. The model was based on the criteria recommended by McLinden et al. [*1987*] for comparing pure and mixed cycles. The cooling load, external temperatures and heat exchanger size were specified by the investigators. The heat exchanger sizes were specified by setting the product of the heat transfer coefficient and the area (the UA value). Log mean temperature differences were calculated on the basis of the inlet and outlet temperatures of the heat exchangers. Although pressure drops were accounted for, the values were specified rather than calculated from correlations. The Carnahan-Starling-DeSantis equation of state [*DeSantis et al 1976*] was used to calculate thermodynamic data. The simulation was carried out to find a drop in replacement for R12 in domestic refrigerators. Initially 15 pure refrigerants were examined. No pure refrigerant could match R12 for specific capacity and COP. R32 and R152a had comparable COPs. Attention then focused on non-azeotropic refrigerant mixtures (or NARMS for short). Twenty one binary mixtures were selected on the basis of sufficiently large temperature glides to boost COP, as well as the pure components having relatively large COPs. Each mixture was simulated across the entire composition range. Most of the mixtures involved a HFC and a HCFC. COPs and specific capacities relative to R12 were listed. The maximum increase in COP for any mixture was 5%. Large increases were not observed because the heat sink air temperature drop was relatively small (10 degrees C). The mixtures with the largest increase were R32/R142b and R22/R142b. R32/R152a and R32/R134a were the HFC mixtures that exhibited the best improvement (1.38% and 1.35% improvement respectively). These have the largest glides of the HFCs. It was suggested that more efficient heat exchangers would lead to improved energy efficiency. The model was ran with a higher UA value for the R22/R142b mixture. Improvements of 20-25% in the COP were realised. The authors recommended that attention should focus on improving heat exchanger efficiency.

The SERCLE model was upgraded by Jung and Radermacher [*1991b*] to model a (domestic) two evaporator refrigerator cycle (called TERCLE), similar to Lorentz and Meutzner's cycle (Figure 2.10 on page 30). As with the single evaporator simulations, pure refrigerants were examined first. With pure fluids COPs increased by 6-15% as a result of having a portion of the evaporator load at a higher temperature. Again no pure fluid could replace R12 without system modification, especially the compressor. With mixtures, increases of 6-18% in COP as compared to pure R12 were recorded. Mixtures with relatively large glides were selected. The air side temperature drop (23 degrees C) was larger than that for the single evaporator model. Good temperature profile matching promoted COP improvements. The best mixtures were R22/R123 and R32/R142b. The best HFC mixture was R32/R152a with an 8.9% improvement. The authors then examined how the ratio of the evaporator areas affected performance. They found that the COP was maximised when the evaporator area ratio was close to the fraction of the load of the higher temperature evaporator. These studies showed that there are modest gains to be achieved in energy efficiency with the use of mixtures. The two models did have some shortcomings. Temperature-enthalpy profiles were assumed to be linear in the heat exchangers. This does occur for some mixtures but not all. Some mixture exhibit curved temperature-enthalpy profiles during condensation and evaporation. (Figure 5.2 on page 142). Pressure drops and heat transfer coefficients were not calculated but specified. The disadvantage of calculating these from correlations is that the results are only valid for a specific type of equipment since correlations for pressure drop and heat transfer depend on system geometry. Nevertheless these studies provided a valuable insight into likely COP benefits of HFC mixtures.

2.5.3 National Institute for Science and Technology (N.I.S.T.), U.S.A.

Domanski [*1986*] developed a rigorous model of a residential heat pump which provided summer cooling and winter heating. The model (HPBI) took into account all the major irreversibilities. It was a development of an earlier model (HPSIM) used and verified by Domanski [*1983*]. Heat losses in the hermetic compressor to the motor windings and valve movements were considered. The pressure drop was modelled using two phase flow theory. The capillary tube, used to expand the working fluid, was also rigorously simulated. The CSD equation of state supplied thermodynamic property data. The model was verified by running an air to air heat pump in two heating and two cooling modes. The working fluid used by the model and in the experiments was a 65/35 wt.% R13B1/R152a mixture. There was good agreement between the model and the experiment on the major parameters. An analysis of the effect of heat transfer coefficients and the pressure drop on the COP was conducted. COP varied by 5-6% when the heat transfer coefficients were varied by 50%. A 50% variation in pressure drop affected a change of less than 1% on the COP.

Domanski et al. [*1992*] used their CYCLE-11 model to simulate a domestic refrigerator. The model is an improvement on the CYCLE-7 model which was used by McLinden et al. [*1987*] to examine how pure and mixed cycles should be compared (Section 2.3.1 on page 21). Compressor heat losses were taken into account. The condenser was divided into three regimes, comprising two phase, superheating and subcooling flow. The two phase flow regime was further subdivided, and a weighted average log mean temperature difference was calculated according to the distribution of the heat transferred in each subsection. Pressure drop was assumed proportional to heat load of each section. The model had three options for modelling the compressor: (1) isentropic process, (2) polytropic process and (3) either of these with an inclusion of a volumetric efficiency. The model calculates temperature differences in the heat exchangers and iterates until these meet the specified values

within a certain tolerance. The CSD equation of state provided the thermodynamic data.

In their tests the authors simulated a domestic refrigerator cooling an air stream from 21.7°C to 17.8°C and heating up another air stream from 32.2°C to 37.8°C. The evaporator average effective temperature difference was specified as 6.2°C, while the corresponding temperature difference for the condenser was 12.0°C. Four fluids were examined (relative to R12): R134, R134a, a 63%/37% R22/R142b mixture and a 38%/62% R22/R152a mixture. Three different models of the refrigeration cycle were simulated. The first was a purely theoretical model which assumed no losses in the compressor; the second assumed a polytropic process with a specified polytropic efficiency of 0.85; a liquid-suction heat exchanger was also included. The final model was that of a real refrigerator which accounted for heating losses in the compressor. Results were expressed relative R12. For the theoretical cycle R134a and R134 had lower COPs than R12 but were higher for the real refrigerator cycle. Mixtures had better COPs than R12 with the theoretical cycle, but in the real refrigerator cycle the COPs were very similar to R12. The mixtures had better specific capacities than R12 for all three cycles while R134a and R134 had reduced capacities. A further set of tests were undertaken to examine the effects of neglecting the effects of the temperature-enthalpy non-linearities in the heat exchangers. Using an R22/R23 mixture, (because of its large GTD) the model overpredicted COP by 8.7% at 20% R22. With this test it is important to model the heat exchangers correctly if a realistic simulation is to be achieved.

2.5.4 Department of Mechanical Engineering, Saga University, Japan

Miyara and co-workers [*1992*] published results from two simulations carried out at Saga University, Japan. The first was a simple model of a heat pump cycle. It was later

modified to take account of heat transfer and the effects of pressure drop [*Miyara et al. 1993*]. The Benedict Rubin Webb (BWR) equation of state provided the refrigerant thermodynamic data. The refrigerant pair used in both models was R22/R114. The compression process was assumed to be isentropic in both cases. In the first model the UA values of the condenser and evaporator were prescribed. The second model assumed the heat exchangers were of the double pipe variety and heat transfer coefficients and pressure drops were calculated from correlations.

The condenser heating load external fluid temperatures and flowrates were specified in the first model. Thus it satisfies McLinden's criterion for comparing pure and mixed refrigerants. A heating load of 2 kW was specified. The heat sink inlet temperature was 40°C and the heat source inlet temperature was set at 30°C. Three values of UA were selected (100, 200 and 300 WK^{-1}). For each UA value, three values of the heat source and sink fluid temperature change (ΔT_s) were specified (0, 10 and 20 degrees K). For each value of UA and ΔT_s, the composition was varied from pure R114 to pure R22. The heating COP was plotted as a function of composition for each value of UA with ΔT_s as a parameter. In each plot the heating COP decreased as ΔT_s increased. With ΔT_s = 20 degrees K, there was an improvement in mixture COP as the value of UA rose. As UA increased a more pronounced maximum near the equimolar point occurred. The opposite happened when ΔT_s was set to zero. A minimum in the COP-composition curve resulted as UA was increased. The authors noted that the degree of improvement in mixture heating COP, is larger when the heat transfer fluids' temperature change are large and when the UA value is large. The improvement is greater when the temperature glide of the working fluid is similar to the temperature change of the heat transfer fluids.

In the second model the values for the overall heat transfer coefficient were calculated. Experimental temperature profiles were compared to those predicted and good agreement was shown for a 76 mol.% R22/R114 mixture. The heat load was again set to 2 kW and the inlet source and sink temperatures were set at 20°C and 30°C

respectively. With these conditions COP seemed independent of composition while the overall heat transfer coefficients did change with composition. These parameters were graphically shown with and without the effect of pressure drop. The effect of pressure drop reduced COP and evaporator heat transfer coefficient, but not by any substantial amount. In a second simulation the same external temperatures were specified but the model was adjusted so that the inlet condensation and evaporation temperatures were fixed. As McLinden pointed out, this can lead to an unfair comparison for the pure refrigerants and unsurprisingly the result, showed a pronounced COP maximum at the 50/50 composition point which was 60% higher than that for pure R22. This is one of the largest increases in COP found in this literature study. COP was also plotted against composition with evaporator and condenser tube length set as a parameter. COP increased with longer tube length. As tube length increased a slight maximum appeared at 60 mol% R22.

2.5.5 Centre de Recherche Industrielle du Quebec, Canada

Parent and Larue [*1989*] compared the results of their heat pump model with experimental values obtained from a 15kW heat pump, using groundwater as the heat source. The model used the CSD equation of state to supply thermodycnamic data on the working fluids. Agreement within 6% for thermodynamic state predictions was claimed. Refrigerants tested included 74/26 wt.% R13B1/R152a, 80/20 wt.% R22/ R114 and a 12.5/87.5 wt.% R23/R22 mixture. The authors found the same accuracy for COP, refrigerant mass flow, and heating capacity although no specific results were published in this article.

2.5.6 Department of Chemical Engineering, University of Leeds, U.K.

Haselden and Chen developed a simulation and design model for an air conditioning unit [1994]. The model accepted air inlet and outlet temperatures and flowrates. It then calculated heat loads, heat exchanger areas and heating COPs. Pressure drops were specified as well as the compressor isentropic efficiency. Pure and mixed refrigerants were compared on the basis of minimum temperature pinches in the evaporator and condenser. Högberg et al. (Section 2.3.2 on page 25) recommended that such a basis of comparison should be avoided since they are on the basis of different areas. In fact the evaporator and condenser areas were displayed as functions of mixture composition. The model used the Redlich-Kwong-Soave (RKS) equation of state to calculate the necessary thermodynamic properties. The thermodynamic data yielded by the RKS equation of state was checked against experimental data for a 55 wt.% R22/R142b mixture. The deviation was less than 1%. With this pair of refrigerants the composition was varied in intervals of 0.1 weight fraction. The model cooled 0.95 m^3s^{-1} of air from 26.7°C to 13.3°C and rejected the heat to an air stream at 35.5°C with a flowrate of 1.25 m^3s^{-1}. The model was simulated with three values for the condenser minimum pinch (1.0, 6.5,and 10.0 degrees C) and three values for the evaporator pinch point (1.0, 5.0 and 10.0 degrees C). For all values of pinch point, the COP showed a maximum at 50 wt.% R22. With a prescribed condenser pinch of 6.5°C the increase in COP was 35%; at a pinch of 10.0°C the COP enhancement was 22%. Evaporator and condenser fin areas also showed a maximum at the midpoint of composition. The results here showed substantial power savings by using mixtures at the expense of increased heat exchanger area. These power savings are some of the largest found in this literature survey. The authors suggested that the optimum design need to take into account capital and operating costs.

Bensafi et al. [*1993*] experimentally examined 50/50 wt.% R22/R142b mixture in an air conditioning unit. An air stream at 27°C was cooled to 14°C with a design duty of

18.7kW. Pure R22 was compared to a the R22/R142b mixture. Power savings of 25% were achieved for the mixture. This particular unit was modelled and various blends of HCFCs and HFCs were applied as working fluids. Heat transfer UA values were prescribed in the model. Binary, ternary and quaternary mixtures were studied as well. A 35/65 wt.% R32/R134a mixture had a 14% improvement in COP compared to R22. With addition of extra heat exchanger area this rose to 32%. Power savings with an R32/R134a were described as disappointing although it could be improved with the addition of more heat transfer surface. A ternary mixture seem to be marginally disadvantageous. The addition of a fourth component straightened the temperature-enthalpy profile hence the best mixture was 10/15/15/60 wt.% quaternary mixture of R23, R32, R125 and R134a.

2.6 Summary of Published Research Work

Different authors use different bases of comparison and different operating conditions in comparing pure and mixed fluid cycles. Consequently comparing results from different authors can be somewhat difficult. In order to facilitate comparison between the various investigators a tabulated summary of the work of each author is given in Table 2.1 to Table 2.5. Listed in each row are: the name and year of each investigator; the mixtures examined; GTD of a 50/50 mole fraction of each mixture (as calculated by the Carnahan-Starling-DeSantis equation of state at 1 bar a); identification of sink and source streams and their temperatures; basis of comparing pure and mixed refrigerants used by each investigator; and significant results i.e. increase (or decrease) in COP. For the publications of McLinden et al. [*1987*], Högberg et al. [*1993*], Miyara et al [*1992*] and the simulation of Kim et al. [*1992*] the percentage change in COP due to mixtures was calculated from graphs presented in the article rather than quoted directly from the publication. Table 2.1 and Table 2.2 list the experimental treatment of mixed refrigerants whilst Table 2.3 and Table 2.4

summarise simulation studies. Some authors have completed experimental and simulation studies together so these are listed separately. Refrigerant mixtures marked with an asterix indicate that the composition was varied. (Note: for the hydrocarbon mixtures of Carr [*1949*] and Haselden et al. [*1958*] the Redlich-Kwong-Soave equation of state in conjunction with the Wilson activity model was used to calculate the GTD).

There has been some extensive research into the field of refrigerant mixtures with the intention of increasing energy efficiency. Most of the investigations used CFC and HCFC mixtures as working fluids rather than HFCs. Recently however, the focus has shifted onto HFCs and other non ozone depleting refrigerants. Specifically Pannock et al. [*1992*], Jung et al. [*1991a, 1991b*] and Bensafi et al. [*1993*] used HFC mixtures in their work. For HFC mixtures increases in efficiency have been modest rather than spectacular. COP increases generally fell in the range -2.5% to 24%. Pannock and Jung found that R32/R134a and R32/R152a were found to be the best performing HFC mixtures. These have the largest GTDs of the HFC mixtures examined. CFC and HCFC mixtures tend to have larger GTDs than HFC mixtures. R22/R114 and R22/ R142b have relatively large GTDs (19.4 and 16.4 degrees C respectively) and both mixtures have been used in a number of studies. With CFCs and HCFCs the improvement in COP tends to fall in the range -5.1% to 35%, with the exception of Miyara et al. [*1993*]. They found an increase of 60% in mixture COP for R22/R114 over the COP of pure R22. However they did specify the temperature at which evaporation and condensation began, which ran counter to the recommendation of McLinden et al. [*1987*]. The results from the literature suggests that improvements in cycle efficiency can be achieved by the use of mixtures rather than pure fluids. However, this depends on how well the temperatures are matched. COP increases tend to be larger when large refrigerant glides and large external fluid glides occur. The work of McLinden et al. [*1987*], Mulroy et al. [*1988*], Kim et al. [*1994*] and Miyara et al. [*1992*] would indicate that matching GTDs and heat source and sink temperature changes lead to increases in COP in the range 10-30%.

In the following chapters investigative work into improvements in refrigeration COP through the application of HFC refrigerant mixtures is described. The R32/R134a pair was examined in an experimental refrigeration cycle previously used by Low. Amongst HFC mixtures, it has a relatively high gliding temperature difference and thus has potential to improve the COP. The experimental apparatus used by Low was substantially modified for this mixture and these changes are described in the next chapter. The results attained in the experimental program are reported and discussed in Chapter 4. As well as experimentally investigating the R32/R134a mixture a simulation of a simple refrigeration cycle was undertaken. Six HFC pairs were examined for their ability to increase the COP beyond what can be achieved with pure working fluids. Cycle parameters were varied to determine those conditions where improvements in mixture COP are greater.

Table 2.1: Summary of literature review of experimental treatment of refrigerant mixtures

Author and Year	Refrigerants	GTD (deg. C)	Heat Source and Sink Temps.	Basis of Comparison	Results
Carr 1949	37/32/31 mol.% $C_2H_6/C_3H_8/C_4H_{10}$	44.9 (80.0 deg. F)	Source: Unspecified liquid 55→ −30°F Sink: water 65→100°F	Evap. LMTD = 20.0°F Cond. LMTD = 20.8°F	71% power of NH_3
Haselden 1958	Propane/n-butane*	15.6 (28.1 deg. F)	Source: water 70→45°F Sink: water 80→105°F	Not given	7% power saving compared to pure n-butane
McHarness 1961	R13B1/R12* R12/R22* R13B1/R22*	0.4 1.4 3.0	Source: R11 Sink: water	Evap. temp.: -20, -10,-40°F Cond. temp.: 110°F	5% increase in COP for R13B1/R12
Arora 1967	R22/R114*	19.4	Not given	Evap. temp.: 0, -5, -10, -15, -20, -25°C	13.8% increase in COP

Table 2.2: Summary of literature review of experimental treatment of refrigerant mixtures (continued)

Author and Year	Refrigerants	GTD (deg. C)	Heat Source and Sink Temps.	Basis of Comparison	Results
Lorenz 1975	50/50 wt.% R22/R12	1.4	Sink: air 32, 25, 16, -10°C	Ambient air temperature	20% power saving compared to R12
Kruse 1981	R22/R114*	19.4	Not given	Evap. temp.: +5, 0, -5, -10°C Cond. temp.: 55°C	25% increase in COP
	R12/R114*	10.3	Not given	Evap. temp.: +10, 0, -10°C Cond. temp.: 50°C	15% increase in COP
Mulroy 1988	R22/R114* R13/R12*	19.4 25.8	Source: water 26.7→12.8°C Sink: water 27.8→47.2°C	Equal HTFs temps and equal capacity	32% & 16% increase in COP for R22/R114 &R13/R12 resp.
Blaise 1989	Unspecified	N/A	Source: NH_3 10.0→12.5 bar Sink: water 58.0→68.0°C	Equal heat source pressure	20% increase in capacity
Trepp 1992	R22/R142b* R22/R114* R22/R12	16.4 19.4 1.4	Source: water/ glycol mix Sink: water	Inlet evap. temp.: 0,-5, -10°C Cond. dewpoint: 40°C	8-16% increase in COP
Pannock 1992a	R32/R134a R32/R152a	7.7 8.8	Source and Sink: water/glycol Four separate temperature configurations	Equal HTF temps. and equal capacity	0-24% improvement compared to COP of R22
Mulroy 1994	R23/R142b* R22/R142b* and ternary mixtures of R23, R22 & R142b	63.5 16.4	Source: water 26.7→12.8°C Sink: water 27.8→47.2°C	Equal HTF temps.	28% increase in COP (R23/ R142) 22% increase in COP (R22/ R142b)
Kim 1994	R22/R142b*	16.4	Source: water 25.0→10.0°C Sink: water 23.0→33.0°C	Equal capacity 2kW & compressor speed	10% increase in COP

Table 2.3: Summary of literature on refrigerant mixture simulation studies

Author and Year	Refrigerants	GTD (deg. C)	Heat Source and Sink Temps.	Basis of Comparison	Results
Stoecker 1981	R12/R114	10.3	Single evap.: Source: air -15→-25°C Sink: air 25→32°C Double evap. Low temp. Source: air -20→-25°C	Equal HTFs, equal evap. loads and equal UA values Single evap. load = 0.2kW Double evap. loads = 0.2kW & 0.1kW	Simple cycle: 7.2% decrease in compressor power Simple with LSHX: 11.4% decrease Two evap. cycle: 12% decrease
Domanski 1986	65/35 wt.% R13B1/R152a	0.4	Indoor and outdoor air temps. depending on mode:	N/A	Model compared well to actuality
McLinden 1987	R22/R114* R12/R11*	19.4 23.5	Source: -5→-15°C & -5→-30°C Sink: 35→45°C & 20→45°C (respectively)	Equal HTF temps and equal value of UA_{tot}/Q_c	27% & 22% increase in COP for R22/R114 & R22/R11 resp., both with large HTF ΔT
Parent 1989	R13B1/R152a R22/R114 R22/R23	0.4 19.4 25.7	Source: water/ glycol mix Sink: air	Evap. capacity: 15 kW	Model verified with experimental results
Jung 1991a	15 pure & 21 mixtures* of HFCs and HCFCs		Source: air -11→-18°C Sink: air 32.2°C	Equal HTF temps; Q_e = 185 W; $UA_E = 20 W°C^{-1}$; $UA_C = 10 W°C^{-1}$	-2.5 to +5% increase in COP compared to R12
Jung 1991b	15 pure & 21 mixtures* of HFCs and HCFCs		Source 1: air 5→0°C Source 2: air -12→-18°C Sink: air 32°C	Equal HTF temps; Q_e = 185 W; $UA_E = 20 W°C^{-1}$; $UA_C = 10 W°C^{-1}$	6-18% increase in COP compared to R12
Domanski 1992	R12, R134a, R134, R22/R142b R22/R152a	16.4 3.0	Source: air 21.7→17.8°C Sink: air 32.2→37.8°C	Equal HTF temps.	Mixture COP ≈ R12 COP

Table 2.4: Summary of literature on refrigerant mixture simulation studies (continued.)

Author and Year	Refrigerants	GTD (deg. C)	Heat Source and Sink Temps.	Basis of Comparison	Results
Pannock 1992	Blends of R23, R32, R125, R134a, R143a & R152a		Source and sink: air Four different temperature configurations	Equal HTF temps.	R32/R134a and R32/R152a had better performance than R22
Miyara 1992	R22/R114*	19.4	Source: water 30→30, 20, 10°C Sink: water 40→40, 50, 60°C	Equal HTF temps. and equal cond. load = 2kW	20% Increase in COP for large glides & matched profiles
Miyara 1993	R22/R114*	19.4	Source: water 20°C Sink: water 30°C	Equal HTF inlet temps & flows; equal inlet cond. and evap. temps; cond. load = 2kW	60% increase in COP
Högberg 1993	R22/R114* R22/R142b*	19.4 16.4	Source: water 15→10°C & 15→0°C Sink: water 60→65°C & 50→65°C resp.	Equal min. pinch points; equal ΔT_{LMTD}; equal areas	R22/R142b: 0-9% increase in COP R22/R114: -10 to +18% increase in COP
Bensafi 1993	R22/R142b and various blends of R23, R32, R134a & R125	16.4	Source: air 27→14°C Sink: air 35°C	Equal HTF temps. and equal evap. load (18.7kW)	Increases up to 14% in COP compared to R22
Haselden 1994	R22/R142b*	16.4	Source: air 26.7→13.3°C Sink: air 35.5°C	Equal HTF temps. & minimum approach temps. (evap.: 1, 6.5, 10 deg C; cond.: 1, 5 10 deg. C)	Increases up to 35% in COP

Table 2.5: Summary of literature on refrigerant mixture simulation studies (continued.)

Author and Year	Refrigerants	GTD (deg. C)	Heat Source and Sink Temps.	Basis of Comparison	Results
Kim 1994	R22/R142b*	16.4	Source: water 25.0→10.0°C Sink: water 25.0→40.0°C	Equal capacity 2kW & HTF temperatures	-19% to +20% increase in COP depending on superheating in evaporator and subcooling in condenser
Domanski 1994b	R23/R142b* R22/R142b* and ternary mixtures of R23, R22 & R142b	63.5 16.4	Source: water 26.7→12.8°C Sink: water 27.8→47.2°C	Equal HTF temps.	Predicted COPs compared with experimental results [*Mulroy et al. 1994*]. Addition of intermediate component to mixture improves COP

2.7 Equations of State Requiring Sparse Data

A computer model of a refrigeration cycle was developed to examine how HFC refrigerant mixtures can enhance the COP of a refrigeration cycle. Cycle perimeters were varied to determine what conditions mixed refrigerants improved COP. The model and its results are presented in Chapter 5. The Cubic Chain-of-Rotators equation of state was used to supply the necessary thermodynamic data needed by the model. The CCOR equation has the advantage of requiring a small amount of data on the fluid it describes. With the phasing out of CFC refrigerants it is advantageous to have a means of predicting the thermodynamic properties of new refrigerants from sparse data. Before applying the model the CCOR equation of state was examined for its suitability to predict the thermodynamic behaviour of HFC refrigerants. Calculated thermodynamic data was compared with published experimental data. Pure and mixed fluids were considered. Its predictions were also compared with the Carnahan-

Starling-DeSantis equation of state. This was used as a reference equation of state. It is more complex than the CCOR equation and theoretically it is more accurate. The investigation of the CCOR equation is detailed in Appendix B for pure fluids and in Appendix F for binary mixtures. In this section articles in the literature pertaining to the CCOR and CSD equations of state are reviewed. A brief description of the equations, and the assumptions behind them is given. This section is intended to run parallel with Appendix B, Appendix F and Section 5.3 which summarises the findings of the examination of the CCOR equation. A brief review of the prediction of refrigerant thermodynamic properties using other equations of state is also given.

2.7.1 Commonly Used Equations of State

2.7.1.1 Ideal Gas

The simplest of all equations of state is the one that describes an ideal gas.

$$Z = \frac{PV}{nRT} = 1 \qquad \text{(Eq 2.1)}$$

where Z is the compressibility factor, P is the pressure, V the volume, n the number of moles, T the temperature and R is the universal gas Constant ($8.314 J mol^{-1} K^{-1}$). This equation is adequate in describing gases below a pressure of 1 atmosphere. As the pressure of a fluid approaches zero the fluids behaves in an ideal manner. At increasingly higher pressures significant deviations arise.

2.7.1.2 Van der Waals Equation of State

Van der Waals was the first worker to apply a cubic function to describe the behaviour of a fluid. An equation of state should be complex enough to describe both liquid and vapour properties but not so complex as to present analytical difficulties when used.

$$P = \frac{RT}{v-b} - \frac{a}{v^2} \qquad \text{(Eq 2.2)}$$

2.7.1.3 Redlich-Kwong-Soave Equation of State

A major improvement to the Van der Waals equation by Redlich and Kwong [*1949*]. The attractive force term was altered. This change yielded a much better accuracy in describing the vapour phase. However, description of the liquid phase was poor.

$$P = \frac{RT}{v-b} - \frac{a/T^{0.5}}{v(v+b)} \qquad \text{(Eq 2.3)}$$

The equation did not predict vapour liquid equilibrium very well. Soave [*1972*] refined the Redlich Kwong equation to remedy the situation. Thus the equation is commonly referred to as the Redlich-Kwong-Soave (RKS) equation of state. A strong temperature dependence in the attractive force term was introduced. As a result of this improvement the RKS equation is often used by industry to calculate the behaviour of multicomponent fluids. Numerous improvements and refinements have been made to the equation and publications continue today. The RKS equation is a three parameter equation of state since the critical temperature, the critical pressure and the acentric factor must be known.

2.7.1.4 Martin Hou Equation of State

In the refrigeration industry one of the most common equations of state is the Martin-Hou equation of state. It is more complex than either the RKS or Peng-Robinson (PR) equations. Usually it is used to describe pure refrigerants only. Mixing rules for each of the seventeen parameters would have to be provided if it were used for mixtures. Very often the terms A_4, B_4 and C_4 are set to zero. It has the form:

$$P = \frac{RT}{V-b} + \sum_{i=0}^{3} \frac{A_i + B_i T + C_i e^{-(KT)/T_r}}{(V-b)^{i+2}} + \frac{A_4 + B_4 T + C_4 e^{-(KT)/T_r}}{e^{\alpha v}(1 + C' e^{\alpha v})} \quad \text{(Eq 2.4)}$$

2.7.2 Chain-of-Rotators Equation of State

Equations of state such as the RKS and Peng Robinson equations are wholly empirical. The equations have been developed and manipulated to fit experimental data. In contrast however, are those equations of state which are derived from a theoretical approach. The properties of the macrofluid are inferred from the behaviour of the molecules. This is a much more rigorous approach. The behaviour of the fluid at the molecular level is reflected in the equation of state. A model of a fluid can incorporate the separate collisions, attractions and other forces that make up the pressure contributions. More powerful computers mean that the relative importance of each of the contributions can be assessed. By simulating a microfluid an equation of state for a macrofluid can be extrapolated and tested against experimental data.

One such equation of state is the Chain-of-Rotators (COR). This was first published by Chien et al. [*1983*]. It is the "father equation" of the Cubic Chain-of-Rotators equation of state which will be examined in this thesis. The equation visualises the molecules as a chain of "hard dumbbell" rotators. The model takes into account the rotational, translational and attractive contributions of each molecule to the overall pressure. The model combined the Carnahan-Starling [*1969*] model of a hard sphere with an equation of state for hard dumbbell molecules proposed by Boublik and Nezbeda [*1977*]. The hard sphere fluid theory visualises the fluid as having infinite repulsion forces below a certain radius and zero beyond. The equation of state is quite complex:

$$\frac{pV}{nRT} = 1 + \frac{4\left(\frac{\tilde{v}}{\tau}\right)^2 - 2\left(\frac{\tilde{v}}{\tau}\right)}{\left(\frac{\tilde{v}}{\tau} - 1\right)^3} + \frac{c}{2}(\alpha - 1)\frac{3\left(\frac{\tilde{v}}{\tau}\right) + 3\alpha\left(\frac{\tilde{v}}{\tau}\right) - (\alpha + 1)}{\left(\frac{\tilde{v}}{\tau} - 1\right)^3} + \qquad \text{(Eq 2.5)}$$

$$\left[1 + \frac{c}{2}\left(B_0 + \frac{B_1}{\tilde{T}} + B_2\tilde{T}\right)\right]\sum_{n,\,m}\frac{mA_{nm}}{\tilde{T}^n\tilde{v}^m}$$

The constants A_{nm}, B_0, B_1 and B_2 are universal for all fluids.The term α is a dumbbell constant which depends on the ratio of the molecules' centre-to-centre diameter to the diameter of the molecules. $\tilde{T}$ and $\tilde{v}$ are reduced parameters and are given as follows:

$$\tilde{T} = T/T^* \qquad \text{(Eq 2.6)}$$

$$\tilde{v} = V/V_o \qquad \text{(Eq 2.7)}$$

$$\tau = \pi\sqrt{2}/6 \qquad \text{(Eq 2.8)}$$

The parameters T^*, c and V_0 are specific for each fluid and are regressed from experimental data.

Chien tested the equation by comparing experimental vapour pressure, saturated liquid and vapour densities of a number of hydrocarbons and benzene against the values predicted by the COR. The Perturbed Hard Chain (PHC) equation of state was compared also. Vapour pressure were within 1% of the experimental data. The Average Absolute Deviation (AAD) for Liquid volumes was 0.5%. The liquid volume prediction was shown to be quite good and much better than that for the RKS and Peng-Robinson (PR) equations of state. PVT data comparison on alkanes were also carried out. The COR equation showed better performance than the PHC equation. A number of VLE comparisons were made and good agreement was observed.

Masuoka and Chao [*1984*] modified the Chain-of-Rotators equation for polar substances. An extra term was added to the equation. Predictive vapour pressures for

H_20, SO_2, NH_3 and other polar compounds were examined for accuracy. Root mean deviations were in the range 0.5-4.2% for vapour pressure and 0.8-4.1% for saturated liquid volume.

2.7.3 Cubic Chain-of-Rotators Equation of State

The Cubic Chain-of-Rotators (CCOR) was first described by Lin et al. [*1983*]. It was intended to use the COR's good prediction of liquid behaviour in a cubic form since a cubic equation is much easier to invert. Most equations of state are pressure explicit and need to be inverted to calculate the volume. The CCOR equation uses a simplification to describe the hard sphere fluid behaviour. The CCOR equation has five parameters which need to be calculated as opposed to the three in the COR equation. These parameters (a, b, c, d, and c^R) depend on three constants: critical temperature, critical pressure and acentric factor. No other parameters dependent on experimental data need to be calculated. This offers a distinct advantage when the properties of new or experimental fluids are needed, since a minimum of data is required. For VLE calculations two interaction constants are used instead of the normal one. The equation has the form:

$$p = \frac{RT}{T}\left[\frac{v+0.77b}{v-0.42b} + \frac{c^R}{2}\left(\frac{0.11b}{v-0.42b}\right)\right] - \frac{a}{v(v+c)} - \frac{a}{v(v+c)(v-0.42b)} \qquad \text{(Eq 2.9)}$$

The first term on the right hand side (of Equation 2.9) is the approximation of the Carnahan-Starling hard sphere model. The second term accounts for the rotational contribution of polyatomic molecules to the pressure. The remaining term expresses the attractive forces.

Lin compared the predictive ability of the CCOR to the RKS and Peng-Robinson (PR) equations. Vapour pressures and saturated liquid volumes of a number of alkanes, and other gases such as carbon dioxide, argon and nitrogen were examined. The results

showed that the CCOR equation was superior to the PR and RKS equations, especially for liquid behaviour. Vapour liquid equilibria comparisons were also carried out. These included mixtures of m-cresol, tertalin and quinoline. The CCOR equation managed to predict the K values with good agreement. Deviations were in the range 3-7%.

During the years 1985-1986 a series of papers were published by the team that developed the CCOR equation, which detailed further examinations of the equation's predictions. Comparisons were made with some n-paraffins. Deviations for vapour pressure were in the region 1-2% and these were slightly better than the errors associated with the PR and RKS equations. A similar examination for heavy non-paraffinic substances yielded errors of 1-3%. Kim pointed out that the definition of the enthalpy departure function is discontinuous at the critical temperature (even if the pressure is not critical). This is because two functions are joined together for the definition of *da/dT*. This has implications for interpolating other properties when the enthalpy is known. An extensive investigation of the equations' ability to predict VLE was undertaken. Solutions containing hydrogen, methane, carbon dioxide and nitrogen were examined. The average absolute deviations (AAD) were in the range 3-5% for these particular substances. The authors noted that the use of two interaction parameters (k_{aij}, k_{cij}) significantly improved the accuracy of the equation. (Most cubic equations of state use one). These were found by minimizing the sum of the square of the relative deviation between calculated and experimental data.

Guo et al. [*1985a*] examined the CCOR equation with polar substances and their mixtures [*Guo et al. 1985b*]. The parameters A_1, A_2, C_1 and C_2 which define α and γ, used to calculate a and c, were regressed from vapour pressure data for water and ammonia. PVT comparisons of water and ammonia were then made. AADs of 0.68% and 0.43% respectively were observed. With the same values for C_1 and C_2, values of A_1 and A_2 were regressed for 45 polar compounds. Deviations for vapour pressure were beneath 1.54%. Comparison of mixtures were divided into low and high

pressure mixtures. The low pressure mixtures consisted of mainly alcohol solutions. Calculated bubble pressures and vapour compositions were within 1% of experimental values. The CCOR equation proved superior to the Wilson activity coefficient model in the majority of mixtures. VLE for high pressure mixtures showed agreement in the range 4-5% with occasional mixtures such as hydrogen sulphide/ water showing discrepancies greater than 10%.

Leet et al. [*1986*] also examined the equation in conjunction with polar substances. Instead of calculating values of Z_c from the acentric factor ω, direct values were used. The vapour pressure and saturated liquid density of twenty four polar fluids were compared with the CCOR equation's values. Good agreement was noted (AADs<1.5%). Symmetric and asymmetric polar binary mixtures were investigated. These included water/ethanol and hydrogen/ammonia mixtures. Predicted K values were close to experimental values. A liquid-liquid equilibrium evaluation was carried out and the CCOR equation behaved well although there were some significant deviations of the solute at dilute concentrations.

2.7.4 Carnahan-Starling-DeSantis Equation of State

Like the Cubic Chain-of-Rotators equation the Carnahan-Starling-DeSantis (CSD) equation of state has been developed from molecular dynamics. It uses the so called hard sphere fluid to model the fluid at the molecular level (Equation 2.10). This was developed by Carnahan and Starling [*1969*]. This was examined by Monte Carlo simulation and found to represent reality quite well.

$$Z = \frac{1 + y + y^2 - y^3}{(1 - y)^3} \qquad \text{(Eq 2.10)}$$

$$y = \frac{b}{4v} \qquad \text{(Eq 2.11)}$$

Desantis et al. [*1976*] proposed that it would be desirable if a single equation of state could be used to describe both liquids and vapour, rather than separate descriptions of the liquid by means of activity coefficients. DeSantis combined the repulsion of the hard sphere model with the attractive term of the Redlich Kwong equation of state, yielding the Carnahan-Starling-DeSantis equation of state:

$$Z = \frac{1 + y + y^2 - y^3}{(1-y)^3} - \frac{a}{RT(v+b)} \qquad \text{(Eq 2.12)}$$

The parameters a and b took account of the temperature dependency and forced the equation to pass through the critical point. The parameter a represents the attractive forces in the fluid. It decreases with increasing temperature. The effective volume of the molecules, which measures the closest approach, is represented by b. The equation was checked by calculating second virial coefficients and comparing with experimental values for a number of alkanes. Good agreement was obtained. Mixture VLE prediction for nitrogen/argon and ethane/propane was good (AADs were less than 2%).

Morrison and McLinden [*1985a*] examined the equation's ability to represent the thermodynamic properties of refrigerants. The a and b parameters were defined in such a manner that the equation was no longer constrained to pass through the critical point. The authors noted that forcing the equation to do so affected its accuracy at temperatures well away from the critical point. With these equations, fluids described by the CSD equation have a critical compressibility of 0.3516. They defined the a and b parameters in terms of temperature only.

$$a = a_0 exp(a_1 T + a_2 T^2) \qquad \text{(Eq 2.13)}$$

$$b = b_0 + b_1 T + b_2 T^2 \qquad \text{(Eq 2.14)}$$

The parameters a_0, a_1, a_2, b_0, b_1 and b_2 are found from experimental pure fluid saturation data. They are found by minimising the function represented by Equation 2.15.

$$F = w_l\left(\frac{v_{l_e} - v_{l_c}}{v_{l_e}}\right)^2 + w_g\left(\frac{v_{g_e} - v_{g_c}}{v_{g_e}}\right)^2 + w_p\left(\frac{p_{sat_e} - p_{sat_c}}{p_{sat_e}}\right)^2 \qquad \text{(Eq 2.15)}$$

where the subscript e represents the experimental value of a particular property and c represents the calculated value. The w terms refer to the relative weighting given to each property and they usually lie between zero and one. Equation 2.12 is the form that is used today. Morrison et al. demonstrated that calculating the a and b parameters from what he described as restricted datasets can produce a universal description of a fluid. Morrison compared the heat capacity (C_p) predictions of the CSD equation for R152a against three data sources. Despite not having included C_p data in the evaluation of the a and b parameters in Equation 2.15, the predicted C_p compared well with the experimental value. This is a particularly stringent test of an equation of state since it results from the second derivative of the equation of state.

2.7.5 Prediction of Refrigerant Properties Using Equations of State

2.7.5.1 Cubic Chain-of-Rotators Equation of State

As part of his thesis, Low examined the suitability of the CCOR equation of state to represent both pure and mixed CFC refrigerants Low [*1991*] compared the CCOR equation to data from thermodynamic property tables in Perry [*1984*] and with high accuracy correlations, for a number of CFC fluids. Fluids examined included R11, R12, R13, R22, R113, R114 and RC318.

The properties studied were vapour pressure, saturated liquid and vapour volume and latent heat of vaporisation. The mean AADs were 1.5%, 3.3%, 6.7% and 7.0%

respectively. Vapour volume was not very well predicted above a reduced temperature of 0.85. Disagreement occurred between the CCOR and CSD equations near the critical point. This was due to the underlying assumptions that led to their development. Low noted that there was room for improvement in prediction ability and pursued an optimisation strategy. The parameters A_1, A_2, C_1 and C_2 which define α and γ were optimised to achieve better predictions. This brought mixed results. Vapour volume and saturated liquid volume predictions at low reduced temperature were improved. Vapour volume at high reduced temperatures could not be improved. The author suggested that the errors were due to the form of the equation and predictions could not be improved without altering the equation.

CFC mixtures were also examined. AADs were in the range 1-5% for the fluids tested. The effect of the interaction constants k_{aij} and k_{cij} were also examined. It was found that for a given mixture an optimum pair of constants should exist. In summary, Low found that the CCOR offered improved prediction of liquid phase properties compared to other equations as state. It was not as accurate as the CSD equation nevertheless it was recommended for predicting the properties of potential replacement fluids with little or no data.

2.7.5.2 Carnahan-Starling Equation of State

In determining if the hard sphere model could successfully model the properties of refrigerants Morrison and McLinden [*1985b*] examined two mixtures: R13B1/R152a and R12/R22. The interaction parameter k_{a12} was optimised for each dataset. Good agreement in predicting the VLE pressures was noted. A good prediction of the heat of vaporisation of the R12/R22 mix was also noted.

The results of a more extensive comparison were published a year later by the same authors [*Morrison et al. 1986*]. The saturation properties of ten CFC fluids were compared against values from ASHRAE standard correlations. Root mean square

errors for vapour pressure and vapour volume were less than 0.5%. Those for liquid volume and latent heat of vaporisation were less than 0.1% and 1.0% respectively. These indicated excellent predictions of CFC thermodynamics. The parameters a and b had been calculated by minimizing the function in Equation 2.12 using saturation data only. With R22 the authors examined if the inclusion of non-saturation data in determining the a and b parameters would improve the predictions. The quality of the predictions was only slightly improved. Thus good representation of non-saturation properties could be made with only saturation data at hand. A number of mixtures were also studied. For each dataset the interaction parameter (k_a) was calculated. Deviations for the 11 mixtures were in the range 0.008-0.02. It was observed the composition dependence of k_a was strongly correlated to the relative volatility of the components.

The CSD equation calculates the data for the refrigerant software package REFPROP (Version 4.0) [*N.I.S.T.*] issued by the U.S. National Institute of Science and Technology. This is a computer program which calculates both pure and mixed properties for CFC, HCFC and HFC mixtures. (For the sake of accuracy this has been upgraded to version 5.0 which uses a modified Benedict-Webb-Rubin equation). It has also been used to calculate the thermodynamic properties for a number of refrigeration cycle simulation studies *[Domanski 1983, 1986, 1992]*, [*Jung et al. 1991a, 1991b*], [*McLinden et al. 1987*], [*Parent et al. 1989*].

2.7.5.3 Other Equations of State and Refrigerant properties

The ability to accurately predict the thermodynamic properties of refrigerants of a number of other equations of state have been studied by a number of investigators. This is a very brief summary of some of the latest work done in this field. Lee et al. [*1992*] compared the VLE behaviour of three equations of state, namely RKS, Patel-Teja (PT) and Iwai-Margerum-Lu (IML) equations. Twenty two different CFC and

HCFC mixtures were studied in all. The PT equation exhibited the best ability to correlate CFC VLE. Optimal interactions were calculated for each equation of state by minimizing the square of the pressure errors and the K value errors. Lee noted that the interaction constant, k_a, was essential to accurate prediction of VLE. On the basis of the calculated optimal values a correlation of k_a for the PT equation was presented. This correlation was a function of acentric factor (ω) difference and critical compressibility factor (Z_c) difference. This correlation, although not as accurate as using a pair specific value for k_a, was more accurate than setting k_a to zero.

Blindenbach et al. [*1994*] examined the Perturbed Anisotropic Chain Theory (PACT). This equation require three different parameters representing the dispersion energy, characteristic volume and shape of the molecule. These are determined from experimental data. Both pure and mixtures of refrigerant were studied. Vapour pressure AADs were less than 2.3% while liquid volume deviations were below 2.6%. Nineteen binary pairs were investigated and comparison were drawn with the PR and SRK equations. The PACT equation had lower deviations ($\approx$5%) than the other two equations ($\approx$11%). The PACT equation was able to predict the behaviour of R23 mixtures despite being a very polar compound. Using correlations for the interaction parameter k_a the data was re-examined. The PR showed slightly better agreement with the experimental data. The authors suggested that the cubic equations could be used with well known refrigerants, but for prediction work the PACT should be preferred.

The Redlich-Kwong-Soave equation of state, in conjunction with mixing Rules proposed by Huron and Vidal, was investigated by Barolo et al. [*1995*]. The most commonly used mixing rules are the Van der Waals mixing rules (Section F.2 on page 277). For accurate prediction of vapour liquid equilibria the interaction parameter k_{ij} must be known or determined. However for predictive purposes large errors can arise if k_{ij} is set to zero. Instead of using the Van der Waals mixing rules to calculate the parameters of the RKS equation the mixing rules proposed by Huron and Vidal were applied. These are based on the activity coefficient evaluated at a reference state of

infinite pressure. A UNIFAC group contribution method was used to reproduce the activity coefficient at infinite pressure ($\ln \gamma_i^{\infty}$). These mixing rules do not use any parameter which is determined from VLE data. This method was compared against VLE experimental data for CFC and HCFC mixtures. Agreement between experimental and calculated data was satisfactory. An overall root mean square (RMS) error of 3.9% on pressure was noted while the average deviation for composition was 0.0148 mole fraction.

2.7.6 Hydrofluorocarbon Refrigerant Experimental Thermodynamic Property Data

Thermodynamic properties determine the efficiency and capacity of a refrigeration cycle. In order to compare how well a given equation of state can predict thermodynamic properties, experimentally determined values of those properties need to be measured. Saturation vapour pressure and pressure-volume-temperature (PVT) data is often used to compare how well a given equation can predict the behaviour of a refrigerant. Before any such comparisons can be made the data must first be experimentally measured in a laboratory. McLinden [*1990*] conducted a survey of the available data on acceptable CFC replacements. His survey focused on HCFCs and HFCs. He found that for some refrigerants, such as R22, there was a considerable amount of data published over an extensive range of temperature and pressure. Other refrigerants, such as HFCs had little or no data except for anonymous undocumented data sheets. In an earlier article McLinden et al. [*1989*] outlined what properties needed to be investigated and they categorised the property needs (Section 1.3.2.1 on page 11). At that time (1989) most of the research into refrigerant properties focused on CFCs despite the existence of the Montreal Protocol. The authors called upon the fluid properties community to shift their focus onto the CFC replacements. By and large their request has been answered. Since then, a tremendous amount of work has gone into determining the properties of HFCs experimentally.

Later McLinden et al.[*1993*] updated their survey of thermodynamic data, focusing on HFCs. R134a is often used as a reference fluid for the thermodynamic properties of ethane based refrigerants because of the volume of published data. Comprehensive data also exists for R32 and R125. Transport data was somewhat less plentiful although the situation will have been remedied somewhat since 1993. Much of the thermodynamic property data research has been conducted by the Thermophysics Division of the National Institute of Science and Technology in the U.S.A. and by the Thermodynamics Laboratory of Keio University, Japan. An extensive bibliography for the thermodynamic and transport properties of HFCs was provided. The Japanese Association of Refrigeration (JAR) [*1994*] issued computer software which allowed one to determine saturation properties of a pure refrigerant using the Peng-Robinson equation of state. It also provide a comprehensive bibliography. It covers all aspects of experimentally determined refrigerant properties from vapour pressure to speed of sound.

Vapour liquid equilibrium (VLE) data for HFC and HCFC mixtures are considerably more scarce. There has been a lot of refrigerant VLE data published but most involves CFCs. The author of this thesis managed to locate eleven sources of VLE data where at least one of the components was a HFC. Bubble point pressure and saturated liquid density are the properties most often published. Since most equations of state can represent vapour reasonably well, this is not such a great problem. The temperature is usually above ambient and rarely below ambient which is of interest in a refrigeration cycle.

In this section a brief summary is given on experimentally determined thermodynamic properties. Rather than laboriously reviewing each publication, an example of each type of source of experimental data used in Appendix B and Appendix F will be given, namely vapour pressure determination, PVT behaviour and bubble pressure and density of a binary refrigerant pair. Most of the publications are very similar in form. The reader is usually referred to an earlier publication, by the same author, for a

description of the experimental equipment and procedure. The data is then given in tabular form. Usually the author will compare his data to an equation of state or a correlation.

2.7.6.1 Vapour Pressure (N.I.S.T.)

Weber et al. [*1993*] published data on the saturation vapour pressure of R32. He noted that little information had been published for R32 at low temperatures. An ebulliometric comparator was used to determine the pressure at a given temperature. Both the fluid under test and a standard fluid (water in this case) were boiled and condensed. The pressure of the refrigerant was calculated from the boiling temperature of the standard fluid. The symmetry of this system means that errors are self-cancelling. Condensation temperatures are insensitive to very volatile or involatile impurities. The accuracy of the platinum resistance thermometer was 3-4mK. Twenty seven values of vapour pressure were recorded over a temperature range of 208-237K. An Antoine type expression for vapour pressure was calculated. It had a relative deviation of 0.036%. This and the experimental data were compared to the data of Kanungo and co-workers [*1987*] (who provided a correlation only) and Malbrunot et al. [*1968*]. The predictions of Kanungo's vapour pressure correlation were systematically 0.44% higher than those of Weber's Antoine equation. Malbrunot's research, although it displayed less precision, did not display any overall systematic difference. Using their own data and Malbrunot's, the authors determined a function for vapour pressure spanning the temperature range of 191K to the critical temperature. It had a relative standard deviation of 0.24%. The authors also calculated second order virial coefficients

2.7.6.2 PVT Properties (Keio University)

The pressure-volume-temperature and the vapour pressure behaviour of R134a was experimentally determined by Piao et al. [*1990*]. One hundred and fifty nine data points, along 24 isochores, were recorded for PVT. Fifty one vapour pressure measurements were made as well. The temperature in a constant volume cell ($139 cm^3$) was varied and the pressure recorded by three pressure gauges, with an uncertainty of 2.0 kPa. The temperature was measured using a platinum resistance thermometer with an accuracy of 10 mK. Experimental density uncertainty fell in the range 0.05 to 0.5 $kg m^{-3}$. Five different samples were used and their purity varied from 99.50% to 99.99%. The vapour pressure measurements were taken between 300 K and the critical temperature (measured as 374.29 K). Based on this data an expression for vapour pressure was provided, which could represent the data within 0.2%. This expression was compared with five other sources of R134a vapour pressure data. The maximum absolute deviations varied from 0.4-2%. The PVT measurements were taken over a wide range of density, 36-1144 $kg m^{-3}$; temperature varied form 310-425 K and the pressure range was 0.7-12 MPa. As with vapour pressure the data was compared with other published data. Piao's data agreed with the data of Wilson and Basu [*1988*] within 0.8% in pressure. An equation attributed to Du Pont agreed within 4.8% of Piao's data. Saturated liquid density was determined on the basis of the PVT data. An expression for the density represented the data to within 0.08% and the maximum deviation was -0.3%.

2.7.6.3 Refrigerant VLE Data: R22 & R152a (Keio University)

The bubble point vapour liquid equilibrium of R22 and R152a was investigated by Maezawa et al. [*1991a*]. The liquid densities were measured using a magnetic densimeter. The uncertainty associated with the densimeter was 0.3%. A 25 Ω platinum resistance thermometer with an uncertainty of 15mK provided the

temperature measurements. Five different compositions (10, 30, 50, 70 and 90 wt.%) were used in the experiments. In total, 66 different points were recorded. The author compared the density data with 2 correlations which allow one to calculate the saturated density of a mixture. The data agreed to within 0.5% for the Rackett correlation and to within 0.5% for the Hankinson-Brost-Thomson equation. With the bubble pressure data, an optimised interaction parameter for the Peng-Robinson equation of state was calculated. This value was implemented in predicting values for bubble pressure with the PR equation of state. It agreed to within 2% of Maezawa's measured data.

Chapter 3

Design and Construction

3.1 Introduction

The motivation for the experimental research was the potential that mixed refrigerants can have higher COPs than those of pure fluids. Temperature changes experienced by a mixed refrigerant when undergoing phase changes in the and evaporator and condenser can be matched with the temperatures changes of the heat source and sink leading to higher COPs. Several researchers have carried out investigative work into improving COPs with mixtures. Most studies examined CFC and HCFC mixtures. The phasing out of CFCs, and eventually HCFCs, has meant that they can no longer be used as working fluids in refrigeration machinery. In the experimental research described in this thesis the objective was to investigate the improvements in COP from the use of non ozone depleting refrigerant mixtures, specifically with mixtures of the hydrofluorocarbon refrigerants R32 and R134a. This chapter describes the design and construction of the refrigeration pilot plant used to examine the R32/ R134a mixtures.

3.2 Plant Design and Requirements

The equipment used by Low [*1991*] in his investigation was re-employed for this research. CFC mixtures had been used as the working fluid. Consequently it was necessary to make substantial modifications to the cycle because of the use of more volatile refrigerants and because of certain specifications outlined in the project remit. The plant was remodified to accommodate R32/R134a mixtures of varying compositions. R32 has quite a high vapour pressure (14 bar g at 20°C). The plant had to be able to contain and store this high pressure refrigerant. A water-ethylene glycol stream was used as a heat source with a separate water stream acting as a heat sink. The experimental refrigeration cycle was instrumented to record cycle parameters.

3.2.1 Project Specifications

A number of requirements regarding the cycle design were included to the project remit. These were as follows:

- **Utilisation of existing equipment**. A dual condenser two fluid heat pump existed in the Department of Chemical Engineering. This had been run previously with CFC mixtures. It was felt that this should be used in experimentally determining the benefits of using non ozone depleting refrigerant mixtures.
- **Use of R32 and R134a mixtures.**
- **Pool boiling Evaporator**. The project was sponsored by both Imperial Chemical Industries and the Engineering Physical Science Research Council. Rather than using a forced convection evaporator with little hold up, I.C.I. were interested in the performance of a flooded pool boiling evaporator. The evaporator was thus designed to operate in a flooded manner.
- **Minimisation of refrigerant hold-up**. R32 is regarded as a flammable refrigerant and it has a relatively high vapour pressure. Safety considerations meant that the cycle was to be designed to use a minimum charge of refrigerant. This was negated

to a certain extent by the use of a pool boiling evaporator. However, other parts of the plant had scope for reduction of inventory, particularly the glass storage tanks immediately after the expansion valves.

- **Direct measurement of refrigerant flowrate**. Low had used the throughputs of the metering pumps to measure the mass flowrate of the CFC refrigerants. It was felt that a more reliable and accurate method of measuring refrigerant mass flow rate was required. A device that would directly measure the mass flowrate was preferred. Pressure drop methods (e.g. orifice plate) require knowledge of the fluid density which would not be readily at hand.

3.3 Plant Design

Before detailing design specifications and describing the intended conditions under which the plant operated a brief description of Low's heat pump will be given. Specification of temperatures, heat loads and heat transfer coefficients would depend on the operation of the heat pump.

3.3.1 Plant Prior to Modifications

The variable capacity heat pump is shown in Figure 3.1. Low gives a detailed description of the design and selection of each piece of equipment in Chapter 3 of his thesis. By using a dual condenser system, in series, partial separation of the mixed refrigerant occurred and the composition of the working fluid could be varied in response to demand conditions to maintain a constant heat output. Superheated vapour entered the compressor (J1) at pressures of 1-2bar g. The vapour was compressed in a rotary sliding vane type compressor. This had a variable drive which allowed the speed to be set by the operator. The vapour was then partially condensed in a brazed plate type heat exchanger (C1) at a pressure of 8-10bar. Water, typically at 60°C, was used to condense the refrigerant. The water stream ran countercurrent to

the working fluid. The two phase refrigerant stream was separated into liquid and vapour by a flash pot (T1). The remaining vapour was condensed in the second condenser (C2). The liquid in each flash pot was further subcooled by mains water (H1 & H2). The condensate leaving the first condenser would we richer in the more volatile component, when a binary working fluid was used. The condensers effected a partial separation of the fluids. The subcooled liquids were expanded across two control valves (CV3 & 4).

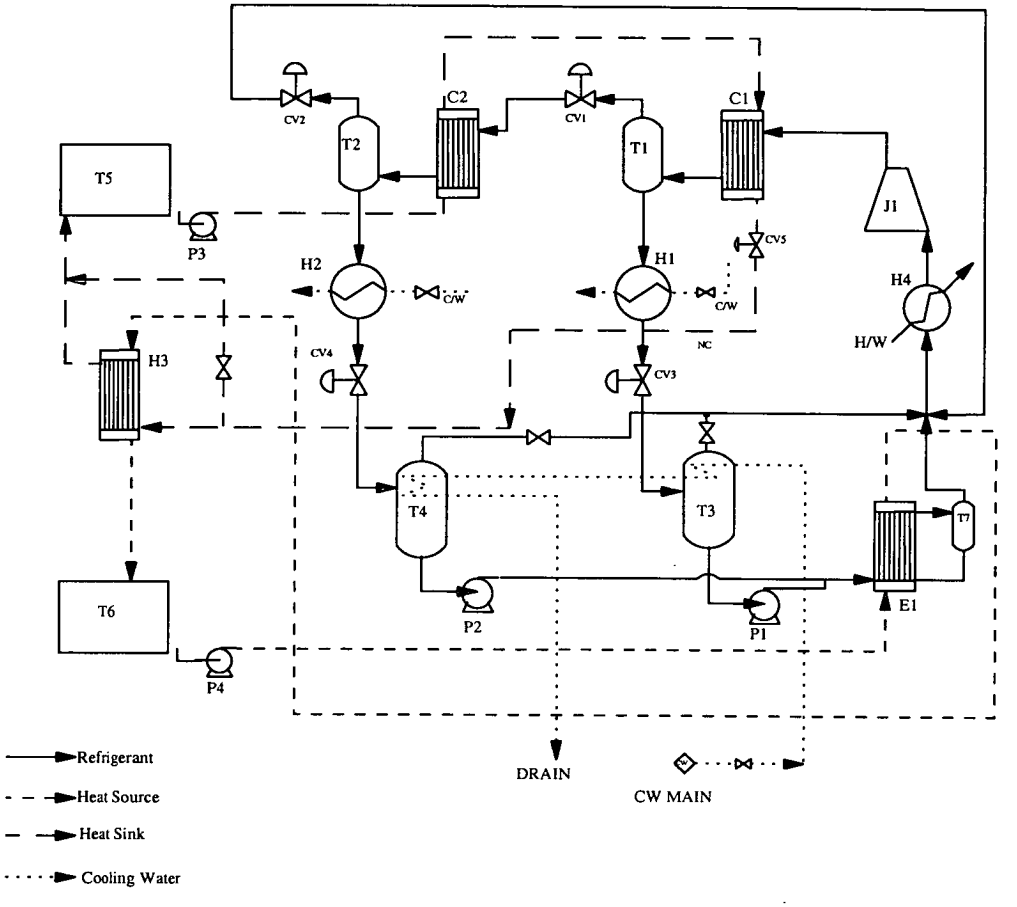

Figure 3.1: Flow diagram of the variable capacity heat pump prior to modifications (Taken from Low [*1991*])

The two-phase mixtures were stored in two glass storage tanks (T3&4). Storage of the separate condensates allowed the circulating fluid composition to be altered without any external control. Excess flash gas was recycled to the compressor suction. Two metering pumpheads (P1 & P2), with a variable stoke setting, transferred the liquid to the evaporator allowing refrigerant composition to be varied. The two liquid streams were blended before transfer to the evaporator. The evaporator consisted of a double pipe heat exchanger. A water stream acted as the heat source and flowed in the inner tube. Turbulence promoters on the inside and a large extended surface area on the outside ensured high heat transfer coefficients. Liquid carry over from the evaporator was separated in a glass separation tank (T7). The saturated vapour was superheated in a double pipe heat exchanger (H4) prior to compression while the heat sink and heat source water streams were held in tank nos. 5 and 6 respectively. A plate heat exchanger (H3) and electrical heaters ensured that the tanks were held at a constant temperature. Pipework was constructed from copper with high pressure refrigerant fittings.

The plant was well instrumented. Five pressures and twenty four temperatures were recorded. The data was logged on an 80286 personal computer. The sink and source flow rates were measured by the pressure drop across an orifice plates. Levels in the evaporator and condenser flash tanks were also recorded. The metering pump stroke setting could also be remotely altered from the computer. Temperature differences in the sink and source streams were measured by a five junction thermopile. The water thermopile measured the temperature change across *both* of the condensers. The control and information display program was written in the TurboC language.

3.3.2 Design Considerations

A number of considerations and constraints had to be taken into account in designing the plant for use as a refrigeration device. These had a large influence on the

replacement and/or modification of individual pieces of equipment on the plant. These factors arose from the specifications laid out in Section 3.2.1 on page 74. The main considerations which had a bearing on the design are discussed in the following sections.

3.3.2.1 Pressure and Safety Considerations

The most significant factor affecting the design of the plant was the intended operating pressures, and also the pressures at which the refrigerant would be stored when the plant was not operational. Both the high and low pressure sections would have significantly higher pressures compared to previous operations. In particular, the volatile nature or R32 would influence the design of many components. Low had designed the pressure limit on the high pressure section (condensers, flash pots and subcoolers) to be 24bar g. This was regarded as sufficiently high for operation with pure R32. At 24bar the saturation temperature of R32 is 40°C. Since the inlet water stream for the condensers was specified as 20°C (vapour pressure = 14.7bar) a maximum allowable pressure of 24 bar seemed sufficiently large. Larger allowable pressures would have meant substantial increases in cost and complexity and would have unnecessarily complicated the safety issues. In addition adequate relief would have to be provided.

Not only would the plant have to be able with stand increased pressures; also it would have to store the working fluid without significant losses. The number of joints would have to be minimised and adequate sealing provided. Fractionation of a non azeotropic mixed refrigerant would lead to a change in the overall composition in the event of a leak. Thus the potential for composition change over a period of time existed. R32 is classified as a flammable substance and this added extra urgency to the removal of leaks at the design stage. Advice from I.C.I. indicated that although

considered flammable, R32 is quite difficult to ignite. Removal and dispersion of any leaked vapour would have to be considered.

The equipment on the high pressure side of the apparatus (apart from some pipework) did not need to be replaced or substantially remodified. Most of the alterations occurred at the low pressure end of the plant. Operating pressures had been in the region of 1-2.5bar g and much of the material was constructed from glass. This would have to be replaced with stronger material. Each piece of equipment had to be able to operate at the desired pressure levels. The pool boiling evaporator would be used to store liquid refrigerant when the plant was not operational. Thus the pressure when the equipment was nonoperational would be *higher* than when it was being run because the normal operating temperature would be less than ambient temperature. The evaporator would have to be able to store the liquid refrigerant with minimum losses. Thus the maximum allowable pressure on the low pressure side was set at 20bar g.

3.3.2.2 Temperature Considerations

The normal boiling point of R32 is -52°C. Equipment on the cold low pressure side would have to have a minimum allowable temperature beneath this. Running the evaporator at sub-atmospheric pressures was to be avoided to prevent air ingress. Use of R32 leads to high compressor discharge temperatures (120-130°C). In addition the discharge pipework and the first condenser would have to be able to withstand such a temperature regime. Refrigerant condensate temperatures were anticipated to be just above ambient.

3.3.2.3 Minimisation of Refrigerant Hold-up

A smaller refrigerant inventory would reduce any risks as a result of leaks or catastrophic failure. Refrigerant costs would also be reduced. A smaller plant would mean fewer joints and reduced likelihood of leaks. Bearing this in mind it was decided to replace the two glass storage tanks (T 3&4) with lengths of $\frac{1}{2}$" high pressure copper pipe. Although the flooded pool boiling evaporator negates the principle of minimising of refrigerant hold-up to a certain extent, the evaporator would be designed in such a manner that a minimum of liquid refrigerant would be needed. Process equipment items were placed as close to each other as possible to reduce the length of interconnecting pipe. Equipment was also positioned in such a way as to reduce bends and joints.

3.3.2.4 Choice of Sink and Source Streams

For simplicity and ease of use, water would be used as the heat sink stream. The source stream would have to remain in the liquid form at temperatures in the region of -45° to -50°C. Operating source temperatures would be higher than this. From a safety point of view it would be necessary for the heat source to be in liquid form at these temperatures to prevent any solidification and consequent damage to pumps and pipes. A 60 wt.% ethylene glycol water solution was chosen. This has a freezing point of -47°C which was considered sufficiently low. This particular concentration was chosen as a trade-off between lower freezing point and increased liquid viscosity. A higher concentration of glycol would only have lowered the freezing point by a one or two degrees, at the expense of increased liquid viscosity and consequent reduced heat transfer performance. Detailed transport property charts are provided in Perry [*1984*] enabling heat transfer coefficients to be calculated. Ethylene glycol (referred to simply as glycol hereafter) is easily available and inexpensive. The solution was made by simply weighing appropriate amounts of water and glycol and transferring the

mixture to the tank. The concentration was regularly checked by measuring the temperature, and the density with a hydrometer and determining the proportion of glycol from a temperate-density concentration chart.

3.3.2.5 Compatibility

The refrigerants R32 and R134a are compatible with most materials of construction including copper, steel and many plastic materials. Advice from I.C.I. indicated that R134a could cause swelling to "Viton" rubber seals therefore these were avoided in the construction of the plant. During operation, no noticeable swelling of seals was observed. Normal mineral oil can not be used as a compressor lubricant if HFCs are used. As an alternative a polyol ester oil would normally be used instead. Consequently two gallons of this specially developed oil were supplied by I.C.I. for use as compressor lubricant.

3.3.3 Flowsheet and Mass and Energy Balance

A flowsheet of the plant was drawn up. This is shown in Figure 3.2. At a first glance it is similar to Low's plant. Most of the changes to the plant occurred in the low pressure side i.e. removal of glass tanks, replacement of the evaporator and metering pumps. Previously the expanded fluids were mixed before being evaporated. On the new plant the fluids were not mixed prior to evaporation; i.e the evaporator had two feed streams. The fluids were mixed and evaporated in the same step. The glass vapour/ liquid separator after the evaporator was removed, again due to increases in the operating pressure. It was anticipated that the heat source and sink streams would be similar in configuration to those on the original plant. Potential changes would arise from changes in the required flowrate which would primarily affect the pump and the flowrate measuring instrumentation.

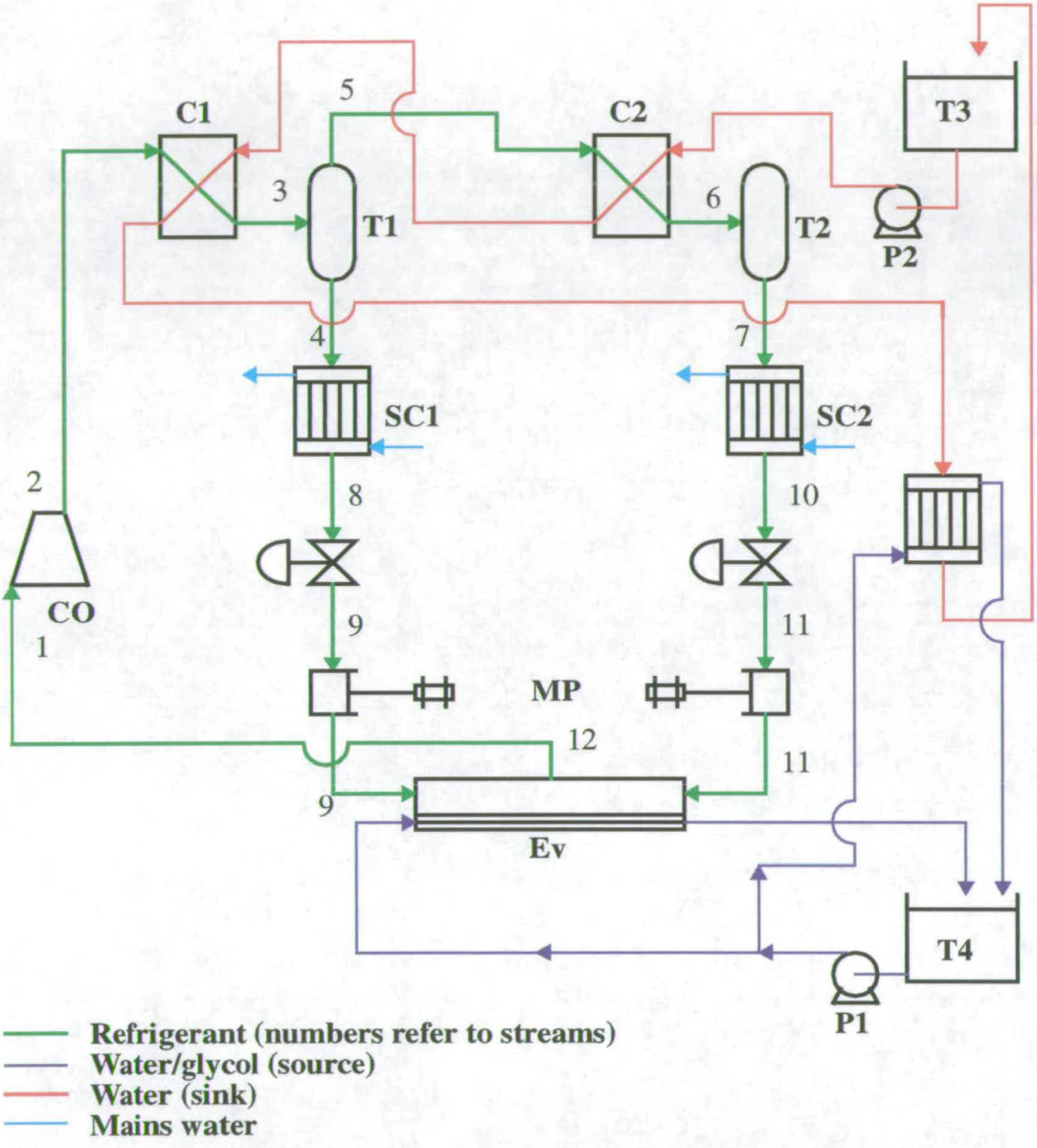

Figure 3.2: Flowsheet of the refrigeration plant

Before designing individual pieces of equipment a mass and energy balance was calculated. This would form a basis on which individual pieces of equipment could be sized. The mass and energy balance was calculated with pure R32 as the working refrigerant. It was known that the compressor had a pressure ratio of 5. The upper and

lower pressures were selected at 5 and 25bar absolute. A heat load of 8 kW in the evaporator was specified. This would allow the mass flowrates, work and heat loads to be calculated. The mass and energy balance calculations are detailed in Appendix A on page 197. Thermodynamic data used in these calculations was supplied by ICI [*I.C.I*]. From the mass and energy balance the design R32 mass flowrate was set at $112.5 kg hr^{-1}$ with a compressor work load of 3.14kW and the total condenser heat load was calculated to be 11.0kW. Table A.1 on page 202 details the conditions of each stream while Table A.2 on page 203 tabulates the energy transfers associated with each piece of equipment. Using this information each item of equipment was sized and selected.

3.4 Equipment Design and Selection

This section describes the rationale behind each piece of equipment. Some of the items were not altered from Low's plant and only a brief description for these items are given. The reader is referred to Low's thesis for a fuller, more detailed design. Most of the design and selection involved checking existing equipment specifications to see whether the increased pressures could be withstood. New equipment was chosen if the operating pressures were above the maximum for a particular piece of equipment.

3.4.1 Compressor

3.4.1.1 Compressor Unit

The existing compressor on the plant was a rotary sliding vane type. It was designed for use with R12 and it had a throughput of $12.6 m^3 hr^{-1}$ at 1500 r.p.m. The drive motor had a power rating of 3.7kW. A 3 phase (415V, 50Hz) supply was needed by the

motor. The design pressure ratio was 5:1. An IMO Jaguar electronic variable speed drive was also supplied. This would allow the supply current to be varied and hence vary the work received by the fluid. It was felt that the compressor would be suitable for the design pressures and work load proposed. The compressor was designed for R12 which meant that more efficient compression would occur with R134a than R32, since R134a is intended as a replacement for R12. The expense, time and effort involved in specifying a HFC designed compressor was not felt to be justifiable. The Jaguar electronic drive failed and was replaced by an Excal variable speed motor controller. A high temperature trip on the compressor discharge had been installed and it was set at 140°C. A pressure relief valve was installed on the discharge of the oil separator. It was set at 350p.s.i. gauge and it discharged to the suction side of the compressor.

3.4.1.2 Oil Circuit

Mineral oil is normally used to lubricate CFC compressors. HFCs are immiscible with mineral oil which means that it cannot be readily used to lubricate HFC compression equipment. Polyol ester based oils have been identified as suitable for use in compression equipment with HFCs. I.C.I supplied 2 gallons of Emkarate RL375 oil. This was found to provide satisfactory lubrication. Immediately after the compressor an oil separator removed the oil from the refrigerant and returned it to the compressor head. After initial operation with R32, a double pipe heat exchanger was installed in the oil return line. This reduced the temperature from 132°C (close to the maximum) to around 120°C, by circulation of countercurrent cooling water. Very high discharge temperatures meant that the temperature limits of the compressor were being approached. The heat exchanger consisted of a $\frac{1}{4}$ " pipe through which the oil flowed, surrounded by a $\frac{1}{4}$ " pipe. The exchanger was 60cm long.

3.4.2 Condensers

The condensers on the original plant were two brazed plate heat exchangers constructed from AISI 316 stainless steel. Alfa Laval supplied the units and they were originally designed for an R114/R11 mixture. The original design heat loads were 5.1 and 4.1 kW. The maximum working pressure was 30 bar which meant that they could be used in conjunction with R32. There seemed little point in redesigning and reordering new condenser, so these condensers were retained.

3.4.3 Condensate Flash Pots

Vapour and liquid from the condensers were separated in two flash pots. The flash pots had been built in the departmental workshop. These were designed for a hold-up of 2 minutes. The pots were constructed from 3" steel pipe and had a height of 93 cm. This gave a volume of 4 litres for each pot. These were pressure tested to 300 p.s.i. These were retained on the plant.

3.4.4 Subcoolers

The condensed refrigerant is further subcooled with two "trombone" double pipe heat exchangers. These were 1.8 m in length and Cal-Gavin "Heatex" turbulence promoters were placed on the refrigerant side (inner tube). According to the original design the condensate would be cooled from 75°C to 25 °C. Operation of the plant as a heat pump meant a much reduced temperature difference between the refrigerant and the mains cooling water and hence a reduced cooling load. Low describes the design of these in detail.

3.4.5 Metering Pumps

Feed to the evaporator was supplied by two reciprocating metering pumps. These were type SS-40C and were manufactured by MPL limited. A single 240V motor drove both pumpheads. The nominal flow was 100lhr.$^{-1}$. The pump was configured in such a way that the stroke percentage could be remotely varied from the computer. The pump could be turned on and off by this method also. The maximum allowable working pressure on the pumpheads was 7bar. Hence the metering pump was replaced by another model, made by the same manufacturers, which had the necessary pressure limits. Four pumpheads with a maximum allowable pressure of 37.5 bar and a stoke rate of 144 strokes per minute were available. These gave a maximum total flow of 150lhr^{-1} which would be sufficient for the plant. The drive motor used a 240V 50Hz electrical supply. The stroke control units were removed from the original pumpheads and installed on the new pumpheads. Thus two of the pumps had remote stroke control and two had manual. One advantage of using pumpheads constructed by the same manufacturer was that the control circuitry and software did not need to be changed. Because of the increased pressure rating two spring loading valves were purchased. These provided a back pressure against which the pumpheads worked. Each loading valve provided back pressure for two pumpheads. When the pumpheads were installed, drain valves were plumbed in to provide drainage if the plant needed to be emptied. Isolation valves were added to the inlet and outlet pipes.

3.4.6 Evaporator

The evaporator was specified to be run in a flooded pool boiling mode. Also the inner tubes and extended area of Low's evaporator were to be reused. Thus the evaporator heat transfer area was already specified. This consisted of three 22mm tubes, 77cm in length. The tube exteriors had a highly extended heat transfer material attached to it. This area was about 50 times the plain tube equivalent area. The inner tubes also had turbulence promoters inserted. Consultations with Mr. Matthew Rea, the department's Technical Services Manager, led to the conclusion that a large pipe with the tubes laid on the bottom parallel to the axis of the pipe would be the simplest to construct. The ends were sealed by end plates bolted onto the pipe. In order to maximise heat transfer coefficients, the glycol made one pass through each tube in series. Thus the glycol would make three passes through the evaporator in all. The evaporator body length would be determined by the length of the tubes from Low's evaporator. Using a number of different evaporator diameters the refrigerant hold-up was calculated. The tubes were placed as close to each other as mechanical joints would allow. A pipe diameter of 6" gave a minimum hold-up and also sufficient height for vapour liquid droplet separation. (Although a diameter of 8" had a slightly lower hold-up the increase in pipe diameter did not justify using this diameter). The evaporator was constructed in the departmental workshop. It is shown diagrammatically in Figure 3.3. An 80cm length of 6" steel pipe was used as the main evaporator body. Four tappings were made in the evaporator body, for the vapour outlet, a thermocouple pocket so the liquid refrigerant temperature could be measured, an analogue pressure dial and a drain valve at the bottom. The drain valve would allow for evacuation of the evaporator. The ends of the evaporator were closed by steel flanges. These were bolted to the pipe with eight bolts and rubber 'o' rings provided sealed the joints. The tubes carrying the glycol went through the end plates. Elbow joints were welded to the ends of the glycol tubes to allow transfer from one tube to the next.

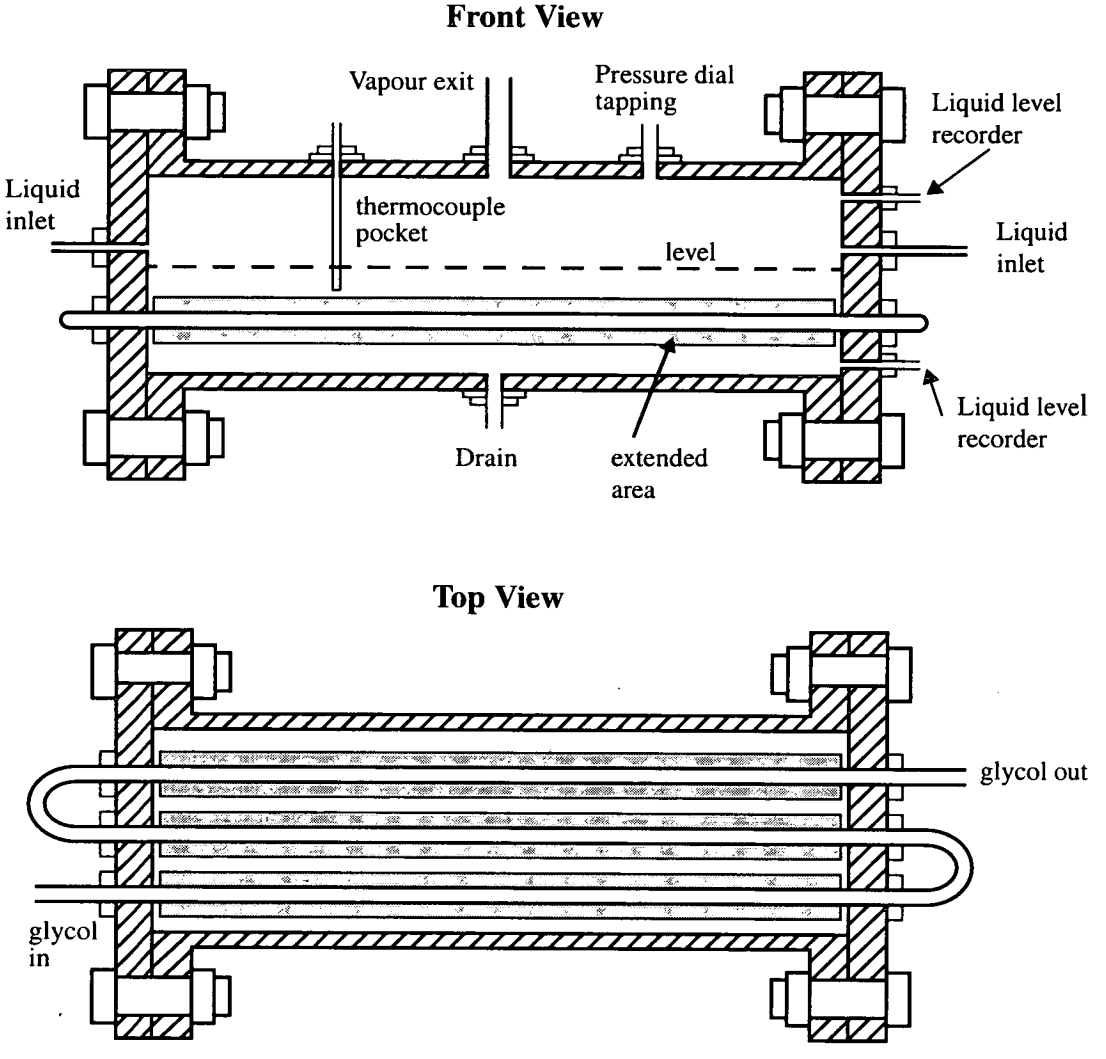

Figure 3.3: Top and front diagrams of pool boiling evaporator

The alignment of the glycol pipes within the body of the evaporator are shown from a side view in Figure 3.4. The figure is to scale and the horizontal dashed line represents the liquid level. The glycol tubes were clamped onto the steel end flanges using high pressure brass fittings. The fittings acted as a seal between the tubes and the flanges.

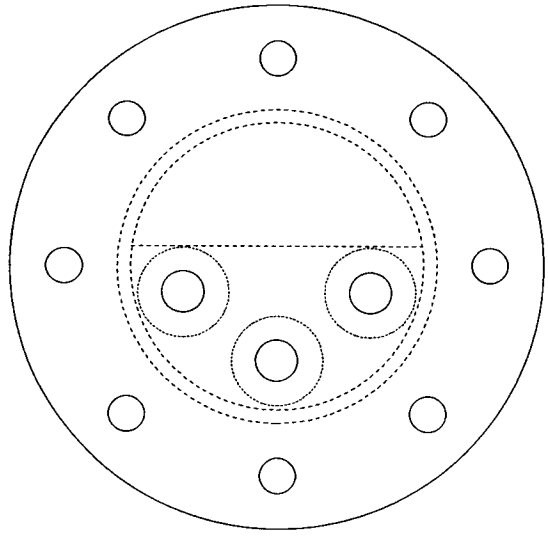

Figure 3.4: Side view of evaporator

A typical example is shown in Figure 3.5. A $\frac{3}{4}$" hole was drilled and tapped into the flange. A $\frac{3}{4}$" high pressure Wade hex male stud coupling was screwed into the hole. A Dowty seal provided sealing between the hex fitting and the flange. The inside of the hex fitting had been bored out to allow the glycol tube to pass completely through it. A brass compression ring was fitted onto the glycol tube and this provided sealing, with a $\frac{3}{4}$" nut which was screwed onto the outer side of the hex fitting. Pipe sealant was also used on the threaded fittings to prevent refrigerant loss.

Each end plate had another hole bored in it about 8cm from the bottom to allow the refrigerant from the metering pump to enter the evaporator. The fittings on these were similar to those for the glycol tubes in Figure 3.5. The right hand end plate had two further holes so the level in the evaporator could be measured. This was carried out using a pressure difference transducer. The level was calculated by measuring the pressure difference between the bottom of the liquid and the vapour above the liquid. Three refrigeration valves on the inlets and outlet were installed to isolate the evaporator, which acted as a refrigerant store when the plant was not operational. On

the vapour outlet a tapping was added for an electronic pressure transmitter which allowed for electronic monitoring of the evaporator pressure. A pressure relief valve was also installed on the evaporator outlet (set at 350 p.s.i.). The discharge vented to atmosphere outside the laboratory. The evaporator was mounted on a special stand. After it was plumbed in, an insulation box was constructed around the evaporator. This was filled with perlite type insulation to minimise heat losses and prevent the build-up of ice from atmospheric moisture.

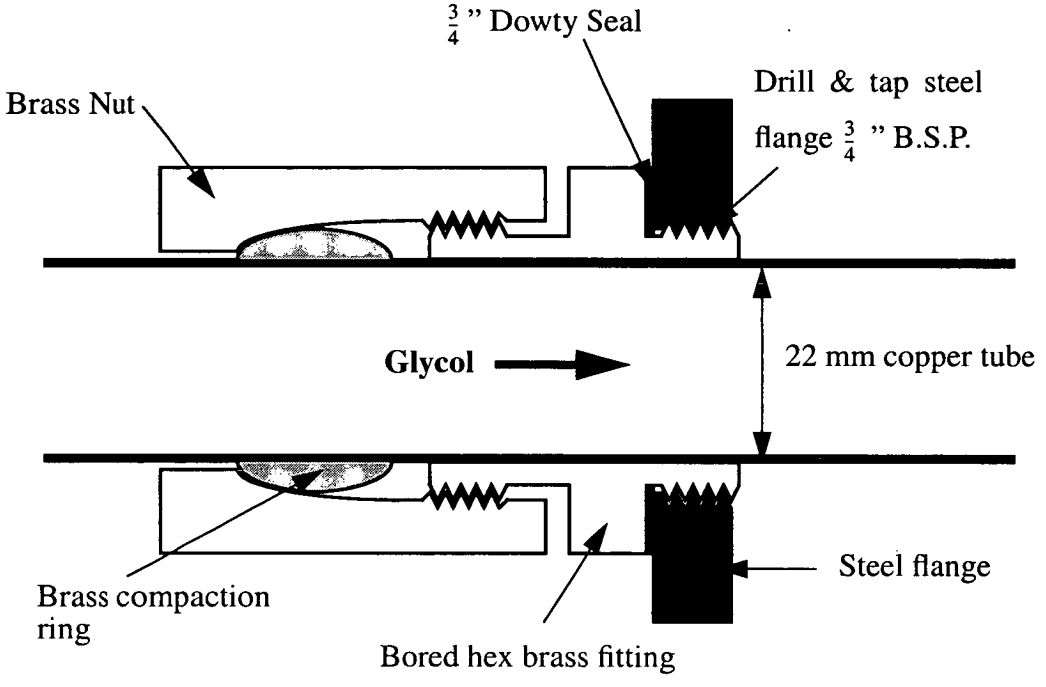

Figure 3.5: Brass fittings between evaporator flange and glycol tubes.

3.4.7 Glycol and Water Stream Equipment

It was intended that the same systems would be used to transfer the heat sink and source streams to and from the evaporator and condensers. The material for each

stream was stored in a metal buffer tank. Electric kettle heaters ensured that the temperature in the tank was kept constant, which could be set from the computer. Regenerative pumps were used in both streams. These had a maximum flowrate of $39 l min^{-1}$ at 0m head pressure. New flowrates and the change in pipework required pressure drop calculations to be undertaken. Flowrates of 18 and 36 litres per minute were selected. Pressure drop calculations indicated that the pumps would be able to deliver these flowrates. New rotameters and flow measuring equipment were installed as a result of changes in flow rates.

3.4.8 Miscellaneous

A number of other pieces of equipment were added to the plant to ensure smooth operation. Each piece of equipment was isolated during shut down by standard ball type vales. These prevented total loss of refrigerant in the event of a leak while the plant was not operational. They also speeded up the location of leaks. Two in line refrigerant driers were installed on the two evaporator feed lines to remove any water in the system. Pipe sealant was placed on all the non brazed joints. Losses due to leaks would have been considerably greater without this. A special hand held electronic HFC refrigerant leak detector was purchased to locate leaks.

All of the refrigerant, water and glycol pipework were wrapped with insulation to prevent heat losses or gains. A fan was mounted beside the plant to remove any vapour leaks to the external atmosphere. A transparent plastic curtain was erected around the plant to ensure that the immediate surrounding air was in circulation around the plant.

3.5 Instrumentation and Control

3.5.1 Previous Plant Instrumentation and Control

Due to the pilot plant's complexity, the instrumentation was based around a microcomputer. This would monitor, log and display pertinent plant variables. Also the system would take action in the event of unsafe operation and warn the operator. In Low's plant, 24 temperatures, 5 pressures, 2 water flowrates, 3 liquid levels (evaporator and two flash pots), 2 differential temperatures and the position of the metering pumpheads were recorded. Five control valves were placed on the plant. Two were located after each flash pot; one control valve was placed before each glass storage tank to provide for the working fluid's expansion.

Low used an IBM 286 compatible personal computer to record the data. The temperatures were measured by K type thermocouples. The signals from these were amplified and filtered by two CIL PCI 1002 units. These were based on the IEE-488 communications protocol. An Amplicon PC-30, interface card dealt with pressure, flowrates, temperature difference in the water streams and the control valves. The card operated with both digital and analogue communication. Analogue inputs were used to communicate process information from the plant e.g. pressure, glycol flowrate etc. Digital outputs enabled the tank heaters to be turned on and off and the metering pump stroke settings to be altered. Analogue outputs were used to vary the stem settings on control valves.

3.5.2 Requirements

Using the plant to examine refrigerant HFC mixtures meant that the plant would be run until the intended steady state conditions were reached and the relevant data recorded. Tight control did not assume the same importance as in Low's plant because no deliberate disturbances would be applied. As outlined in Section 2.3 on page 20,

comparing pure and mixed refrigerant should be done on the basis of the same heat and sink temperatures and the same log mean temperature differences. Manual intervention would prove to be more efficient in meeting these requirements. Data collection assumed a greater importance than control. A full piping and instrumentation diagram of the plant is given in Figure 3.6 on page 94.

3.5.3 Modifications of Control and Instrumentation

3.5.3.1 Microcomputer and Software

A number of modifications and alterations were made to the plant's instrumentation and control system. Since the plant itself was modified the measurement of plant data would also change. The PC was upgraded to a 386. Later this was superseded by a 486 type computer which allowed for much faster scanning of the data. Thermodynamic properties could be calculated on-line using the Carnahan-Starling-DeSantis equation of state. Parameters such as COP could also were displayed in real time. The original TurboC software was retained. Over time the program was substantially altered. This was necessary to accommodate new instruments. The basic windows format of the program was retained but a colour monitor meant that a more user friendly display was developed. The program was also altered to include a number of alarms which would warn the operator of any unusual developments such as a high or low temperatures etc.

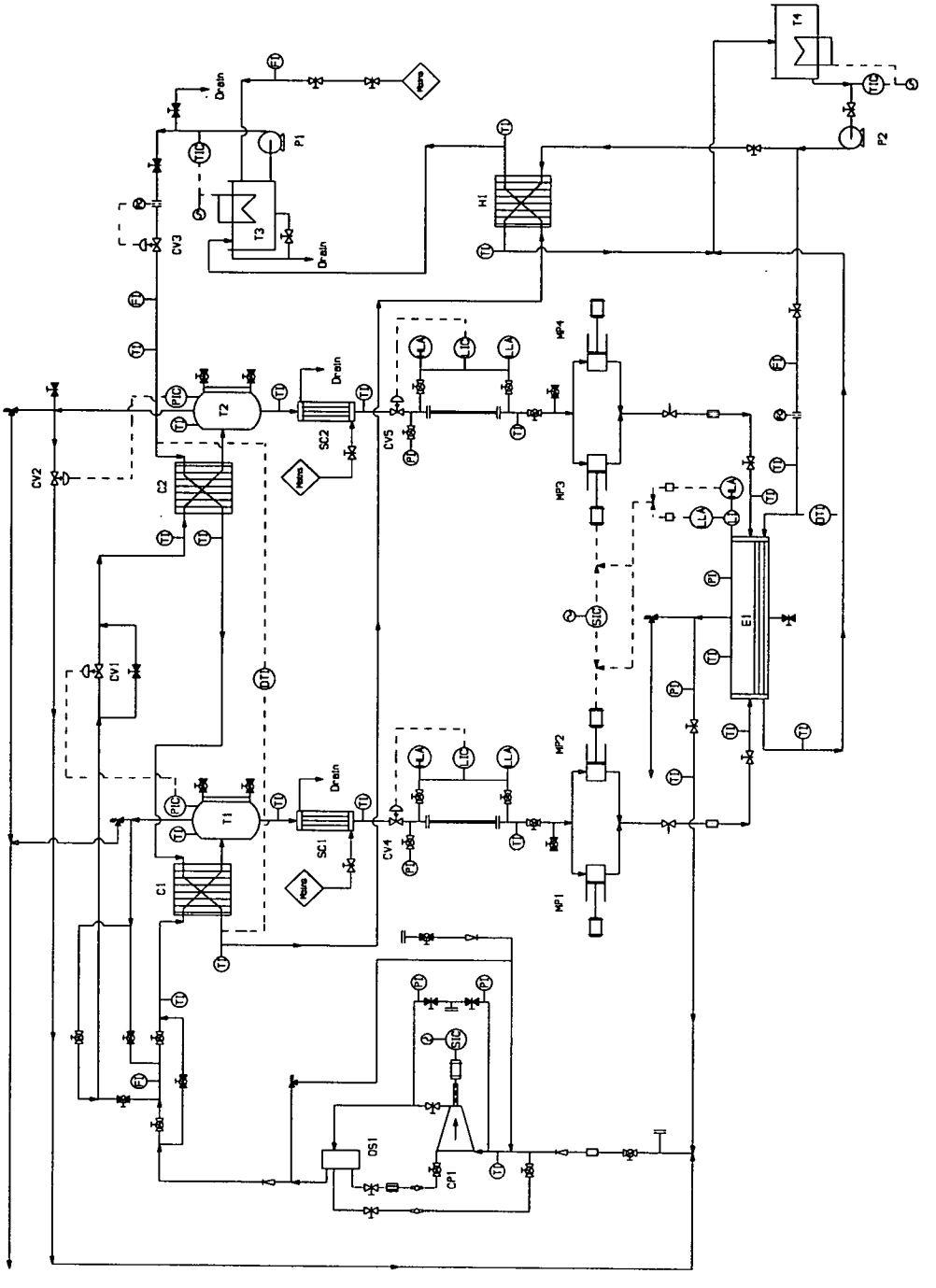

Figure 3.6: Piping and instrumentation drawing of refrigeration plant

3.5.3.2 Temperature Measuring System

A temperature measurement system similar to that used by Low was employed. The two CIL PC1002 amplification boxes were reused. These boxes converted the thermocouple voltage into a 255 bit number which was communicated to the computer. The bit numbers were converted into meaningful temperature by the software. Each box sent the data on request from the PC. All the K type thermocouples were replaced.

Table 3.1: Locations and channels of thermocouples

Locations of Thermocouples for Box 1	Channel	Locations of Thermocouples for Box 2	Channel
Compressor Suction	4	Evaporator Outlet	4
Condenser 1 Inlet	5	Compressor Discharge	5
Flash Pot 2	6	Condenser 2 Water In	6
Subcooler 1 Outlet	7	Condenser 2 Water Out	7
Expanded Liquid in Leg 1	8	Condenser 1 water Out	8
Flash Pot 1	9	Plate Heat Exchanger Water Out	9
Subcooler 2 Outlet	10	Evaporator Liquid Refrigerant	10
Expanded Liquid in Leg 2	11	Evaporator Glycol In	11
Plate heat exchanger glycol out	12	Evaporator Glycol Out	12
Condenser 2 Vapour Outlet	13	Condenser Vapour Outlet	13
Evaporator Feed 1	14	Water Mains	14
Evaporator Feed 2	15	Glycol Tank	15

Apart from the compressor discharge, the locations of the thermocouples on the high pressure side of the plant remained the same since this part of the plant was not altered. A thermocouple was located directly at the compressor discharge port. Previously the compressor temperature had been recorded from the vapour entering

the first condenser. Since the evaporator side of the plant was reconstructed, new thermocouple locations were specified. The location and channel number of each thermocouple is detailed in Table 3.1. A new IEE-488 interface card was purchased to ensure faster communication between the boxes and the computer.

3.5.3.3 Pressure, Flowrate, Temperature Difference, Miscellaneous Measurements and Control Output

The original Amplicon interface card and conditioning cards were preserved and reused. This system provided more than enough gremlins to ensure the author satisfied his contractural obligations as regards time spent on the job! Much of the instrumentation was based on a 4-20mA current signal. Signal conditioning cards constructed by Mr. Matthew Rea converted these signals to 5V. The signal was then transferred to the Amplicon card which converted the voltage to a bit number between 0 and 4095. This required a separate calibration for each instrument connected to the Amplicon card to provide a relationship between the measured variable and the bit number recorded by the card.

The pressure transmitters on the condenser flash pots were retained. New pressure transmitters, with a maximum allowable pressure of 35barg, were installed on the evaporator and on the pipework on the metering pump inlet. Before installation, these had to be calibrated to ensure accurate measurement. The metering pump stroke setting control system and the system used to remotely turn on and off the pump motor were not altered. The same on/off control system was employed to maintain a constant temperature in the sink and source tanks.

The control valves on the plant were not removed or relocated. These had a pressure rating of 300bar and so they were suitable for use with R32. Originally the level in the flash pots was controlled by the expansion valves on Low's plant. These were hardware controlled. For ease of use these were converted to software control i.e. the

operator could vary the stem setting if so desired. This initially provided an awkward problem since the Amplicon had only four analogue output channels and six analogue outputs were required. An ingenious solution was developed by Mr. Matthew Rea, whereby sixteen digital channels were manipulated to provide an "analogue" output.

Two differential thermopiles were used to provide a measurement of the temperature difference in both sink and source streams. These provided a more accurate estimation of the temperature difference rather than relying on the difference of two thermocouples. Level measurement in the $\frac{3}{4}$" pipes was achieved by taking the pressure differential transmitters used by Low to measure fluid flow and recalibrating them to measure the height of liquid in the legs. Table 3.2 tabulates the location and channel number of each of the 4-20mA instruments used.

Table 3.2: Location of analogue instruments

Instrument and Location	Channel	Instrument and Location	Channel
Condenser 1 Pressure	13	Evaporator Liquid Level	5
Condenser 2 Pressure	7	Expanded Liquid Level in Leg 1	3
Expanded Liquid in Leg 1	4	Expanded Liquid Level in Leg 2	6
Expanded Liquid in Leg 2	14	Stroke Setting on Metering Pumphead 2	8
Evaporator Pressure	15	Stroke Setting on Metering Pumphead 3	9
Glycol Flowrate	0	Glycol Thermopile	11
Water Flowrate	1	Water Thermopile	12

3.5.3.4 Heat Sink and Source Temperature Control

The same on/off system as used by Low was retained to maintain a constant temperature in the heat sink and source streams. When the temperature went below

the setpoint the computer sent a signal via the Amplicon card to an electrical relay. Originally these relays were located in a box underneath the glycol tank and beside the pump. The relays were replaced and the box was relocated above the tank. This was done to reduce any risks resulting from glycol leaks from the pump which could find their way into the box.

3.5.3.5 Flow Measurement

Sink and Source Streams

The flowrates of the sink and source streams were originally measured using orifice plates. Pressure difference transducers, based on a 4-20mA signal, were then used to record the pressure difference allowing the flowrate to be calculated. On the modified refrigeration plant the transducers were relocated to measure the height of liquid in the pipes on the suction side of the metering pumps. On the water stream the same orifice plate/pressure drop system was used. The diameter of the orifice was increased from 11 to 13mm. The pressure drop across the orifice plate was measured by a simple pressure differential measuring device constructed by Matthew Rea. This was calibrated against a size 18 stainless steel water rotameter. The orifice in the glycol stream was replaced by a turbine flowmeter. This gave a linear output which meant it was far easier to calibrate. This was calibrated against a size 24 stainless steel rotameter. The rotameter calibration had to be recalculated because the 60% ethylene glycol has a higher density ($\approx 1080 kg m^{-3}$) than water. The calibration also had to take into account the fact that the density of the glycol would change as its temperature changed. The glycol could experience a temperature change of 40 degrees C, as it went from ambient to the desired heat source temperature. Using formulae from the rotameter manual [*Rotameter Manufacturing Co.*] new calibration charts for the glycol were calculated and drawn. Since density changes with temperature a calibration curve was calculated for 20, 0,-5, -10, -15 and -20°C.

Refrigerant Flowrate Measurement

One of the specifications in the project remit was that the refrigerant flowrate should be directly measured. The flowrate could be measured using an orifice plate or some similar method. However, an accurate value of the density would be needed to calculate the mass flowrate. With mixtures of new HFC refrigerants accurate values of density could not be guaranteed. It was decided that an instrument that recorded a direct measurement of the flowrate would give a more accurate value of the plant's flowrate. Hence a coriolis type mass flowmeter was purchased. These type of flowmeters measure the difference in frequency between two vibrating loops through which the vapour flows. The flowmeter came in two parts: a sensor which had a maximum measurable flowrate of $150 kg hr^{-1}$, and a flow transmitter which allowed the information to be sent to a computer. The sensor was plumbed in to the pipework immediately after the oil separator. The sensor measured the temperature, density and total flowrate. This was connected to an RFT9712 flow transmitter which processed the data and sent it to the PC. In order to correctly read the data a PCI_743 PC-Labcard was purchased. This used the RS-485 communications protocol to read the data. This particular coriolis flowmeter was a "semi-intelligent" device. It could give back the data in the format required by the user e.g $kg hr^{-1}$, lbs^{-1}, °F etc. Also it had the great advantage that it was calibrated at the point of manufacture.

Originally it was intended to have two flowmeters: one on the compressor discharge and one on the vapour flowing from flash tank no. 1 to condenser 2. However the high cost meant that only one could be bought. A bypass system of valves was constructed so that either the compressor flow or the vapour flow to condenser 2 could be measured, but not simultaneously by the same flowmeter (Figure 3.6 on page 94).

3.6 Plant Layout

The plant is shown by a series of photographs. Individual pieces of equipment are labelled.

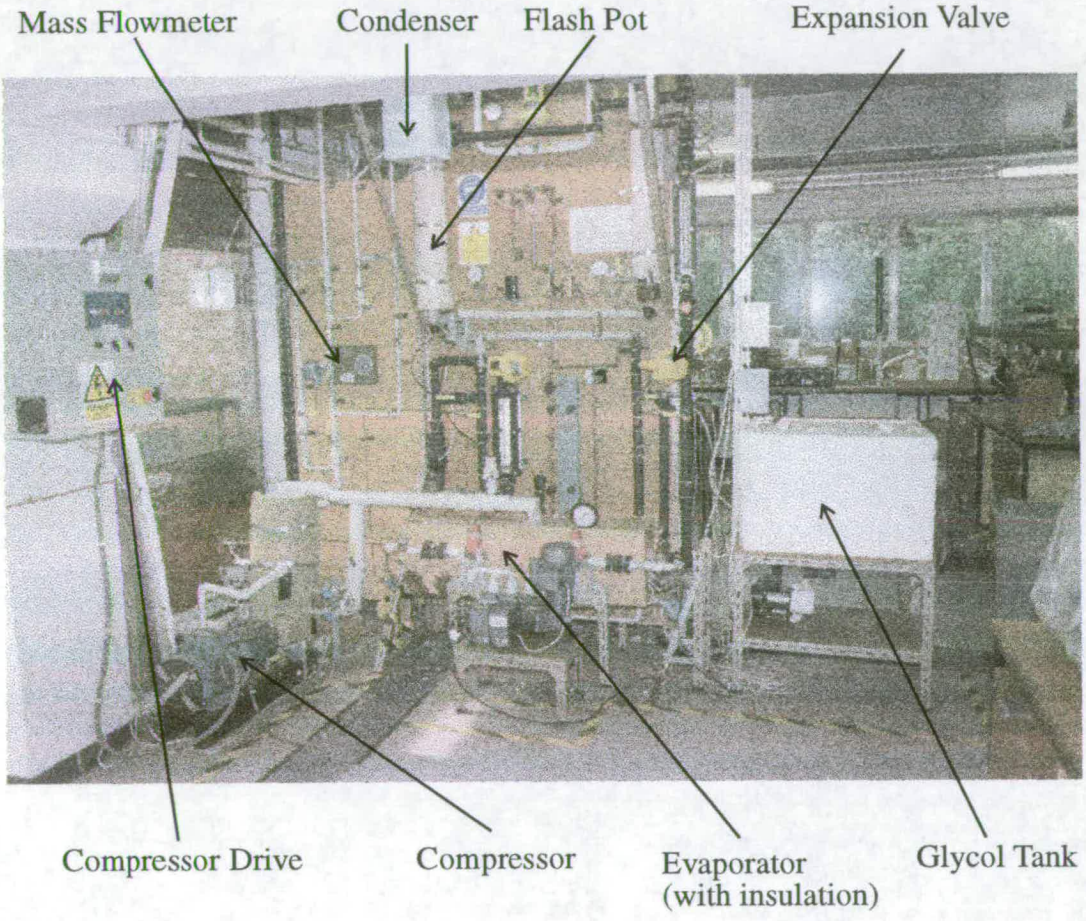

Figure 3.7: Front view of plant

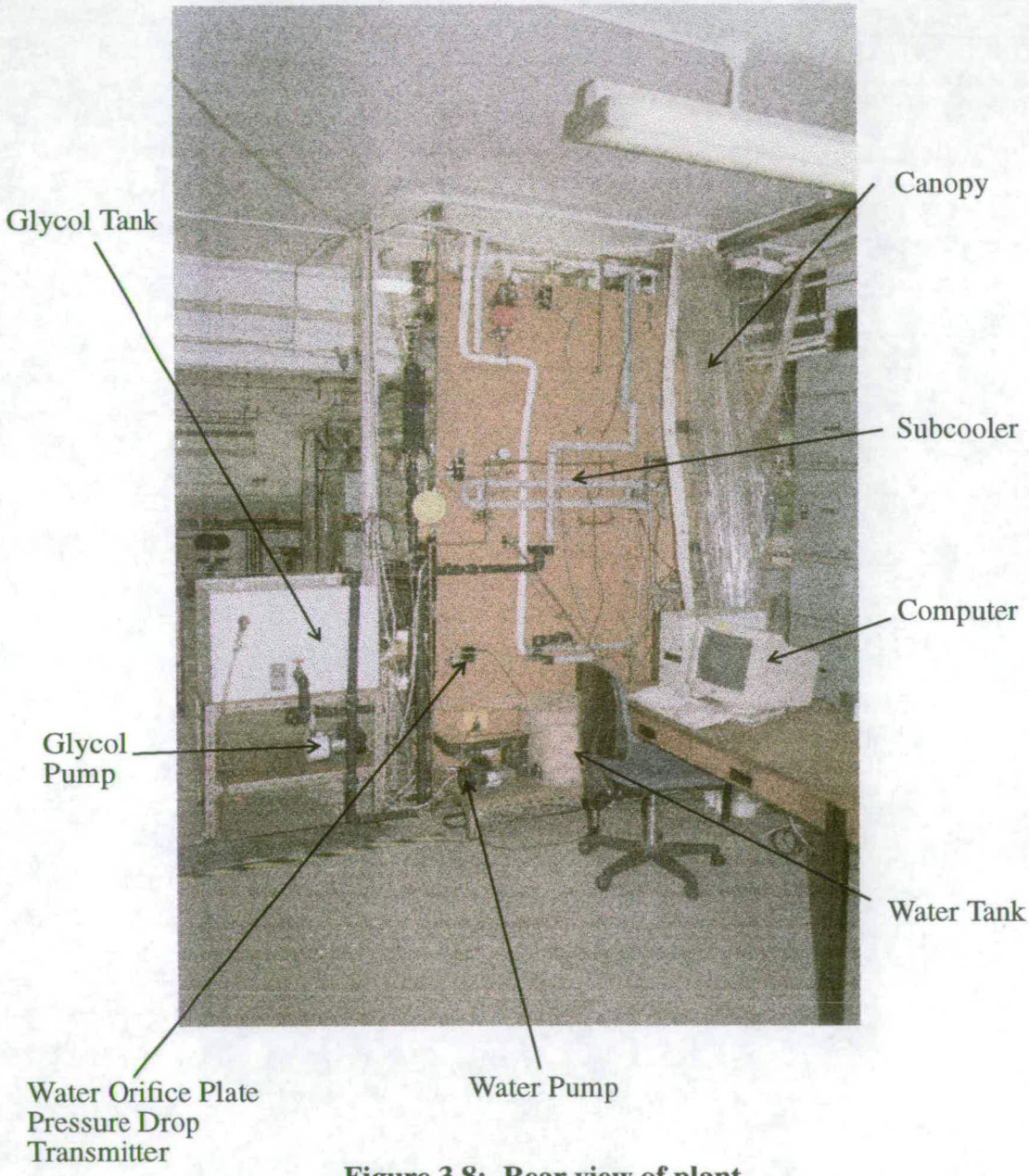

Figure 3.8: Rear view of plant

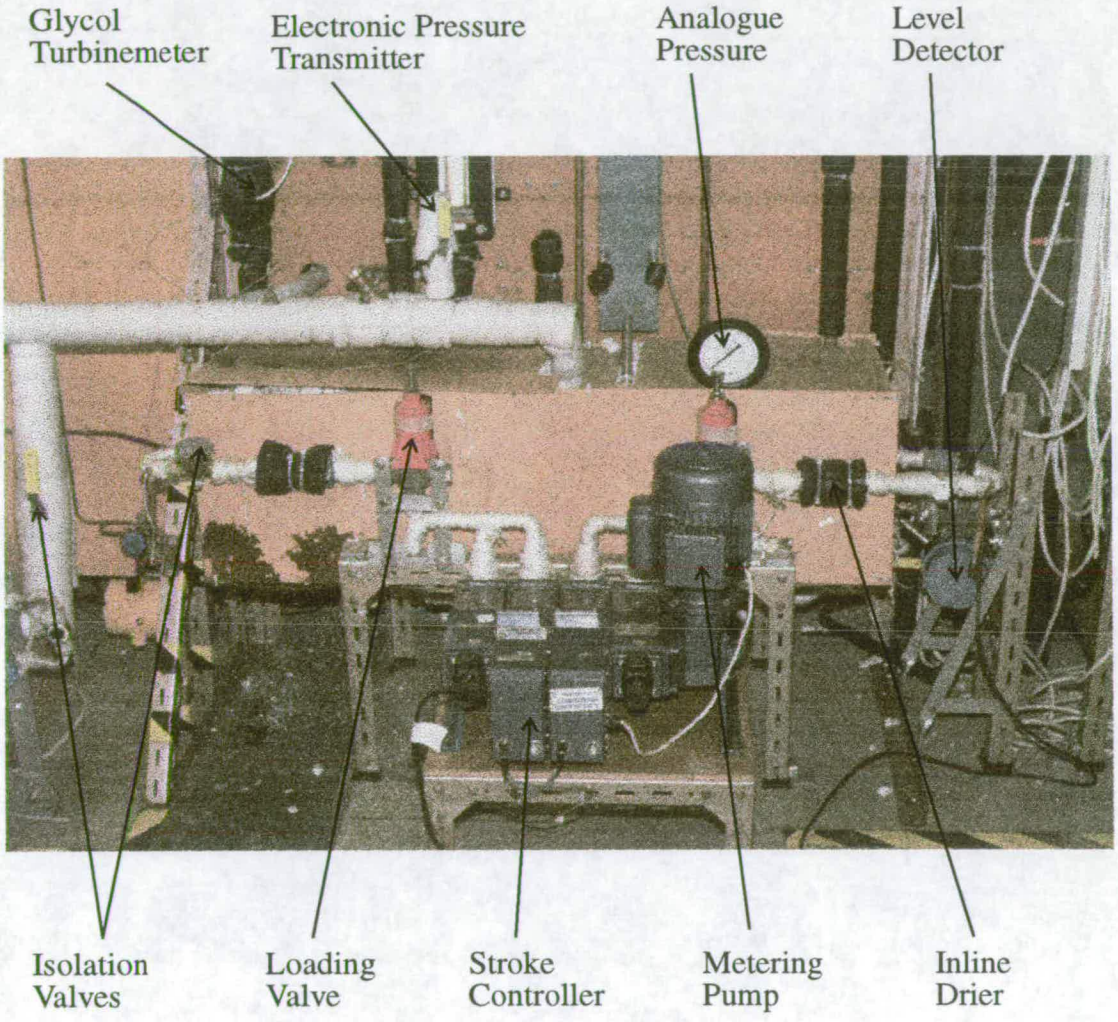

Figure 3.9: Evaporator and ancillary equipment

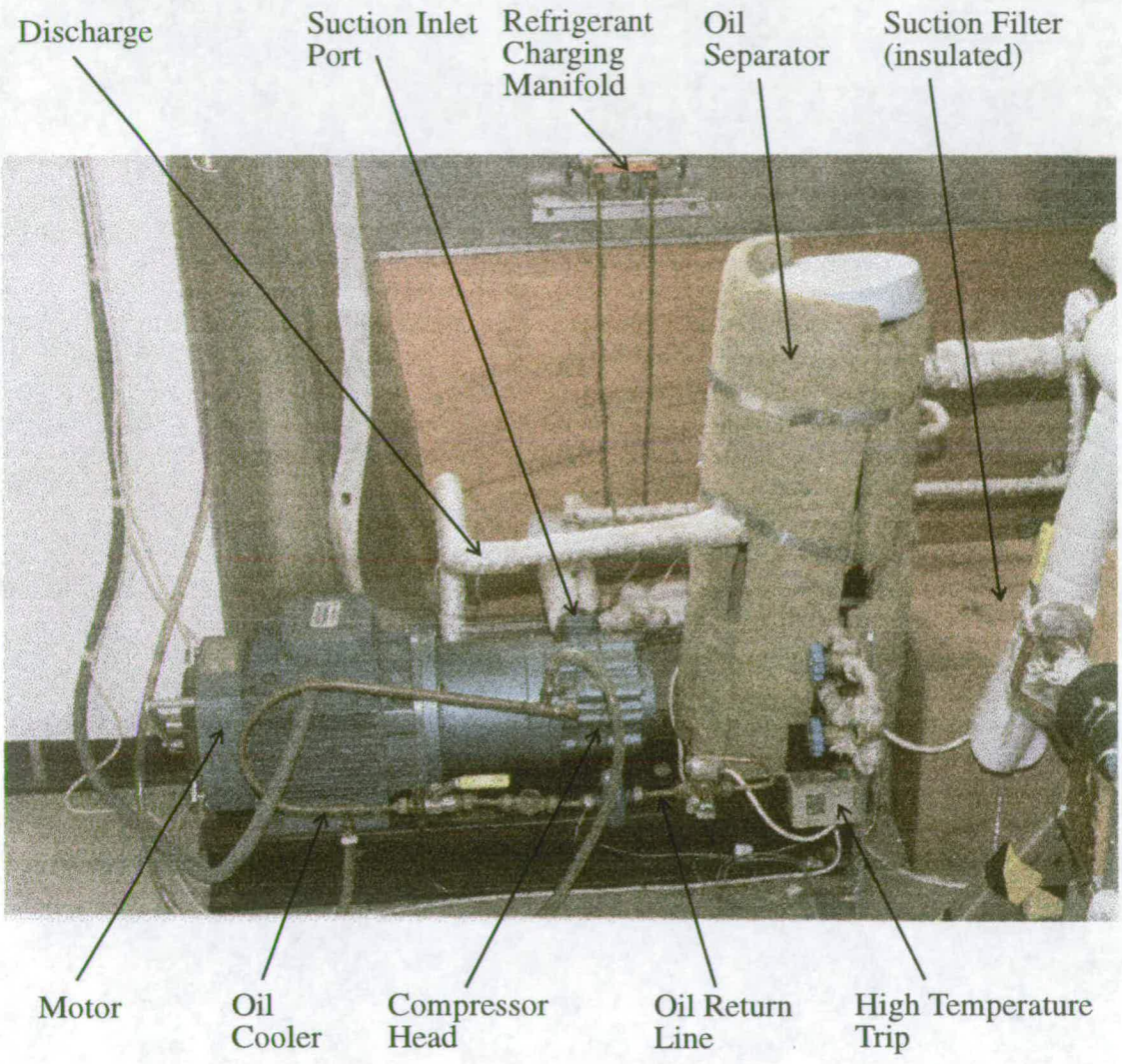

Figure 3.10: Compressor and ancillary equipment

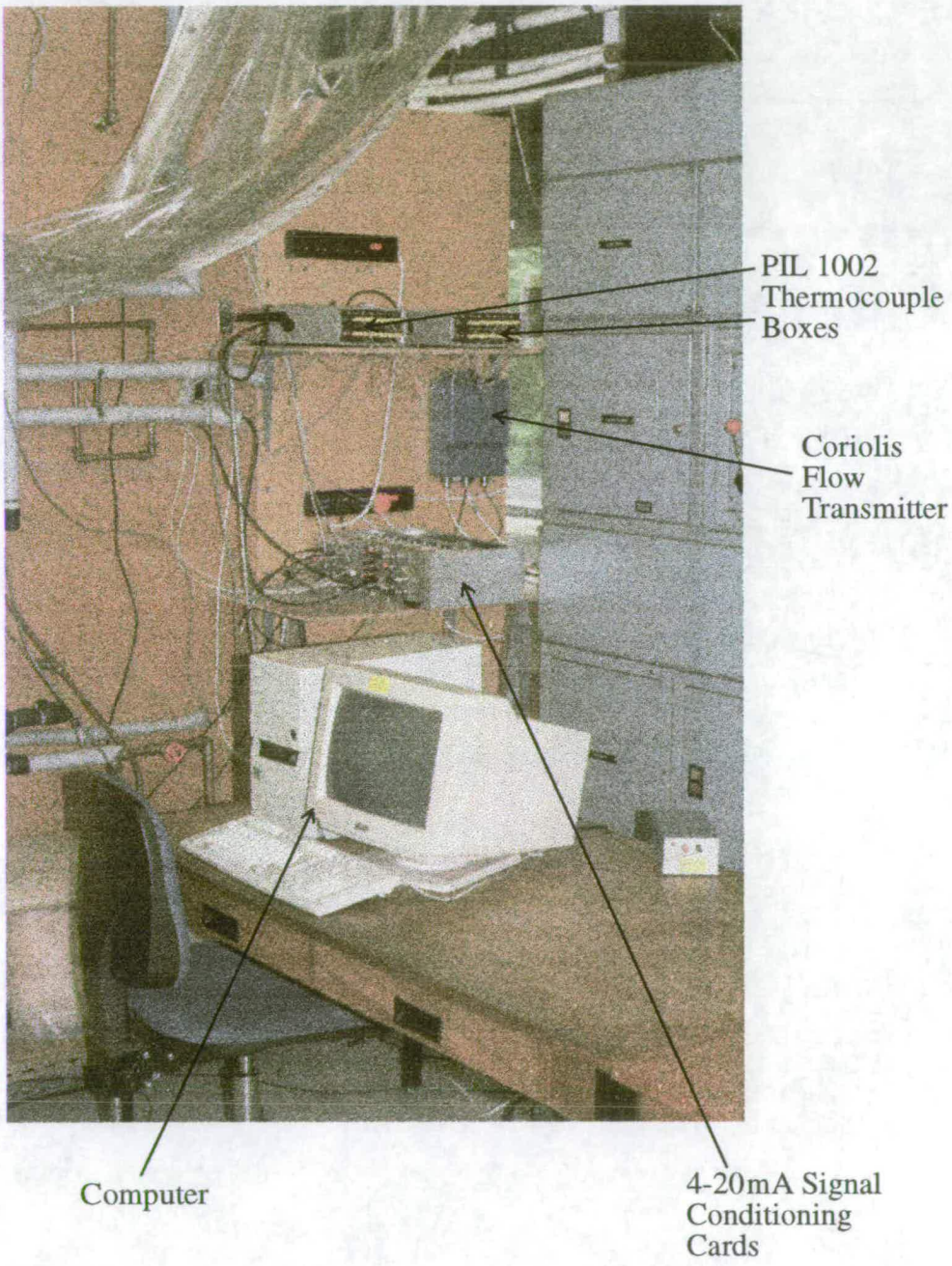

Figure 3.11: Electronic instrumentation and communications equipment

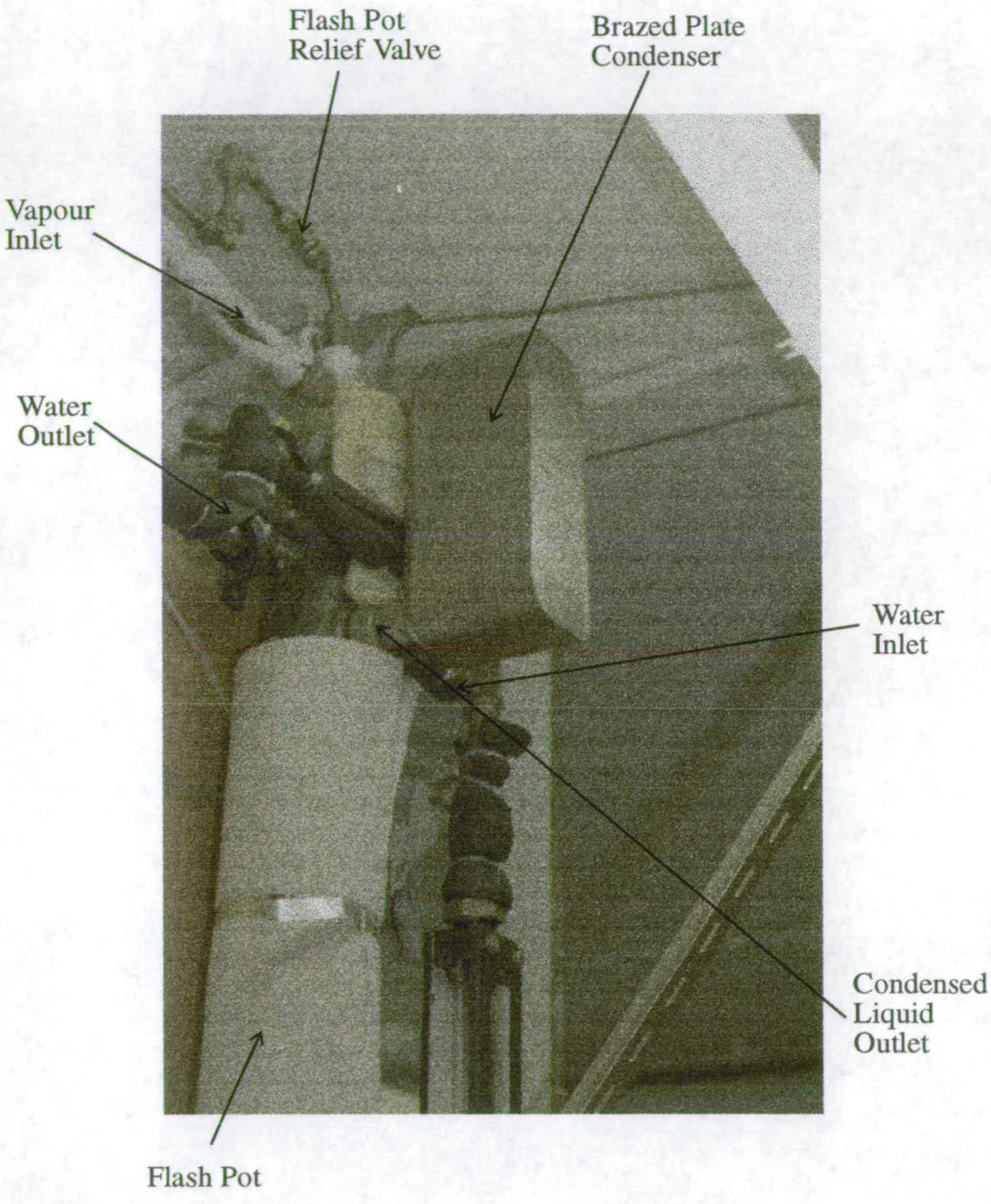

Figure 3.12: Condenser number 2

Chapter 4

Pilot Plant Experimental Investigation of Hydrofluorocarbon Mixed Refrigerant Working Fluids

4.1 Introduction

Once the modifications to the pilot plant were completed, commissioning of the plant was undertaken. Each piece of equipment was individually tested to ensure correct and satisfactory operation. A substantial part of the commissioning work was in ensuring that the plant was leak tight. Differential fractionation of the more volatile component (R32) could have lead to the composition of the plant altering over time. Once the commissioning was complete and sufficient operational experience gained, the experimental program could commence. The experimental results obtained from operation of the pilot plant are described here. The composition of an R32/R134a mixture was to have been varied from pure R134a to pure R32 in composition intervals of 20 wt.% R32. to ascertain if the COP for the mixtures was larger than those of the pure fluids. However the experimental program was prematurely terminated by the theft of the computer, which measured and recorded data from the plant's instrumentation. This represented a fatal setback in the progress of the experimental investigation since the electronic interfaces, used to record data from the

plant's instruments were also misappropriated. Considerable time and effort had been invested in getting the computer to correctly interact with all of the plant's instruments, as well as overcoming other operational problems associated with the plant. Although the experimental objectives of the project were not achieved, research work was successfully carried out on the prediction of HFC thermodynamic properties from sparse data (Appendix B and Appendix F). A simulation model of a refrigeration cycle with binary mixed working fluids was developed and used to investigate the efficiency benefits of HFC mixtures. Results were obtained from the model and these are presented in Chapter 5.

A number of commissioning runs with pure R32 and pure R134a were made prior to the theft of the computer. One experimental series of runs had been made with a 21.9/ 78.1 wt.% mixture of R32/R134a. Data from these runs are presented in this chapter along with general conclusions about the operation of the plant.

4.2 Plant Commissioning

The commissioning and initialisation of the plant prior to the first runs are described in this section. After construction the plant underwent an extensive leak testing program. Instrumentation and control systems were checked. A number of modifications were made for a variety of different reasons and are outlined in the chapter.

4.2.1 Condenser Water Circuit

Commissioning of the water circuit was embarked upon first since it was relatively straight forward. The thermocouples were checked for consistent readings and they were found to record a steady and even temperature over a number of hours.

Calibration of the flow measuring instruments was then implemented. The water stream flowrate was calculated by measuring the pressure drop across an orifice plate. An 8mm diameter had been previously used. This gave too high a pressure drop for the pressure transmitter at the flowrate that was to be used. The transmitter did not have an adjustable range and zero so the diameter of the orifice plate was increased to 10mm. The pressure transmitter was calibrated against a standard water rotameter (size 18 steel float). A TurboC program (CALIB.EXE) was used in all calibrations of 4-20mA instruments connected to the Amplicon interface card: five pressures transmitters, two temperature difference thermopiles, two liquid flowrate measuring devices and three liquid level detectors (Section 3.5.3.3 on page 96). Calibration required that each variable was measured by another instrument, in this case the water rotameter. The program measured and recorded the incoming voltage from the instrument into the Amplicon card and converted this into a bit number between 0 and 4095 (12 bit accuracy).

Air bubbles were flushed from the transmitter's connecting pipework. The temperature in the water tank was brought to the temperature used in the experiments (20°C). Using a hand valve the flow was set to a prescribed value and was allowed to settle. The computer then recorded the average of a total of 1000 individual readings of average flow. The flow was then readjusted and recorded again. This was repeated over the full range of flow. A relationship was established between the actual flow, as determined from the rotameter chart, and the average bit number which the computer read from the Amplicon card. For the orifice plate this had the form:

$$Flow = Offset + \frac{\sqrt{Bit\ Number}}{Gain} \qquad \text{(Eq 4.1)}$$

The values of the offset and the gain were determined by regression of the calibration data. These values were then installed into the control software. The flow measured by the pressure transmitter and the computer were then checked against the flow from the rotameter. The discrepancy was $0.1 l hr^{-1}$ (1.4% of full flow).

4.2.2 Temperature Control of Sink and Source Streams

Operation of the plant would require satisfactory operation of the temperature measuring systems. As described in Section 3.5.3.2 on page 95, 2 PCI 1002 thermocouple junction boxes sent 255 ASCII characters, for each thermocouple, to an IEEE 488 interface card. This card transferred the data to the computer enabling it to calculate and record a temperature. The manufacturer's supplied software written in QuickBasic allowed the computer to correctly read the data from the junction boxes. Since the program to control the whole plant was written in TurboC, attempts were made to translate the QuickBasic program into TurboC. However, the C programs proved unreliable over a period of a number of hours. After an initial period of ten minutes or so of satisfactory operation, data would not be completely read from an arbitrary channel, by the IEEE interface card. This would then stop all data transfer from the other junctions. The solution was to implement a routine in the plant control program which called the manufacturer's Basic program. The manufacturer's program was altered so that the thermocouple data was transferred to a binary file. This was then read by the control program and displayed on the screen. Although this approach would not draw gasps of breath from the electronic engineering profession, it proved reliable in supplying temperatures from the plant.

4.2.3 Coriolis Flowmeter

Communication with the coriolis flowmeter was carried out in a similar manner to the CIL thermocouple boxes. The computer sent a signal via an PCL_743 interface card to the RFT9712 flowtransmitter requesting information on the refrigerant flowrate being measured. This then sent back data in the form of ASCII characters which the PC could convert into a meaningful flowrate. The interface card (PCL 743B) used the RS 485 serial communications protocol. The suppliers of the flowmeter (Rosemount) also included some of their own software. Initially the PCL card was tested by

sending text to a BBC microcomputer which then displayed the text. However successful communication between the PCL card and the flowtransmitter proved extremely difficult to obtain. Signals to the flowtransmitter were successfully sent out by the PCL card but the RFT9712 remained obstinately mute. After much tinkering and cajoling by Mr. Matthew Rea and the author, meaningful data eventually emerged from the transmitter. This was achieved by setting one of the jumpers on the PC-743 to allow direct control of the transmitter and receiver. This meant that the software program instructed the card to turn on and off the transmitter and receive at the appropriate times. To reduce variations in measurement, an average of five individual readings was taken each time the flow was measured.

4.2.4 Other Instruments

The five pressure transducers were calibrated using a special pressure calibrator. These had a linear output of bit number vs. pressure i.e.:

$$Pressure = Offset + \frac{Bit\ Number}{Gain} \qquad \text{(Eq 4.2)}$$

As with the water stream the offset and gain were found using the CALIB.EXE program. The transducers were set up so that the maximum pressure that could be measured was 40bar g. This was because the maximum allowable pressure for the transmitter was 35bar g. The conditioning card for the evaporator pressure was later altered so that the full scale pressure was 20bar g which allowed for greater accuracy at lower evaporator pressure. During operation, the pressure transmitter on the leg 2 after the expansion failed and had to be replaced by a transmitter which had a maximum allowable pressure of 20bar g.

The water and glycol thermopiles were calibrated by placing the cold junction in a beaker of water at ambient temperature. The hot end was placed in an insulated beaker

of warmer water. Boiling water was added to increase the temperature difference. The temperature of each beaker was measured by using a digital multichannel thermometer. Five measurements from each beaker were taken by separate thermocouples and averaged. This was to ensure that a less accurate method was not used to calibrate an instrument with a greater accuracy (the thermopiles used the average temperature difference of 5 thermocouple junctions). Water in a glass tube whose height was measured was used to calibrate the level detectors. The inlet pipe of the detectors was placed at the zero mark of the tube. The height of water was varied allowing the gain and offset to be calculated. The thermopiles and level detectors had linear outputs similar to pressure and used an equation similar to Equation 4.2.

4.2.5 Compressor

The compressor control system was checked by Mr. Mathew Rea. All the necessary trips and controls were found to be in good working order. The compressor head was removed and the vanes were cleaned. No damage or significant wear were discovered. Before turning the compressor over, oil was added via a port on the oil separator. All the valves were opened on both oil return lines. The compressor was turned over slowly to ensure that rotation was in the correct direction.

4.2.6 Leak testing

The refrigeration plant had to be made as leak tight as possible. Leaks would alter the global composition of refrigerant mixtures and leaks of flammable material could pose certain risks. After construction, an extensive and lengthy program of locating and removing leaks was undertaken. Throughout the experimental research for this thesis, a constant and often losing battle was fought against the insidious behaviour of leaks. Removal of leaks involved a process with a number of different stages.

Before detection of leaks the interior of the plant had to be vacuumed and cleaned. The plant had been fitted with a number of different tappings to allow any gas to be removed. The plant was connected to a vacuum pump and this was operated almost continuously for a week. All pieces of dirt and loose debris were removed. The vacuumed gas was passed through a liquid nitrogen bath. Thus water or any other foreign material was removed. The plant was then pressurised with nitrogen. All isolation and control valves were opened before addition of nitrogen to ensure that all parts of the plant were pressurised. Each section of the plant was then isolated so that, if a leak occurred, the number of possible joints responsible would be reduced. The plant was then allowed to stand for a number of hours. A computer program was written for the control computer which monitored the loss in pressure over time. If a leak occurred a soap solution was passed over the joints. Leaking nitrogen would blow a fine froth of bubbles. The joint would be then tightened. This eliminated all the larger leaks.

The nitrogen was removed and the plant was filled with R22. A special propane gun was then used to detect leaks. This was a simple propane gas blowtorch. In the presence of chlorine containing compounds the flame would change from blue to green. A pipe connected to the flame was passed over a suspected joint and if the joint leaked the flame would change colour. To improve the plants ability to hold refrigerant vapour, leaky joints were sealed with a special joint sealant. This helped to seal most of the threaded joints on the plant. Losses would have been considerably greater without this. The sealant was applied to both parts of the joint. The sealant required 18 hours at normal pressure to properly seal a given joint. This meant that the section of plant where the leak occurred had to be isolated and allowed to stand for 18 hours. It was decided at this stage to apply the Loctite sealant to all threaded joints that came into contact with the refrigerant working fluid.

Once this was completed, the plant was charged with R32 refrigerant to a low pressure and this was monitored by the computer. Leaks were then detected by the

hand held leak detector (Section 3.4.8 on page 91). This could detect leaks of HCFCs and HFC refrigerants. The detector's probe was passed over a joint. A leak was signalled by a buzzing noise whose intensity was proportional to the size of the leak. This instrument proved invaluable in helping to locate refrigerant losses. It was sufficiently sensitive to pinpoint a leak on a joint but not so sensitive that a tiny leak would cause it to activate far away from the plant. The process of leak detection proved extremely tedious and time consuming. Once a leak was detected the joint was manually tightened. Care had to be taken in not over tightening or rupturing the pipe sealant. Some leaks proved quite difficult to track down and showed an irritating ability to camouflage themselves. Once the loss in pressure was undetectable from the background variation in pressure due to the variation in ambient temperature, the pressure was raised and the process repeated until the normal vapour pressure of R32 was reached. The process of leak detection was conducted until the plant was deemed sufficiently gastight for operation. Although leaks were never fully eliminated, they were reduced to an acceptable level given the number of joints on the plant.

4.2.7 Refrigerant Charging

Refrigerant was supplied by I.C.I. In 9kg gas canisters. All isolating valves were opened and the plant was evacuated. The refrigerant was charged through a special refrigerant charging manifold which was mounted on the compressor. Both the heat sink and source streams were circulated as the refrigerant was added. Refrigerant was charged until the vapour pressure at ambient pressure was reached. The compressor was then started up slowly. Initially the secondary oil return line was left open. This meant that the vapour flow was circulated through this line and not around the plant. After a few minutes a valve on this line was shut causing the compressor to draw vapour from the evaporator. The speed of the compressor was gradually increased. Refrigerant vapour was added through the suction side of the compressor. As increasing amounts of refrigerant were added the liquid level in the evaporator rose.

Refrigerant was added until there was sufficient to ensure that the glycol tubes were covered by liquid refrigerant (a liquid level of 8cm). Once stable operation was reached, the control valves across which the working fluid was expanded were closed causing the temperature on the low pressure side to drop. The glycol flow rate could be adjusted so that the correct operating conditions could be reached.

4.2.7.1 Glycol Turbinemeter

The glycol turbinemeter was calibrated using a similar procedure to the water flow. However because the glycol temperature would vary from 20°C to around -25°C calibration at regular temperature intervals was carried out. This required actual operation of the plant so the turbine meter was the last instrument to be calibrated. Based on transport data from Perry [*1984*] and on methods outlined in the manufacturer's calibration handbook [*Rotameter Manufacturing Co.*], rotameter calibration curves for the 60% ethylene glycol/water solution were calculated. A curve was calculated at intervals of 5 degrees. Maintaining the glycol at low temperature required actual operation of the plant so the glycol turbinemeter was the last to be calibrated. The plant was run until the glycol reached the desired temperature. The flow was varied across the whole range for each temperature. The turbinemeter gave a linear output of bit number vs. flow. The offset remained constant across the range of temperatures. The error associated with this system was 0.1–0.2$l hr.^{-1}$ depending on the temperature (0.5-1.0% of full flow).

4.2.8 Problems Encountered During Plant Operation

The progress of research on the refrigeration plant was slow. A number of problems arose during the commissioning and operation of the plant. These added considerable delays to the research program. The most significant hold up in the progress was the

regular cracking of the brass nuts which clamped the glycol tubes to the evaporator end plates

4.2.8.1 Cracked Nuts

High pressure brass nuts were used to tighten joints throughout the plant. These operated satisfactorily on the high pressure side of the plant. However on the low pressure cold side they were the cause of much frustration. The pipes carrying the glycol into the evaporator were held in place by such nuts (Section 3.4.6 on page 87). They prevented the liquid refrigerant inside the evaporator from leaking. Pipe sealant was applied to the nuts. The nuts had a tendency to fracture along the longitudinal axis on a regular basis leading to complete loss of refrigerant from the evaporator. Once a nut cracked, the evaporator had to be evacuated. If discovered before all the refrigerant was lost, then the working fluid was transferred and stored in the condenser flash pots. The cracked nut was replaced and re-sealed. After the required 18 hours for the nut to be sealed, the evaporator was evacuated and leak tested by incrementally increasing the pressure and ensuring there was no loss over time until it was sufficiently gas tight. It was important to ensure the evaporator was as leak tight as possible since it was here most of the refrigerant was stored when the plant was not operational. Very often after a nut had been replaced other leaks would arise in the repressurisation process. These considerably increased the length of time the plant was nonoperational when a cracked nut was discovered. Often the process of replacing the nut, repressurisation and examining for further leaks took up to a week. The cause of the cracking was never fully established. Fracture also occurred on other brass nuts such as on the compressor suction inlet pipe and on the metering pumpheads. A combination of low temperatures and possible overtightening may have been responsible. It was postulated that contact between the refrigerant and the sealant at low temperatures may have caused expansion of the sealant and consequent fracture of the nuts. The possibility of replacing the nuts on the evaporator with

stainless steel was examined. Since both nuts and bolts must consist of the same material this would have required removing the evaporator from the plant and engaging in time consuming engineering work.

4.2.9 New Electronic Drive

The Jaguar compressor electronic drive shorted out during one experimental run. The cost of repairs was comparable to the purchase price of a new drive. It was replaced by an Excal drive. The Excal could deal with higher currents. The control panel had to be remodified since the Excal was physically much larger than the Jaguar. However the unit had to be returned to the manufacturers on two occasions because some of the safety trips did not work satisfactorily. Eventually the drive was successfully operated. A fan had to be installed in the control panel to keep the Excal cool. Without it the drive would overheat.

4.2.10 Stolen Computer

As has been mentioned in the introduction to this chapter a break-in occurred in the department. The PC controlling the refrigeration plant was among the items stolen. This represented a major inconvenience since the three electronic interface (Amplicon PC-30, IEE 488 & PCL-743) cards were also misappropriated. No data or significant amounts of software were lost since these were backed up on the department's Unix network. The main delay came from the fact that the electronic cards had to be repurchased and reconfigured so that communication could be re-established with the instruments. Considerable time and effort had been invested in getting the original PC to correctly interact with all of the plant's instruments. The theft occurred towards the end of the project and there was insufficient time to set up a new system hence the experimental facet of the research project was abandoned with great reluctance.

4.3 Preliminary Results

This section describes data obtained from some of the experimental preliminary runs obtained from the refrigeration pilot plant. These runs allowed the author to familiarise himself with the operation of the plant. The data acquisition and processing software were also examined to ensure correct operation.

4.3.1 Data Analysis

The refrigeration plant control program allowed data to be stored in files in the computer's memory. Two programs were written to take the information held in these files and analyse the performance of the plant. One was written for pure fluids (PURECSD.EXE) and the other dealt with mixtures (MIXCSD.EXE). Both programs used the Carnahan-Starling-DeSantis equation of state to provide thermodynamic data on the working fluid. The programs calculated values of enthalpy, entropy and exergy at every location on the plant where the temperature and pressure were recorded (Table 3.1 on page 95 and Table 3.2 on page 97). Knowledge of the flowrate, measured by the coriolis meter, allowed refrigerant (working fluid) heat and work loads to be calculated. The results were sent to five separate output files; the first tabulated the conditions at every measurement point in the plant, the second detailed overall cycle performance parameters such as COP, specific volumetric capacity etc., the third detailed the heat and work loads, the fourth described aspects of the compressor performance and the final results file contained an exergy analysis of the plant.

4.3.2 Commissioning Runs With Pure R32

The first results obtained from the plant were completed with pure R32 as the working fluid. Five individual runs were completed. As a basis of comparing results from different runs the following conditions were kept constant: evaporator log mean temperature difference, glycol temperature change (as measured by the thermopile), condenser water inlet temperature and the water flow rate. No refrigerant working fluid conditions were specified, except of course the pressure and temperature limits of the plant. This basis of comparison was chosen from the recommendations of McLinden and Radermacher (Section 2.3.1 on page 21). Fixing the conditions of the external sink and source streams allows a meaningful comparison to be drawn between the performance of pure and mixed refrigerants. Table 4.1 lists the values of these conditions for the runs involving pure R32. For each run the glycol inlet temperature was varied in approximately 5 degree intervals from +5.0°C to -15°C. The actual temperatures were 4.5, -0.3, -3.7, -10.5 and -13.0°C.

Table 4.1: Conditions of preliminary R32 runs

Parameter	Value
Evaporator ΔT_{LM}	13.3 degrees C
Glycol ΔT	5.0 degrees C
Water temperature	15.0°C
Water flow rate	3.3 l min.$^{-1}$

For all the experiments undertaken it proved very difficult to ensure that all of the conditions in Table 4.1 and that the inlet glycol temperature were at the desired level. The plant was quite interactive and adjusting a flow or a valve so that a given condition was at its desired set point usually lead to another variable moving away from its setpoint. Adjustments to the operating conditions had to be done incrementally and very slowly. A run could typically take 2-3 hours.

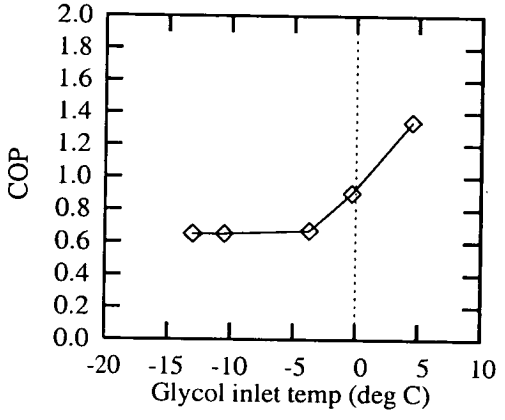

Figure 4.1: R32 COP

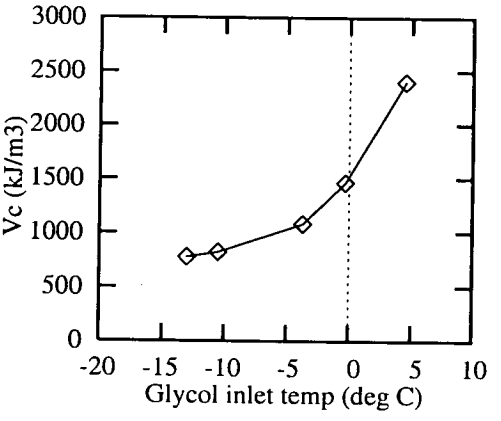

Figure 4.2: R32 specific volumetric capacity

The plant was quite interactive and adjusting a flow or a valve so that a given condition was at its desired set point usually lead to another variable moving away from its setpoint. Adjustments to the operating conditions had to be done incrementally and very slowly. A run could typically take 2-3 hours. After adjustment the plant was allowed to run for a period of time until steady state was achieved. The main cycle parameters are shown in Figure 4.1 to Figure 4.6. For this series of runs the data was not very consistent. The COPs achieved with R32 were quite low, especially at the lower glycol temperatures. (Figure 4.1). A smoother continuously increasing plot of COP vs. glycol inlet temperature would be expected. The graph of specific volumetric capacity (Figure 4.2) is slightly better in this regard.

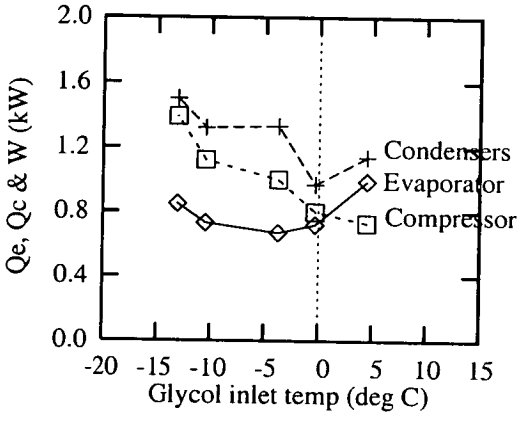

Figure 4.3: R32 Heat and work loads

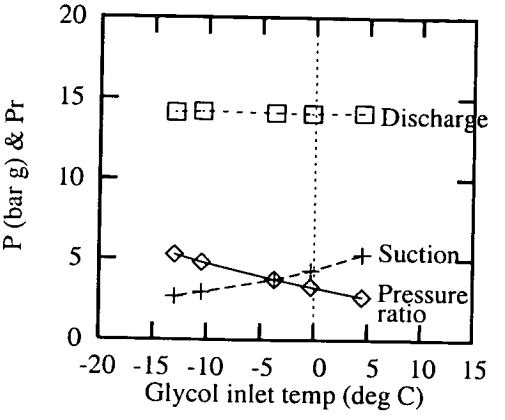

Figure 4.4: Pressures and pressure ratio

The graph of heat and work loads vs. evaporator glycol inlet temperature exhibits quite a bit of scatter. The evaporator heat load goes through a minimum at -3.7°C rather than displaying a continuous increase. The actual values of the heat loads are quite small (0.7-1.6kW). Figure 4.4 shows the pressures in the plant and the pressure ratio.

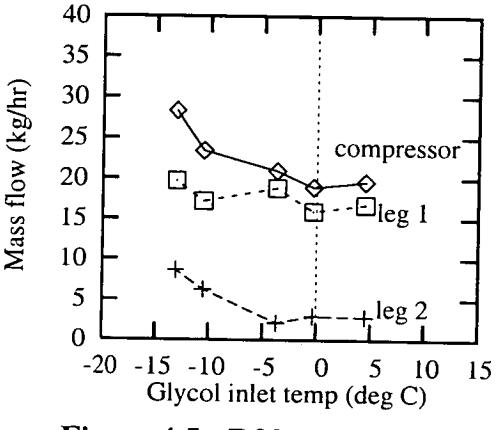

Figure 4.5: R32 mass flowrate

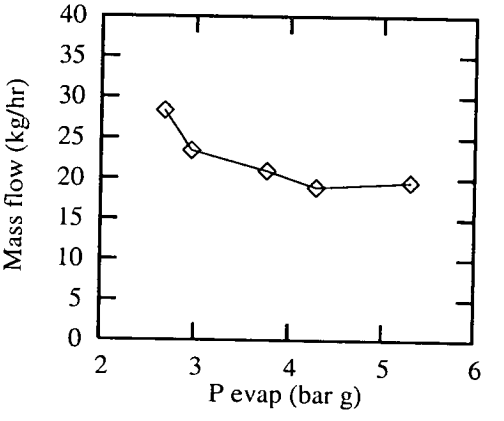

Figure 4.6: R32 compressor mass flow rate vs. evaporator pressure

The higher pressure in the condensers did not vary substantially with the glycol inlet temperature. From Figure 4.4 it is apparent that both the pressure ratio and the suction pressure varied in a regular fashion with reduced glycol inlet temperature. Advice from I.C.I. Suggested that a plot of mass flow rate vs. evaporator pressure could be used as a consistency check. If the graph exhibited a smooth curve or a straight line then the data could be considered consistent. In Figure 4.6 such a plot is presented for the series of initial R32 runs. The graph is not very smooth or continuous in character a certain lack of consistency in the results.

4.3.3 Commissioning Runs with Pure R134a

A second series of preliminary runs was made with pure R134a (Figure 4.7-Figure 4.12). R134a has a lower vapour pressure than R32, hence evaporator temperatures were higher than those of R32. Consequently the evaporator inlet glycol temperatures were also higher. The compressor had a much higher isentropic efficiency compered to R32. This was to be expected since the original compressor was designed with R12 as a working fluid. R134a is intended to an R12 replacement and its properties are similar, but not identical, to those of R12. The conditions of this series of trial runs are given in Table 4.2.

Table 4.2: Conditions of preliminary R134a runs

Parameter	Value
Evaporator ΔT_{LM}	15.0 degrees C
Glycol ΔT	5.0 degrees C
Water temperature	20.0°C
Water flow rate	3.3 $l min.^{-1}$

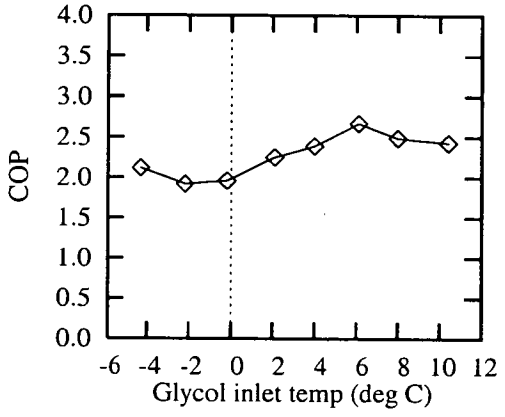

Figure 4.7: R134a COP

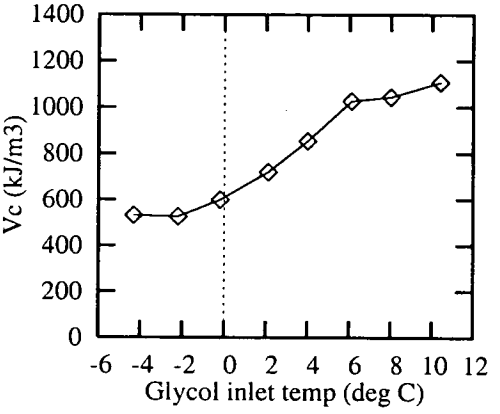

Figure 4.8: R134a specific volumetric capacity

Eight runs were conducted at glycol temperatures from approximately 10°C to -4°C in 2 degree intervals. As with the preliminary R32 data the graphs are not very smooth and show some scatter. The plot of COP vs. glycol inlet temperature (Figure 4.7) exhibits a maximum and a minimum rather than an increasing curve as one would expect. This scatter is reflected in the plots of heat and work loads (Figure 4.9) and mass flow rates (Figure 4.11).

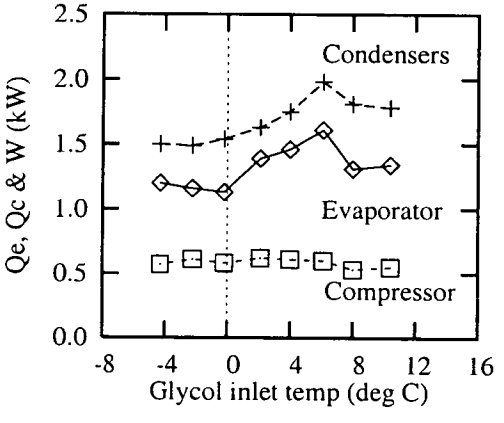

Figure 4.9: R134a heat and work loads

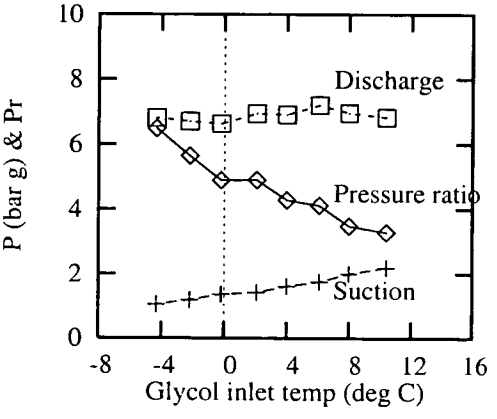

Figure 4.10: R134a pressures and pressure ratio

As in the operation with pure R32, the heat and work loads were found to be rather small, in the region 0.5-2.0kW. When the mass flow rate is plotted against the evaporator pressure, a smooth curve does not result, indicating a lack of consistency in the results. Ideally Figure 4.12 should be a straight line. The compressor was run in the lower third of its speed range for both sets of preliminary runs. Hence the relatively low values for heat and work loads. For the experimental runs involving the R32/R134a mixture described in the next section the full range of the compressor speed was used and more consistent results were reported.

Although not shown here, the compressor was more efficient with pure R134a. The compressor was originally designed to operate with CFC refrigerant R12. R134a is a replacement refrigerant for R12 and it resembles thermodynamically R12 more closely than R32.

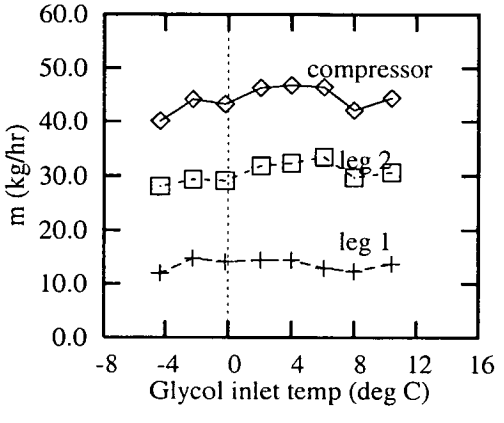

Figure 4.11: R134a mass flow rates

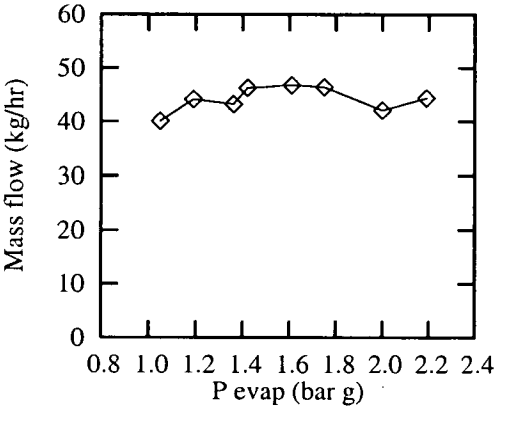

Figure 4.12: R134a compressor mass flow rate vs. evaporator pressure

4.3.4 21.9/78.1 Wt.% R32/R134a Mixture Results

Four runs were conducted with a 21.9/78.1 wt.% mixture of R32/R134a. The plant was charged with 9.5kg of R134a. A balance was used to weigh each gas canister before and after each charging. 2.525 kg of R32 were then added to the R134a already in the plant. The conditions held constant as a basis of comparison are outlined in Table 4.3. In order to increase the work and heat loads the plant was operated with a higher compressor speed, higher water and glycol flowrates. For both pure fluid commissioning runs the compressor had been operated in the lower half of its rotational speed range, hence it was decided to operate at a higher speed for the mixture runs. The specified log mean temperate difference in the evaporator was increased to 25.0 degrees C. It was anticipated that these measures would improve the consistency of the results obtained from the plant. The evaporator inlet glycol temperature for the four runs were 4.8°C, -0.4°C, -5.0°C and -10.8°C.

Table 4.3: Conditions of preliminary R134a runs

Parameter	Value
Evaporator ΔT_{LM}	25 degrees C
Glycol ΔT	4 degrees C
Water temperature	20°C
Water flow rate	6 l min.$^{-1}$

Important cycle parameters are plotted as a function of glycol inlet temperature in Figure 4.13-Figure 4.26. The graphs are considerably smoother in profile than those obtained for the commissioning runs of R32 and R134a. The plot of compressor mass flowrate vs. evaporator pressure (Figure 4.13) is close to a straight line. This indicates a satisfactory degree of consistency in the results, in contrast to those for R32 (Figure 4.6) and R134a (Figure 4.12). The results reported here for the pure R32, pure R134a and 21.9/78.1 R32/R134a were completed at different external conditions hence immediate comparisons between them cannot be drawn. The water flowrates

and specified log mean temperature differences are different for each working fluid, hence a direct comparison between the runs cannot be made. For a fair comparison between the mixed and pure fluids the external conditions and log mean temperature difference should be the same (as recommended by McLinden et al. [*1987*]). The pure R32 and R134a runs were intended as commissioning runs and not as actual experimental runs.

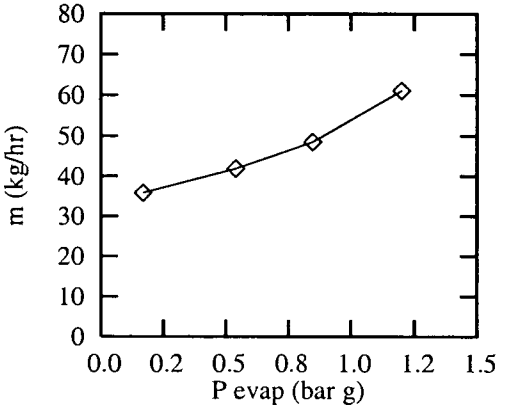

Figure 4.13: 21.9/78.1 wt.% R32/R134a compressor mass flow vs. evaporator pressure

Figure 4.14 shows the mixture COP plotted as a function of the evaporator glycol inlet temperature. As one would expect the COP decreases as the glycol temperature is reduced. The values of the COP (in the range 1.4-1.8) do not indicate exceptional performance. With an R32/R134a mixture at a composition of 20 wt.% R32 Jung et al. [*1991a*] calculated a COP of 1.35 for a simulation of a domestic refrigerator. An air stream was cooled from -11°C to -18°C while the heat was rejected to another airstream with a temperature of 32.2°C.

Although not immediately comparable since the heat sink temperatures and temperature changes are different, it can be seen that at a glycol inlet temperature of -10.8°C the mixture COP observed by the author for the R32/R134a is 1.38 which is

similar to the COP calculated by Jung et al. The heat and work loads are shown in Figure 4.15. The condenser heat load is that calculated from the temperature change recorded by the water thermopile, i.e. across both condensers.

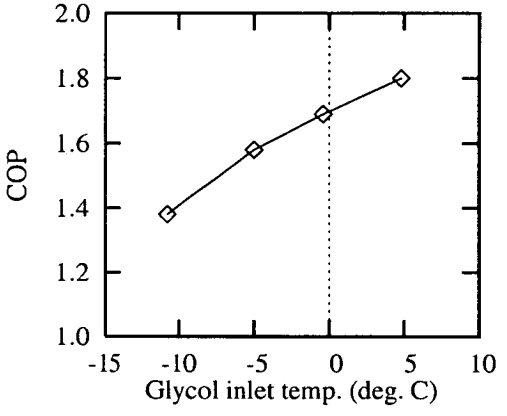

Figure 4.14: 21.9/78.1 wt.% R32/R134a COP

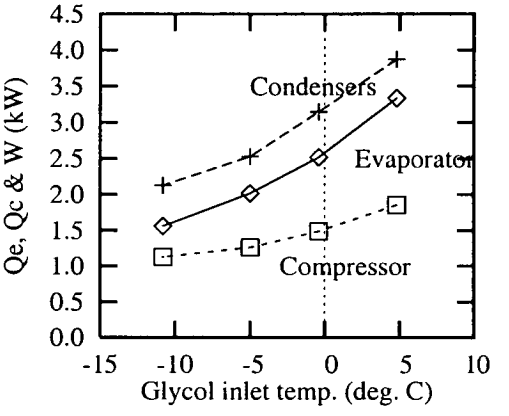

Figure 4.15: 21.9/78.1 wt.% R32/R134a heat and work loads

All three energy transfers increase as the glycol temperature increases. Although more work is done at the higher glycol temperatures, proportionally higher amounts of heat is removed form the glycol stream, hence the increase in the COP. Better heat transfer occurs at higher glycol temperatures. This is shown in the graph of UA values vs. glycol temperature (Figure 4.16). Since the area of the evaporator is a constant throughout ($0.0138 m^2$ inside pipe area), the evaporating heat transfer coefficient is improved as the glycol temperature increase. The viscosity of the 60% ethylene glycol-water heat sink decreases as the temperature increases while the specific heat capacity increases with temperature [*Perry 1984*]. Thus there is an improvement in the amount of heat transferred to the glycol from the refrigerant mixture as the glycol temperature increases.

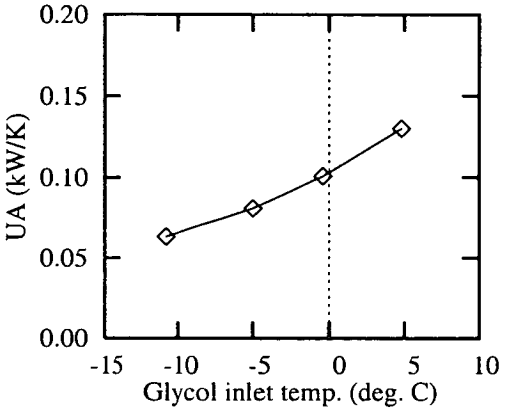

Figure 4.16: 21.9/78.1 wt.% R32/R134a evaporator UA values

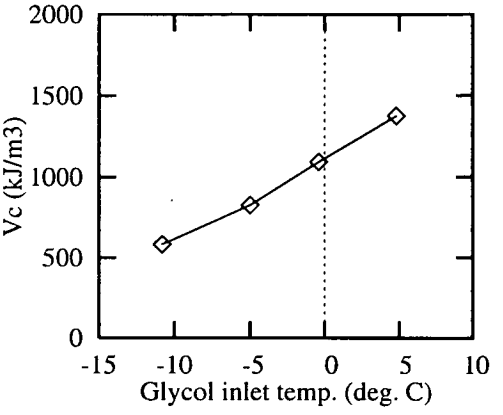

Figure 4.17: 21.9/78.1 wt.% R32/R134a specific volumetric capacity

From Figure 4.17 it can be seen that the specific volumetric capacity increases almost linearly with the glycol inlet temperature.

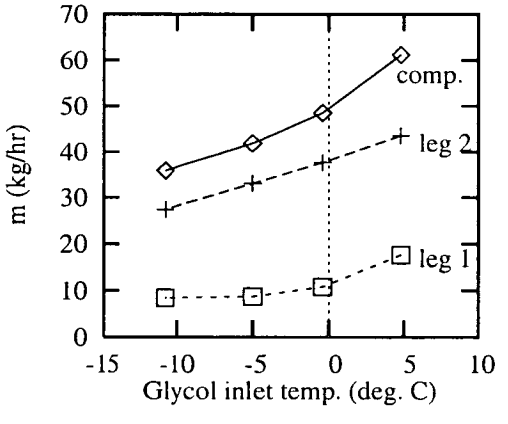

Figure 4.18: 21.9/78.1 wt.% R32/R134a mass flowrates

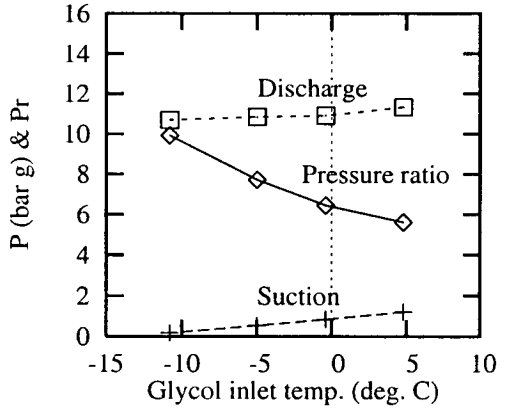

Figure 4.19: 21.9/78.1 wt.% R32/R134a pressures and pressure ratio

Although the compressor mass flowrate (Figure 4.18) exhibits an increase with higher glycol temperatures, it is offset by the increase in the evaporator heat load and lower vapour volumes; hence V_c increase as the glycol temperature increases. The mass flowrate in leg 1 of the refrigeration plant is much less than that of leg 2. All of the vapour is desuperheated in condenser 1 and as a result much of its duty is in de superheating. Consequently most of the refrigerant is condensed in condenser 2 resulting in a higher flowrate through leg1. The discharge pressure increases slightly as the glycol temperature increases. Fixing the glycol temperature change and the log mean temperature difference in the evaporator means that the suction pressure increases with increasing glycol temperature. Consequently the pressure ratio decreases with increasing glycol temperature.

Figure 4.20 and Figure 4.21 show the isentropic compressor efficiency as a function of the evaporator glycol inlet temperature and of the pressure ratio respectively. From inspection it can be seen the compressor is less efficient at higher heat source temperatures.

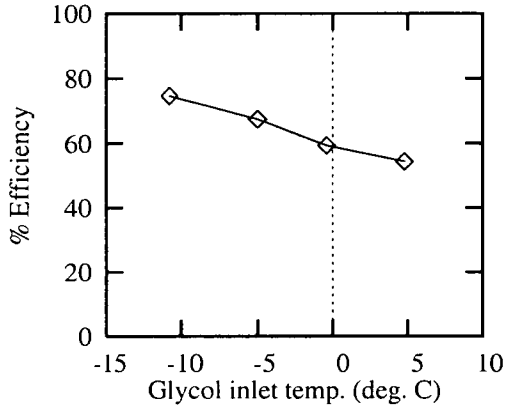

Figure 4.20: 21.9/78.1 wt.% R32/ R134a compressor isentropic efficiency

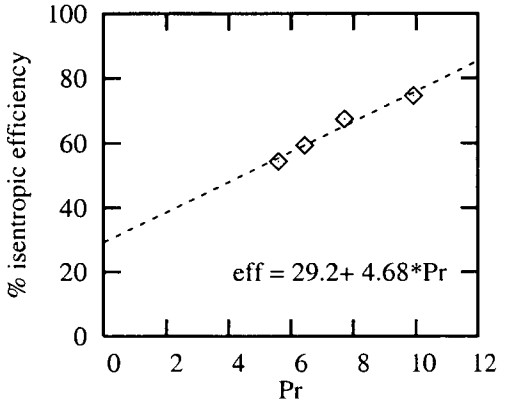

Figure 4.21: 21.9/78.1 wt.% R32/ R134a compressor isentropic efficiency vs. pressure ratio

There is a linear relationship between the isentropic efficiency and the pressure ratio. An equation of a straight line was regressed and is shown in Figure 4.21. The r^2 value was found to be 0.986 indicating a strong linear relationship over the range considered (Low had also found a linear relationship between the isentropic efficiency and the pressure ratio when the compressor was used in conjunction with CFC fluids). The compressor discharge temperature remains fairly constant at a value of around 105°C over the four values of glycol inlet temperature considered (Figure 4.22). For this mixture and conditions the discharge temperature is not unduly large compared to that of pure R32 (which could reach 135°C, close to the compressors's limit). The compressor suction temperature and the amount of superheat in the compressor suction are shown in Figure 4.22.

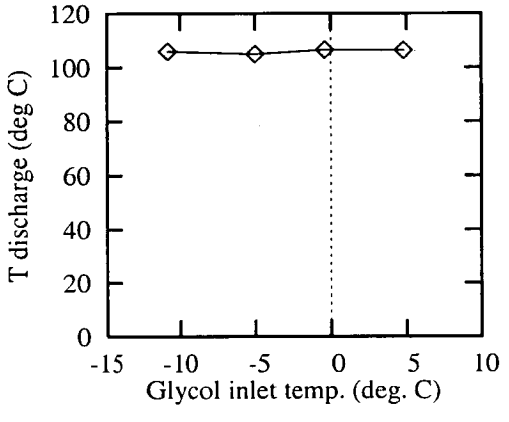

Figure 4.22: 21.9/78.1 wt.% R32/R134a compressor discharge temperature

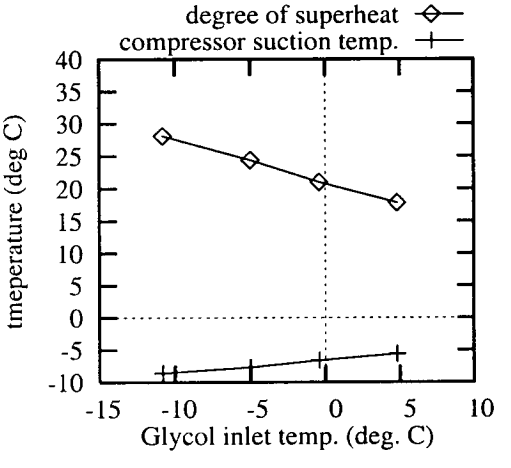

Figure 4.23: 21.9/78.1 wt.% R32/R134a temperature & superheat in compressor suction

The compressor suction temperature decreases almost linearly with decreasing glycol temperature. The degree of superheat in the compressor suction vapour exhibits a noticeable increase as the glycol temperature decreases. At the lowest glycol temperature (-10.8°C) the suction vapour has a temperature 28.1 degrees C greater than the saturation temperature at the same pressure. At lower glycol temperatures,

the larger difference in temperature between the vapour entering the compressor and the ambient air and the reduced mass flowrate meant that the vapour had a higher degree of superheat compared to the higher glycol temperatures. The pipe length between the evaporator and the compressor suction inlet port was about 2.5m. Although the pipe was well insulated, its length would have promoted the amount of superheat in the suction. Rough calculations indicated that heat transfer coefficients for the pipe were in the range 25-44 $Wm^{-2}K^{-1}$ whilst the heat absorbed by the pipe fell in the range 161-259 W.

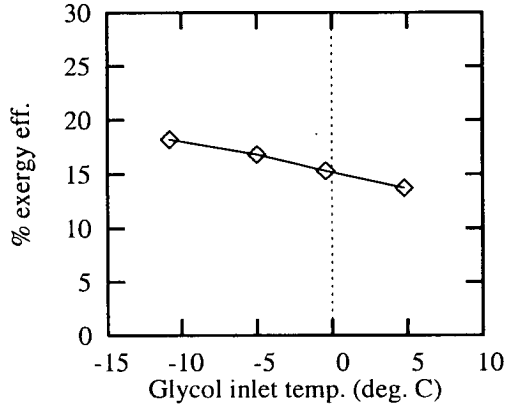

Figure 4.24: 21.9/78.1 wt.% R32/R134a cycle exergy efficiency

The overall exergy efficiency of the cycle is displayed in Figure 4.24 as a function of the glycol inlet temperature. The values of the efficiency are quite low (14-18%). The relatively large temperature difference in the evaporator (25 degrees C) reduces the exergy efficiency. The efficiency is higher at lower glycol temperature. This is because the compressor isentropic efficiency is better at lower glycol temperatures. The exergy loss for each piece of equipment is shown cumulatively in Figure 4.25. The space below a given plot and between the plot beneath represents the actual exergy loss for a particular piece of equipment. The compressor and the evaporator are responsible for the majority of the exergy loss. All of the equipment except for the compressor show a

relatively constant exergy loss over the range of glycol temperature considered. The compressor exergy loss decreases from 0.690kW to 0.227kW. The reduction in compressor exergy loss reflects the fact that the compressor performs better at high pressure ratios.

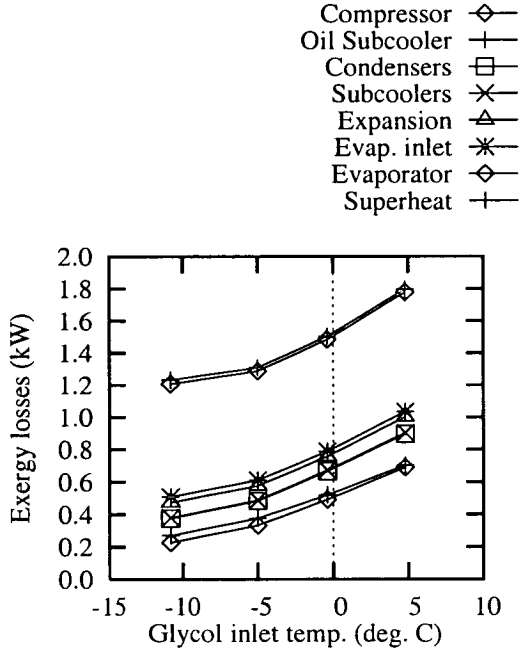

Figure 4.25: 21.9/78.1 wt.% R32/ R134a equipment exergy losses

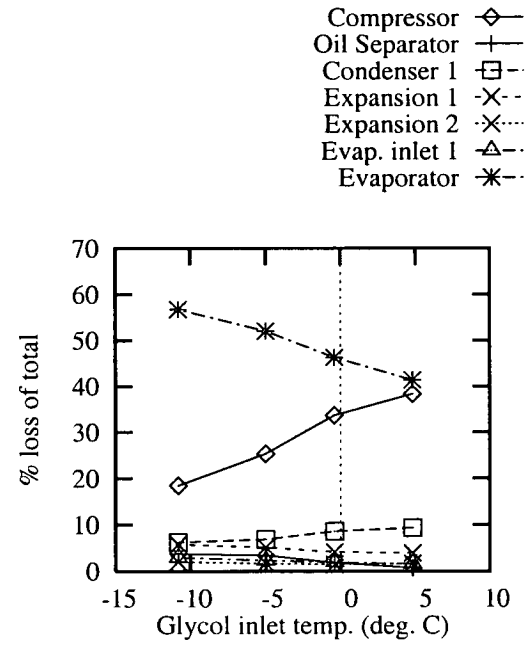

Figure 4.26: 21.9/78.1 wt.% R32/ R134a equipment exergy losses as a percentage of the total

Figure 4.26 displays the percentage exergy loss for each piece of equipment relative to the total exergy loss. At the lowest glycol inlet temperature the evaporator is responsible for over half the total exergy loss. As the glycol temperature increases the inefficiencies in the compressor increase its proportion of the total exergy losses. The actual evaporator exergy loss actually remains constant but the increase in the compressor exergy loss as the glycol temperature increases mean that the evaporator's proportion of the total falls. The large exergy losses in the evaporator result from the large log mean temperature difference used.

4.4 General Remarks and Summary

A few general qualitative comments are made here about the limited operation of the experimental refrigeration pilot plant. The most serious problems encountered in using refrigerants R32 and R134a was the occurrence of leaks, testing the patience of technicians and researchers alike. A considerable amount of time was involved in tracking down and removing leaks throughout the course of the experiments. Both refrigerants showed almost the same propensity for leaking despite the fact that R134a is much less volatile and is a larger molecule. The pure R134a commissioning runs were completed after the pure R32 runs. When the plant was first charged with pure R134a it exhibited a high tendency to leak, even though the plant had been made almost leakproof for R32. With any future plant brazed joints would be better. There were only one or two occurrences of these leaking during the operation of the plant.

The compressor operated with R32 and R134a without any major problems even though it was designed for R12. The compressor operated more efficiently with pure R134a than with R32. High discharge temperatures were experienced with R32 resulting from a lower efficiency. The relatively long length of pipe between the evaporator and the compressor suction inlet port promoted relatively large amounts of superheat in the suction vapour. There were no problems experienced with the polyol ester oil used to lubricate the compressor. From the limited operation of this plant it seems that a R32/R134a mixture can be used with equipment designed for R12 without any serious operational problem, although there can be a loss of efficiency.

Since the evaporator heat transfer area was rather small the evaporator was run at a high log mean temperature difference (25 degrees C) in order to get consistent results. The large temperature difference led to a low overall exergy efficiency (14-18%). At the lowest glycol inlet temperature the evaporator was responsible for around 55% of the total exergy losses of the plant. A temperature difference of 25 degrees C meant that the lowest glycol temperature achievable with a 21.9/78.1 wt.% R32/R134a

mixture was -11.0°C, without the pressure in the evaporator going below 0 bar g. A lower temperature would have meant that operation at lower glycol temperatures could have been accomplished.

Glycol temperature change, condenser inlet water temperature and flowrate and the log mean temperature difference between the glycol and the refrigerant were selected as the parameters to be used as a basis of comparison as recommended by McLinden et al. [*1987*]. These were kept constant in the various runs. In practice this was quite difficult to achieve. It proved difficult to independently adjust the glycol temperature change and the log mean temperature difference in the evaporator. The evaporator log mean temperature difference could be adjusted by changing the flowrate of the glycol or opening or closing the expansion valves to increase or decrease the temperature in the evaporator. This usually then caused the temperature change of the glycol stream to move away from its specified value. Changes to the glycol flowrate or percentage expansion valve opening had to be small so as not to unduly disturb the operating conditions. The on-off nature of the temperature control system in the glycol storage tank tended to cause fluctuations in the evaporator inlet temperature. This added to the difficulty of the task of controlling the plant conditions. In contrast the water flowrate and temperature proved quite easy to adjust to their specified values.

The coriolis mass flowmeter worked quite well and gave consistent data throughout the operation of the plant. It did take quite along time to correctly configure the computer and RS485 interface so that communication with the coriolis flowmeter could be achieved but once it was functioning its operation was satisfactory. Use of a 486 computer meant that parameters such as COP, specific volumetric capacity and log meant temperature difference could be calculated and displayed every time the instruments were scanned. These proved useful in analysing the performance of the plant while it was in operation. Altering the control program so that it included a number of alarms, when the plant went outside the realm of intended operation proved a useful safety feature.

Fraying of thermocouple sheaths provided a constant source of irritation. Sometimes it was necessary to remove thermocouples from their pockets if a particular piece of equipment was being removed or examined. The pockets were quite narrow (2-3mm) and if the outer thermocouple sheath frayed, which it often did, then it was impossible to re-insert back into the pocket. This meant that the thermocouple had to be replaced.

Although the experimental program of the thesis was prematurely terminated, due to circumstances beyond the control of the author, research was conducted into the potential enhancement of COP through the application of HFC refrigerant mixtures. This was completed by means of a computer simulation study. Also methods of calculating the thermodynamic properties of HFC refrigerants from sparse data were examined. The simulation study and results emanating from it and are presented in the following chapter.

Chapter 5

Simulation of Refrigeration Cycles with HFC Mixtures

5.1 Introduction

Even though the experimental program of this thesis came to an unsatisfactory and discouraging end, research work into improving refrigeration COPs using mixtures of non ozone depleting refrigerants was accomplished. A computer model was used to simulate a refrigeration cycle containing hydrofluorocarbon refrigerant mixtures as the working fluid. Simulation models can be a very useful tool in designing refrigeration cycles. A simulation model allows engineers to vary a great number of cycle parameters so that the most efficient configuration can be identified. A large proportion of the research on refrigerant mixtures has been carried out using simulation models, mainly with CFC and HCFC refrigerants. In this chapter results are obtained from the model are presented. Six different binary HFC mixtures were simulated to determine if the COP of the refrigeration cycle improved with the application of mixtures of refrigerants. A number of cycle parameters were also varied to ascertain the conditions under which mixtures had better performance than pure fluids.

A factor taken into account in the model was that the method of calculating the necessary thermodynamic properties should only require sparse data. As CFCs, and eventually HCFCs, are phased out, a means of evaluating the performance of prospective replacement refrigerants is needed. Many models use an equation of state based approach to calculate the necessary values of the thermodynamic properties. Very often these equations require experimental data to determine the coefficients that are used in the equations. With new and experimental refrigerants there may be a paucity of experimental thermodynamic data. In order to assess the behaviour of new fluids in a refrigeration cycle, a model may be required to make accurate predictions of thermodynamic behaviour from a relatively small amount of information. The model developed in this chapter requires a minimum of knowledge about the working fluid. Consequently the model can used to asses the likely performance of a mixtures where minimal information about one of the components exists.

5.2 Algorithm and Assumptions of Model

5.2.1 Logic and Assumptions Underpinning the Cycle

A model of a simple refrigeration cycle using the Cubic Chain-of-Rotators equation of state to calculate thermodynamic data was developed. It was called CCORSIMPLE. Provision was made to include a liquid-suction heat exchanger. This configuration was chosen for sake of simplicity, which would mean less computation time. The cycle and its temperature-entropy diagram are shown in Figure 5.1. The following is a description of the states numbered in Figure 5.1

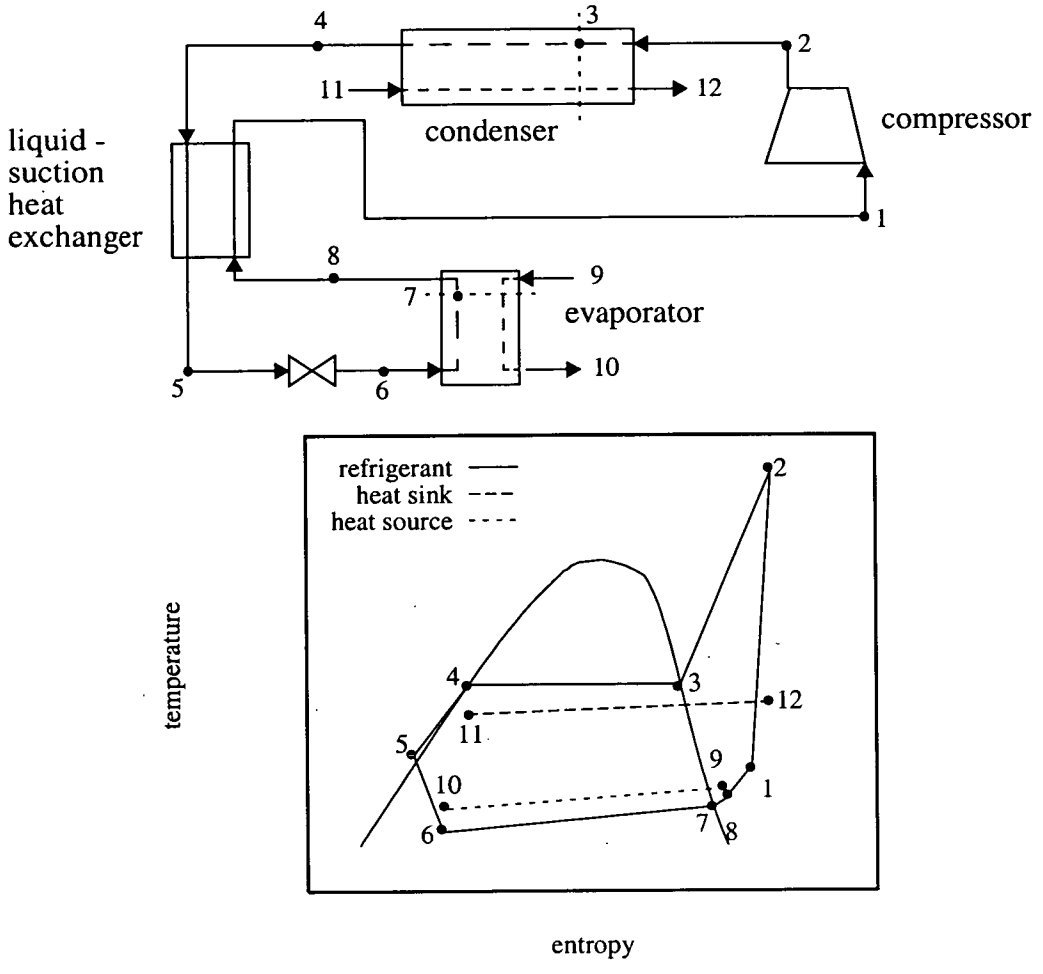

Figure 5.1: Schematic and temperature-entropy diagram of modeled refrigeration cycle

1. compressor inlet (shown here as superheated, but may be saturated)

2. superheated vapour from compressor outlet

3. condenser dew point

4. liquid at bubble point leaving condenser

5. subcooled liquid exiting liquid-suction heat exchanger (LSHX)

6. Throttled fluid entering evaporator

7. evaporator dewpoint

8. (slightly) superheated vapour exiting evaporator and entering liquid-suction heat exchanger.

9. heat source fluid entering evaporator

10. cooled heat source fluid exiting evaporator

11. heat sink fluid entering condenser

12. heat sink fluid leaving condenser

In order to make a fair and meaningful comparison between pure and mixed working fluids, the required evaporative heat load (Q_e) was fixed as well as the heat sink and source conditions. Rather than fixing cycle conditions such as temperature or pressure, the heat load and the external fluid temperatures were fixed and used as a basis of comparison. The recommendations regarding the comparison of pure and mixed refrigerant working fluids, made by McLinden et al. [*1987*] were incorporated into the model (Section 2.3.1 on page 21). The model adjusts the cycle conditions to satisfy the mass and energy balances and the specified sink and source temperatures. The model was based upon an algorithm used by Jung et al. [*1991a*] to compare a binary refrigerant mixtures. The heat sink inlet temperature and flowrate are fixed. The outlet temperate is allowed to vary so as to satisfy the energy balance. Heat exchanger information is provided by specifying the product of the heat transfer coefficient and the area of the condenser and the evaporator (i.e. UA values). As the evaporator heat load and UA value are fixed, the mean temperature differences between the working fluid and the heat transfer fluids are thus fixed. Consequently the model iterates temperatures in the evaporator until the prescribed value has been reached. For a completely accurate representation, the heat transfer coefficient would be calculated from the available correlations. However, this would mean that the

geometry and size of the heat exchangers would have to be specified and the model would become tied to a particular geometric setup. While the model was set up to reflect reasonably a real cycle, strict representation of all the facets of a refrigeration cycle was not the intention.

Table 5.1: Input data need by simulation model

Input Parameter	Units	Input Parameter	Units
M.v.c. component	(-)	Glycol outlet temperature	°C
L.v.c. component	(-)	Evaporator UA value	kWK^{-1}
M.v.c. composition	wt.%	Evaporator Pressure drop	kPa
Equation of state interaction constant(s)	(-)	Superheat in evaporator	°C
Refrigeration Load	kW	Water inlet temperature	°C
Compressor polytropic efficiency	0 -1.0	Water flow	$kg\ s^{-1}$
LSHX used	Yes or No	Condenser UA value	kWK^{-1}
Degree of condensate subcooling if LSHX used	°C	Condenser pressure drop	kPa
Glycol inlet temperature	°C		

Other cycle parameters that are specified by the user are: compressor polytropic efficiency; degree of vapour superheat in the evaporator, heat exchanger pressure drop and amount of subcooling in the liquid-suction heat exchanger. Table 5.1 is a list of the input data needed by the model. A sample input file used by the model to simulate a cycle is given in Section C.2 of Appendix C

5.2.1.1 Compressor

Initially the compression process was modelled by simply specifying the isentropic efficiency. The isentropic efficiency is the ratio of the isentropic enthalpy rise to the real enthalpy rise and is given by:

$$\eta_i = \frac{h_d^* - h_s}{h_d - h_s} \qquad \text{(Eq 5.1)}$$

where the subscripts d and s refer to suction and discharge respectively and the symbol * refers to the enthalpy of an isentropic compression. The actual discharge enthalpy can be calculated by finding the isentropic discharge enthalpy and then calculating h_d from Equation 5.1. Jung and Radermacher used this approach in their simulation of a domestic refrigeration cycle. Domanski et al. [*1992*] recommended that a polytropic analysis should be used. A polytropic description better describes the compressor process at various operating conditions. The isentropic efficiency varies with pressure ratio. The compressor polytropic efficiency is a specified input (Table 5.1). The exit enthalpy is given by Equation 5.2:

$$h_d = h_s + \frac{W}{\eta_p} \qquad \text{(Eq 5.2)}$$

where W is the compressor work and η_p is the polytropic efficiency. The subscripts *s* and *d* refer to suction and discharge conditions respectively. The compressor work is given by the relation:

$$W = \frac{n}{n-1} P_s V_s \left[\left(\frac{P_d}{P_s} \right)^{\left(\frac{n-1}{n} \right)} - 1 \right] \qquad \text{(Eq 5.3)}$$

The polytropic index n is defined by:

$$\frac{n-1}{n} = \frac{\gamma - 1}{\eta_p \gamma} \qquad \text{(Eq 5.4)}$$

Domanski et al recommended for consistency that the isentropic index γ is evaluated according to Equation 5.5 rather than as the ratio of heat capacity at constant pressure and constant volume (i.e. $\gamma = C_p/C_v$). Domanski et al. found that for R12 and operating at pressures used in a domestic cycle the value of γ as calculated by Equation 5.5 differed was 14% lower than the ratio of heat capacities.

$$h_d^* - h_s = \frac{\gamma}{\gamma - 1}(P_d v_d^* - P_s v_s) \qquad \text{(Eq 5.5)}$$

Again the superscript * denotes isentropic conditions. These equations have been taken from Domanski et al.[*1992*].

5.2.1.2 Heat Exchangers

A proper treatment of the heat transfer is needed to simulate a refrigeration cycle. Counterflow heat transfer is assumed in the evaporator and condenser. This is necessary in order to maximise the benefits of refrigerant mixtures. The performance is prescribed by specifying the product of the overall coefficient heat transfer and the area (UA value) for both heat exchangers. Each flow regime in the heat exchangers is treated separately (i.e. two phase and superheated sections). Each section is then subdivided into a number of different subsections of equal heat load. The two phase regimes in both heat exchangers are divided into 50 subsections while the desuperheating section in the condenser is divided into 25 sections. Ten subsections are considered in the superheating section in the evaporator. This gives a more accurate representation of the temperature profile. For some mixtures the enthalpy-temperature profile is not linear, especially if there is a large difference in the components' normal boiling points. Calculation of the average effective temperature

differences based only upon the inlet and outlet temperatures can lead to errors. Domanski et al. [*1992*] found that for an R22/R123 mixture neglecting the nonlineraity of the temperature-enthalpy profile lead to errors of up to 8.9% in COP. Hence in this model, the evaporator and condenser are split into subsections to obtain a more accurate value of the average temperature differences.

An arbitrary evaporator subsection 'i' is shown in Figure 5.2. The heat load Q_i is the total two phase load divided by the 50 subsections. The inlet conditions (t_i, h_i, T_i) are known. The flowrate of the refrigerant (m_{refrig}) is also known hence the outlet enthalpy (h_{i+1}) can be calculated according to:

$$h_{i+1} = h_i + \frac{Q_i}{m_{refrig}} \qquad \text{(Eq 5.6)}$$

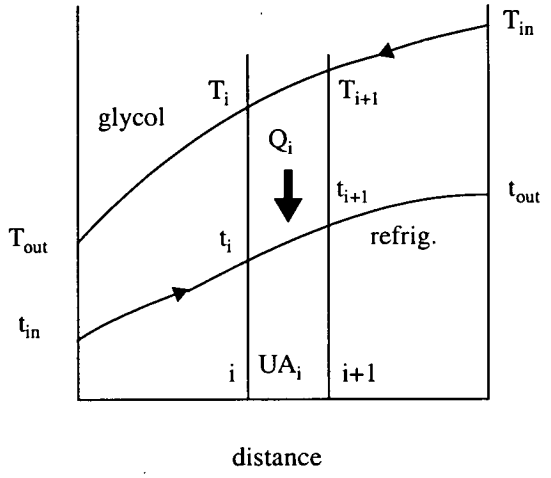

Figure 5.2: Temperature-Distance profile of subsection i in evaporator

T_{i+1} is estimated and an iterative procedure is carried out to find t_{i+1}. The log mean temperature difference for section i is simply given by the relation:

$$\Delta T_{LM_i} = \frac{(T_{i+1} - t_{i+1}) - (T_i - t_i)}{\ln\left(\frac{T_{i+1} - t_{i+1}}{T_i - t_i}\right)} \quad \text{(Eq 5.7)}$$

The overall log mean temperature difference of the heat exchanger is the arithmetic mean of the temperature differences of each subsection weighted with the UA value of each section:

$$\Delta T_{LM_{hx}} = \sum \frac{UA_i \Delta T_{LM_i}}{UA_{hx}} \quad \text{(Eq 5.8)}$$

The UA value of each subsection is simply calculated by Equation 5.9:

$$UA_i = \frac{Q_i}{\Delta T_{LM_i}} \quad \text{(Eq 5.9)}$$

This gives a better representation of the temperature difference rather than relying solely on the inlet and outlet temperatures.

In the model the *total* pressure loss in the condenser and evaporator is specified by the user. The pressure at each subsection is calculated by assuming that the pressure loss is distributed in the heat exchangers according to the heat load. Referring to Figure 5.1, the pressure at states 3, 7 and 8 are given by:

$$P_3 = P_2 - \Delta P_c f_{desupc} \quad \text{(Eq 5.10)}$$

$$P_7 = P_6 - \Delta P_e (1 - f_{tpe}) \quad \text{(Eq 5.11)}$$

$$P_8 = P_6 - \Delta P_e \quad \text{(Eq 5.12)}$$

f_{desupc} is the fraction of desuperheating in the condenser and f_{tpe} is the fraction of two-phase heat transfer that takes place in the evaporator. A more rigorous approach would be to apply two-phase pressure drop correlations to each heat exchanger and

distribute the pressure drop accordingly. No pressure drop is assumed to take place in the liquid-suction heat exchanger or in any of the pipework connecting the pieces of equipment.

5.2.2 Cycle Algorithm

The successive substitution method was used to implement the model. This method involves a number of iterative loops so that energy balances and other constraints could be met. An estimate is made of a particular variable within an inner iteration loop. On the basis of this assumed value, other values such as enthalpy and entropy are calculated. The variable is altered until a convergence criteria has been reached. The model continues until all of the convergence criteria have been met. A flow sheet of the model is shown in Figure 5.3. The subscripts correspond to the points in Figure 5.1. The input data is read from a file or it can be typed in manually. The following is a list of the major assumptions of the model:

- There is no accumulation of material in the cycle. The overall composition at each point is constant throughout the cycle. The composition of the liquid and vapour phases in the evaporator, condenser and after expansion will be different from the prescribed global composition.
- Pure fluids and binary mixtures are considered by the model.
- A 60% ethylene glycol/ water solution is used as the heat source. The density and heat capacity were found in Perry [*1984*]. Expressions relating the density and heat capacity to the temperature were regressed. The expression for heat capacity was used to determine the glycol temperature profile in the evaporator
- The heat sink fluid was water. A constant value of heat capacity was used ($4.186 kJkg^{-1}K^{-1}$). A temperature dependent function was used for density.
- The expansion is assumed to be isenthalpic.

5.2.2.1 Explanation of Algorithm

The saturation temperature of the condensate (T_4) is estimated. Since the condensate is assumed to be saturated, the pressure (P_4) can be determined from the vapour pressure in the case of a pure refrigerant, or from the bubble pressure if a mixed refrigerant is used. The specific volume, enthalpy and entropy of state 4 can then be calculated. Since the degree of subcooling is specified as an input parameter, T_5 can be calculated. The state properties at point 5 are then computed as is the amount of heat transferred (Q_{LSHX}). The temperature after the expansion (T_6) is then estimated and since the expansion is isenthalpic, the remaining state properties of point 6 can be found by iteration. This gives the conditions at the inlet to the evaporator. The pressure at point 7 is given by subtracting the evaporator pressure drop (ΔP_e) from P_6. Saturation is assumed at this point, hence T_7, v_7, h_7 and s_7 may be calculated by the equation of state. The degree of superheat in the evaporator is prescribed from the input data, hence all the state properties at point 8 can be found.

Since the entrance and exit conditions of the evaporator are known, the two phase flow regime is divided into 50 subsections and the temperature profile of the refrigerant and heat source fluid is calculated, as described in Section 5.2.1.2. This allows the log mean temperature difference to be calculated. Since the heat load (Q_e) and the UA value in the heat exchanger have been specified then the log mean temperature difference in the evaporator has been specified (called DTE). The calculated ΔT_{LM} value, based on the estimate of T_6 is compared with the prescribed value. T_6 is adjusted until the two values fall with in the required tolerance.

The state properties of the suction vapour are determined since the pressure is known and the enthalpy is the sum of the inlet enthalpy (h_8) and the amount of heat transferred in the liquid-suction heat exchanger. Based up on the entropy of the suction vapour (s_1) the isentropic discharge conditions are determined. The polytropic efficiency of the compression process is specified and hence the work can be calculated according to Equation 5.3.

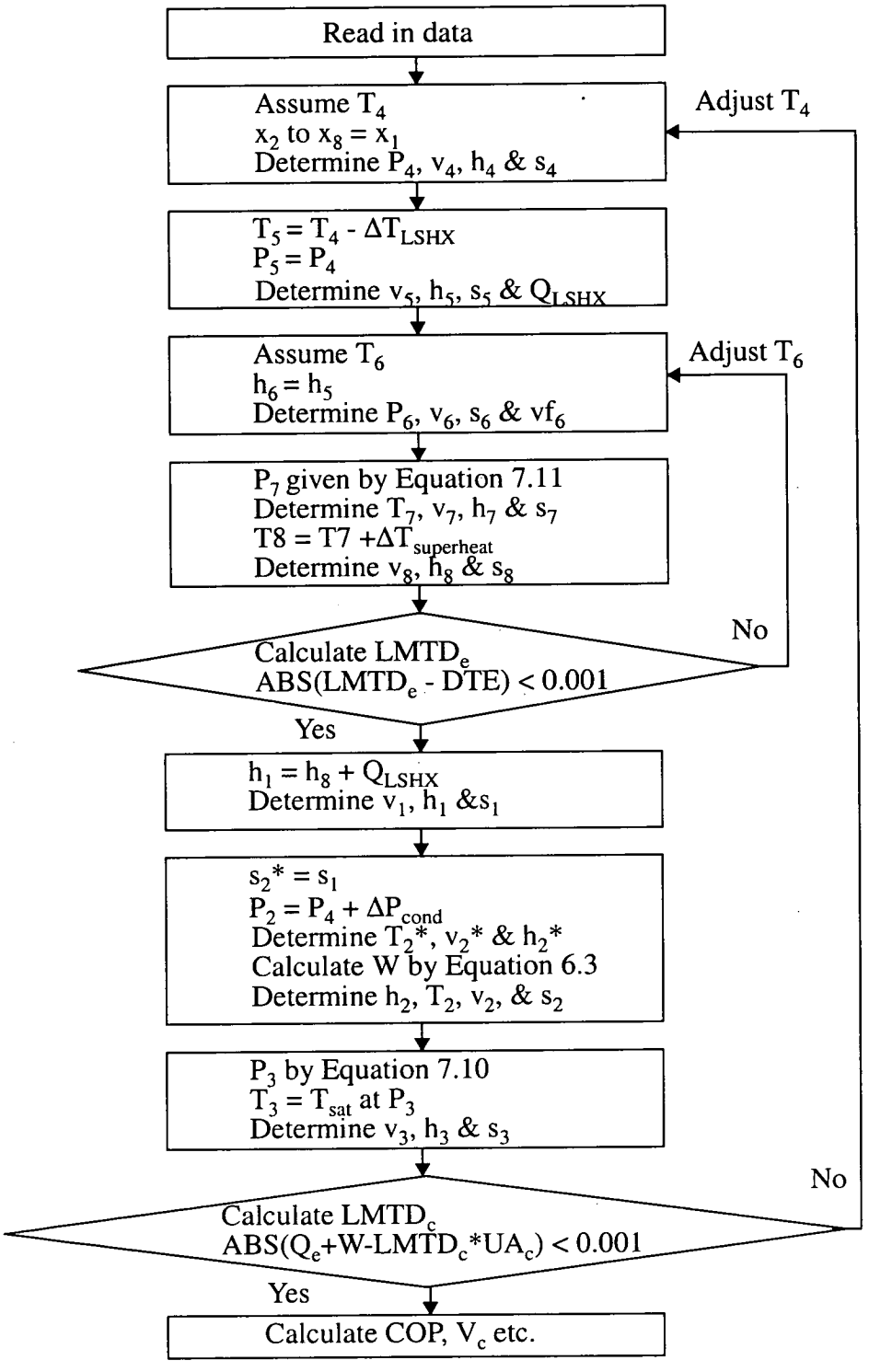

Figure 5.3: Flowsheet of the simulation model

This allows the real discharge conditions to be determined. In a similar fashion to the treatment of the evaporator the log mean temperature difference ($\Delta T_{LM\ cond}$) is calculated. An energy balance, described by Equation 5.13, is carried out.

$$Qe + W - (\Delta T_{LM\ cond} \times UA_c) \qquad \text{(Eq 5.13)}$$

If the balance is within the tolerance set in Table 5.2 on page 153 then the model has reached convergence otherwise the initial estimate of the condenser exit temperature (T_4) is adjusted. When the model has converged parameters such as COP, pressure ratio etc. can be calculated and the results sent to an output file.

5.2.2.2 Parameters calculated by the Model

The model calculates all the state properties at each point of the refrigeration cycle. The results are printed out to an output file. An example of a typical output file from CCORSIMPLE is given in Section C.2 of Appendix C. Each point in the cycle is listed along with the following calculated properties: temperature, pressure, specific volume, enthalpy, entropy, exergy, composition and vapour fraction (where applicable). A number of cycle parameters are also calculated. These include:

- coefficient of performance (COP)
- compressor work (W)
- condenser heat load, (Q_c)
- pressure ratio ($P_{r)}$
- compressor isentropic efficiency (η_i)
- refrigerant mass flow (m)
- exergy efficiency (η_{ex})
- temperature change of water (ΔT_w)

- specific volumetric capacity (V_c) This is the evaporator heat transferred per unit volume flow of refrigerant. It is given by:

$$V_c = \frac{Q_{evap}}{m_{flow} \times v_{suction}} \quad \text{(Eq 5.14)}$$

- evaporator gliding temperature difference (GTD_e). This is the temperature difference between the dew point in the evaporator and the *entering* temperature. This is usually less than the difference between the dew and bubble temperatures: the entrance temperature will be greater than the bubble temperature because refrigerant enters the evaporator as a two-phase fluid.
- condenser gliding temperature difference (GTD_c). This is weighted to take account of the temperature change due to the desuperheating that takes place in the condenser. Subtracting the bubble point temperature from the dew point temperature does not take into account the temperature change that occurs in the desuperheating section, which can be substantial. The condenser GTD is the sum of the desuperheating and two-phase temperature difference weighted by the fractional heat load in each section. This was recommended by Jung et al. [*1991a*], [*1991b*] in their simulations of a single and double evaporator domestic refrigerator.

$$GTD_{condenser} = (GTD_{desup} \times f_{desup}) + (GTD_{two\ phase} \times f_{two\ phase}) \quad \text{(Eq 5.15)}$$

5.3 Calculation of Thermodynamic Properties

In modelling a refrigeration cycle the vapour pressure, enthalpy, entropy and specific volume of the working fluid need to be calculated. It is desirable that engineers have access to methods which can supply accurate thermodynamic data. CFCs have been used since the 1930s and a large body of methods to predict their thermodynamic properties have been built up as a result. These include both tabular methods (pressure-enthalpy charts) and equations of state. Accurate equations of state, especially dedicated to a particular refrigerant, have been developed to provide data

for applications not covered by correlations. However for new and experimental refrigerants there is not the same abundance of information. In order to estimate the effect of new or proposed refrigerants on a cycle, with some degree of confidence, it is necessary to have some means of estimating the refrigerant's properties from sparse amounts of data. Values of the critical properties, acentric factor and boiling point may be at hand, but vapour pressure curves and PVT data may not exist. The method of calculating the thermodynamic data needed to be as accurate as possible yet require a minimum of experimental information.

The Cubic Chain-of-Rotators equation of state visualises the molecule as chains of rotating hard dumbbells. It has been derived by examining the interactions at the molecular level and extrapolating these to the macrofluid. It does not depend on empirically derived coefficients. For this research, the CCOR equation was chosen because it offered a means of calculating thermodynamic information from very little data. This equation does not need any experimentally derived parameters. If the critical temperature, critical pressure and acentric factor are known then thermodynamic data for a particular refrigerant could be calculated. It has been developed from an analysis of the behaviour of fluids at the molecular level. It is thus much more rigorous than empirically derived equations. The fact that it is cubic in form offers computational advantages (i.e. when the pressure is known, and the volume is desired it is easier to invert a cubic equation).

A detailed examination of the ability of the CCOR equation to predict the thermodynamic properties of HFC refrigerants was carried out before implementing the model. Both pure and mixed fluids were investigated. These are described in Appendix B on page 204 and in Appendix F on page 276 respectively. Comparisons were made between properties predicted by the CCOR equation and published experimental data. Comparisons were also made against the Carnahan-Starling-DeSantis equation of state which has been commonly used to predict refrigerant properties and is theoretically a more accurate equation. For pure fluids the properties

examined were saturated vapour pressure, saturated liquid density, saturated vapour density and PVT behaviour. Five HFC refrigerants were examined: R32, R125, R134a, R143a, and R152a. It was found that the CCOR equation predicted the saturated vapour pressure quite well, with an overall average absolute deviation of 1.57%. Likewise the vapour pressure of superheat vapours was also predicted quite well (AAD=1.94%). Liquid and vapour saturated densities were not quite predicted so well (AAD=10.05% and 8.63% respectively). In mitigation the CCOR equation was slightly more accurate in predicting vapour density than the CSD equation. For liquid density, below a reduced temperature of 0.85, the error was independent of temperature and depended only on the refrigerant examined. Neither equation predicted compressed liquid pressure very well.

The ability of the CCOR equation to predict HFC VLE properties was also examined. Despite needing less data the CCOR equation predicted bubble pressure, vapour and liquid composition to a higher accuracy than the CSD equation. Use of optimum interaction parameters (based on whole datasets from the literature) reduced errors by about 50% for both equations. Investigations were undertaken to see how the optimum interaction constants varied with temperature and composition. This is described in much more detail in Appendix F

In summary it was found that the CCOR equation made reasonable predictions of the thermodynamic properties of HFCs given the paucity of data it needs. For mixtures it s predictions were as good if not better than the CSD equation of state which requires six parameters calculated from pure fluid saturation data. For new refrigerants where initial rough estimations of the thermodynamic data was needed then the CCOR equation could be used to predict the thermodynamic properties. A model of a refrigeration cycle based upon the CCOR equation would allow the likely performance of an experimental or proposed refrigerant fluid to be determined with minimal information about the fluid itself.

5.4 Implementation of Code

The model was written in ANSI C on the departmental UNIX workstation network. The programs are also compatible for a PC. Two versions of the model were written: the first (CCORSIMPLE) used the CCOR equation of state to calculate the necessary thermodynamic data, and the second used the CSD equation (CSDSIMPLE). These two programs carried out one single simulation of a refrigeration cycle. The model invokes numerous calls to the routines developed for the property prediction routines in Appendix B and Appendix F so that the necessary thermodynamic data could be calculated. CCORSIMPLE was written initially to ensure that the algorithm converged on a solution and produced sensible results.

In order to compare the behaviour of pure and mixed refrigerants, the model was adapted so that the working fluid composition could be varied. The actual simulation and thermodynamic property calculation routines were identical to CCORSIMPLE. The program CCORCOMPVARY was a development of CCORSIMPLE, which allowed the composition to be varied between 0-100% wt. of the m.v.c. at a composition interval specified by the user. The cycle parameters (COP, V_c etc.) were sent to a file as a function of composition. As well as calculating the parameters outlined in Section 5.2.2.2, CCORCOMPVARY also calculated the fraction of the condenser heat load that is used to desuperheat the vapour (F_{desup}) and it also sends the rise in water temperature to the output file (ΔT_{wat}). This allowed a graph of COP (or any other parameter) vs. composition to be plotted. Research work described in this chapter was carried out using CCORCOMPVARY. An identical model which used the CSD equation of state to calculate thermodynamic properties was also written. This was called CSDCOMPVARY.

5.4.1 Iteration Methods

The secant method was used to carry out the majority of the iterations in the algorithm. This method uses the two previous estimates to linearly interpolate the next estimate. A full description is given by Press et al. [*1992*]. The method was found to converge quite quickly in most cases. For example, the secant method would converge after 3 or 4 iterations when trying to find the exit temperature of a heat exchanger subdivision, when the enthalpy was known (Section 5.2.1.2). The main outer loop would typically converge in 4-5 iterations. One disadvantage of the secant method is that two initial estimations are needed. Normally a first guess is made and this is slightly perturbed for the second. If care is not taken in making the second estimate, the algorithm can disappear to infinity. When determining the refrigerant temperatures in the desuperheating section of the condenser in conjunction with the CCOR equation, the bisection method was used. It was found to be more reliable, but slower. Occasionally the secant method failed in this application.

As has been pointed out in Section 2.7.3 on page 60, two functions for the α term are used in the CCOR equation. These meet at the critical point and are discontinuous. This means that there is a slight discontinuity in the value of enthalpy as the temperature varies from subcritical to supercritical. This difference in enthalpy before and after the discontinuity is usually below 23 kJ $kmol^{-1}$($\approx$ 0.44$kJkg^{-1}$ for R32), depending on the refrigerant. This can lead to convergence problems when iterating for enthalpy since the enthalpy iteration tolerance is 0.01$kJkmol^{-1}$. To avoid, nonconvergence the enthalpy tolerance was set to 23$kJkmol^{-1}$ when the temperature was within 0.02 °C of the critical temperature. This problem did not occur with the CSD equation.

In picking the iteration tolerances there is a trade off between accuracy and the time taken to reach a solution. Smaller tolerances mean longer execution times to converge on a solution, while larger tolerances can lead to inaccurate solutions. Using larger tolerances with CCORCOMPVARY led to discontinuities plots of cycle parameters

vs. composition. Tolerances were selected to achieve convergence within a reasonable time frame and to give smooth curves when the results were subsequently plotted. The tolerances for the iteration loops are given in Table 5.2. Entropy tolerance is used when the compression process is modelled. The treatment of the compressor (Section 5.2.1.1) requires the calculation of the isentropic discharge conditions. As an initial guess the discharge entropy is set equal to the suction entropy. The temperature is varied, using the secant method, until the temperature which returns an entropy within the tolerance given in Table 5.2. It was found that cycle parameters such as COP, Vc etc. are quite sensitive to the entropy tolerance hence the need for a narrow tolerance. A larger entropy tolerance leads to discontinuities in cycle parameter-composition curves.

Table 5.2: Thermodynamic property iteration tolerances

Property	Tolerance	Units
Enthalpy	0.01	$kJkmol^{-1}$
Entropy	0.001	$kJkmol^{-1}K^{-1}$
Evaporator log mean temperature difference	0.001	°C
Main loop	0.001	kW

5.4.1.1 Run Time

The model was run on the Sun workstation network which uses the UNIX operating system. The model was executed much quicker when a pure fluid is used. Calculation of the equation of state parameters rather than the iterations needed to converge on a particular solution, is responsible for most of the processing time. When a mixture is modelled many more parameters need to be calculated and hence a larger processing time is required. As a comparison the processing times of the various models are given in Table 5.3 (CCOR) and in Table 5.4 (CSD). Two different types of machine

are compared. This gives an indication of the time needed to complete a simulation. The same input data was used for each machine and equation of state. CCORCOMPVARY and CSDCOMPVARY altered the composition for 0 to 1 weight fraction (m.v.c.) with an interval of 0.05 (i.e. 21 cycle simulations). Because the CSD only uses two parameters the execution time is much less; about half that needed for the CCOR equation.

Table 5.3: Processing times of model with CCOR equation

Machine Type	CCORSIMPLE Pure refrigerant	CCORSIMPLE Mixed refrigerant	CCORCOMPVARY
Sun Sparc station 1	6 sec	1 min. 34 sec.	28 min. 15 sec.
Sun Sparc station 20	2 sec.	13 sec.	2 mins. 57 sec.

Table 5.4: Processing times of model with CSD equation

Machine Type	CSDSIMPLE Pure refrigerant	CSDSIMPLE Mixed refrigerant	CSDCOMPVARY
Sun Sparc station 1	4 sec.	49 sec.	15 min. 24 sec.
Sun Sparc station 20	1 sec.	4 sec.	1 min. 7 sec.

5.5 Mixtures Considered

In examining the benefits of refrigerant mixtures, the same five hydrofluorocarbon fluids that were examined in Appendix F were considered. These were R32, R125, R134a, R143a, and R152. With these five fluids there were ten possible binary combinations. The efficiency benefits of refrigerant mixtures arises from the temperature matching in the condenser and evaporator (Section 2.2 on page 17). Rather than examining all ten of the possible mixtures only those whose maximum gliding temperature difference at 1 bar was greater than 4°C were considered.

Table 5.5: Maximum GTDs of binary HFC mixtures

Mixture	GTD at 1bara (°C)	GTD at 5bara (°C)	GTD at 15bara (°C)
R32 - R152a	8.79	8.23	6.89
R32 - R134a	7.71	6.87	5.48
R125 - R152a	6.55	5.34	3.85
R143a - R152a	5.79	4.44	3.04
R125 - R134a	5.36	4.09	2.75
R143a - R134a	4.68	3.30	2.08
R32 - R143a	0.52	0.72	0.77
R32 - R125	0.36	0.45	0.46
R134a - R152a	0.07	0.09	0.09
R125 - R143a	0.02	0.04	0.05

Because the benefits of refrigerant mixtures stems from the exploitation of the temperature glide, mixtures with a small glide were not examined. The glides are shown in Table 5.5. Six binary pairs were therefore selected: R32/R134a, R32/R152a, R125/R134a, R125 R152a, R143a/R134a and R143a/R152a. The remaining combinations were not considered since they exhibit azeotropic or near azeotropic behaviour.

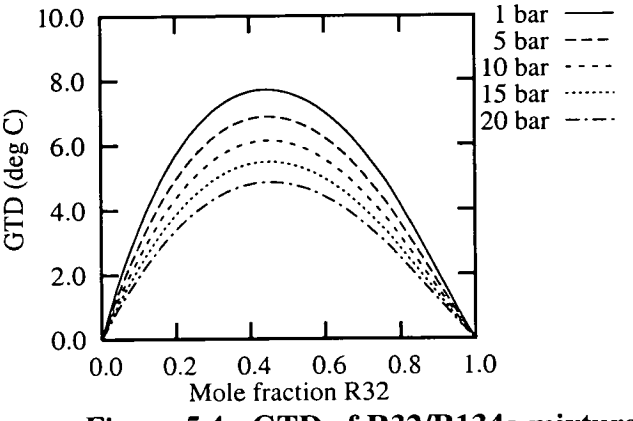

Figure 5.4: GTD of R32/R134a mixture

Effectively R32, R125 and R143a are considered as low boiling volatile compounds and are combined with two heavy or less volatile compounds (R134a and R152a). Figure 5.4 shows the GTD of the R32/R134a mixture. GTD is plotted as a function of R32 composition. As expected the largest GTD occurs close to the equimolar composition. The GTD reduces with increasing pressure.

5.6 Comparison of Results of CCOR & CSD Models

Before using the model to determine the advantages of hydrofluorocarbon mixtures, the results obtained from the model using the CCOR equation were compared with the results where the thermodynamic data was supplied by the CSD equation. The CCOR can supply thermodynamic data with little prior knowledge of experimental data. With the CCOR equation the performance of a new or proposed refrigerant can then be estimated without detailed experimental data. In this section the results from the model when the CCOR equation was used will be compared to the cycle parameters calculated by the model when the more accurate CSD equation is used. The equations will be examined with the same working fluids and conditions.

5.6.1 Conditions of Comparison

Three refrigerant mixture pairs were considered in the comparison; R32/ R134a, R32/ R152a and R125/R134a. If a new or experimental refrigerant pair were to be tested, there would be no interaction coefficients available. Thus if the performance of such a mixture were to be calculated, the interaction coefficients would be set to zero. The interaction constants (k_a and k_c of Equation F.1 and Equation F.3) were set to zero when using the model with the CCOR equation in the comparison test. However the thermodynamic data calculated by the CSD were calculated using *optimised* interac-

tion parameters. The CSD equation, in conjunction with an optimised value for k_a offers a theoretically more accurate prediction of mixture thermodynamic data. With bubble point VLE data and the interaction parameters the average error associated bubble pressure was found to be 3.61%, while the error associated with the CSD, in conjunction with an *optimum* value for k_a was 1.30%. The corresponding errors for bubble density were 6.72% and 3.02%. The CCOR model was examined to see how its results compared to that of a model where a more accurate source of thermodynamic data existed. Since the CCOR equation can be used with minimal fluid information, it will be advantageous to compare its model's results with those of the CSD equation whose interaction constant has been optimised. At the time of writing, published experimental data only existed for the above mentioned pairs, hence optimum interaction constants could only be determined with these particular mixtures (Section F.5.2 on page 303).

For a given refrigerant pair, six different operating conditions were chosen. Within each set of operating conditions the composition was varied from pure m.v.c. to pure l.v.c. in steps of 5 wt.%. Thus 378 individual simulations were carried out for each equation of state. Some of the input parameters were fixed for each simulation. The following is a list of the parameters and their values that were constant throughout the comparison:

Table 5.6: Values of parameters kept constant in model comparison

Input Parameter	Value
Evaporator load	3kW
LSHX Used	Yes
Subcooling in LSHX	10.0 degrees C
Evaporator pressure drop	15kPa
Water inlet temperature	20.0°C

Table 5.6: Values of parameters kept constant in model comparison

Input Parameter	Value
Water flowrate	$0.07 kgs^{-1}$
Condenser pressure drop	15kPa

Table 5.7 shows the value of the input parameters that were varied. Two values of each parameter were taken. For example both the CCOR and the CSD models were run with evaporator the UA_e values set at 0.2 and $1.0 kWK^{-1}$.

Table 5.7: Values of variable parameters in model comparison

Variable	Values when varied		Values when constant	Units
UA_e	0.2	1.0	0.60	kWK^{-1}
UA_c	0.26	1.3	0.78	kWK^{-1}
compressor poly. eff.	0.55	0.77	0.75	none
glycol inlet temp.	-6.75	0.0	-5.0	°C
glycol outlet temp.	-8.25	-15.0	-10.0	°C

The other parameters were set to those values in column 3 of Table 5.7 and to the values in Table 5.6. (Note: when UA_e was set to $0.2 kWK^{-1}$, UA_c was set to $0.26 kWK^{-1}$ i.e. 1.3 times UA_e). Similarly when the glycol inlet temperature was 0.0°C, the outlet temperature was set at -15.0°C). The programs CCORCOMPVARY and CSDCOMPVARY were used to generate the results for comparison.

A special program (imaginatively called COMPARE) was written, which took the results file from both models and calculated the differences. The comparison program read both output files (Section C.3 on page 234 for a typical example) and expressed the CCOR result as a percentage deviation from the CSD result, see below.

$$\%\ difference = \left(\frac{CSD\ result - CCOR\ result}{CSD\ result}\right) \times 100 \qquad \text{(Eq 5.16)}$$

Since CCORCOMPVARY expresses cycle parameters as a function of composition the comparison program listed this difference in this manner also. In addition an average difference over the whole composition range for each cycle parameter was calculated.

N.B: Differences between the CSD and CCOR evaporator gliding temperature differences (GTD_e) are not expressed as a percentage. They are simply represented as the difference between the CSD and CCOR value i.e.

$$difference\ in\ GTDe\ =\ GTD_{e\ CSD} - GTD_{e\ CCOR} \qquad \text{(Eq 5.17)}$$

In some instances the evaporator GTD may sometimes be close to zero or negative. This would lead to a large misleading percentage difference if Equation 5.16 was used.

5.6.2 Comparison Results

Using the program COMPARE, the differences between the two models were calculated for the three refrigerant pairs considered. The values of the optimum interaction constant k_a used with the CSD equation were: -0.00789 for R32/R134a; 0.00292 for R125/R134a and -0.00584 for R32/R152a (Appendix E). The composition was varied from zero weight fraction R32 to 1.0 weight fraction in intervals of 0.05. The overall average differences were calculated across all the conditions and compositions and these are summarised in Table 5.8.

Table 5.8: Average differences across all conditions and refrigerants

Parameter	% Difference	Parameter	% Difference	Parameter	% Difference
COP	2.01	P_r	1.04	η_{ex}	1.88
Vc	2.39	m_{flow}	5.36	η_i	5.95

Table 5.8: Average differences across all conditions and refrigerants

Parameter	% Difference	Parameter	% Difference	Parameter	% Difference
W_{comp}	2.06	GTD_e	0.31 (°C)	F_{desup}	25.16
Q_{cond}	0.49	GTD_c	16.97	ΔT_{wat}	0.44

Differences in the major cycle parameters are quite small (<3%). The parameters with the largest difference (F_{dsup} & GTD_c) are associated with the condenser. The compressor discharge temperature is the state point at which the equations of state differ most markedly (e.g. for pure R32 with the above conditions the CCOR equation discharge conditions are 80.8°C and 18.8bar a while those for the CSD equation are 86.8°C and 18.7bar a). Thus the parameters that depend on the condenser conditions show the largest differences. Using the CCOR equation of state in a refrigeration cycle simulation compares well with the CSD equation of state, for which optimised interaction constants have been calculated. In simulating a refrigeration cycle, the method used to calculate the thermodynamic data does not significantly influence the cycle results, assuming that reasonably accurate thermodynamic data is provided. Specifications such as heat load, sink and source temperatures have a larger influence on the COP, pressure ratio etc.

Application of the CCOR model to a HFC refrigerant mixture (for which there exists little data) would yield a value of COP and exergy efficiency which would compare favourably to the same model using the CSD equation of state. Thus a reasonably accurate value of the main refrigeration cycle parameters could be estimated from a comparatively small amount of fluid data. The CCOR model would allow one to make an assessment of a proposed new refrigerant, within a certain margin of error. Credible value of COP, compressor work, pressure ratio and condenser heat load could be predicted. The model is reasonably easy to use and allows the performance of a cycle to be determined relatively quickly and easily.

These comparisons indicates that the method used to supply the thermodynamic data does not have a very significant bearing on cycle parameters. Factors such as heat

transfer UA values, compressor efficiency etc. have a greater influence. The values for these parameters would not be as accurate compared to an experimental investigation or a model which rigorously accounted for pressure drops and heat transfer coefficients.

5.6.2.1 Comparison of CCOR Model with Optimised Interaction Parameters

In Section 5.6.2 the results of the model using the CCOR equation with zero interaction constants were compared to the same model where the thermodynamic data was supplied by the CSD equation of state with an optimised interaction constant. It was decided to examine if the application of optimum interaction constants, as calculated in Section F.5.2 on page 303 (i.e from whole sets of VLE data), with the CCOR equation would make the differences between the CCOR model and the CSD model any smaller. The differences in the models should be smaller with optimum interaction constants as the thermodynamic data should be more accurate. The values of the CCOR optimised interaction constants are shown in Table 5.9.

Table 5.9: Optimised CCOR interaction constants

Mixture	Optimised k_a	Optimised k_c
R32/R134a	-0.00546	0.00962
R32/R152a	-0.00379	0.00984
R125/R134a	0.01274	0.00992

The models were rerun with exactly the same refrigerants, the same operating conditions and the same range of compositions. This comparison should give a measure of how much the interaction constants can effect the calculation of the overall cycle parameters (for HFCs at least). The differences between the models are displayed in Table 5.10.

Table 5.10: Overall average differences for the three fluids with the optimised CCOR model

Parameter	% Difference	Parameter	% Difference	Parameter	% Difference
COP	1.89	P_r	1.32	η_{ex}	1.73
Vc	3.15	m_{flow}	4.83	η_i	5.91
W_{comp}	1.93	GTD_e	0.20°C (*)	F_{desup}	24.03
Q_{cond}	0.49	GTD_c	17.01	ΔT_{wat}	0.44

(* GTDe has units of °C since it is not a percentage difference; Equation 5.16).

All of the parameters except the specific volumetric capacity and condenser GTD have smaller differences when compared to the zero interaction constant CCOR model of Table 5.8. The reductions in most of the parameter differences are not very large (0.2-1.0%). The mass flowrate and the pressure ratio (P_r) show the largest reductions. Optimised interaction constants do reduce the differences between the models but not by any great extent. Optimised interaction constants can mitigate the differences to some extent but they cannot eliminate the differences altogether. The differences stem from the derivation and of the equations and the logic which underpins them. Both fluids use the hard sphere fluid theory as their basis (Section 2.7.4 on page 62). However, the CCOR equation uses a simpler function to describe hard sphere behaviour. Also, the CCOR equation has been derived from theories which visualise a fluid composed of rotating dumbbells. This is absent from the CSD equation. The CSD equation contains a Redlich-Kwong type term which does not appear in the CCOR equation of Table 5.10. With a new refrigerant mixture, determination of binary interaction CCOR constants does not seem to substantially improve the accuracy of the model.

5.7 Results of Mixtures Application

Mixtures of refrigerants can offer efficiency benefits over pure fluids in vapour compression cycles under certain circumstances. In this section binary HFC mixtures will be examined to quantify the efficiency gains. The effects of cycle parameters such as heat transfer coefficient, compressor efficiency etc. will be examined. The model CCORCOMPVARY was used to simulate a simple refrigeration cycle across the composition spectrum. Comparison between pure and mixed cycles were then made.

5.7.1 Conditions and Fluids Examined

Six different binary HFC mixtures were selected on the basis of the maximum gliding temperature difference (Section 5.5 on page 154). The mixtures considered were R32/ R134a, R32/R152a, R125/R134a, R125/R152a, R143a/R134a and R143a/R152a. The composition was varied from 0% m.v.c. to 100% m.v.c. in 5% intervals (i.e. 21 simulations at a given set of operating conditions). Six separate input parameters were varied to gauge their effect on COP, specific volumetric capacity and the other parameters calculated by the model. The six input parameters chosen were: condenser and evaporator UA value (considered together); compressor polytropic efficiency, water flowrate; glycol inlet and outlet temperatures (considered together), pressure drop in the heat exchangers and degree of subcooling of the condensate in the liquid-suction heat exchanger. Each variable was considered separately with the remaining input parameters set at a fixed value. The values of those input parameters whose values were adjusted, are tabulated in Table 5.11. Each parameter was considered separately. Table 5.11 also shows the values for a parameter when it was kept constant.

Table 5.11: Values of model variable input parameters

Parameter	Variable values	Values when constant	Units
UA_e	0.2, 0.3, 0.6, 1.0	0.6	kWK^{-1}
UA_c	0.26, 0.39, 0.78, 1.3	0.78	kWK^{-1}
Compressor polytropic efficiency	0.55, 0.65, 0.75, 0.85	0.75	(-)
water flow rate	0.07, 0.1, 0.15, 0.2	0.078	kgs^{-1}
Glycol inlet temperature	-6.25, -5, -2.5, 0.0	-5	°C
Glycol outlet temperature	-8.75, -10, -12.5, -15	-10	°C
Heat exchanger pressure drop	5, 15, 25, 35	15	kPa
Degree of subcooling in liquid suction heat exchanger	0, 5, 10, 15	10	deg. C

Condenser and evaporator UA values were considered together. Throughout the refrigeration cycle simulation, UA_c was kept to a fixed ratio of UA_e i.e. $UA_c = 1.3 \times UA_e$. For these values of UA the values of compressor polytropic efficiency, water flowrate, glycol inlet and outlet temperatures and the heat exchanger pressures drops were set to 0.75, $0.078 kgs^{-1}$, -5°C, -10°C and 15kPa respectively. The glycol inlet and outlet temperatures were similarly linked, with values selected so that the arithmetic mean of the two temperatures would equal -7.5°C. Thus the effect of the glycol's temperature change was being examined at a constant average temperature. This would be a fairer comparison as opposed to fixing the inlet glycol temperature and lowering the glycol outlet temperature Table 5.12 details the values of those parameters that were not varied throughout the investigation. When the value of the

pressure drop was varied from 5 to 35kPa, both the evaporator and condenser pressure drops were set to the same value.

Table 5.12: Values of model fixed input parameters

Parameter	Value
Evaporative Load	3kW
Water inlet temperature	20°C

5.7.2 Results with R32/R134a

In this section, calculated values of some of the main cycle parameters are presented for an R32/R134 mixture. The effect of mixture composition upon the refrigeration cycle are graphically illustrated in Figure 5.5-5.14.

At low UA values there is little extra benefit to be gained from using a mixture as shown in Figure 5.5. The COP does not change very much with increasing R32 weight fraction. A graph of the percentage change in COP over the *higher pure fluid COP* as a function of composition is shown Figure 5.6. This percentage change is given by:.

$$\%\ COP\ change\ = \left(\frac{COP_{mixture} - COP_{pure}}{COP_{pure}} \right) \times 100 \qquad \text{(Eq 5.18)}$$

where COP_{pure} is the *larger* of the two pure fluid COPS. This parameter measures the relative change in COP as the composition of the mixture changes. The percentage COP change is relative to the higher of the two pure fluid COPs so that any COP benefits attributable to mixtures can be estimated.

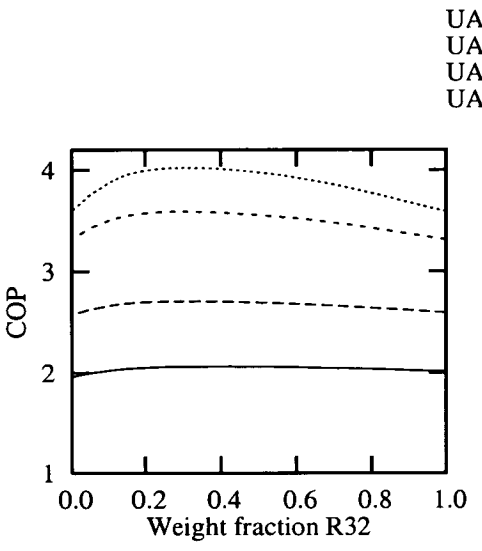

Figure 5.5: R32/R134a COP vs. composition

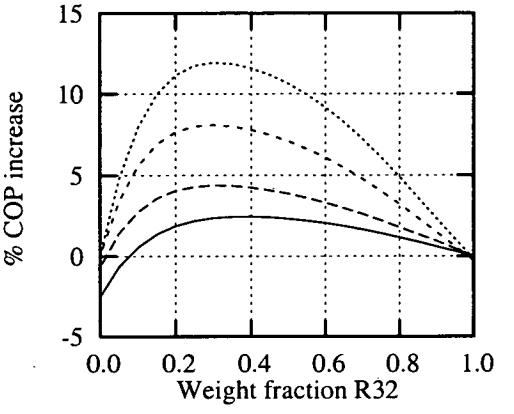

Figure 5.6: R32/R134a percentage change in mixture COP over higher pure COP vs. composition

With UA_e at $0.2 kWK^{-1}$ (and UA_c at $0.26\ kWK^{-1}$) the largest increase in COP over the pure R32 COP (the higher of the two pure fluids) is 2.4%. With the specified heat load of 3kW the evaporator log mean temperature difference (ΔT_{LMe}) is 15 degrees C; while the corresponding value for the condenser is 17 degrees C. Larger log mean temperature differences in the heat exchangers mean that mixture benefits to COPs are reduced. Since the heat transfer fluid temperatures are specified, larger values of ΔT_{LM} mean higher condenser pressures and lower evaporator pressures. The enhancement that mixtures can make to the COP are reduced at larger values of ΔT_{LM}. As the values of UA are increased (proportionately) not only does the absolute value of COP increase (because of improved heat exchange) but also the gain in COP due to mixtures also increases. The temperature matching means that the benefit due to the mixed fluid increases as the UA values increase.

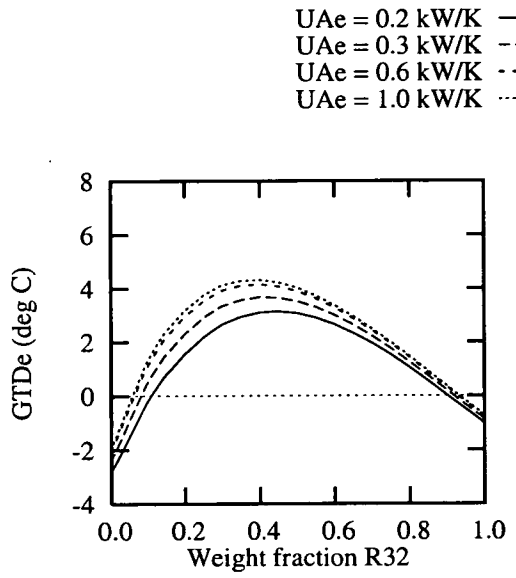

Figure 5.7: R32/R134a evaporator GTD vs. composition

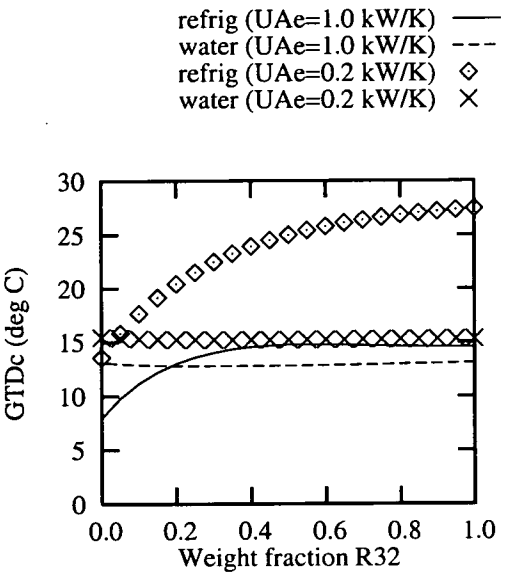

Figure 5.8: R32/R134a condenser GTD and water ΔT vs. composition

The peak COPs occur at 30 wt.% R32 for UA_e = 0.3, 0.6 and 1.0kWK^{-1} (35% for UA_e = 0.2kWK^{-1}). The gliding temperature differences in the evaporator have their maximum values at around 40 wt.% R32 Figure 5.7). The largest GTD in the evaporator (when UA_e = 1.0 kW K^{-1}) is 4.31 degrees. This is similar to the specified glycol temperature change of 5 degrees. As the UA values increase, the maximum GTD in the evaporator approaches temperature difference of the glycol, which leads to better temperature profile matching, hence improved COPs. For the condenser, both the gliding temperature difference and the water temperature difference are shown in Figure 5.8. For reasons of clarity, only the profiles associated with the highest and lowest UA values are displayed. The condenser GTD and water ΔT are denoted by points for UA_e = 0.2kWK^{-1} and by lines for UA_e = 1.0kWK^{-1}.

With UA_e = 0.2kWK^{-1} the water ΔT and the condenser GTD have the same value at low concentrations of R32 (profiles are denoted by dots). As the proportion of R32

increases, the condenser GTD increases while the water ΔT stays roughly the same. This results in a temperature mismatch and consequently there is little improvement in the COP. However when $UA_e = 1.0 kW K^{-1}$ the condenser GTD and the water ΔT are quite similar over most of the composition range (at 20 wt.% R32 they have the same value). Hence the COP of the mixture is improved because of the better match.in temperature changes. For the evaporator it has been noted that the evaporator GTD is similar to the glycol ΔT at 40% R32. The compositions where the condenser and evaporator GTDs are closest to the heat transfer fluid temperature change (20% and 40% respectively) lead to the maximum COP being located at 30 wt.% R32. From these simulations, good temperature matching in both exchangers led to improvements in COP for the R32/R134a mixture. COPs are enhanced when the log mean temperature differences are comparable to the refrigerant temperature glide. Large values of ΔT_{LM} reduce the potential benefits of binary mixtures.

Other Parameters

The compressor work requirement reduces as the heat transfer in the exchangers is improved. Increasing the UA values leads to reduced compressor work. Since the evaporative heat load is fixed by the algorithm in all of the simulations, the trends in compressor work with composition inversely reflect the trends in COP. The combination of specifying the evaporative load and the requirements of the overall energy balance (Equation 1.1 on page 3) mean that the condenser heat load will vary with composition and UA values in exactly the same manner as the compressor work.

The compressor pressure ratio is reduced as the heat exchanger UA values are increased, as shown in (Figure 5.10). Increasing the UA values (at constant evaporator heat duty) means lower ΔT_{LM} values. The convergence in condenser and evaporator conditions reduce the pressure ratio (and consequently decrease the work requirement).

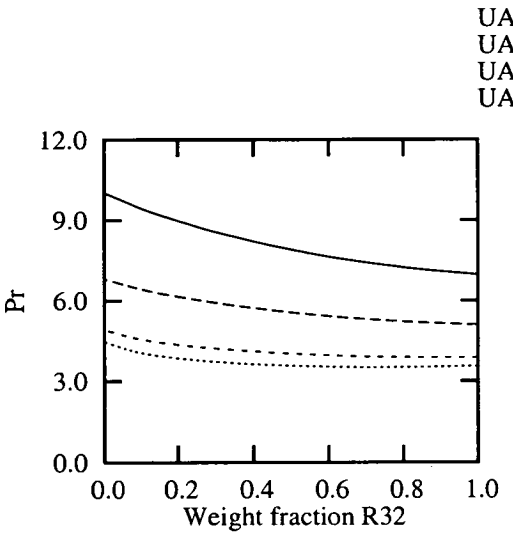

Figure 5.9: R32/R134a compressor pressure ratio vs. composition

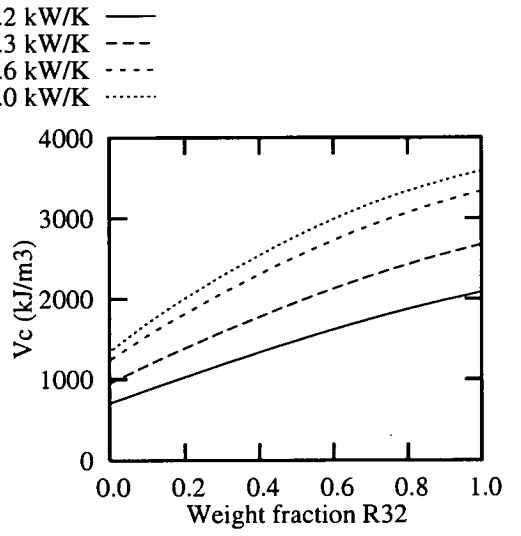

Figure 5.10: R32/R134a specific volumetric capacity vs. composition

For all four UA values R32, has a lower pressure ratio than R134a. At lower UA values the change in pressure ratio with composition is reduced. With $UA_e = 1.0 kW K^{-1}$ and $UA_c = 1.3 kW K^{-1}$ there is little change in the pressure ratio with composition.

Examining the graph of specific volumetric capacity vs. composition (Figure 5.11), it can be seen that V_c increases as the value of UA becomes larger. The specific capacity depends mainly on conditions in the evaporator. With increasing UA the pressure and temperature in the evaporator increases, which means a smaller specific volume. Hence a smaller volume of vapour is needed to effect the same evaporative heat transfer. The specific capacity increases dramatically as the R32 concentration increases. R32 is more volatile than R134a and has a smaller specific saturation volume at the same temperature (Figure B.5 on page 221). In order to achieve an evaporative heat load of 3kW the pressure in the evaporator is higher for R32 and the specific suction volume is smaller. The refrigerant mass flow rate decreases as the R32

concentration increases (Figure 5.12). Consequently the specific capacity increases as the proportion of R32 increases.

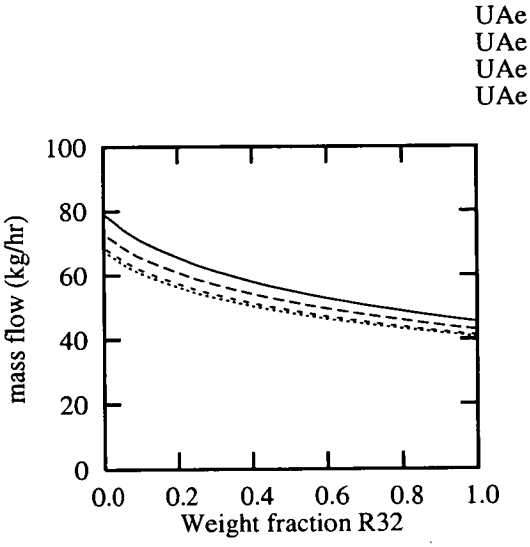

Figure 5.11: R32/R134a refrigerant mass flow vs. composition

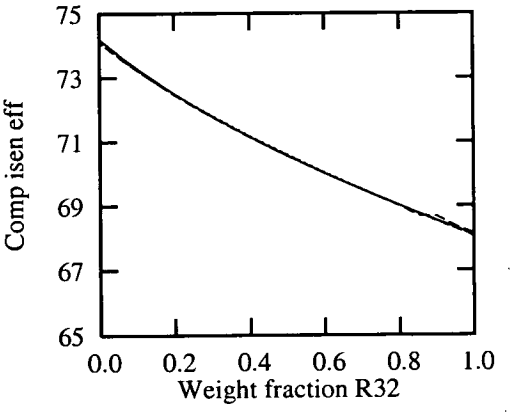

Figure 5.12: R32/R134a compressor isentropic efficiency vs. composition

The mass flowrate decreases slightly with increasing UA values. At a constant value of UA_e and UA_c, the flowrate decreases as the proportion of R32 in the refrigerant mixture is increased. R32 has a higher latent heat than R134a; hence less fluid needs to be circulated around the cycle. With increasing UA values the average temperature on the evaporator refrigerant side rises. The latent heat of a refrigerant reduces with increasing temperature; thus at higher temperature more refrigerant needs to be circulated to achieve a given duty. However, the effect of this is counteracted as the proportion of liquid entering the evaporator is higher. More liquid is available for evaporation to achieve the given evaporative heat load, so a lower flowrate is required, despite the fact that the latent heat of R32 is smaller than R134a, hence less needs to be circulated around the cycle.

UA values do not have much effect on the compressor isentropic efficiency. From Figure 5.12 it can be seen that the composition of the mixture has a larger influence. The polytropic efficiency of the compression process was specified at value of 75%. At any given composition the isentropic efficiency was very similar for all four heat transfer conditions examined. The isentropic efficiency is reduced as the proportion of R32 is increased. A higher proportion of superheat in the condenser is associated with R32. This can be seen in Figure 5.15. As the proportion of R32 in the mixture increases the amount of superheat increases leading to a reduction in isentropic efficiency.

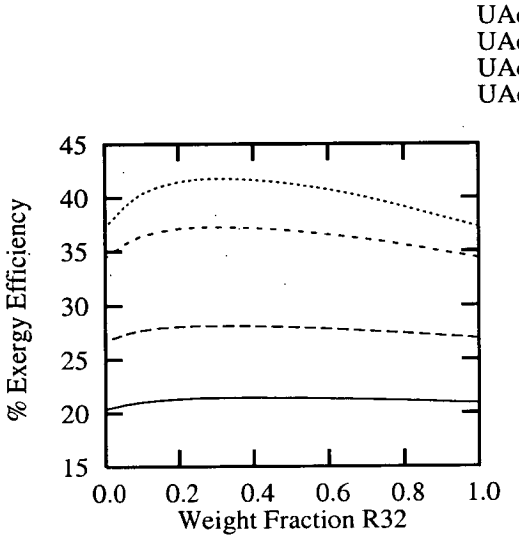

Figure 5.13: R32/R134a exergy efficiency vs. composition

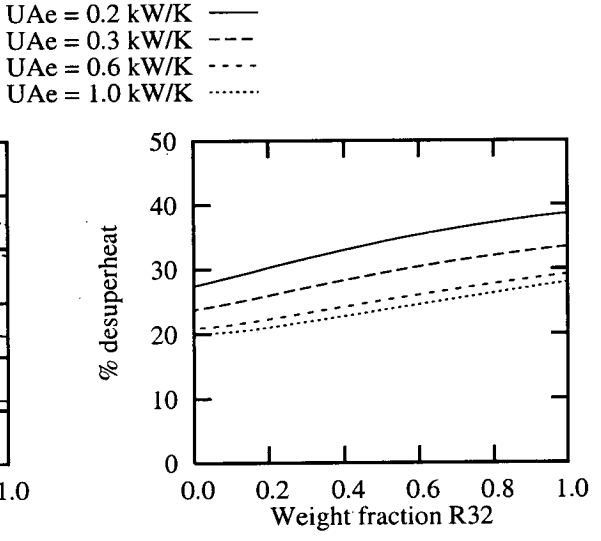

Figure 5.14: R32/R134a percentage desuperheating of condenser heat load vs. composition

The exergy efficiency shows very similar trends to that of the COP (Figure 5.14). Increasing the UA value improves the exergy efficiency. As the UA value is increased the mean temperature differences between working fluid and sink and source fluids are reduced. The exergetic efficiency is the ratio of desired or theoretical exergy to

that which is needed or actually used by the process. For a vapour compression cycle the exergetic efficiency is the ratio of exergy removed from the heat source to the work put in by the compressor i.e.:

$$\eta_{ex} = \frac{\Delta e_{glycol}}{w} \qquad \text{(Eq 5.19)}$$

The exergy absorbed by the glycol (Δe_{glycol}) can also be given by Equation 5.20 [*I.I.R 1980*]:

$$\Delta e_{glycol} = q\left|\left(1 - \frac{T_{datum}}{T_{glycol}}\right)\right| \qquad \text{(Eq 5.20)}$$

Substituting Equation 5.20 in Equation 5.19 yields:

$$\eta_{ex} = \frac{q}{w}\left|\left(1 - \frac{T_{datum}}{T_{glycol}}\right)\right| \qquad \text{(Eq 5.21)}$$

The datum temperature was selected as 293.15 K throughout the simulation. With this particular algorithm, the glycol inlet and outlet temperature are specified; hence the average glycol temperature will remain fixed and thus the term ($1-T_{datum}/T_{glycol}$) will be constant. Thus the exergy efficiency can be described as the COP multiplied by a constant (K):

$$\eta_{ex} = K\frac{q}{w} \qquad \text{(Eq 5.22)}$$

$$\eta_{ex} = K \times COP \qquad \text{(Eq 5.23)}$$

Hence the exergy efficiency will have the same trends as the COP.

5.7.3 Comparison of COP and Mixture COP Change Relative to Pure Fluid COP with Mixture Composition

Rather than tediously examine each refrigerant mixture with each varied parameter, the COP and percentage change relative to the higher pure fluid COP for each mixture (i.e. Equation 5.18) were plotted together on the same graphs. These are shown in Appendix H. Six individual input parameters were varied as part of the simulation exercise: UA values, compressor polytropic efficiency, glycol temperature change, condenser water flowrate, heat exchanger pressure drop and amount of subcooling in the liquid-suction heat exchanger. (See Table 5.11). The model was run with four values of each parameter across all compositions of the six refrigerant mixtures considered. For each of the values of the cycle parameters considered, a graph of the COP and the percentage difference between the mixture COP and the highest pure fluid COP is presented, for each of the six mixtures. Each parameter was considered in turn and its influence upon the mixture COP could be examined. All six refrigerants are shown on the same graph, allowing comparisons between the different mixture pairs to be drawn.

5.7.3.1 UA_e and UA_c Values

The UA values have a significant effect on the absolute value of the COP and the relative improvement that mixtures can offer. Both the absolute value of the COP and the percentage change over the higher pure fluid COP, increase as the heat transfer improves. Proportionately improving the heat transfer of both the condenser and evaporator increases both the absolute value of the COPs and the mixture COP enhancement. Graphs of COP and of the percentage COP change relative to the best performing of the two pure fluids vs. weight fraction of the m.v.c., for the four values of UA_e and UA_c are shown in Figure H.1 to Figure H.8 on page 324. Table 5.13 shows the percentage improvement for the best performing composition for each binary

mixture considered. The composition at which the maximum in COP occurred is also given. At the lowest value of UA_e and UA_c (0.2 and 0.26kWK^{-1} respectively) only R32/R152a and R32/R134a mixtures show any significant improvement over the pure fluid COPs. These two mixtures display a broad maximum rather than a peak. With the other binaries, mixed refrigerants do not confer any additional COP benefits. The mixed COP is not better than the higher of the pure fluid COPs. At a constant evaporator load, increasing UA means that the log mean temperature differences are reduced and the required work is reduced. Addition of R125 to R134a and R152a, causes the COP to reduce sharply, at these heat transfer conditions.

As the UA values increase, the maxima in both graphs become more pronounced. The conditions become more suitable for mixtures and they show superior performance to the pure fluids. At the largest UA value, the maximum percentage increase in the mixture COP for each refrigerant pair lie in the range 5-13%. These improvements in COP are of a similar, if somewhat smaller, magnitude as those reported by other investigators (Section 2.6 on page 49). The enhancements in COP are not exceptionally large. Högberg et al. [*1993*] pointed out that refrigerant mixtures with large glides have more scope for COP improvement. The glides associated with the HFC pairs examined here are not particularly large: they lie in the range 5-9 degrees C. A HFC pair with a gliding temperature difference of 12-15 degrees C would probably produce larger COP improvements. The largest improvement (12.8%) in mixture COP is associated with the R32/R152a mixture, which occurs at a composition of 40 wt.% R32. This pair has the highest COP and the highest mixture enhancement for all four conditions examined. With a few exceptions this refrigerant pair displayed the highest COP and the highest percentage change in mixture COP across all variables examined.

Table 5.13: Maximum percentage improvement in COP relative to higher pure fluid COP and occurring composition (wt.% m.v.c.) with UA_c and UA_e varied.

Binary Mixture	UA_e=0.20kWK^{-1} UA_c=0.26kWK^{-1}	UA_e=0.30kWK^{-1} UA_c=0.39kWK^{-1}	UA_e=0.60kWK^{-1} UA_c=0.78kWK^{-1}	UA_e=1.0kWK^{-1} UA_c=1.3kWK^{-1}
R32/ R152a	3.0%	4.4%	8.3%	12.8%
	35	35	35	40
R32/ R134a	2.5%	4.4%	8.1%	11.9%
	40	30	30	30
R125/ R152a	0.05%	1.3%	5.2%	9.0%
	10	35	55	60
R143a/ R152a	0.1%	1.4%	4.7%	7.9%
	10, 15	35	50	55
R125/ R134a	-	0.7%	3.6%	6.5%
	R134a	25	40	45
R143a/ R134a	0.1%	0.9%	3.2%	5.5%
	10	25	40	40

This is also the pair with the highest glide. R32/R134a is the pair with the next largest COP improvement. In his simulation of a domestic refrigerator Jung et al. [*1991a*], [*1991b*] found that R32/R152a and R32/R134a were the best performing HFC pairs. Pannock [*1992*] also found that of the mixtures examined by him, these two had the highest COPs. Further studies, both experimental and more rigorous simulations, would be recommended to fully ascertain the COP enhancements that these mixtures offer.

5.7.3.2 Compressor Efficiency

With the same six refrigerant mixtures the compressor polytropic efficiency was varied from 55% to 85% in steps of 10%. The composition of each mixture was changed at 5% intervals from pure m.v.c. to pure l.v.c. The evaporator UA value was set to 0.6kWK^{-1} and the corresponding condenser value was 0.78kWK^{-1}. The plots of

COP and percentage COP change relative to the higher pure fluid COP are shown in Appendix H, Figure H.9 to Figure H.16. The results of the best performing mixtures are given in Table 5.14. From the plots it can be seen that improving the compressor efficiency increases pure and mixture COPs. Examining the graphs of the absolute value of COP on the left hand side, it can be seen that the COP rises as the compressor efficiency improves. As the efficiency increases, proportionately less of the compressor work is used in heating the vapour beyond the isentropic discharge conditions. Hence for a specified evaporative load less work is required, and the COP increases. The R32/R152a mixture has the largest values of COP and the largest mixture increase. There is a broad maximum in the COP vs. composition plots. The remaining mixtures have more pronounced maxima. The order of the mixtures with the largest COPs and largest mixture increase coincides with the order of decreasing gliding temperature difference.

Table 5.14: Maximum percentage improvement in COP relative to higher pure fluid COP and occurring composition (wt.% m.v.c.) with compressor polytropic efficiency varied.

Binary Mixture	$\eta_{cmp} = 55\%$	$\eta_{cmp} = 65\%$	$\eta_{cmp} = 75\%$	$\eta_{cmp} = 85\%$
R32/R152a	8.8%	8.5%	8.3%	8.2%
	40	40	35	35
R32/R134a	7.7%	7.9%	8.1%	8.2%
	30	30	30	30
R125/R152a	6.8%	5.9%	5.2%	4.7%
	60	55	55	50
R143a/R152a	5.9%	5.2%	4.7%	4.3%
	55	50	50	45
R125/R134a	4.4%	3.9%	3.6%	3.4%
	45	45	40	40
R143a/R134a	3.5%	3.3%	3.2%	3.1%
	40	35	40	35

Increasing the compressor efficiency seems to affect all the mixtures to the same extent. Pure and mixed refrigerants are influenced to the same degree. Consequently there is no substantial change in the percentage change in COP due to mixtures. The graphs of percentage COP change vs. composition, on the right hand side, are quite similar to each other. In conclusion the compressor efficiency does not seem to have a significant effect on the enhancement of the COP due to mixtures, although it does influence the actual value of the COP.

5.7.3.3 Glycol Temperature Change

Four separate values of the glycol temperature change were examined for the six mixtures across all compositions. The results are shown in Figure H.17-H.24 in Appendix H. The best performing mixtures are summarised in Table 5.15. The glycol inlet and outlet temperatures were *both* adjusted so that the arithmetic average temperature of the inlet and outlet remained constant at -7.5°C. Keeping the inlet glycol temperature constant, and successively lowering the outlet temperature would not be a fair comparison since the average temperature of the glycol would be reduced, requiring a lower pressure in the evaporator and hence lower COPs. Adjusting the inlet temperature upwards and the outlet temperature downwards, so that the average remains constant, should lead to a more meaningful comparison. The four values of glycol temperature drop selected were 2.5, 5, 10 and 15 degrees. The actual inlet and outlet temperatures are shown in Table 5.11 on page 164.

Examining the graphs of COP vs. m.v.c. weight fraction with glycol ΔT as a variable parameter, it is apparent that the absolute value of the COP decreases as the average glycol temperature difference increases (R32/R152a is an exception to this trend). As the glycol ΔT is increased, the plots of COP vs. composition show increasingly pronounced maxima. This is reflected in the plots of mixture COP change relative to the higher pure fluid COP. As the ΔT increases, the mixed refrigerants are more

efficient. In a refrigerant system where the heat sink experiences a relatively large change in temperature the evidence here would suggest that refrigerant mixtures with large glides would be more beneficial to the COP. The shape of the curves follows previous patterns: i.e. R32/R152a has the maximum near the 40% point; the plot for R32/R134a is skewed to the left and the maximum is near 30 wt.%; the remaining mixtures are skewed to the right with the maxima of R125/R152a and R143a/R152a located near 60 wt.% of the m.v.c.; the maxima of R125/R134a and R143a/R134a are located around the 50 wt.% point. Many of the plots of percentage of mixture COP relative to the higher pure fluid COP exhibit this shape throughout this simulation exercise.

Table 5.15: Maximum percentage improvement in COP relative to higher pure fluid COP and occurring composition (wt.% m.v.c.) with glycol temperature change varied

Binary Mixture	ΔT_{gly} = 2.5 deg. C	ΔT_{gly} = 5 deg. C	ΔT_{gly} = 10 deg. C	ΔT_{gly} = 15 deg. C
R32/R152a	5.7%	8.3%	12.1%	14.5%
	30	35	45	45
R32/R134a	5.8%	8.1%	10.7%	12.3%
	25	30	30	35
R125/R152a	3.4%	5.2%	7.5%	9.2%
	50	55	60	60
R143a/R152a	3.0%	4.7%	6.7%	8.2%
	45	50	50	55
R125/R134a	2.3%	3.6%	5.3%	6.5%
	35	40	45	45
R143a/R134a	2.0%	3.2%	4.7%	5.7%
	35	40	40	45

The degree of improvement in mixture COP is proportional to the refrigerant pairs' gliding temperature difference. The order (in terms of maximum improvement in mixture COP) of the mixtures again coincides with the order of the gliding

temperature difference. The refrigerant pair, whose mixture COP is improved most by larger values of glycol ΔT is R32/R152a. With ΔT = 15 degrees C, the improvement over the COP of pure R152a is 14.5%. This was the largest improvement in COP obtained throughout this simulation exercise. This confirms the fact that, in order to maximise the enhancement of mixed refrigerant working fluids, large heat transfer fluid temperature changes coupled with large working fluid temperature glides are best.

5.7.3.4 Heat Exchanger Pressure Drop

The heat exchanger pressure drop was examined for its effect on mixture COP. Four values were chosen (5, 15, 25 and 35kPa). The evaporator and condenser were *both* set to the particular chosen value (i.e. $\Delta P_{cond} = \Delta P_{evap}$). Results for the variation in the pressure drop are presented in Figure H.25-Figure H.32. Table 5.16 tabulates the mixtures which had the best improvement in mixture COP. As with the glycol temperature drop, increasing the pressure drop causes a decrease in the absolute value of the COP, but an *increase* in the percentage mixture enhancement. Large pressure drops mean reduced evaporator exit pressures and increased condenser entrance pressures.

However, in a system with relatively large pressure drops, mixtures seem to perform progressively better than pure fluids. The percentage increase in mixture COP gets larger as the pressure drop increases. With ΔP = 5kPa the maximum improvement in mixture COP lie in the range 2.1%-6.4%. At ΔP =3 5kPa the range is 5.9% to 8.1%. A pressure drop causes the condenser gliding temperature difference to increase and the evaporator gliding temperature difference to decrease. In the situations examined here, the water temperature change is more or less constant at 13.2 degrees C. The mixture R125/R152a is improved most as the pressure drop increases. The increase in pressure drop increases its condenser gliding temperature difference to match the

water temperature change. At the largest pressure drop, and at a composition of 65 wt.% R125, the condenser GTD for the R125/R152a mixture is 13.3 degrees C while the water temperature change is 13.2 degrees C. This mixture has the highest improvement in mixture COP (9.1%). The 50/50 mixture of R32/R152a has a condenser GTD of 19.5 degrees C which means it is not as well matched to the water temperature change as is R125/R152a.

Table 5.16: Maximum percentage improvement in COP relative to higher pure fluid COP and occurring composition (wt.% m.v.c.) with pressure drop varied.

Binary Mixture	ΔP = 5kPa	ΔP = 15kPa	ΔP = 25kPa	ΔP = 35kPa
R32/R152a	6.4%	8.3%	8.6%	8.1%
	30	35	45	50
R32/R134a	6.5%	8.1%	7.9%	7.4%
	25	30	35	35
R125/R152a	3.7%	5.1%	7.0%	9.1%
	50	55	60	65
R143a/R152a	3.2%	4.7%	6.4%	7.0%
	45	50	55	60
R125/R134a	2.5%	3.6%	4.9%	6.5%
	35	40	45	50
R143a/R134a	2.1%	3.2%	4.4%	5.9%
	35	40	45	50

5.7.3.5 Condenser Water Flow Rate

Plots of COP and percentage change in mixture COP vs. composition with the condenser's water flowrate as a parameter are shown in Figure H.33-Figure H.40. The maximum percentage increase in COP for each mixture and water flowrate simulated is tabulated in Table 5.17. High water flowrates promote higher COPs but reduce the

mixture enhancement. At a water flowrate of $0.07 kgs^{-1}$ ($252 kghr^{-1}$), most of the COPs lie in the range 3.2 to 3.6. At the highest water flowrate, $0.2 kgs^{-1}$ ($720 kghr^{-1}$), the range of COPs is 3.7 to 4.2. Increasing the water flowrate seems to have the opposite effect on the percentage change in COP (over the higher pure fluid COP). As an example, with the mixture R32/R134a the maximum COP increase with the flow at 0.07 kg s^{-1} is 8.1%. When the flowrate is set to 0.2 kgs^{-1}, then the maximum COP increase is 4.1%. At the lowest water flowrate (0.07 kgs^{-1}) the maximum percentage increase in mixture COP for R32/R152a and R32/R134a are 8.3% and 8.1%. The plots of percentage increase for these two refrigerants are noticeably larger than the remaining four refrigerant mixtures.

Table 5.17: Maximum percentage improvement in COP relative to higher pure fluid COP and occurring composition (wt.% m.v.c.) with water flowrate varied.

Refrigerant Mixture	m_{water} = 0.07kg/s	m_{water} = 0.1kg/s	m_{water} = 0.15kg/s	m_{water} = 0.2kg/s
R32/R152a	8.3%	7.3%	4.7%	3.8%
	35	30	25	20
R32/R134a	8.1%	6.4%	4.8%	4.1%
	30	25	25	20
R125/R152a	5.1%	4.6%	3.8%	3.3%
	55	55	50	50
R143a/R152a	4.7%	4.2%	3.5%	3.1%
	50	50	45	45
R125/R134a	3.6%	3.2%	2.7%	2.3%
	40	40	35	35
R143a/R134a	3.2%	2.8%	2.3%	2.1%
	40	35	35	35

Raising the water flowrate flattens the graph of percentage change in COP for these two mixtures. At the highest water flowrate (0.2 kg s^{-1}) the percentage increase for R32/R134a and R32/R152a is not substantially different from the other mixtures. The

plots of percentage change in COP converge as the water flowrate increase. For the R32 containing mixtures, as the flowrate increases the composition at which the maximum percentage increase in COP occurs is shifted to the left, towards a lower R32 weight fraction. For the mixtures R125/R152a, R32/R134a, R143a/R152a and R143a/R152a, the composition where the maximum increase in COP occurs, tends to have a higher proportion of the m.v.c. than R32 containing mixtures. As the flowrate increase the composition of the best performing mixture has less and less of the m.v.c.

5.7.3.6 Liquid-Suction Heat Exchanger Temperature Drop

The effect of the degree of subcooling to the liquid condensate upon the mixture COP was examined. The liquid-suction heat exchanger removes heat from the liquid condensate leaving the condenser and transfers it to the vapour entering the compressor. Reduction in the liquid temperature entering the throttling valve normally leads to a lower vapor quality in the two-phase fluid entering the evaporator. More refrigerant liquid is available for evaporation in the evaporator. This is achieved at the expense of higher inlet temperatures into the compressor and consequently higher discharge temperatures. In the model used in this simulation, the drop in temperature experienced by the liquid condensate in the liquid-suction heat exchanger was specified as an input variable. Four values were selected: 0, 5, 10 and 15 degrees C. With values of ΔT_{lshx} greater than 15 a temperature cross occurred in the liquid-suction heat exchanger for some of the refrigerant mixtures. The composition for each refrigerant mixture was varied in the same manner as that of the previous simulations. Plots of COP and change in mixture COP relative to the higher pure fluid COP are shown in Figure H.41-H.48. Table 5.18 tabulates the largest percentage increase in COP for each mixture, relative to the higher of the pure fluid COPs. The composition at which this occurs is also given.

Inspecting Figures H.41, H.43, H.45 and H.47, it can be seen that the COP of all refrigerants, both pure and mixed increases as the temperature drop experienced by the condensed liquid increases. The mixtures are not affected equally. Subcooling of the liquid condensate affects the COP of the mixtures R125/R134a, R125/R152a, R143a/R152a and R143a/R134a to a greater extent than those in which R32 is a component. With ΔT_{lshx}= 0 degrees C, the above four mixtures exhibit a relatively large reduction in COP at high composition of the more volatile component. However, with the largest value of ΔT_{lshx} (15 degrees C) the reduction in mixture COP with increasing m.v.c composition, is much smaller. Above a weight fraction of 0.8 the COP of the mixture R125/R152a is very similar to the COP of the mixture R32/ R152a. For the former mixture the peak COP increases from 3.3856, at ΔT_{lshx} = 0, to 3.5778 at ΔT_{lshx}=15. This represents a 5.7% change in COP. For the R32/R152a mixtures the corresponding COPs at ΔT_{lshx} = 0 deg. C and ΔT_{lshx} = 15 deg. C are 3.5470 and 3.6527 respectively. The increase in peak COP for this mixture is a 3.0%. As ΔT_{lshx} increases there is a convergence of the COP vs. composition curves. Mixtures that do not perform as well in the cycle with no liquid-suction heat exchange are affected to a greater extent than those mixtures which perform best in the basic cycle (ΔT_{lshx}= 0 degrees C). Domanski et al. [*1994a*] conducted an investigation using a simulation model into the effect of a liquid-suction heat exchanger on the refrigeration cycle. Pure refrigerant fluids were used in their study. They came to the conclusion that liquid-suction heat exchange benefit fluids that perform poorly in the basic cycle more than fluids which perform well.

Figures H.42, H.44, H.46 and H.48 show the percentage change in mixture COP relative to the higher of the pure fluid COPs. With no liquid-suction heat transfer R32/ R152a shows the largest increase relative to the COP of pure R152a (R152a has the higher pure fluid COP in this case). From Figure H.42 it is apparent that both mixtures which have R32 as one of their components, show a markedly larger percentage increase in COP than the other four mixtures. As ΔT_{lshx} increases the gain in COP of all the mixtures increases. The degree to which the maximum COP is larger than the

higher of the pure fluid COPs, increases as the temperature drop in the liquid-suction heat exchanger increases. These four plots also show that there was a greater impact on COP for those mixtures which performed least well in the basic cycle. With no liquid-suction heat transfer, the COP of a 40 wt.% mixture of R125/R152a is 2.8% better than that of pure R152a. This is the best performing composition of this mixture. When ΔT_{lshx} = 15 degrees C a maximum in COP occurs at 60 wt.% and this is 6.4% higher than the COP of pure R152a at the same conditions. The corresponding maximum COP enhancements for the R32/R152a mixtures are 7.7% and 8.7%. R32/R152a outperforms the mixture R125/R152a, but R125/R152a is more responsive to liquid-suction heat transfer. The mixture COP enhancement of R125 and R143a mixtures was improved proportionately better as the amount of liquid-suction heat exchange was increased.

Table 5.18: Maximum percentage improvement in COP relative to higher pure fluid COP and occurring composition (wt.% m.v.c.) with condensate temperature change in LSHX varied.

Refrigerant Mixture	ΔT_{lshx} = 0 deg. C	ΔT_{lshx} = 5 deg. C	ΔT_{lshx} = 10 deg. C	ΔT_{lshx} = 15 deg. C
R32/R152a	7.7%	8.0%	8.3%	8.7%
	35	35, 40	40	35, 40
R32/R134a	6.8%	7.6%	8.1%	7.9%
	35	30	30	30
R125/R152a	2.8%	4.0%	5.2%	6.4%
	40	50	55	60
R143a/R152a	2.9%	3.7%	4.7%	5.6%
	40	45	50	50
R125/R134a	2.0%	2.8%	3.6%	4.5%
	30	35	40	45
R143a/R134a	2.2%	2.7%	3.2%	3.7%
	30	35	40	40

Use of liquid-suction heat transfer helps to increases the efficiency gains of mixed refrigerants. Those mixtures which do not perform particularly well in the basic cycle are affected to a greater extent than those mixtures which show relatively good performance in the basic cycle. Cycles using mixtures containing R125 or R143a are more responsive to the addition of liquid suction heat transfer than cycles which have R32 mixtures as a component of the working fluid.

5.8 Summary and Conclusions

A model of a refrigeration cycle was developed and successfully ran. The model used the Cubic Chain-of-Rotators equation of state to calculate the necessary thermodynamic data. Calculated refrigeration cycle parameters, using the CCOR equation were compared to the results where the Carnahan-Starling-DeSantis equation of state was used to supply the thermodynamic data. Zero interaction constants (k_a & k_c) were used with the CCOR model, whereas an optimum interaction constant was used in conjunction with the CSD equation. The models agreed to within 2-5% for most of the cycle parameters. Disagreements focused on the condenser. Using the CCOR equation allowed estimates of cycle performance to be made from small amounts of data on the working fluid. The model can be used to provide preliminary information on the performance of an experimental refrigerant or refrigerant mixture. The model is not a rigorous representation of a real refrigeration cycle. At the stage of screening potential refrigerants it is not necessary to simulate exactly every facet of a cycle. The model can be used as guide to determine if the performance of a proposed refrigerant is sufficient to warrant further investigation.

The CCOR model was used to quantify the likely benefits of using HFC mixtures in a refrigeration cycle. Six refrigerant HFC mixtures were compared at constant evaporative load. It was found that improved heat transfer increased the COP benefits of mixtures. As the UA value in the heat exchangers increased, the improvement in

mixture COP increased. With the best heat transfer conditions the COP was improved by 5.5-14.5% compared to the best performing pure fluid refrigerant of each binary mixture. The compressor polytropic efficiency affected pure and mixed working fluids to the same extent. The improvement in COP by mixtures was independent of the compressor polytropic efficiency. Increasing the heat source temperature change, at constant average heat source temperature, decreased the absolute value of the COP. However, as the temperature change of the heat sink was increased, mixtures became progressively more efficient than pure working fluids. Larger temperature changes in the glycol helped to improve the COP of mixtures beyond that which could be achieved with pure fluids. The refrigerant mixtures with the largest glides, (R32/ R152a and R32/R134a) experienced the largest increase in COP at higher heat sink temperature changes. For the largest heat sink temperature change, increases in COP were in the range 6.0-14.4%. Refrigerant mixtures are best applied when large changes in heat transfer fluid temperature are combined with mixtures with large gliding temperature differences.

Similarly, increasing the pressure drop in the heat exchangers caused the actual value of COPs to reduce. However the mixture COP enhancement actually increased.The six mixtures examined performed better by 5.9-8.1% than pure fluids at the highest value of pressure drop examined. Increased water flowrate boosted the COP. Larger water flowrates reduced mixture COP enhancement. Subcooling the liquid leaving the condenser with the vapour leaving the evaporator helps to improve mixture COPs. The impact upon mixtures which do not perform relatively well in the basic cycle, is greater than those mixtures which do perform well in the ordinary refrigeration cycle.

The increases in COP found in this simulation study are not very large. The largest increases in mixture COP, compared to pure fluid COPs, were in the range 0-15% depending on the conditions. Improved heat transfer and better matching of temperature profiles leads to improvements which fall near the upper limit of this range. These increases fall within the range found by other most other investigators.

The gliding temperature difference of a refrigerant pair strongly influenced its ability to improve mixture COPs beyond the COPs for pure fluids. R32/R152a has the largest gliding temperature difference of the six mixtures examined and it was consistently the best performing mixture in this investigation. The gliding temperature differences of the HFCs examined were relatively small; all were less than 8 degrees C. HFC mixtures with larger temperature glides could improve COPs to a greater extent. Parameters such as heat transfer coefficient and compressor efficiency have a far stronger influence on the COP of a refrigeration cycle than the use of mixed working fluids. The potential of mixtures to improve COP are enhanced when the heat transfer fluids experience large changes in temperature. Application of refrigerant mixtures should be considered as part an overall strategy to improve the efficiency of refrigeration cycles. On their own, refrigerant mixtures will not necessarily lead to very large energy savings.

Chapter 6

Conclusions

This chapter describes the main conclusions resulting from the research work described in this thesis. Each facet of the work is considered separately: experimental work, thermodynamic property prediction and examination of hydrofluorocarbon mixtures in refrigeration a cycle by modelling. Recommendations for possible future work are also given.

6.1 Experimental Work

A limited amount of experimental work was carried out on the refrigeration plant. Not as much research work as the author would have wished was completed. The theft of the computer was a serious and fatal setback to the experimental aspect of the research. An appreciable amount of time and effort went into configuring the computer and the pilot plant instruments so that they communicated correctly. It was not possible to repeat this work before the end of the project. The plant had been successfully commissioned with a number of runs completed with pure R32 and R134a. A series of experimental runs was completed with a 21.9/78.1 wt.% R32/ R134a refrigerant mixture. The compressor's isentropic efficiency was found to decrease linearly with the pressure ratio. An exergy analysis demonstrated that the

evaporator and compressor were responsible for the majority of the inefficiencies in the plant. At lower glycol inlet temperatures the evaporator was responsible for most of the inefficiencies since the compressor was more efficient at higher pressure ratios. Most of the condensation took place in the second condenser, hence the second leg of the plant had a higher mass flowrate. Compressor discharge temperatures with pure R32 were found to be quite high.

Use of hydrofluorocarbon refrigerants in equipment designed for R12 did not lead to any serious operational problems. Replacing mineral oil with a polyol ester oil led to satisfactory operation of the sliding vane compressor. High discharge temperatures were experienced with R32 but were alleviated by installation of a small heat exchanger in the oil circuit. Relatively high amounts of superheat in the compressor suction vapour were noted at lower glycol temperatures.

It was found that the use of HFC refrigerants leads to sealing problems on a refrigeration plant which uses screwed joints. It was found that brazed joints are far superior in the prevention of leaks although they lead to less flexibility. Brass nuts should not be used at low temperatures with pipe sealant and HFC refrigerants. It was found that they had a high tendency to fracture, leading to complete loss of refrigerant charge.

McLinden et al. [*1987*] recommended that pure and mixed refrigerants be compared on the basis of equal heat sink and source temperatures. Equal log mean temperature differences is also a valid means of comparison and this was used in the experimental examination. In practice it was found that it was quite difficult to achieve. Prescribing the inlet and outlet heat source fluid temperatures, the log mean temperature difference between the refrigerant in the evaporator and the heat source fluid lead to long run times. It was found that the plant was quite interactive and adjusting one parameter to a specified value usually meant that another parameter moved away from its prescribed value.

6.2 Thermodynamic Property Prediction from Sparse Data

The Cubic Chain-of-Rotators equation of state was examined for its ability to predict hydrofluorocarbon thermodynamic properties. This equation was chosen because it requires a minimal amount of data on the fluid it describes, namely the critical temperature, critical pressure and acentric factor. No other experimentally derived parameters are needed. Thermodynamic properties, as calculated by the CCOR equation, were compared with published experimental data. Pure and mixed fluid properties were investigated. The ability of the Carnahan-Starling-DeSantis equation of state to predict the same thermodynamic properties was also examined. The CSD equation was used as reference equation of state. It is more complex and requires parameters calculated from pure fluid experimental data. It has been used to supply thermodynamic data in software packages and in refrigeration cycle simulations by other investigators.

Pure fluid thermodynamic properties were compared to those calculated by the Cubic Chain-of-Rotators equation. The CCOR equation predicted the saturation and superheated vapour pressure of pure fluids quite well. Vapour pressure is one of the properties that determines a refrigerant's suitability. The CCOR equation seemed to predict it quite well. Saturated liquid density was not predicted particularly well (average error was 10.1%). Below a reduced temperature of 0.85 the error was independent of temperature and depend on the particular refrigerant. The CSD equation was far superior in describing the liquid phase. Saturated vapour density was not predicted very accurately by the CCOR equation (average error 8.6%). The error associated with vapour density was dependent on temperature and not on the fluid examined. In mitigation, the CCOR equation did predict vapour density slightly more accurately than the CSD equation. Compressed liquids were poorly predicted by both equations of state. Despite the errors in predicting liquid and vapour density, the size of the errors indicate that the CCOR equation could be used to provide preliminary

estimates of the thermodynamic properties of an experimental refrigerant. It could be used to calculate initial data for a new refrigerant, if such data need not be exceptionally accurate. It would not be recommended to use the equation as a high accuracy equation of state for refrigerants.

The CCOR equation was examined for its ability to predict HFC and HFC/HCFC binary refrigerant VLE behaviour. It was found that the CCOR equation represented refrigerant vapour-liquid equilibrium quite well. Prediction of bubble point pressure, bubble point density liquid and vapour composition were superior to the CSD equation. The CCOR equation can be used to provide reasonably accurate VLE data of binary refrigerants. Use of two non-zero interaction constants, derived from *each set* of published experimental VLE data reduced the error of the predictions by approximately 50%. Attempts were made to see if there was any relationship between interaction constants, derived from whole sets of data, and the difference in the ratio of the dipole moment divided by the cube root of the excluded molecular volume. None appeared to exist. Similarly there did not appear to be any relationship between the interaction constants and the difference in the acentric factors of the components of the mixture.

Optimum CCOR interaction constants were calculated for *every point* in an experimental VLE data sets. The application of two interaction constants meant that, with VLE bubble point data, the errors associated with bubble pressure and density were forced to negligible values. Both optimum interaction constants were found to have a regular dependence on temperature and composition for all bubble point data sets. This seemed to indicate that the mixing rules used with the CCOR equation of state could be refined so that the interaction constants are replaced by more complex functions which take account of factors such as temperature, composition and possibly characteristic properties of the fluids in the mixture.

The CCOR equation of state described the properties of HFCs reasonably well. Some properties were better described than others. The equation of state can be used to give

a reasonable estimate of the properties of a new or proposed refrigerant on which little information exists. The equation can be used as an exploratory tool to estimate the thermodynamic properties of an experimental refrigerant or a refrigerant mixture. Such an experimental refrigerant can be examined for its suitability for use in a working fluid in a refrigeration cycle. The CCOR equation would not be recommended for use as a high accuracy equation of state in conjunction with fluids about which a large amount of thermodynamic data was known. In the future stricter environmental constraints may lead to new fluids being proposed as refrigerants. The CCOR equation could be used to provided an estimate of such a proposed fluid's properties with a reasonable degree of confidence.

6.3 Refrigeration Cycle Modelling

A simulation model of a refrigeration cycle was developed. The model was used to quantify the COP benefits of hydrofluorocarbon binary refrigerant mixtures. The CCOR equation of state was used to calculate the necessary thermodynamic data. Comparisons between pure and mixed fluids were made on the basis of equal evaporative heat loads, and equal sink and source fluid temperatures. This ensured a fair means of comparison between pure and mixed refrigerants. The model did not rigorously model pressure drops and heat transfer coefficients. Temperature profiles in the evaporator and condenser were calculated by subdividing the two phase regions. This accounted for non-linear temperature profiles. An identical model based upon the CSD equation was also developed. A number of simulations were carried out and the results of the two models were compared. It was found that for many cycle parameters such as COP, pressure ratio and exergy efficiency, the difference between the models were quite small (under 3%). Parameters such as heat transfer coefficients and compressor efficiency have a much greater dependence on the cycle conditions and performance than on the method used to calculate the thermodynamic data. The

CCOR refrigeration cycle model allowed the performance of an experimental working fluid in a refrigeration cycle to be assessed.

A refrigeration cycle was simulated with six HFC refrigerant mixtures.: R32/R134a, R32/R152a, R125/R134a, R125/R152a, R143a/R134a and R143a/R152a. A number of cycle parameters were varied to find the conditions which improved mixture COP beyond that achievable with pure fluids. For each mixture and set of conditions, a cycle was simulated across the whole composition range. For a given mixture the percentage change in mixture COP relative to the higher of the pure fluid COPs was plotted as a function of composition. As the heat transfer in the evaporator and condenser improved, the degree to which mixtures outperformed pure fluids increased. Increased compressor polytropic efficiency affected mixtures and pure fluids to the same extent. Increasing the heat source temperature drop, at constant average temperature decreased COPs for all refrigerants, pure and mixed. However as the temperature drop of the heat sink increased, the degree to which mixtures outperformed pure fluids increased. At the highest heat source temperature change mixtures were 5.7-14.5% better than the higher of the pure fluid COPs. Under the conditions examined, increasing the heat exchanger pressure drop led to better temperature profile matching and better mixture COPs, although the improvements were below 10%. It was found that liquid-suction heat transfer affected mixtures which performed relatively poorly in the basic cycle, more than those mixtures which performed relatively well. R32/R152a was consistently the best performing mixture. It also had the largest gliding temperature difference. If for each variable examined, the mixtures were placed in descending order of maximum COP, then this order was the same as the order of mixtures if classified according to size of the gliding temperature difference.

The improvement in COP due to the use of mixtures was modest (0.0-14.5%). Parameters such as heat transfer coefficient and compressor efficiency had a more profound effect upon COP. All of the gliding temperature differences were under 9

degrees C (at 1 bar a). Compared to the glides of some CFC and HCFC mixtures, this is not particularly large. It was found the largest improvements in COP in this study occurred when the temperature change of the heat sink was greatest. Improvements in COP with the mixtures considered here are restricted because the temperature glides of the mixtures are not very large. In order to fully maximise the energy benefits of mixtures, refrigerant mixtures with as large as possible glides, coupled with relatively big changes in heat sink or source temperature are required. Use of refrigerant mixtures should be considered as one component as part of an overall strategy of improving refrigeration cycle efficiency.

6.4 Future Work and Recommendations

The most obvious recommendation to be made is that the program of experimental results for which the plant had been constructed should be completed. Experimental runs for mixtures of 40, 60 80, 100 wt.% R32 and 100 wt.% R134a at the conditions detailed in Table 4.3 on page 124 should be carried out. Hence improvements in COP, specific volumetric capacity and other parameters can be quantified from an actual experimental refrigeration plant.

The heat transfer area of the evaporator should be increased. The log mean temperature difference of 25 degrees C, used in the 21.89/78.1 wt.% R32/R134a series of run was rather large. In any new investigation this should be reduced to near a value of 8-12 degrees C or smaller if possible. This would mean replacement of the current pool boiling evaporator since its design is not amendable to increases in the heat transfer area. On a practical note it would be desirable to simplify the low pressure side of the refrigeration plant. This could be achieved by removing the metering pump and associated pipework and using a brazed pate heat exchanger as the evaporator (similar to those used in the condensers). A simpler plant would lead to less maintenance, downtime and would have fewer components to malfunction. Brass

nuts and pipe sealant should not be used at low temperatures (they may be used on the high temperature-high pressure side of a refrigeration plant). Brazed type joints should be used even though this may lead to problems of flexibility if individual pieces of equipment need to be repaired or individually examined. The distance between the evaporator exit and the compressor suction inlet port should be reduced to decrease the amount of superheat in the suction vapour. A certain amount of superheat is needed to prevent liquid droplets entering the compressor but it should not be excessive.

One final matter concerning practical alterations to the experimental apparatus is the matter of security. In any academic investigation it is not normally considered a pressing priority unless confidential information is being dealt with. Bitter experience has taught the author of this thesis otherwise. Customised and specialized electronic equipment which has a potential black-market resale value should be adequately protected. Loss of such equipment can prove catastrophic to research and does not inspire a great deal of confidence in researchers.

In any new investigation of the efficiency benefits of mixtures, refrigerant mixtures with large temperature glides should be examined. These are more likely to yield improvements in cycle efficiency. With the phasing out of CFCs the range of substances to choose from has been reduced. Such mixtures could involve hydrocarbons and other non-halogens. There may be practical and safety difficulties associated with these. Ternary refrigerant mixtures could also be examined. Mulroy, Domanski and Didion noted that certain ternary mixtures may exhibit linear temperature-enthalpy profiles during phase changes, unlike binary mixtures which often have curved temperature-enthalpy profiles which can lead to pinch points in the condenser and evaporator [*Domanski et al. 1994a*] [*Mulroy et al. 1994*]. Linear temperature-enthalpy profiles in refrigerant mixtures help to improve COPs (Section 2.4.10 on page 36).

It would be worthwhile to carry out a cost-benefit analysis on the use of mixed refrigerant working fluids. Mixture COPs are enhanced at higher UA values. In order to increase the UA value it is often necessary to increase the area of the heat exchangers. There is trade-off between increased capital cost and reduced operating cost. A proprietary chemical process plant simulation package could be used in such an investigation. Some of these can carry out economic calculations. Ultimately there is little point in using mixed refrigerants if the gain in efficiency is outweighed by increases in the capital cost of the equipment. This trade-off should be investigated.

The apparent regular dependence of optimised CCOR interaction constants k_a and k_c with bubble point VLE temperature and composition should be further investigated. Such a study should extend over a broad range of mixture VLE data encompassing hydrocarbons, non-organic compounds etc. The regular variation in k_a and k_c may possibly point towards more complex but improved mixing rules which take into account more parameters but lead to better predictions of mixture VLE data. Other equations of state should be examined as well. The phenomena found here may indeed only occur with the CCOR equation and HFC refrigerant mixtures, but it warrants further investigation.

Appendix A

Design Mass and Energy Balance

A.1 Assumptions and Specifications

Refrigerant is pure R32.

High pressure = 25 bar a.

Low pressure = 5 bar a.

Stream numbers refer to Figure 3.2 on page 82. A temperature-entropy diagram is shown in Figure A.1.

R32 enthalpy and entropy values are taken from thermodynamic tables published by I.C.I Chemicals and Polymers [*I.C.I.*].

Initial calculation basis: flowrate through compressor is $1\,kg\,s^{-1}$.

A.2 Calculations

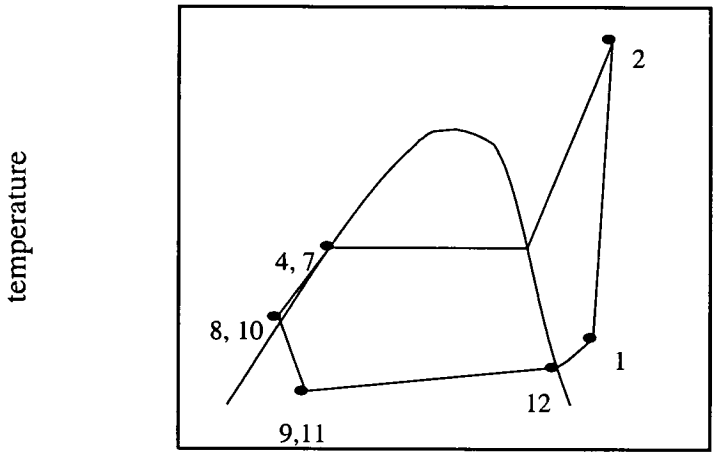

Figure A.1: Temperature-entropy diagram of the experimental cycle.

Compression

$p_{suct} = 5\,\text{bar a}$

$p_{disch} = 25\,\text{bar a}$

Assume 15 degrees of superheat in compressor suction. R32 is a volatile refrigerant and will be superheated if there is a relatively long distance between the evaporator and the compressor suction (as there is in this plant). Saturation temperature at 5 bar a = -14.4°C; hence T_{12} = -14.4°C. Therefore $T_1 = T_{12} + 15 = 0.6°C$

From the thermodynamic tables $h_1 = 426.8\,\text{kJ kg}^{-1}$ and $s_1 = 2.2670\,\text{kJ kg}^{-1}\text{K}^{-1}$

The pressure ratio (p_r) of the compressor (Section 3.4.1.1 on page 83) is 5. With this compressor, Low [62] had correlated a relationship between the pressure ratio and the compressor isentropic efficiency:

$$\eta = 0.041 + 0.14 p_r \qquad \text{(Eq A.1)}$$

Although this correlation was obtained with CFCs it was felt that it would provide a reasonable estimate of the compressor isentropic efficiency. With a pressure ratio of 5 the efficiency according to Equation A.1 would be 0.741. This allows the exit conditions to be calculated.

The exit isentropic enthalpy $h_2^* = 501.4 kJkg^{-1}$ (by linear interpolation from the thermodynamic tables)

By definition the compressor isentropic efficiency η is:

$$\eta = \frac{h_2^* - h_1}{h_2 - h_1} \qquad \text{(Eq A.2)}$$

Rearrangement for h_2, the real discharge enthalpy, gives:

$$h_2 = \frac{h_2^* + h_1(\eta - 1)}{\eta} \qquad \text{(Eq A.3)}$$

With $h_2^* = 501.4 kJkg^{-1}$, $h_1 = 426.8 kJkg^{-1}$ and $\eta = 0.741$ gives $h_2 = 527.4 kJkg^{-1}$. Interpolating for temperature $T_2 = 126.1°C$

Hence the work of compression is 527.4 - 426.8 = 100.6 kJ per $1.0 kgs^{-1}$ of refrigerant.

Condensation

Assume the first condenser desuperheats the vapour and condenses 45% of the vapour with the remaining 55% being condensed in condenser 2. This was the split assumed by Low. If $m_2 = 1\ kg\ s^{-1}$ then $m_4 = 0.45 kg s^{-1}$ and $m_5 = 0.55 kg s^{-1}$.

Since they are saturated the specific enthalpies of stream 4 and stream 6 are $175.1 kJ kg^{-1}$ and $411.3 kJ kg^{-1}$ respectively and the temperatures is 40.6°C.

The heat load in condenser 1 is given by:

$$Q_{c1} = m_2(h_2 - h_3) \qquad \text{(Eq A.4)}$$

$$Q_{c1} = m_3 h_3 - m_4 h_4 - m_5 h_5 \qquad \text{(Eq A.5)}$$

This yields $Q_{c2} = 222.4 kJ$ per $1.0 kg s^{-1}$ mass flowrate of refrigerant in the compressor.

Thus h_3 can be found from Equation A.4 and is $305.1 kJ kg^{-1}$.

The specific enthalpy of stream 6 is also $175.1 kJ kg^{-1}$

Hence the load on condenser 2 is simply:

$$Q_{c2} = 0.55(411.3 - 175.1)$$

$$Q_{c2} = 129.9 \text{ kJ (per 1.0 kg/s of refrigerant in compressor)}$$

Subcooling

Assume 10 degrees of subcooling in each subcooler i.e. $T_8 = T_{10} = 30.6°C$. From the tables the saturated specific enthalpy at this temperature $h_8 = h_{10} = 155.0 kJ kg^{-1}$.

The heat load in subcooler 1, Q_{sc1}:

$$Q_{sc1} = 0.45(175.1 - 155.0)$$

$$Q_{sc1} = 9.0 kJ$$

Likewise $Q_{sc2} = 11.1\,kJ$

Expansion

The expansion process is assumed to be isenthalpic i.e. $h_9 = h_8 = 155\,kJkg^{-1}$ and $h_{10} = h_{11} = 155\,kJkg^{-1}$.

The pressure after expansion is assumed to be 5bar a. The vapour and liquid saturation enthalpies (h_{vap} & h_{liq}) at this pressure are $75.8\,kJkg^{-1}$ and $411.8\,kJkg^{-1}$ respectively.

The vapour quality (x) is given by:

$$x = \frac{h - h_{liq}}{h_{vap} - h_{liq}} \qquad \text{(Eq A.6)}$$

Thus:

$$x = \frac{155 - 75.8}{411.8 - 75.8}$$
$$x = 0.236$$

Similarly the vapour quality for stream 11 will be 0.236

Evaporation and Superheating

Streams 9 and 10 are mixed in the evaporator and vaporised. The heat load Q_{ev} is given by the energy balance:

$$Q_{ev} = m_{12}h_{12} - m_9h_9 - m_{11}h_{11} \qquad \text{(Eq A.7)}$$

At 5 bara the saturation vapour enthalpy of R32 is $411.8\,kJkg^{-1}$. Therefore:

$$Q_{ev} = 1 \times 411.8 - (0.45 \times 155.0) - (0.55 \times 155.0)$$
$$Q_{ev} = 256.8\text{kJ (per 1 kg/s of refrigerant)}$$

15 degrees of superheating from the pipework was assumed hence the heat lost is simply:

$$Q_{sup} = 426.8 - 411.8$$
$$Q_{sup} = 15.0\text{kJ}$$

Heat and Work Loads and Mass Flowrates

The evaporative heat load was specified as 8kW. Thus the flowrates and energy transfers for the rest of the plant can be determined.

The compressor mass flow is simply found from Equation A.7:

$$m_{cmp} = \frac{8}{256}$$
$$m_{cmp} = 0.03125\text{kg/s} = 112.5\text{ kg/hr}$$

The remaining heat and work loads have been calculated. The thermodynamic information describing the cycle has been summarised in Table A.1 and Table A.2.

Table A.1: Calculated stream conditions of experimental pilot plant

Stream Number	Stream Name	Temp (°C)	Pressure (bar a)	Mass flow ($kghr^{-1}$)	Enthalpy ($kJkg^{-1}$)
1	Compressor Suction	-0.6	5	112.5	426.8
2	Compressor Discharge	126.1	25	112.5	527.4
3	Condenser 1 Exit	40.6	25	112.5	305.1
4	Tank 1 Liquid	40.6	25	50.6	175.1
5	Condenser 2 Vapour	40.6	25	61.9	411.3
6	Condenser 2 Exit	40.6	25	61.9	175.1
7	Tank 2 Liquid	40.6	25	61.9	175.1
8	Leg 1 Subcooled Liquid	30.6	25	50.6	155.0
9	Expanded Leg 1 Liquid	-14.4	5	50.6	155.0
10	Leg 2 Subcooled Liquid	-14.4	5	61.9	155.0
11	Expanded Leg 2 Liquid	-14.4	5	61.9	155.0
12	Evaporator Vapour	-14.4	5	112.5	411.8

Table A.2: Equipment work and heat loads

Equipment	Heat & Work Loads (kW)
Compressor	3.14
Condenser 1	6.95
Condenser 2	4.06
Subcooler 1	0.28
Subcooler 2	0.34
Evaporator	8.00
(Superheat)	0.47

Thus the refrigerating COP with R32 is 8/3.14 = 2.55. These conditions were used to specify new equipment and to ensure that existing equipment could be used.

Appendix B

Prediction of Pure Fluid Hydrofluorocarbon Thermodynamic Properties using the Cubic Chain-of-Rotators Equation of State

B.1 Introduction

The Cubic Chain-of-Rotators (CCOR) equation of state will be examined for its ability to predict correctly the thermodynamic properties of non ozone depleting hydrofluorocarbon refrigerants. Pure fluid properties are examined in this appendix. Prediction of binary vapour-liquid-equilibrium properties are examined in Appendix F on page 277. The CCOR equation requires only the critical temperature, critical pressure and acentric factor. No other experimental data is needed to calculate coefficients or parameters. Since 1991-92, a large amount of HFC thermodynamic data has been published. The properties calculated by the CCOR will be compared with this experimental data. There is, to a certain extent, a contradiction in examining the behaviour of an equation of state which needs very little data, with fluids for which a reasonably large amount of data already exists. However, it is worth examining how well the CCOR equation can predict the thermodynamic properties of replacement refrigerants. Some commentators have queried whether some HFCs are

suitable replacements because of their relatively high greenhouse warming potential. In the future stringent environmental standards may place the HFC refrigerants in jeopardy. It is therefore useful to have tools which can describe properties without the need for experimentally derived coefficients. Thermodynamic data on new refrigerants for which little published data exists may be needed in the future.

B.1.1 Carnahan-Starling-DeSantis Equation of State

The Carnahan-Starling-DeSantis equation of state was used as a reference equation. The predictive ability of the CCOR equation was compared to that of the CSD equation. The CSD has also been developed from molecular theory. It is more complex than the CCOR equation. The equation uses six experimentally derived coefficients and it is theoretically more accurate than the CCOR equation. It has been found to accurately represent the behaviour of CFC refrigerants, both pure and mixed [*Morrison et al.1985a, 1986b*]. The six coefficients are usually calculated from pure saturation data (Section 2.7.4 on page 62). If has been used to calculate refrigerant thermodynamic properties (pure and mixed) in a number of refrigeration simulation studies published in the literature and in proprietary software (Section 2.7.5.2 on page 65). Hence it was decided to use the CSD equation as a reference equation in this research.

B.2 Data Required by the CCOR Equation of State

The Cubic Chain-of-Rotators equation was first presented by Lin et al. [*1983*] and is as follows:

$$p = \frac{RT}{T}\left[\frac{v+0.77b}{v-0.42b} + \frac{c^R}{2}\left(\frac{0.11b}{v-0.42b}\right)\right] - \frac{a}{v(v+c)} - \frac{a}{v(v+c)(v-0.42b)} \qquad \text{(Eq B.1)}$$

The reader is referred to Low [*1991*], Lin et al. [*1983*] and Kim et al. [*1986*] for the formulae for pure fugacity coefficient, departure enthalpy and entropy functions and mixture fugacity coefficient derived from the CCOR equation of state. Low also gives a good synopsis of thermodynamic fundamentals.

Table B.1: General thermodynamic properties of refrigerants to which CCOR equation was applied

Refrigerant	M_w kg kmol^{-1}	T_b (K)	T_c (K)	P_c (bar a)	ω (-)
R22	86.468	232.34	369.30	49.90	0.221
R32	52.024	221.50	351.26	57.77	0.277
R125	120.022	224.66	339.17	36.18	0.301
R134	102.031	250.16	391.74	46.06	0.290
R134a	102.031	247.07	374.27	40.65	0.326
R141b	116.950	305.25	477.31	42.50	0.225
R142b	100.495	263.40	410.26	40.40	0.235
R143a	84.041	225.92	345.97	37.69	0.262
R152a	66.051	249.10	386.41	45.12	0.277

In order to apply the CCOR equation to a given substance the *critical temperature*, *critical pressure* and the *acentric factor* must be known. The Japanese Association of Refrigeration [*1994*] have published a table of these properties for CFCs, HCFCs and HFCs. These values were used in the authors application of the CCOR equation. The refrigerants to which the CCOR equation was applied, and the values of the properties required by the CCOR are listed in Table B.1. The values of molecular weight, normal boiling point are also given, even though they are not actually needed by the CCOR equation.

B.2.1 Terms of Carnahan-Starling-DeSantis Equation

Basic Pressure Explicit Equation

The full pressure explicit form of the Carnahan -Starling-DeSantis equation of state is given by Equation B.2. It is much simpler in form than the CCOR equation.

$$Z = \frac{1 + y + y^2 - y^3}{(1-y)^3} - \frac{a}{RT(v+b)} \qquad \text{(Eq B.2)}$$

The term y is simply given by:

$$y = \frac{b}{4v} \qquad \text{(Eq B.3)}$$

The parameters a and b are functions of temperature:

$$a = a_0 \exp(a_1 T + a_2 T^2) \qquad \text{(Eq B.4)}$$

$$b = b_0 + b_1 T + b_2 T^2 \qquad \text{(Eq B.5)}$$

The terms a_0, a_1, a_2, b_0, b_1 and b_2 are regressed from experimental data for each fluid. Below are listed the thermodynamic functions describing the pure fluid fugacity coefficient, chemical potential, residual entropy and enthalpy.

Pure Fluid Fugacity Coefficient

$$\ln\phi = \ln\frac{RT}{pv} - \frac{a}{RT}\left(\frac{\ln\frac{v+b}{b}}{b} + \frac{1}{v+b}\right) + \frac{\beta(8v^2 - 3\beta(3v-\beta))}{(v-\beta)^3} \qquad \text{(Eq 2.6)}$$

The term β is simply:

$$\beta = \frac{b}{4} \qquad \text{(Eq B.7)}$$

Enthalpy Residual Function

$$h^R = \frac{a\frac{db}{dT}T - b\frac{da}{dT}T - ab}{b^2}\ln\left(\frac{v+b}{v}\right) + \frac{a\frac{db}{dT}T - ab}{b(v+b)} + \frac{RT(4v^2 - 2v\beta)\left(\beta - T\frac{d\beta}{dT}\right)}{(v-\beta)^3} \quad \text{(Eq B.8)}$$

The temperature derivatives of a and b are easily obtainable from Equations B.4-B.5.

Entropy Fugacity Residual Function

$$s^R = \frac{b\frac{da}{dT} - a\frac{db}{dT}}{b^2}\ln\left(\frac{v+b}{v}\right) + \frac{a\frac{db}{dT}}{b(v+b)} - \frac{R\beta(4v-3\beta)}{(v-\beta)^2} - \frac{RT\frac{d\beta}{dT}(4v^2 - 2v\beta)}{(v-\beta)^3} \quad \text{(Eq B.9)}$$

B.2.1.1 Data Needed by CSD Equation

In order to use the CSD equation, six experimentally determined parameters are needed. These are a_0, a_1, a_2, b_0, b_1 and b_2 in Equation B.4 and Equation B.5. These are specific to a given fluid. They are determined from experimental pure fluid saturation data by minimising Equation 2.15 on 64. Parameters for many refrigerants have been published by Morrison and McLinden [*1993*]. The coefficients published in this source were used to implement the CSD equation of state. The author discovered that these coefficients caused discontinuities and errors when used with R152a. Updated coefficients were received from McLinden for R152a and no further problems was experienced. The values of the a parameters are displayed in Table B.2 and Table B.3 shows the b parameters for the refrigerants examined.

Table B.2: Values of the a_0, a_1 and a_2 parameters used with the CSD equation of state

Refrigerant	a_0 (kJm^3kmol^{-2})	a_1 ($kJm^3kmol^{-2}K^{-1}$)	a_2 ($kJm^3kmol^{-2}K^{-2}$)
R22	2.54146×10^3	-2.38706×10^{-3}	-1.83653×10^{-6}
R32	2.11437×10^3	-3.97431×10^{-3}	1.33419×10^{-6}
R125	2.94443×10^3	-2.04973×10^{-3}	-3.83296×10^{-6}
R134	4.42503×10^3	-3.95618×10^{-3}	4.06627×10^{-6}
R134a	3.61180×10^3	-2.89497×10^{-3}	-1.28106×10^{-6}
R141b	5.45053×10^3	-2.27552×10^{-3}	-5.52009×10^{-7}
R142b	4.12561×10^3	-2.64418×10^{-3}	-6.80275×10^{-7}
R143a	2.86677×10^3	-2.78421×10^{-3}	-1.32581×10^{-6}
R152a	3.19863×10^3	-2.96134×10^{-3}	-3.21897×10^{-7}

Table B.3: Values of the b_0, b_1 and b_2 parameters used with the CSD equation of state

Refrigerant	b_0 (m^3kmol^{-1})	b_1 ($m^3kmol^{-1}K^{-1}$)	b_2 ($m^3kmol^{-1}K^{-2}$)
R22	1.13681×10^{-1}	-1.16201×10^{-4}	-9.24562×10^{-8}
R32	9.47768×10^{-2}	-1.99441×10^{-4}	1.72802×10^{-8}
R125	1.45797×10^{-1}	-1.53606×10^{-4}	-1.71292×10^{-7}
R134	1.65176×10^{-1}	-3.14598×10^{-4}	1.68947×10^{-7}
R134a	1.44618×10^{-1}	-1.84368×10^{-4}	-2.53676×10^{-8}
R141b	1.81581×10^{-1}	-1.66736×10^{-4}	-5.46722×10^{-8}
R142b	1.67490×10^{-1}	-2.30449×10^{-4}	5.09031×10^{-8}
R143a	1.30367×10^{-1}	-1.40115×10^{-5}	-9.29504×10^{-8}
R152a	1.33264×10^{-1}	-2.03633×10^{-4}	7.77251×10^{-8}

B.3 Algorithms and Coding of the Equations of State

The C language computer code developed by Low for the CCOR and CSD equations were used to calculate the required thermodynamic properties. No major modifications were made to the routines which calculated the thermodynamic properties and parameters. However, modifications were made to iteration routines to make them more stable, especially as the critical point was approached. New programs incorporating Low's code were written which allowed the published experimental data to be compared to the calculated values. All of the experimental data was typed manually into files which was the most time consuming part of the process. The runtime of the programs were less than a few seconds. For saturation properties a program called SATERRORPLOT was written. All of the saturation properties given in the literature were tabulated as functions of temperature. The program read the temperature and the experimental property in question from the data file. The property in question was then calculated at the temperature that has been read. The program then created an output file to store the results. A typical example of an output file from SATERRORPLOT is given in Appendix C on page 230 for vapour pressure. These are tabulated in columns as follows: temperature, calculated property, experimental property and percentage error. When all of the datapoints have been compared the *percentage average absolute deviation* (%AAD) is calculated i.e.

$$\%AAD = \frac{\sum_{i=1}^{N_{pts}} \left| \frac{P_{exp} - P_{calc}}{P_{exp}} \right| \times 100}{N_{pts}} \qquad \text{(Eq B.10)}$$

The *absolute* value of the percentage error of each datapoint is used to prevent cancellation of error, which would occur if both over and underprediction occurred in the same set of data (e.g. Figure D.20 on page 247). (This would yield a smaller average error than actually existed). At the end of the output file, the number of points

in the dataset, the AAD and the absolute standard deviation of the error is given. The program was able to handle many different units for temperature, pressure etc. since a wide range of units are employed in the literature. The units of the experimental data were converted into the units used by the program. These were Kelvin, Nm^{-2}, m^3kmol^{-1}, $kJkmol^{-1}$ and $kJkmol^{-1}K^{-1}$ for temperature, pressure, specific volume, specific enthalpy and specific entropy respectively. The value of R was taken to be $8314Jkmol^{-1}K^{-1}$. These units were used in all the thermodynamic property programs used by the author, including the refrigeration cycle simulations used in Chapter 5.

Similar programs were written for the PVT behaviour and for VLE comparisons. The experimental data is read in, properties calculated using either the CCOR or CSD equation of state, and the results sent to an output file. After each set of experimental data was processed the AAD and the number of points considered was entered into a spreadsheet. This allowed overall average errors associated with a given thermodynamic property and refrigerant to be calculated (e.g. liquid density of R152a).

B.3.1 Enthalpy and Entropy Reference States

When calculating the enthalpy and entropy of a fluid, mixed or pure, a reference state is needed. There are three main reference states which are commonly used. A commercially used reference state sets the liquid saturation enthalpy is set to 100 $kJkg^{-1}$ at 0°C and the entropy is set to $1kJkg^{-1}K^{-1}$. This was the convention used in this work and for the simulation studies in Chapter 5. The second convention sets the liquid saturation enthalpy at 0°C to $200kJkg^{-1}$ and the entropy to $1kJ\ kg^{-1}K^{-1}$. This is used by the International Institute for Refrigeration in their refrigerant thermodynamic tables. The last convention which is commonly used, sets the enthalpy at -40°C to $0kJkg^{-1}$ and the entropy at this temperature to $0kJkg^{-1}K^{-1}$. All of the programs were adapted so that the user can use any of these conventions. The user

can also specify his own reference enthalpy and entropy at whatever temperature is desired.

B.4 Pure Fluid Results

The property prediction behaviour of the CCOR and CSD were examined with five hydrofluorocarbon refrigerants. The five refrigerants were: R32, R125, R134a, R143a and R152a. These are the main CFC replacement candidates. An examination of the literature revealed that a considerable amount of experimental data existed for comparison purposes (Section 2.7.6 on page 68). The properties examined were: saturation vapour pressure, saturated liquid volume, saturated vapour volume and PVT behaviour. Over 3500 different experimental points published by authors were compared. It would be rather tedious to display each author's experimental values and the values given by both equations. For a given set of experimental data (e.g. vapour pressure of R125 by Baroncini et al. [*1993*]) the AAD was calculated. Comparison of other author's data for the each of the same property and refrigerant allowed a more complete picture of the equation of state's accuracy to be determined. *Overall* average absolute deviations were calculated for each refrigerant and property, using a spreadsheet. The averages were weighted according to the number of points published. Error temperature plots for each property and refrigerant are shown in Appendix D. Both CCOR and CSD errors are graphically displayed. A representative sample of experimental points are shown with the corresponding calculated values in the following sections. Appendix E contains a tabulated analysis of the average errors of each published set of data. The errors are grouped together according to each thermodynamic property. References for each set of experimental data are also given. Pure fluid properties are dealt in Section E.1 on page 262. Tabulated results for the prediction of mixture thermodynamic properties (described in Appendix F) are displayed in Section E.2.

B.4.1 Vapour Pressure

The CCOR prediction of vapour pressure for R32 is shown in Figure B.1. For the 229 points examined the average absolute average deviation is 1.84%. This indicates that the CCOR equation can give good prediction of R32 vapour pressure. At low temperatures the vapour pressure is underpredicted. The largest error is 9.8% and occurs at -82°C (T_r = 0.54). The deviation reduces as the temperature increases. The equation is more accurate in the temperature region of 230-340 K, which would be the region of interest in a refrigeration cycle (depending on application). The error is zero at the critical point because the CCOR equation is forced through the critical point. Figure B.1 also displays the consistency of results between the seven authors who measured vapour pressure of R32. This consistency extends to the other refrigerants as well. The prediction of R32 vapour pressure would seem to be very good above a temperature of 230K, given the paucity of data needed by the CCOR equation of state.

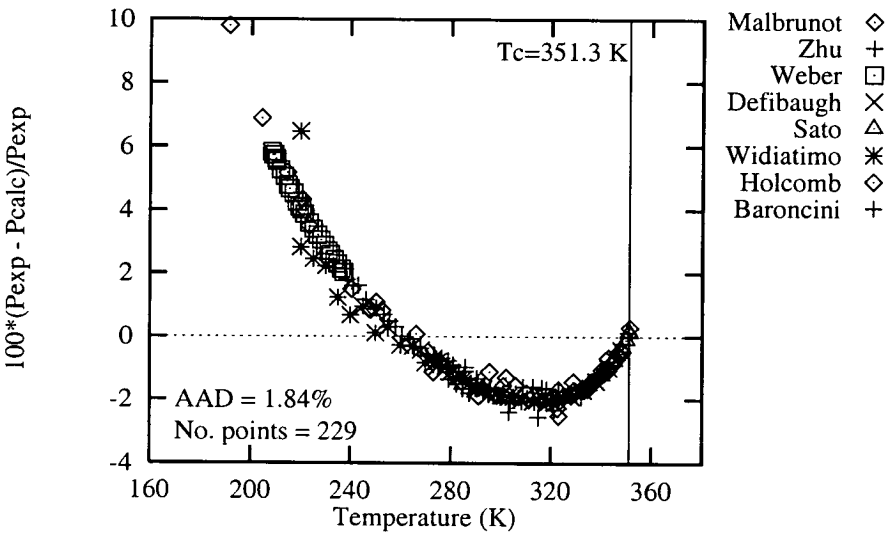

Figure B.1: Deviation of CCOR equation with R32 vapour pressure

The error plots for the remaining refrigerants are shown in Appendix D. The AADs for each published set of experimental data are tabulated in Appendix E for both equations of state. The references for the published experimental data are also given in Appendix D. The plots for R125, R134a, R143a and R152a shows very similar error temperature profiles. Figure D.8 on page 241 shows the AAD as a function of reduced temperature, for the CCOR equation. What is apparent for both equations is the similarity in the error temperature profiles across all five refrigerants examined. As the temperature decreases the over prediction of vapour pressure increases until a turning point is reached at an error of around -2%. As the temperature further decreases the error changes towards the direction of underprediction The zero axis is reached at a reduced temperature in the range $T_r = 0.71\text{-}0.81$. As temperature further decreases the vapour pressure is increasingly underpredicted. There seems to be quite a good agreement between the experimental values of vapour pressure for the same refrigerant as reported by different authors.

Table B.4 shows the number of experimental points compared and the average error associated with each refrigerant. This table summarises the information given in Section E.1.1 for both equations of state.

Table B.4: Average AADs of HFC vapour pressure

Refrigerant	No. Points Compared	AAD % CCOR	AAD % CSD
R32	229	1.84	0.27
R125	142	1.13	0.31
R134a	328	1.17	0.42
R143a	12	1.04	0.45
R152a	363	1.94	0.55
Overall	1074	1.57	0.42

As can be seen, the overall average error for the vapour pressure prediction of the CCOR equation of state is 1.57%. Given the minimal amount of data need by the

CCOR equation this represents quite a good prediction of vapour pressures. It should be noted that there is no great scatter between the individual refrigerants. All the average errors lie between one and two percent. As a graphical illustration the CCOR predicted vapour pressure is shown with a representative sample of experimental data for all five refrigerants in Figure B.2. The CCOR vapour pressure is represented by the lines, whilst experimental data is shown by the points. Although not conclusive by itself, the plot shows the comparison between calculated and predicted vapour pressure.

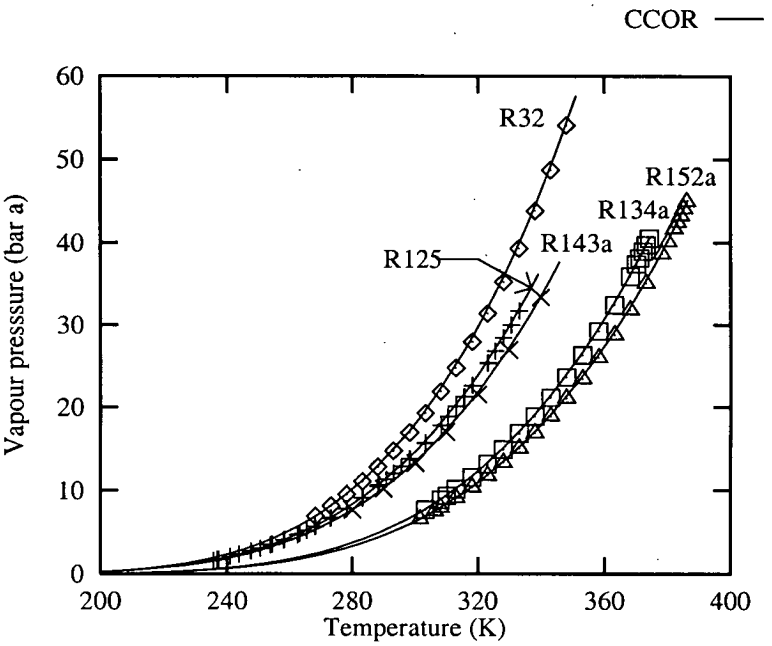

Figure B.2: CCOR calculated and experimental vapour pressures

The same experimental data has been compared with the CSD equation of state. As with the CCOR equation, the error plots for each refrigerant are given in Appendix D and the average absolute deviation associated with each publication is tabulated in Section E.1.1. From the comparison with the experimental data the CSD equation appears to be more accurate than the CCOR, with an overall AAD of 0.42%.

Derivation of the CSD equation's *a* and *b* parameters from saturation sate experimental data means that it can predict vapour pressure to a greater degree of accuracy than the CCOR equation.

The CSD is not forced through the critical point. The deviation at this point is greater than that for the CCOR. However, in the subcritical region the CSD equation is more accurate. Morrison and McLinden [*1986a*] noted that forcing an equation of state to go through the critical point can adversely affect its accuracy in the subcritical region. Hence the equations for the a and *b* parameter do not refer to the critical temperature. This is borne out in the plots of error vs. reduced temperature (Figure D.6 and Figure D.9). The error-temperature plot for predicted R32 vapour pressure with the CSD equation is shown in Figure B.3. If a comparison is made with the corresponding plot for the CCOR it can be seen that the errors are much less for the CSD equation of state.

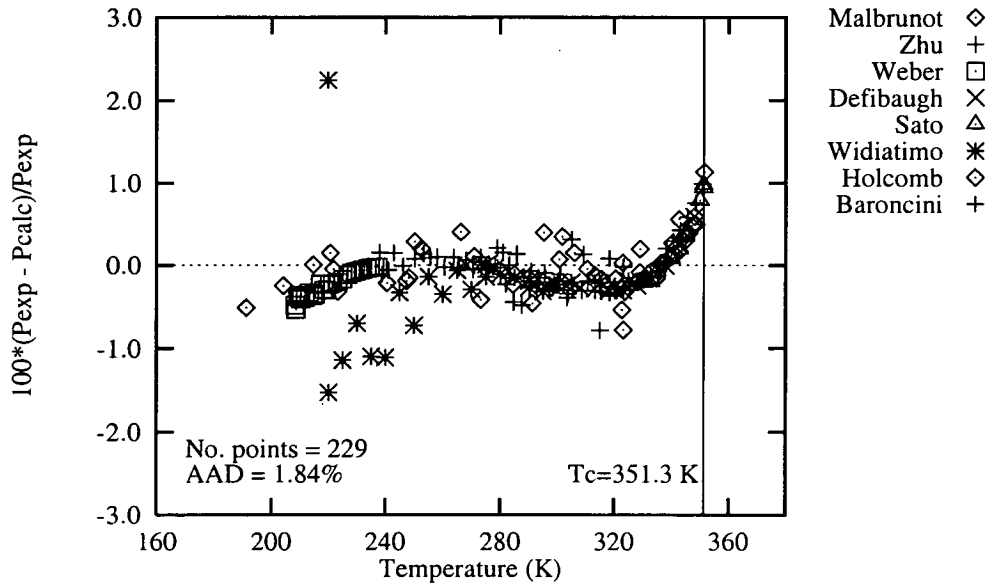

Figure B.3: Deviation of CSD equation with R32 vapour pressure

The vapour pressure at the critical point is underpredicted. As temperature decreases, the error profile goes through a minimum and then a maximum on either side of the zero axis. At low temperatures the vapour pressure is increasingly overpredicted. Also at lower temperature, differences in reported vapour pressures emerge. The sub-ambient vapour pressure data of R134a (Figure D.4 on page 239) as reported by Lavrenchenko et al. [*1992*] seems to disagree with the other reported values.

B.4.2 Saturated Liquid Density

Nearly three hundred saturated liquid density data points were found in the literature. The data covered all five refrigerants; although over a third of the data was for R32. The error plots are shown in Figure D.10 to Figure D.19 of Appendix D. AADs of each set of published liquid density data are tabulated in Section E.1.2 of Appendix E. Comparing the CCOR liquid density to published experimental data an overall average error of 8.63% was found.

Table B.5: Average AADs of HFC saturated liquid density

Refrigerant	Points Compared with CCOR	Points Compared with CSD	CCOR AAD %	CSD AAD %
R32	119	123	13.91	3.04
R125	25	25	2.64	0.40
R134a	72	72	2.61	1.37
R143a	17	17	5.99	0.66
R152a	60	60	8.62	0.81
Overall	293	297	8.63	1.83

The average error is not as small as one would like ideally. Although the errors describing liquid density are not extremely large, an overall AAD closer to that of the CSD equation would be preferable. There is a large degree of variability in the AADs

between the five refrigerants: R32 has the highest average error with a deviation of nearly 14%, whilst R125 and R134a have more acceptable average deviations at around 2.6%. The overall average is somewhat distorted because of the larger proportion of R32. The CCOR equation could be used to give a rough indication of the liquid properties of a new refrigerant. It would not be recommended to use it to describe faithfully liquid behaviour. The CCOR algorithm would not converge for the last four datapoints of Kuwabara et al. [*1995*], hence the difference in the total number of points compared.

The CCOR AADs for all five refrigerants are shown as functions of reduced temperature in Figure D.18 on page 246. The CCOR error does not vary with temperature below a reduced temperature of 0.85. At $T_r < 0.85$ the error depends on the fluid being described and not on the temperature. This indicates that improvements in liquid density prediction could be made by modifying a fluid dependent parameter of the equation. Low [*1991*] suggested that inaccuracies in describing liquid behaviour may arise from the fact that the critical compressibility (Z_c) is calculated from the Pitzer correlation. Originally the CCOR equation was developed to provide the improved liquid phase predictions of the Chain-of-Rotators equation of state in a cubic format. With hydrofluorcarbons it would seem that there is further scope for improvement. The error plots for the CSD equation show that it gives a superior description of the liquid properties. The CSD predictions are quite good compared to those for the CCOR equation. The AAD-T_r profiles for the CSD show a much better consistency between the five refrigerants. Morrison and McLinden's philosophy of not constraining the equation to go through the critical point manifests itself in the large errors near the critical point. However away from the critical point the errors are much smaller (compared to the CCOR) and most of the points lie quite close to the zero error line. There is very little disagreement between the various refrigerants.

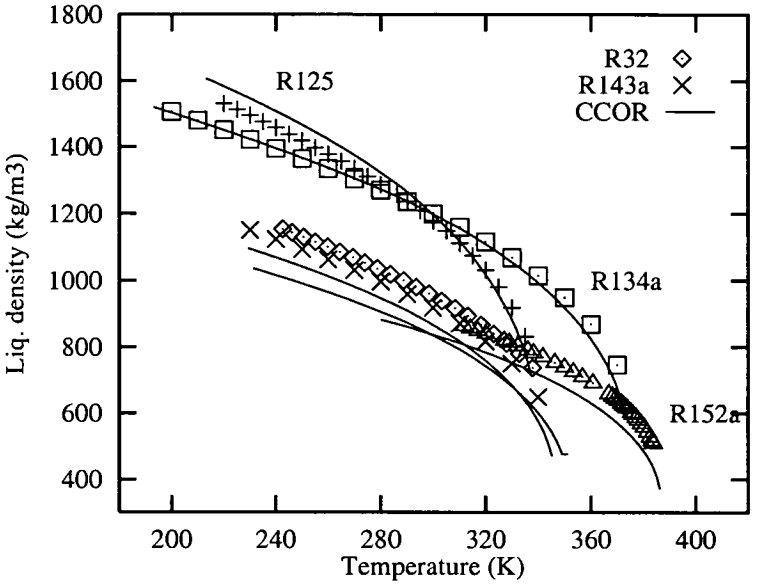

Figure B.4: CCOR calculated and experimental saturated liquid density

Figure B.4 shows the saturated liquid density, as calculated by the CCOR equation, with some typical experimental points for all five refrigerants. The relative agreement with R125 and R134a is clear. Also obvious is the discrepancy between experimental and calculated liquid density for the refrigerants R32, R152a and R143a.

B.4.3 Saturated Vapour Density

A substantially smaller number of experimental saturated vapour density points were located in the literature; 116 in total. Vapour density data was only published for refrigerants R32, R134a and R152a. Individual error plots for the refrigerants are shown in Figure D.20 to Figure D.27 with the corresponding errors tabulated in Section E.1.3 of Appendix E. With an overall AAD of 10.05% for the CCOR equation, the prediction of saturated vapour density is not particularly accurate.

Table B.6: Average AADs of HFC saturated vapour density

Refrigerant	No. Points Compared	CCOR AAD %	CSD AAD %
R32	57	8.38	12.34
R134a	26	14.49	9.66
R152a	33	11.03	12.54
Overall	116	10.05	11.80

A plot of CCOR error vs reduced temperature is shown in Figure D.26 on page 250, for the refrigerants R32, R134a and R152a. Near the critical region the vapour volume is substantially overpredicted. Near $T_r = 0.95$ the curves go through a turning point and the degree of overprediction reduces almost linearly with temperature. Unlike the errors associated with liquid density prediction the error is a strong function of temperature. Also in contrast with the liquid errors, there is a much wider degree of similarity in the errors of each refrigerant. Although there is not complete unanimity, there is sufficient agreement to suggest the vapour volume error is not strongly dependent upon the refrigerant being described. The prediction of vapour volume is not perfect, but at the same time it is not wildly inaccurate. Rough indications of vapour volume can be supplied by the CCOR equation.

One redeeming feature is that the error for the CCOR equation is slightly less than the corresponding average error for the CSD equation, even though the latter is a more complex equation. One would have expected the error associated with the CSD equation to be much smaller, since the values of the a and b parameters are determined from experimental saturation data. Neither equations seems to adequately describe the vapour behaviour of HFC refrigerants with very great accuracy. As the number of points examined was not particularly large it was felt that a more complete picture would emerge with further publication of vapour density data. For the CSD equation all three error-temperature plots show very similar profiles. CSD error vs. reduced temperature plots are shown in Figure D.27. At the critical volume there is a

substantial difference between the calculated and measured volume (underprediction at around 47%). In the region $1.0 < T_r < 0.95$ the error reduces dramatically. Below $T_r = 0.95$ the error decreases linearly with temperature. As with the CCOR equation the errors are strong functions of the temperature and are independent of the refrigerants described. With the CSD equation there is a larger degree of similarity between the errors of each refrigerant.

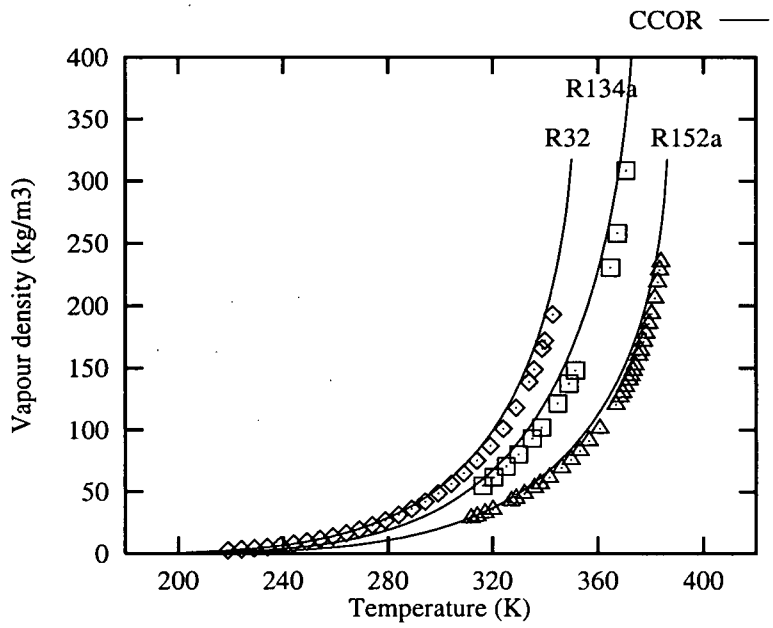

Figure B.5: Calculated and experimental saturated vapour densities

Figure B.5 shows calculated (CCOR) and predicted vapour density data for the three refrigerants considered where the overprediction of the vapour density can be seen. The scale of the plot hides the errors to some extent.

B.4.4 PVT Behaviour

Over half of all the pure fluid experimental datapoints found in the literature were associated with the pressure-volume-temperature (PVT) behaviour of four of the five HFC refrigerants (no PVT data was located for R143a). These data sets tabulate the pressure, temperature and density of non-saturation conditions. Normally pressure and temperature were tabulated at a constant density or constant volume. The majority of the data was concerned with the behaviour of superheated vapour. Some publications included information on non saturated liquids. A similar comparison program to SATERRORPLOT was written for PVT behaviour, called PVTERRORPLOT. Experimental data was read from an input file and using the density and temperature data points, the pressure was calculated and the percentage error was sent to the output file. The error associated with each publication are tabulated in Section E.1.4 on page 267 of Appendix E.

The predicted and experimental predictions for superheated vapour and non saturated liquid were examined separately. Table B.7 shows the average superheated vapour pressure error for both equations of state. With an average percentage error of 1.94% it would seem that the CCOR equation can predict the pressure of a non saturated vapour HFC quite well. The error is of a similar magnitude to that for saturated vapour pressure. This average error is the same as that for the CSD equation.

Table B.7: Average AADS of HFC PVT superheated vapour pressure

Refrigerant	Number of Points	CCOR AAD %	CSD AAD %
R32	361	1.49	3.61
R125	173	3.17	1.59
R134a	720	1.95	1.39
R152a	571	1.83	1.64
Overall	1765	1.94	1.94

With the exception of R32, the average error for each refrigerant is lower for the CSD equation. Since the amount of data needed by the CSD equation to describe a fluid is greater, it would seem that the errors for the CCOR equation are quite satisfactory. The prediction of compressed or non saturated liquid behaviour by the CCOR equation is not as impressive. As can be seen from Table B.8 the CCOR equation does not predict liquid behaviour, away from the saturation zone, very well. The errors for each of the three refrigerants are quite large. The CCOR equation should not be used to predict liquid behaviour away from saturation. The CSD equation is better than the CCOR equation although with an average error of around 10% it is not spectacularly accurate.

Table B.8: Average AADS of HFC PVT compressed liquid pressure

Refrigerant	Number of Points	CCOR AAD %	CSD AAD %
R32	35	17.98	3.55
R134a	104	6.61	13.78
R152a	81	30.24	7.01
Overall	191	15.13	10.06

B.4.4.1 R32

In Section D.4 on page 251 plots of percentage error vs. temperature for the PVT behaviour of the four refrigerants and the two equations of state are given. Figure D.28 displays the CCOR AAD for R32 superheated vapour, as a function of temperature. With the exception of a few points most of the error points lie in the range 0 to 3%. A good agreement exists with the error points of Defibaugh et al.[*1994*], Sato et al. [*1994*] and Baroncini et al. [*1993*]. The data of Malbrunot et al. [*1968*] shows a greater amount of scatter. The CCOR exhibits a characteristic

underprediction of R32 superheated vapour pressure and this manifests itself with the other refrigerants as well. The data of Defibaugh, Sato and Baroncini was presented as a series of isochores. At constant density the error decrease as the temperature increases. Isochores with lower densities tended to have smaller errors. This trend was reflected in all refrigerants and for both equations of state. In Figure D.29 the difference between the predicted pressure of R32 compressed liquid and reported experimental pressure is given. The very large errors (-25% to -125%) arise from a very poor prediction. In his data Sato included tabulated temperature and pressure at a constant density of $850 kg m^{-3}$ and $675 kg m^{-3}$. The CCOR equation seriously over predicted the pressure of these two liquid isochores.

The corresponding error plots for the CSD equation are displayed in Figure D.30 and Figure D.31. Unlike the CCOR equation the CSD equation overpredicts the pressure of R32 superheated vapour. For R32 the CSD equation is less accurate than the CCOR. The error points lie over a wider range (-0.5% to -7.5%). The isochores of Defibaugh's and Baroncini's data are clear. The trend of decreasing error with increasing temperature, at constant density, is apparent. The isochores with the smallest error were those with the smallest density. The compressed liquid errors or the CSD equation (Figure D.31) were smaller than those of the CCOR but were still quite significant.

B.4.4.2 R125, R134a and R152a PVT Prediction

The prediction of the superheated vapour state by the CCOR equation for R125, R134a and R152a is quite good. The CCOR equation underpredicted the superheated vapour pressure, with errors in the range 0.0-5.0%. The CSD equation overpredicted the pressure by the same amount. For both equations of state, errors decreased with temperature, at constant density, for all refrigerants. It was found that isochores with the lowest density showed the smallest errors. The CCOR equation could be used to

predict the PVT properties of a vapour with a reasonable degree of confidence. Both equations of state poorly describe the compressed liquid state for these refrigerants. The CCOR equation was worse in this respect.

Figure B.6 shows the calculated (CCOR) and experimental PVT behaviour of R134a. This shows the experimental PVT data of Piao et al. [*1990*] and the corresponding CCOR predictions. The data was tabulated as a series of isochores (i.e. lines of constant density) For the sake of clarity the density of only a number of isochores are detailed. The density of the experimental isochores of Piao decrease in a clockwise fashion. The isochores predicted by the CCOR equation are represented by the lines. The saturation vapour pressure of R134a is represented by the dashed line.

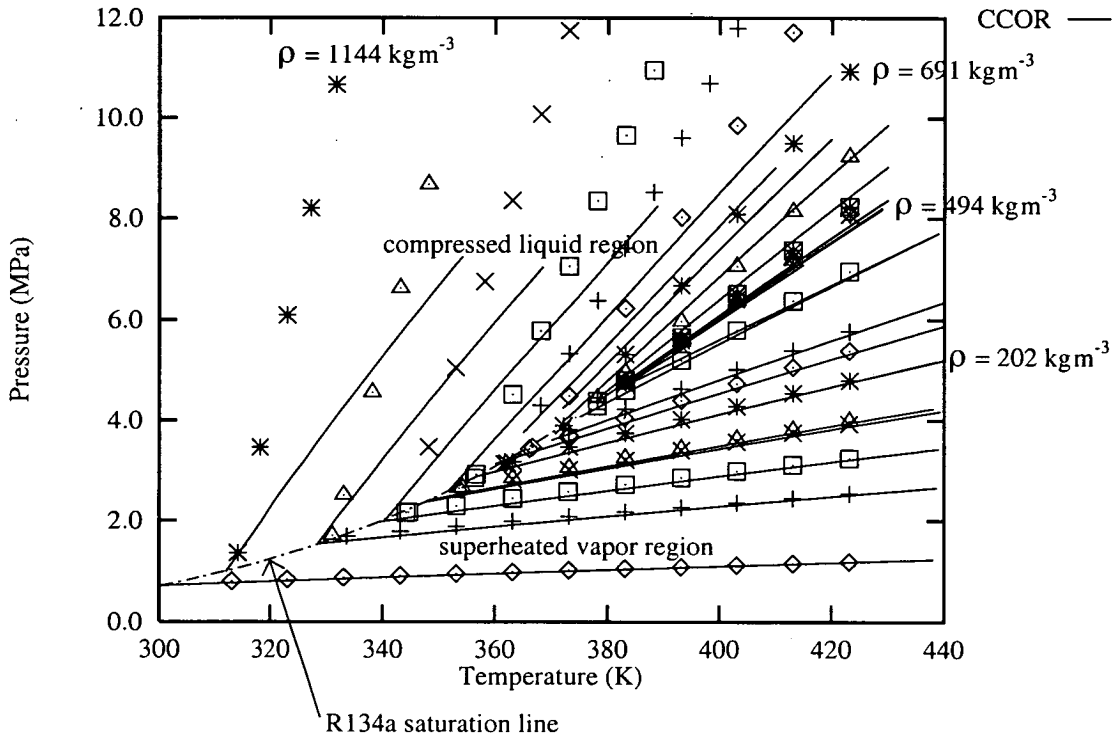

Figure B.6: Experimental and predicted PVT behaviour of R134a compared with data of Piao et al.

It can be seen that the CCOR equation predicts the PVT behaviour of superheated vapour quite well. (AAD = 2.50%). The predicted isochores lie close to the experimental points. Also apparent is the large discrepancies between the predicted isochores and the experimental points in the compressed liquid region (AAD = 21.98%.) At saturation the errors are relatively small. However, as one travels along an isochore, the deviations become very large. In conclusion both equations of state are unsuitable for describing liquids under pressure, but describe superheated vapours quite well. In a refrigeration cycle, liquids are usually in the saturated state are at or near saturation and rarely in the compressed liquid region.

B.5 Summary of CCOR Pure Fluid Predictions

From the investigation of using the CCOR equation to predict non ozone depleting refrigerant thermodynamic properties, a number of conclusions were drawn. From a bare minimum of data the Cubic Chain-of-Rotators could be used to predict the properties of HFC refrigerants with a mixed degree of success. Saturated and superheated vapour pressure were predicted more accurately than either liquid and vapour volume. The CCOR equation predicted the vapour pressure of the five HFC fluids to within 1.6%. Given the paucity of data required, this represents a good prediction. Likewise the superheated vapour pressure is predicted with a satisfactory degree of accuracy (average error = 1.9%). The overall average error for superheated vapour pressure was exactly the same as that for the CSD equation. The CSD equation is more complex and it requires larger amounts of information about the fluid being described yet the CCOR equation can describe superheated vapour pressure to the same degree of accuracy. The comparisons carried out here would seem to indicate that the CCOR equation can be used to predict the vapour pressure of a proposed or refrigerant to an acceptable accuracy.

With the exception of R134a, the CCOR equation did not describe the saturated liquid phase volume with as much accuracy as one would like (average error of 8.6%). The liquid density of R32, R152a and R143a was underpredicted. For R125 the density was overpredicted. Below $T_r = 0.85$ the error was independent of the temperature and depended on the refrigerant being described. Above $T_r = 0.85$ (45°C for R134a) the errors increased dramatically and it would not be recommended to use the CCOR equation in this temperature range. It would seem that a temperature independent parameter of the CCOR equation could be adjusted to improve the liquid phase description. The CSD equation of state was clearly superior at predicting liquid phase behaviour. Errors were much smaller and there were no dissimilarities between the refrigerants examined. Close to the critical region the CSD errors were very large. Both equations of state were very poor at predicting the behaviour of compressed liquids especially the CCOR equation. It would not be recommended to use this equation to describe non-saturated liquid behaviour.

As with liquid volume description the CCOR equation did not show an outstanding ability to predict saturated vapour volumes (over all error of 10.1%). The error varied strongly with temperature, and there was a strong similarity between each refrigerant's error profile. However the CSD equation showed slightly larger errors. Despite needing much less initial data, the CCOR equation is no worse than the more complex CSD equation. Both equations employ the hard sphere fluid theory in their derivation (although the CCOR equation uses a modified form, as well as the rotating hard dumbbell theory). Its application with hydrofluorocarbon refrigerants indicate that there is room for improvement and further refinement.

In summary the CCOR equation displays good vapour pressure predictions. Liquid and vapour phase behaviour is not so well described. If the properties of an experimental refrigerant were to be investigated and highly accurate thermodynamic data was not needed at that stage to decide if the fluid possessed the necessary thermodynamic properties to be considered as a refrigerant, then the CCOR equation

could be used to supply reasonably accurate predictions of the data. This data could be used to determine the likely performance of such a fluid in a refrigeration cycle. There is an inevitable trade-off between accuracy and the amount of data needed by an equation of state. The CCOR equation seems to find an acceptable balance point.

Appendix C

Sample Program Input and Output Files for Thermodynamic Property Comparisons and Refrigeration Cycle Simulation

Appendix C contains typical examples of input and output files of computer programs written by the author, used in the analysis of the Cubic Chain-of-Rotators equation of state in Appendix B and Appendix F. Input and output files used in the simulation modelling described in Chapter 5 are given in Section C.3.

C.1 Thermodynamic Property Comparison Output File

The program SATERRORPLOT was used to compare experimental and predicted values of saturated refrigerant thermodynamic properties. The user specifies the property to be compared and the program reads a data input file with tabulated experimental data (usually the property is tabulated against temperature). SATERRORPLOT calculates the predicted values and sends the experimental values, the calculated values and the percentage errors to an output file The program records

the number of points and calculates the overall percentage absolute average deviation (AAD). The standard deviation of the errors of each individual data point is also given. In the example below the vapour pressure data of Widiatmo et al. [*1994b*] et al. is being compared with the vapour pressure as calculated by the Cubic Chain-of-Rotators equation of state. The '#' is required by the graphing package 'gnuplot', which produced the error plots in Appendix D, so that the subsequent text is ignored. SATERRORPLOT can use the CSD equation of state to predict saturated properties. The output file is identical in format.

```
# Gnuplot error comparison data file:
# properties of R-32 from the CCOR equation
# X variable: Temperature
# Y variable Pressure
#
# Property: Temperature   Units: Kelvin
#
# Property: Pressure   Units: MPa
#
 # Temp    Calc      Exp       Percent Error
 #~~~~~~~~~~~~~~~~~~~~~~~~~~~~~~~~~~~~~~~~~
 219.71    0.0887    0.0948    6.4564
 219.99    0.0900    0.0926    2.8156
 225.00    0.1167    0.1196    2.4484
 229.97    0.1489    0.1523    2.2180
 235.00    0.1885    0.1908    1.2273
 240.00    0.2354    0.2370    0.6708
 244.98    0.2908    0.2936    0.9489
 249.99    0.3563    0.3567    0.1123
 254.54    0.4325    0.4338    0.2953
 260.00    0.5208    0.5194    -0.2781
 264.99    0.6220    0.6201    -0.3102
 269.99    0.7378    0.7317    -0.8320
 274.99    0.8692    0.8624    -0.7905
 274.99    0.8691    0.8610    -0.9382
 279.99    1.0174    1.0060    -1.1294
 284.99    1.1840    1.1680    -1.3660
 289.99    1.3702    1.3490    -1.5732
 289.99    1.3703    1.3480    -1.6515
 294.99    1.5775    1.5490    -1.8376
 304.99    2.0605    2.0220    -1.9037
 314.98    2.6442    2.5930    -1.9751
 319.99    2.9775    2.9190    -2.0027
 324.98    3.3399    3.2780    -1.8879
# No of data points              =   24
# Absolute Average Deviation  = 1.5641
# Absolute Standard Deviation = 0.0661
```

C.2 CCORSIMPLE and CSDSIMPLE Input and Output Files

A typical input data file which is used by the refrigeration simulation program CCORSIMPLE is shown below. In this case a 50/50 wt.% R32/R134a mixtures is used as the working fluid. The input file for the CSD model (CSDSIMPLE) is exactly the same except the k_c interaction constant lines are removed. The output files for the CCOR and CSD models are exactly the same in format. Most of the terms are self explanatory. The term "lshx_used" refers to the use of a LSHX. If the value is one the model includes a LSHX with the degree of subcooling determined in the next row. If the value is zero it is not included.

```
mvc
      r32
lvc
      r134a
mvc_composition
      0.5
ka
      0.0
kc
      0.0
refrigeration_load(kW)
      3.0
compressor_ploytropic_efficiency
      0.75
lshx_used
      1
condenser_liquid_subcool(degC)
      10.0
glycol_inlet_temp(degC)
      -5.0
glycol_outlet_temp(degC)
      -10.0
evaporator_UA_value(kW/K)3
      0.6
evaporator_pressure_drop(kPa)
      15.0
evaporator_superheat(degC)
```

```
      2.0
water_inlet_temp(degC)
      20.0
water_flowrate(kg/s);
      0.07
condenser_UA_value(kW/K)
      0.78
condenser_pressure_drop(kPa)
      15.0
```

The following is a typical results file from the program SIMPLESIM using the previous input data file. The following is an explanation of the acronyms used in the file:

- rho: fluid density
- vf: vapour weight fraction
- m: refrigerant mass flowrate
- Pr: pressure ratio
- Comp isen eff: compressor isentropic efficiency
- GLY DT: Temperature change experienced by glycol
- GTD: Gliding temperature difference
- Qtpc: two phase heat transfer load in condenser
- Qdsupc: desuperheating heat load in condenser
- WAT DT: temperature change experienced by water (heat sink)
- Qlshx: Liquid suction heat exchanger

==========

Results of a simulation of a refrigeration cycle with a 50.0/50.0 R-23/R-134a blend using the Cubic Chain of Rotators Equation of State (with ka=0.00 & kc=0.00)

==========

STREAM DATA

Stream	T deg C	P bar a	flow kg/hr	X wt.%	rho m3/kg	h kJ/kg	s kJ/kgK	e kJ/kg
Comp Suction	9.85	3.731	48.9	0.5	11.96	370.3	2.1137	22.25
Comp Discharge	77.63	14.103	48.9	0.5	38.72	429.2	2.1652	66.09
Cond Dew pt	30.08	14.066	48.9	0.5	53.38	360.0	1.9481	60.51
Cond Bubble pt	25.23	13.953	48.9	0.5	936.4	149.3	1.2470	55.39
LSHX Outlet	15.23	13.953	48.9	0.5	986.5	129.6	1.1782	55.87
Exp Valve Exit	-14.32	3.881	48.9	0.5	65.2	129.6	1.1870	53.30
Exp Liquid	-14.32	3.881	48.9	0.459	1099.5	75.9	0.9798	57.09
Exp Vapour	-14.32	3.881	48.9	0.682	12.6	367.6	2.1052	36.50
Evap Dew Pt	-10.37	3.732	48.9	0.5	13.35	348.4	2.0300	24.95
Evap Vapour	-8.37	3.731	48.9	0.5	13.19	350.6	2.0386	24.58
Cond Water In	20.0		360.0		998.4	83.7	0.296	0.0
Water at Dew Pt	26.8		360.0		996.8	112.3	0.392	0.33
Cond Water Out	29.1		360.0		996.2	121.7	0.423	0.58
Evap Glycol In	-5.0		764.1		1087.6	-14.5	-0.054	3.42
Evap Glycol Out	=10.0		764.1		1090.6	-28.7	-0.107	4.89

OVERALL CYCLE PARAMETERS:

COPr (-)	Wcomp kW	m kg/hr	Vc kJ/m3	Pr (-)	Comp isen eff (%)
3.750	0.800	48.88	1273.07	3.780	70.545

EVAPORATOR:

Qe kW	UA kW/K	LMTD deg C	GLY DT deg C	GTD deg C
3.000	0.600	5.00	5.00	3.93

CONDENSER:

Qc kW	Qtpc kW	Qdsupc kW	UA kW/K	LMTD deg C	WAT DT deg C	GTD deg C
3.800	2.860	0.940	0.78	4.872	9.08	15.42

Liquid Suction Heat Exchanger

Qlshx
kW

0.267

CYCLE EXERGY ANALYSIS

Equipment	Irreversibility (kW)	% of Total
Compressor	0.205	41.93
Condenser	0.145	29.74
Liq - Suct HX	0.025	5.13
Expansion	0.035	7.16
Evaporator	0.078	16.05
Total	0.488	100.0
Exegetic Efficiency	38.94%	

Exergy absorber by glycol = 0.312 kW
Exergy losses + exergy absorbed = 0.8 kW
Work = 0.8 kW

C.3 CCORCOMPVARY Output file.

The following is a typical output file from the refrigeration simulation program CCORCOMPVARY. This uses exactly the same model as CCORSIMPLE. The composition is varied from 0.0 weight fraction m.v.c. to 1.0 weight fraction m.v.c. in intervals selected by the user. The input file in Section C.2 has been used to generate the output file (i.e. an R32/R134a mixture). The output files for the CCOR and CSD models are the same except that there is no reference to the CCOR interaction parameter k_c in the CSD model output file. The composition has been varied in steps of 0.2 weight fraction R32. Most of the abbreviations are self explanatory. "Exereff" is the exergy efficiency. The term "Fracht" is the fraction of the condenser heat load that is used for desuperheating.

Variation in Refrigeration cycle Parameters with
Composition using a binary mixture. The equation of
state used is the CUBIC CHAIN OF ROTATORS (CCOR)
#
Input Cycle Parameters are:
#
Refrigerant 1 : R-32 Refrigerant 2 : R-134A
ka = -0.005461 kc = 0.009620
Qevap = 3.00 kW Comp poly Eff = 0.75
Glycol inlet temp = -5.00 deg C outlet temp = -10.00
deg C
UA evap = 0.6000 kW/K pressure drop = 15.0 kPa
Condenser water inlet temp = 20.0 deg C water flowrate =
0.100 kg/s
UA cond = 0.7800 kW/K pressure drop = 15.0 kPa
Evaporator superheat = 2.0 deg C
liquid-suction heater used : YES, liquid_subcool = 10.0
deg C
#
#

# X R32 (wt fr)	COPr (-)	Vc kJ/m3	Wcomp kW	Qcond kW	Pr (-)	Mflow kg/hr
1.0	3.542	1090.68	0.8470	3.8470	3.650	40.39
0.8	3.630	1120.86	0.8266	3.8267	3.665	43,53
0.6	3.718	1204.48	0.8070	3.8070	3.721	46.94
0.4	3.773	1364.34	0.7951	3.7952	3.862	51.06
0.2	3.795	1637.16	0.7906	3.7906	4.082	56.64
0.0	3.571	2098.50	0.8402	3.8402	4.555	66.95

# X R32 (wt fr)	GTDe deg C	GTDc deg C	Exereff (-)	Compeff (-)	Fracht (-)	Wat DT (-)
1.0	-0.76	14.77	36.78	67.986	27.264	9.190
0.8	0.96	14.95	37.69	68 920	26.912	9.142
0.6	3.05	15.28	38.60	69.976	25.564	9.095
0.4	4.48	15.36	39.18	71.146	23.808	9.066
0.2	3.71	13.99	39.40	72.470	21.696	9.055
0.0	-2.03	8.06	37.08	74.040	20.026	9.174

Appendix D

Temperature - Error Plots for Pure Fluid HFC Refrigerants

Appendix D contains temperature-error plots for the Cubic Chain-of-Rotators and carnahan-Starling-Desantis equations of state as described in Appendix B. Error-temperature plots for five hydrofluorocarbon pure fluid refrigerants are shown, namely: R32, R125, R134a, R143a and R152a. The properties examined are vapour pressure, saturated liquid and vapour density and PVT behaviour. Each graph shows a percentage error as a function of temperature. The error is the discrepancy between a thermodynamic property as calculated by either the CCOR or the CSD of state and the published experimental value. Each particular author of published experimental properties is individual denoted in the legend of each graph. The percentage absolute average deviation associated with each author and the calculated grand average errors are tabulated in Appendix E. The references for the experimental data is also given in Appendix E.

D.1 Vapour pressure

D.1.1 R125

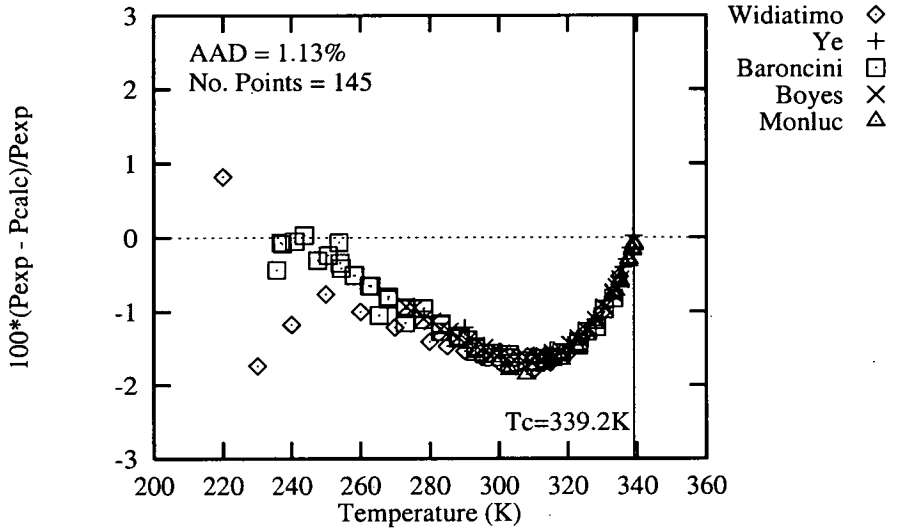

Figure D.1: Deviation of CCOR equation from R125 vapour pressure

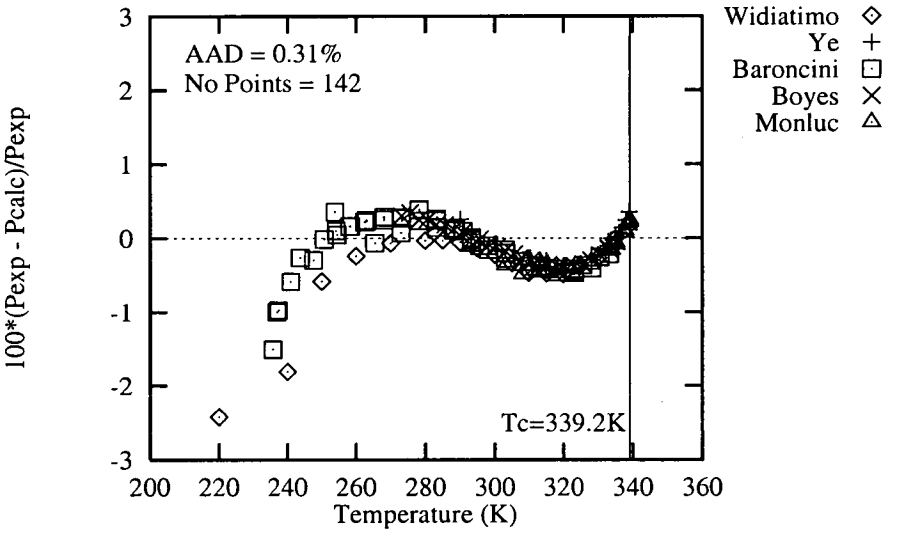

Figure D.2: Deviation of CSD equation from R125 vapour pressure

D.1.2 R134a

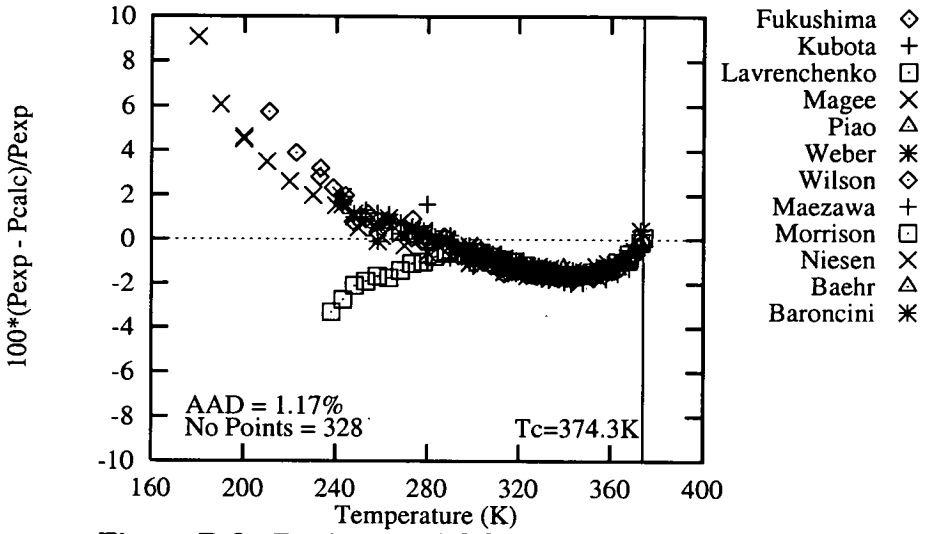

Figure D.3: Deviation of CCOR equation from R134a vapour pressure

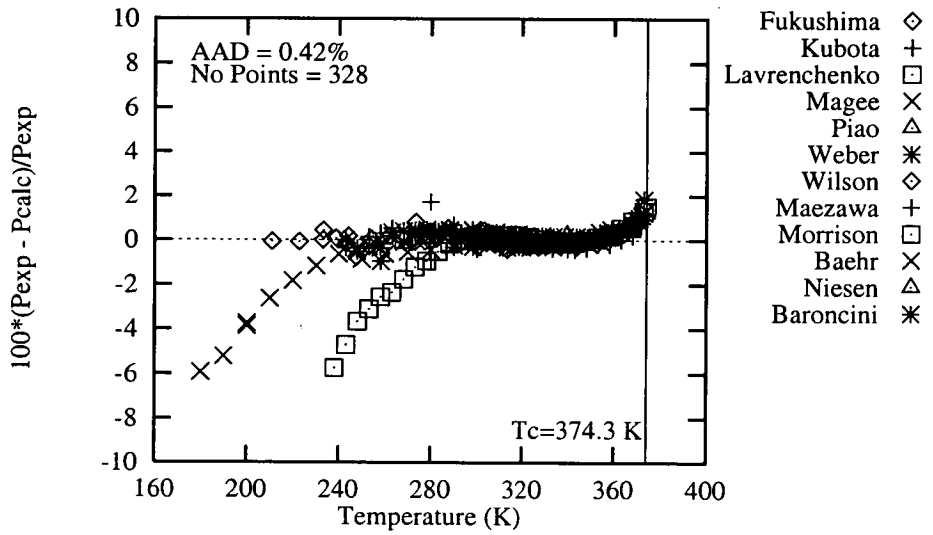

Figure D.4: Deviation of CSD equation from R134a vapour pressure

D.1.3 R143a

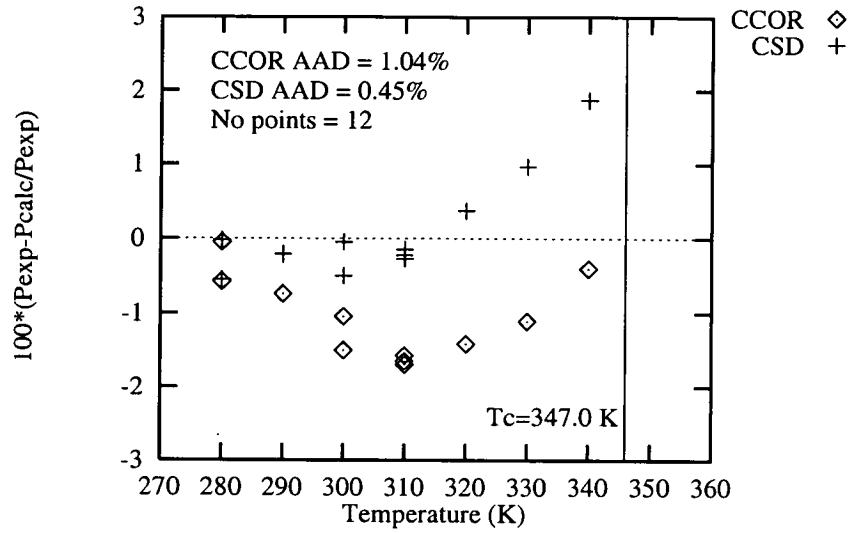

Figure D.5: Deviation of CCOR and CSD equations from R143a vapour pressure

D.1.4 R152a

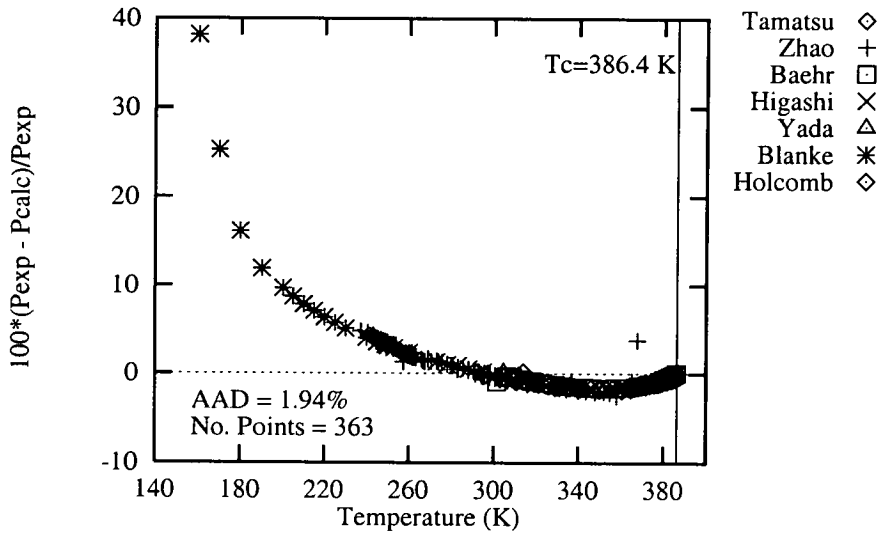

Figure D.6: Deviation of CCOR equation from R152a vapour pressure

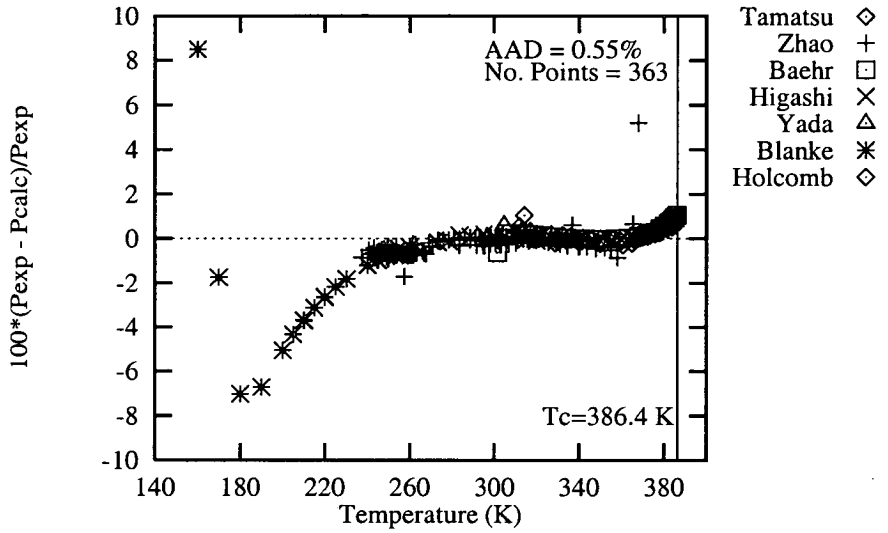

Figure D.7: Deviation of CSD equation from R152a vapour pressure

D.1.5 Vapour Pressure Error vs. T_r Plot for all Refrigerants

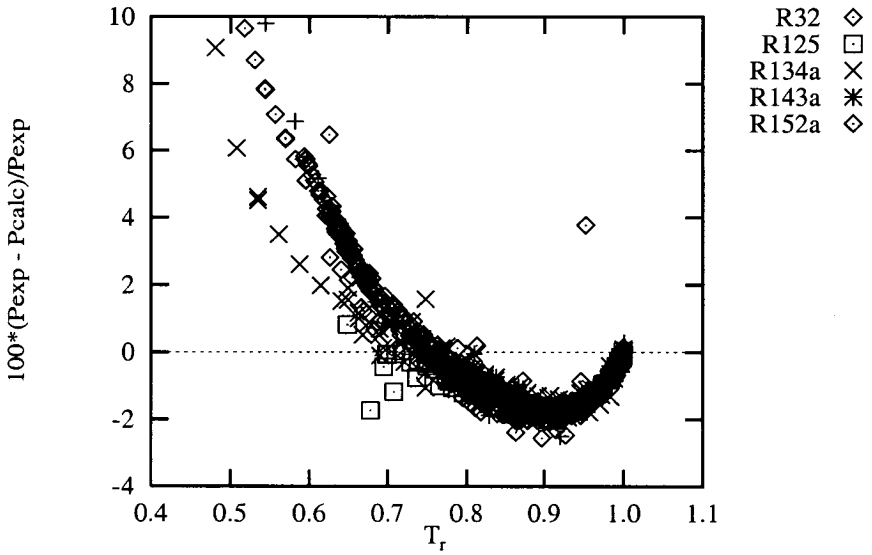

Figure D.8: CCOR error vs. T_r for HFC vapour pressure

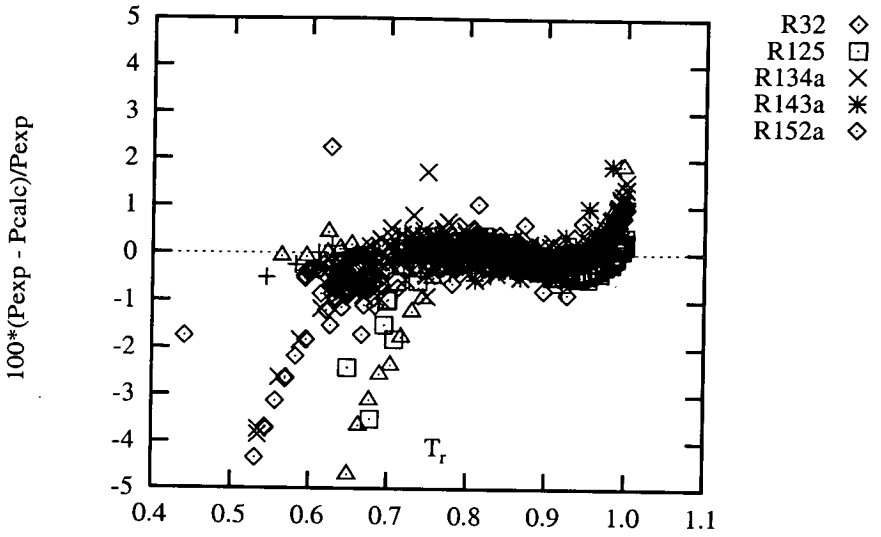

Figure D.9: CSD error vs. T_r for HFC vapour pressure

D.2 Liquid Saturated Density

D.2.1 R32

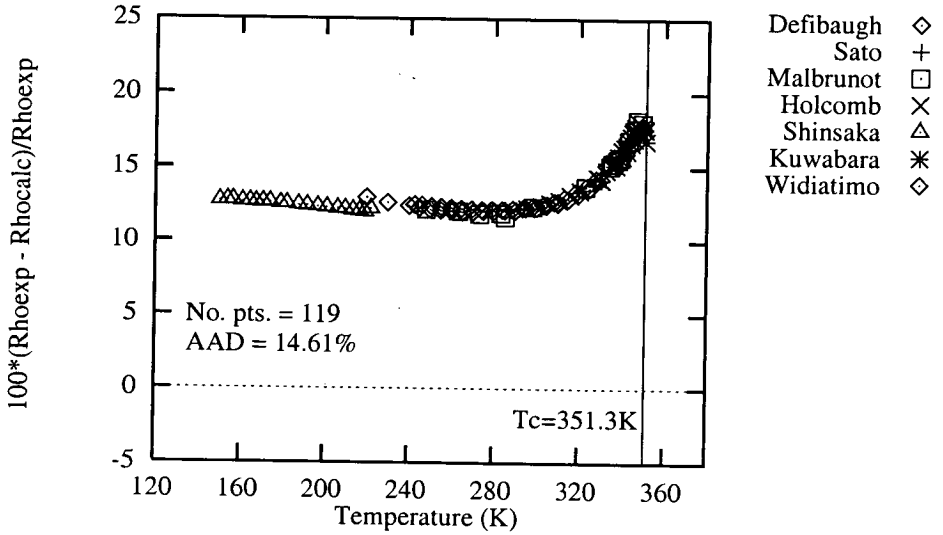

Figure D.10: Deviation of CCOR equation from R32 liquid density

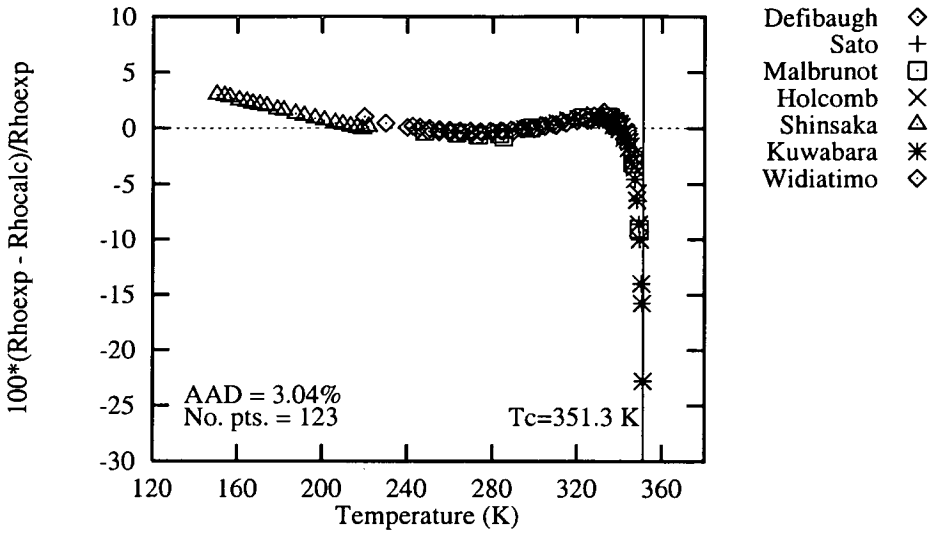

Figure D.11: Deviation of CSD equation from R32 liquid density

D.2.2 R125

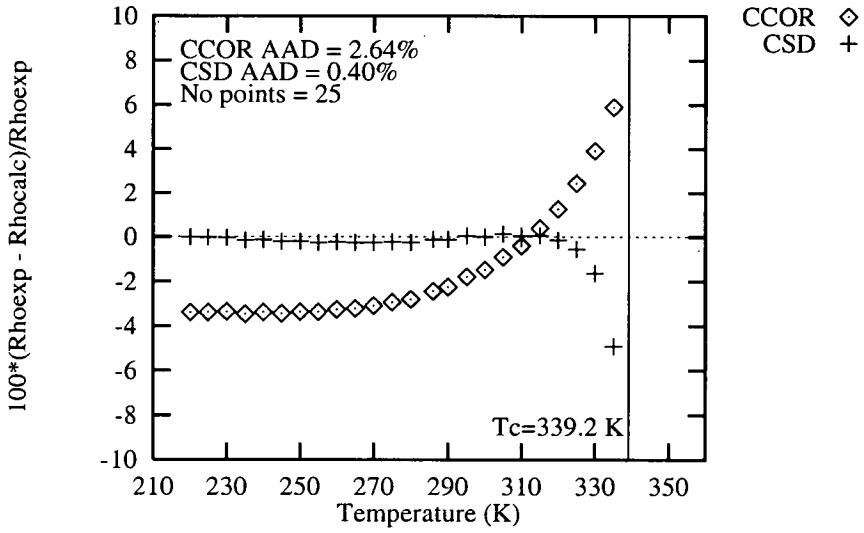

Figure D.12: Deviation of CCOR and CSD equations R125 liquid density

D.2.3 R134a

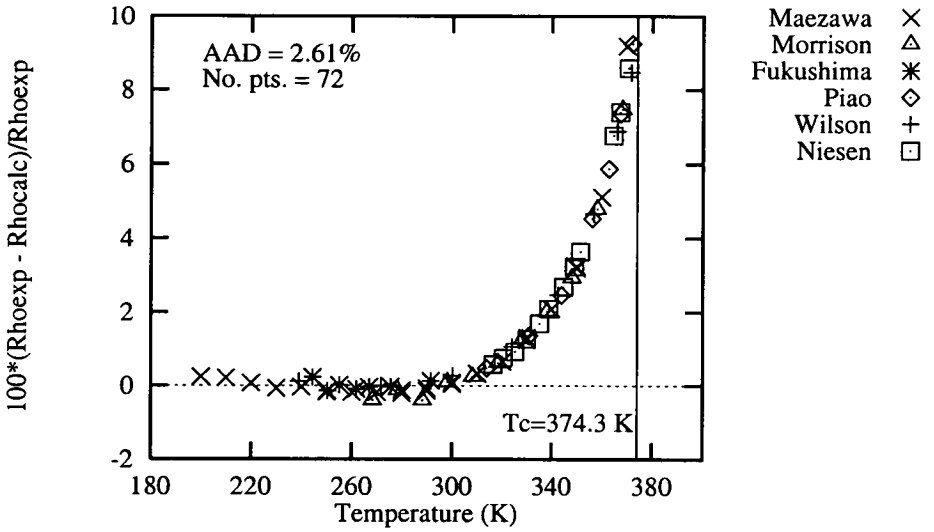

Figure D.13: Deviation of predictions of CCOR equation from R134a saturated liquid density

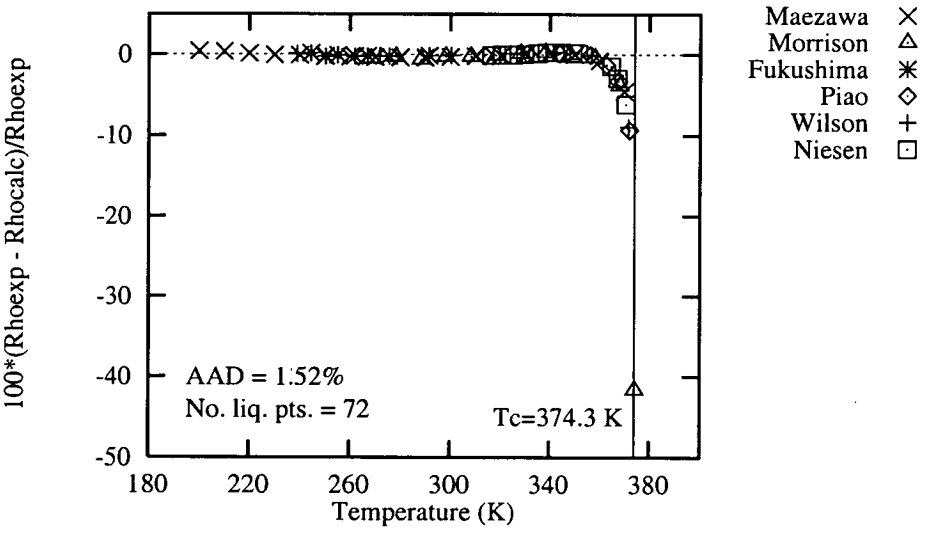

Figure D.14: Deviation of predictions of CSD equation from R134a saturated liquid density

D.2.4 R143a

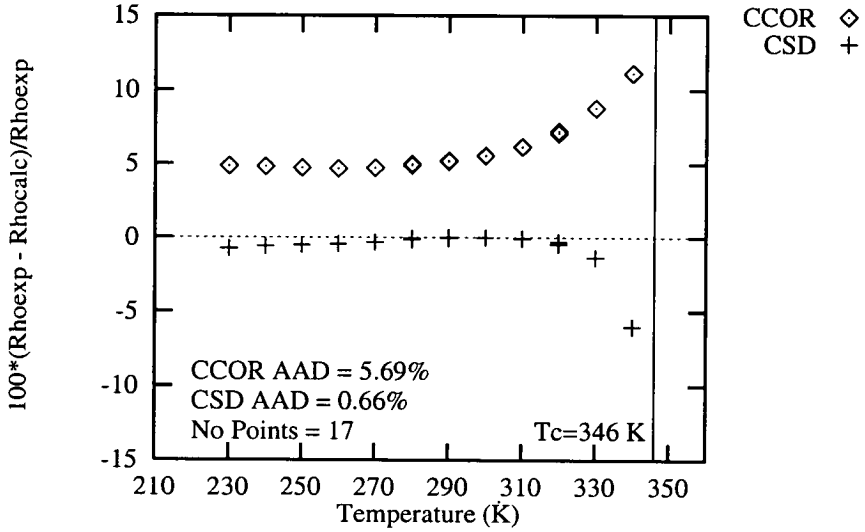

Figure D.15: Deviation of CCOR and CSD equation from R143a saturated liquid density

D.2.5 R152a

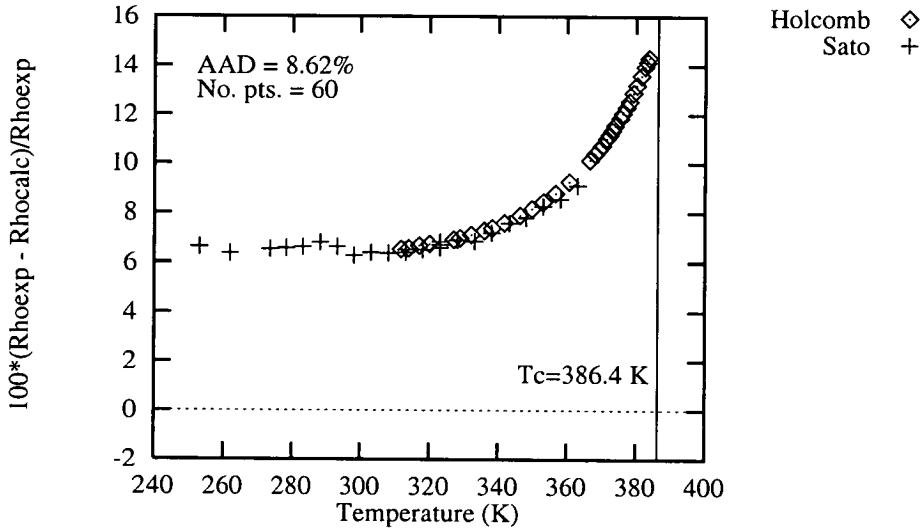

Figure D.16: Deviation of predictions of CCOR equation from R152a saturated liquid density

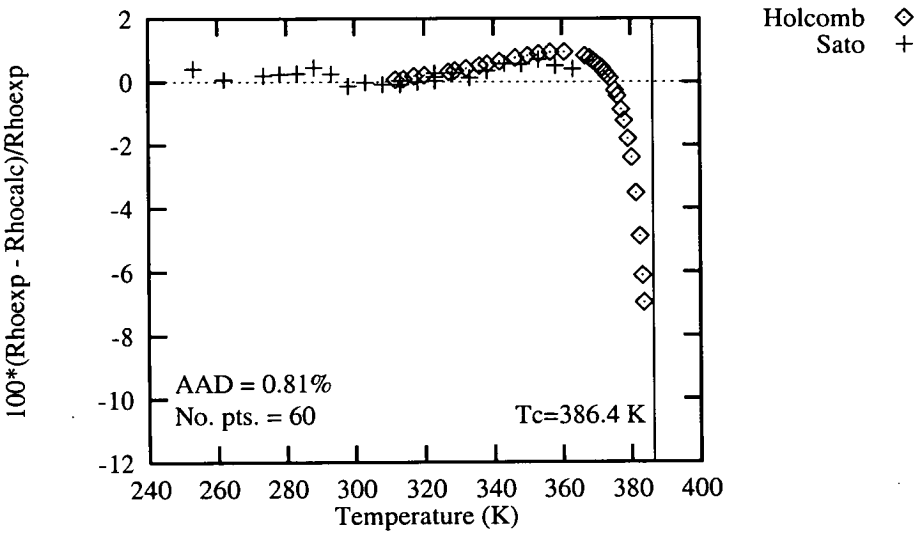

Figure D.17: Deviation of CSD equation from R152a saturated liquid density

D.2.6 Error vs. T_r for Liquid Density of all Refrigerants

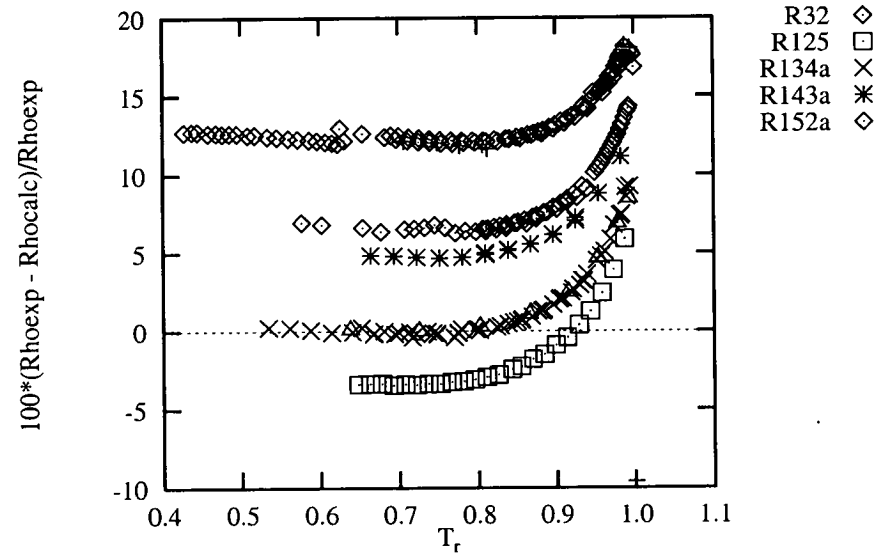

Figure D.18: CCOR error vs. T_r for HFC liquid density

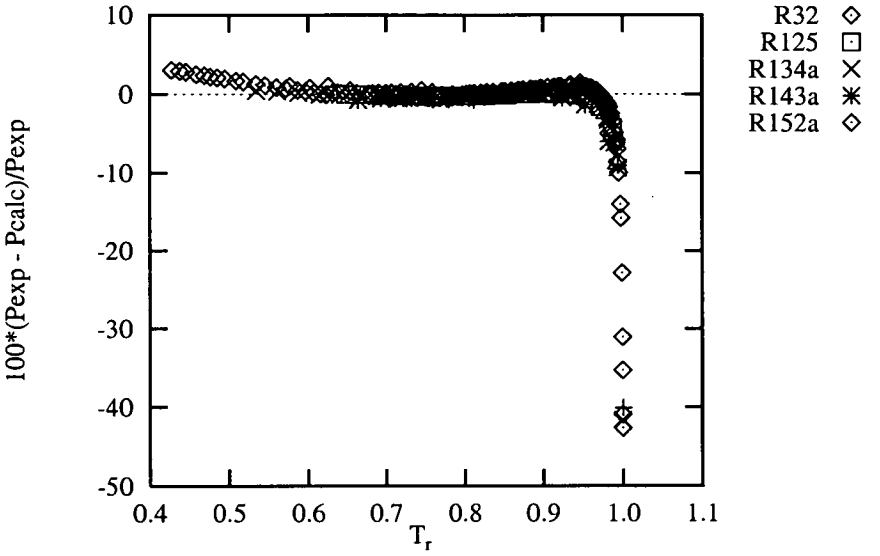

Figure D.19: CSD error vs. T_r for HFC liquid density

D.3 Saturated Vapour Density

D.3.1 R32

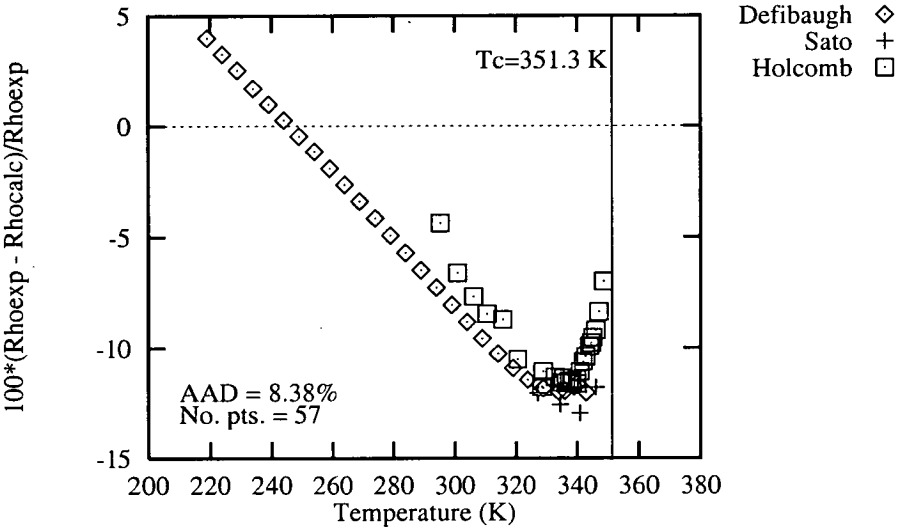

Figure D.20: Deviation of CCOR equation from R32 saturated vapour density

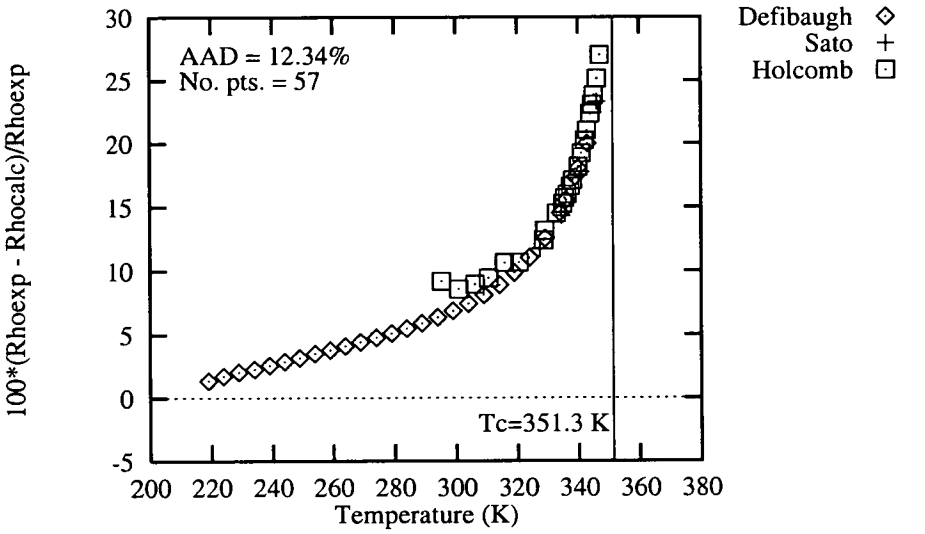

Figure D.21: Deviation of CSD equation from R32 saturated vapour density

D.3.2 R134a

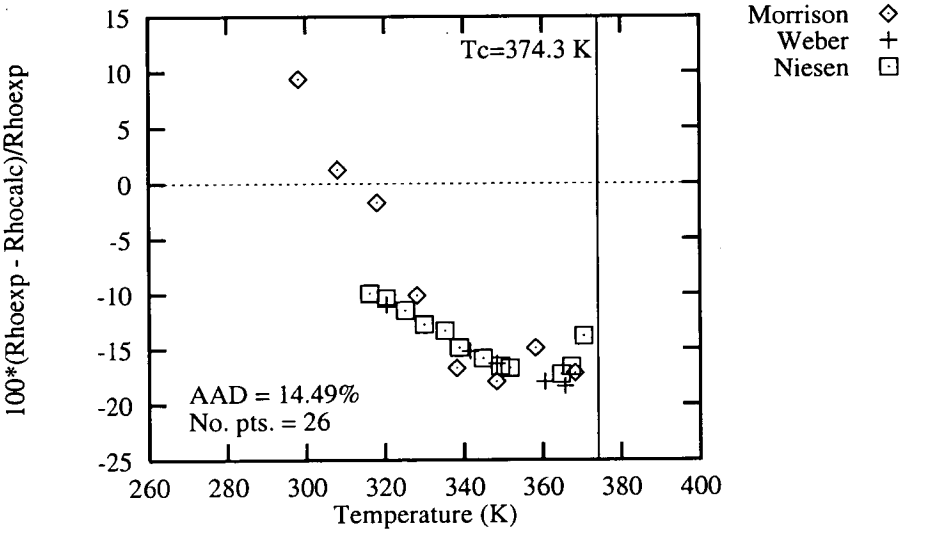

Figure D.22: Deviation of predictions of CCOR equation from R134a saturated vapour density

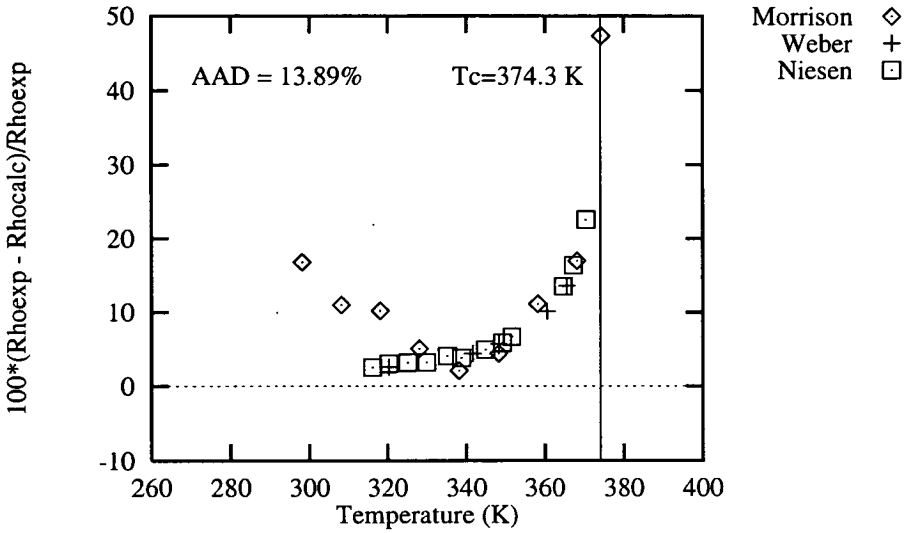

Figure D.23: Deviation of predictions of CSD equation from R134a saturated vapour density

D.3.3 R152a

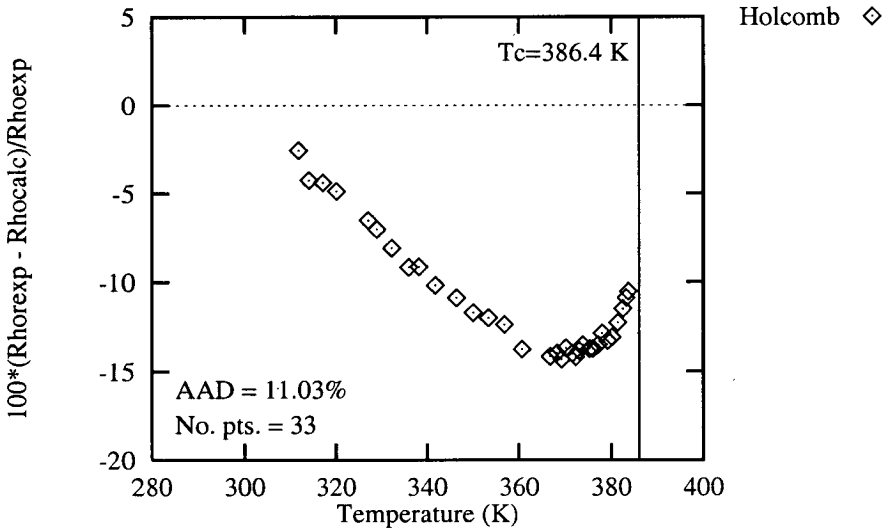

Figure D.24: Deviation of predictions of CCOR equation from R152a saturated vapour density

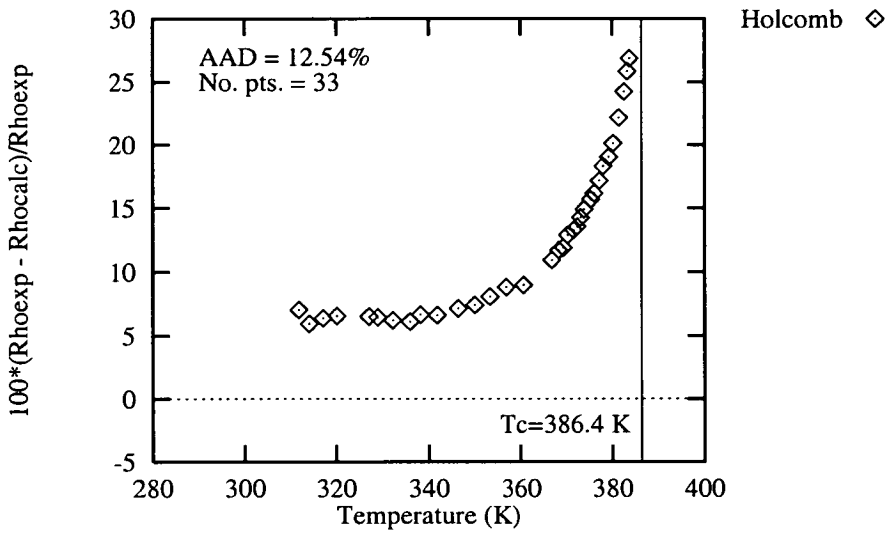

Figure D.25: Deviation of predictions of CSD equation from R152a saturated vapour density

D.3.4 Error vs. T_r for Vapour Density of All Refrigerants

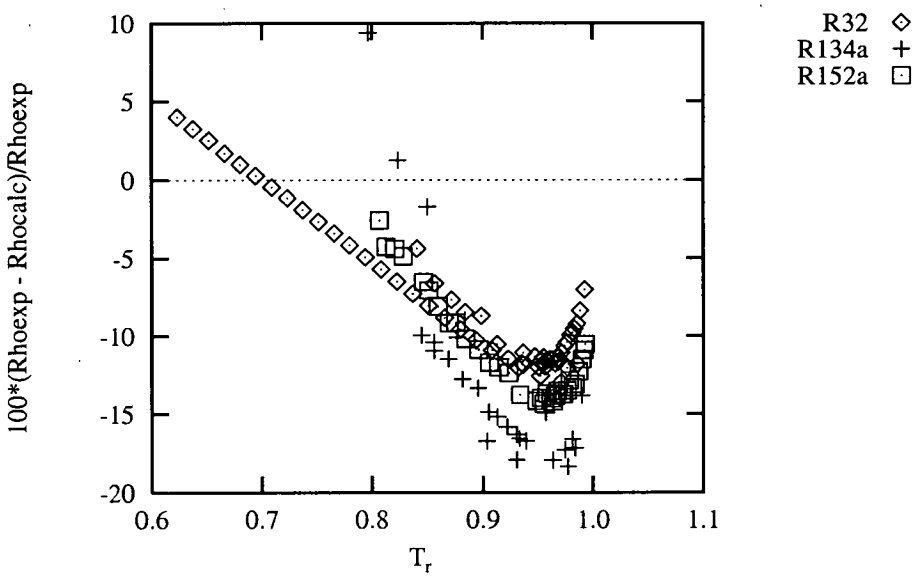

Figure D.26: CCOR error vs. T_r for HFC vapour density

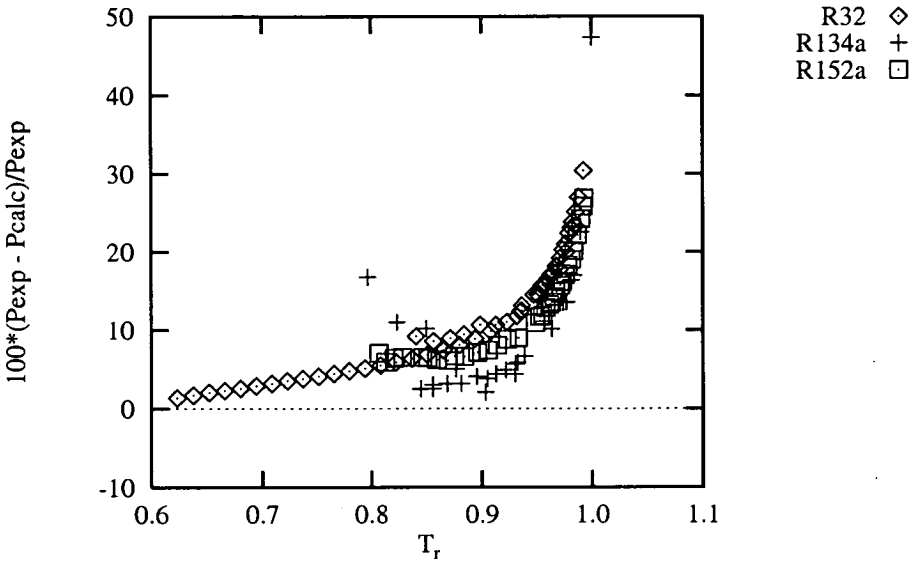

Figure D.27: CSD error vs. T_r for HFC vapour density

D.4 PVT Behaviour

D.4.1 R32

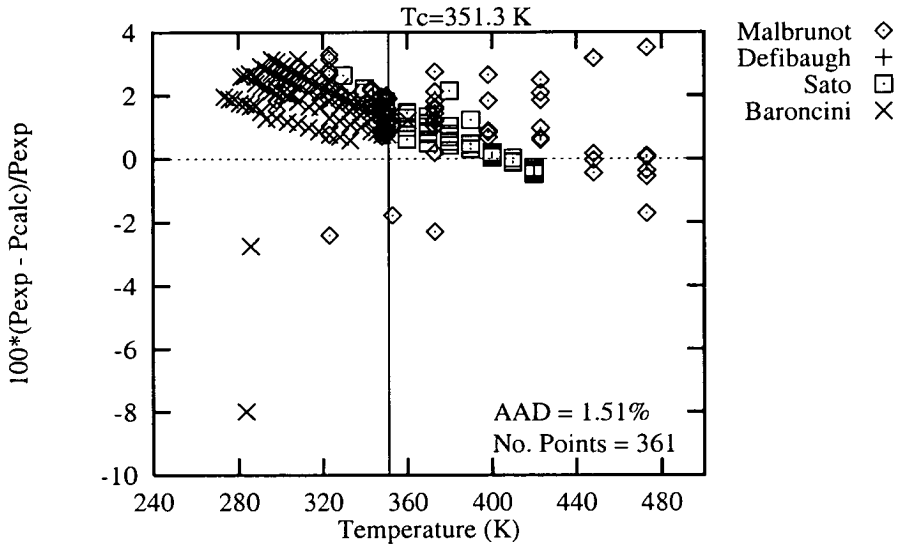

Figure D.28: Deviation of CCOR equation from R32 PVT superheated vapour pressure

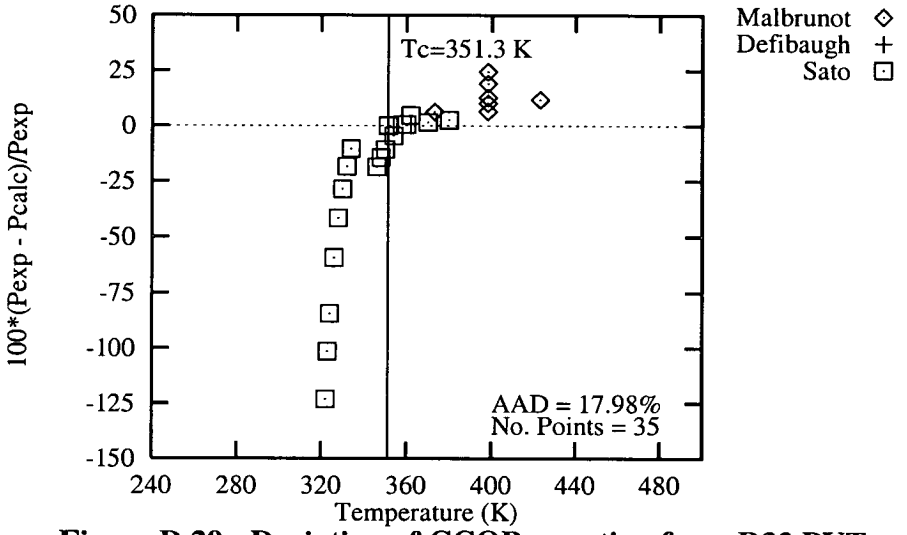

Figure D.29: Deviation of CCOR equation from R32 PVT compressed liquid pressure

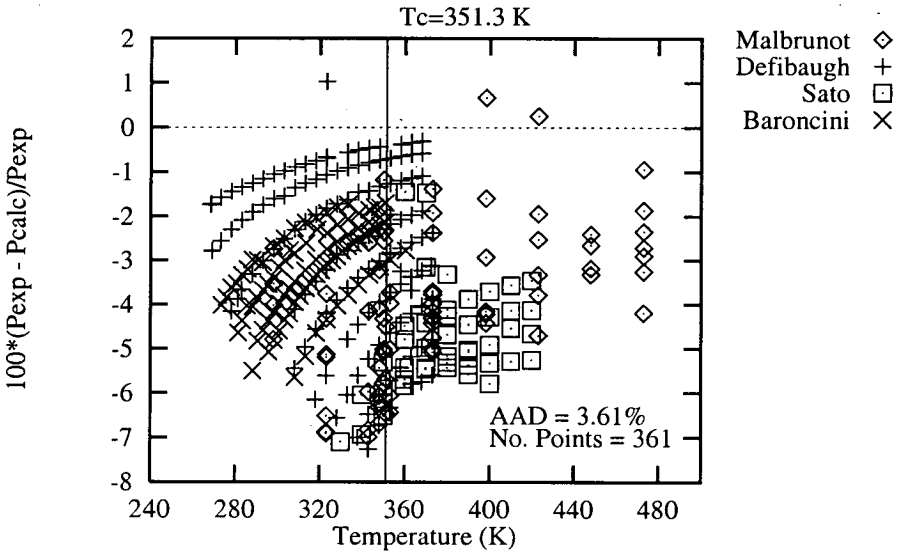

Figure D.30: Deviation of CSD equation from R32 PVT superheated vapour pressure

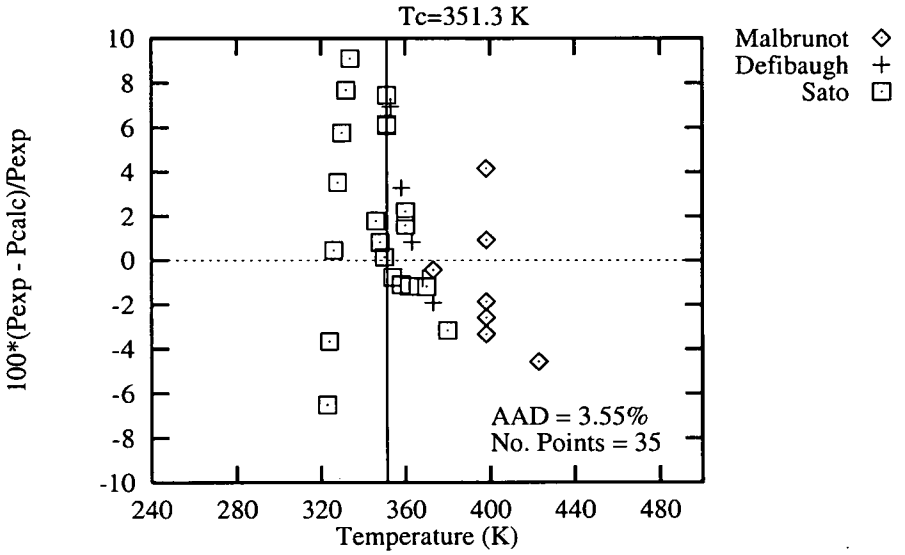

Figure D.31: Deviation of CSD equation from R32 PVT compressed liquid pressure

D.4.2 R125

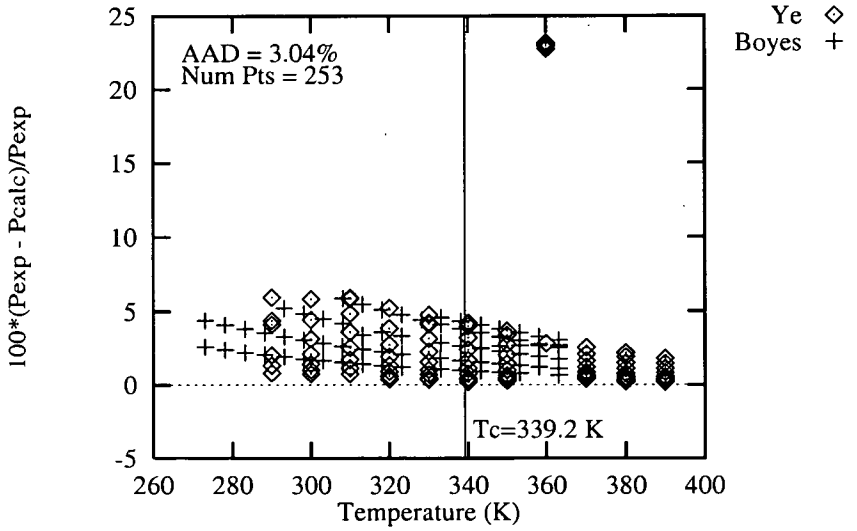

Figure D.32: Deviation of CCOR equation from R125 PVT superheated vapour pressure

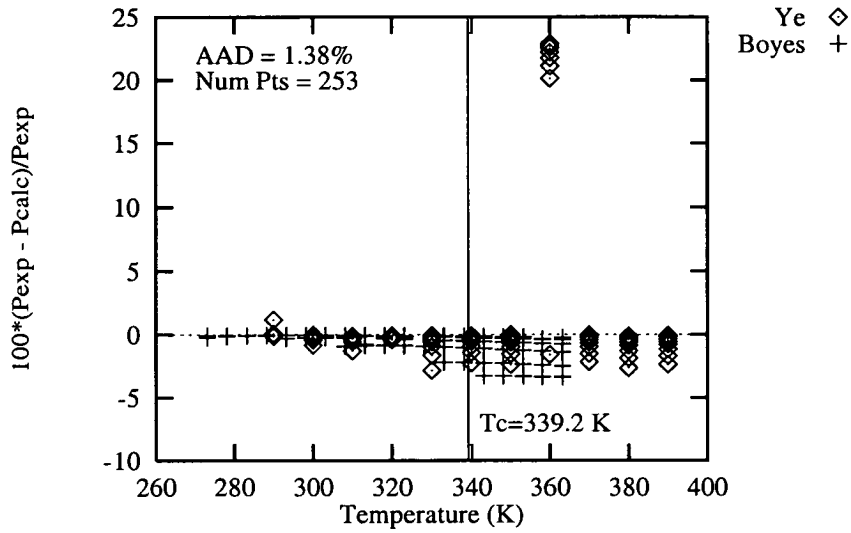

Figure D.33: Deviation of CSD equation from R125 PVT superheated vapour pressure

D.4.3 R134a

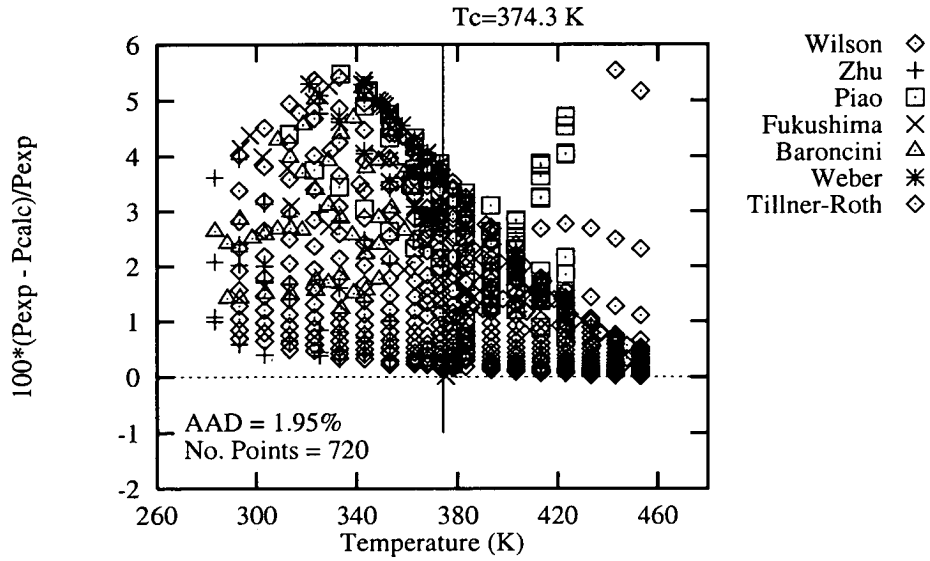

Figure D.34: Deviation of CCOR equation from R134a PVT superheated vapour pressure

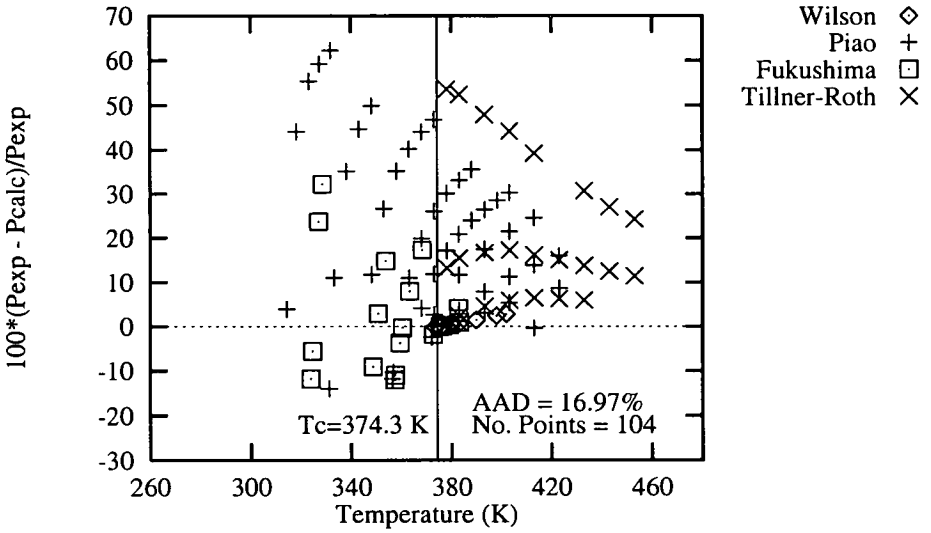

Figure D.35: Deviation of CCOR equation from R134a PVT compressed liquid pressure

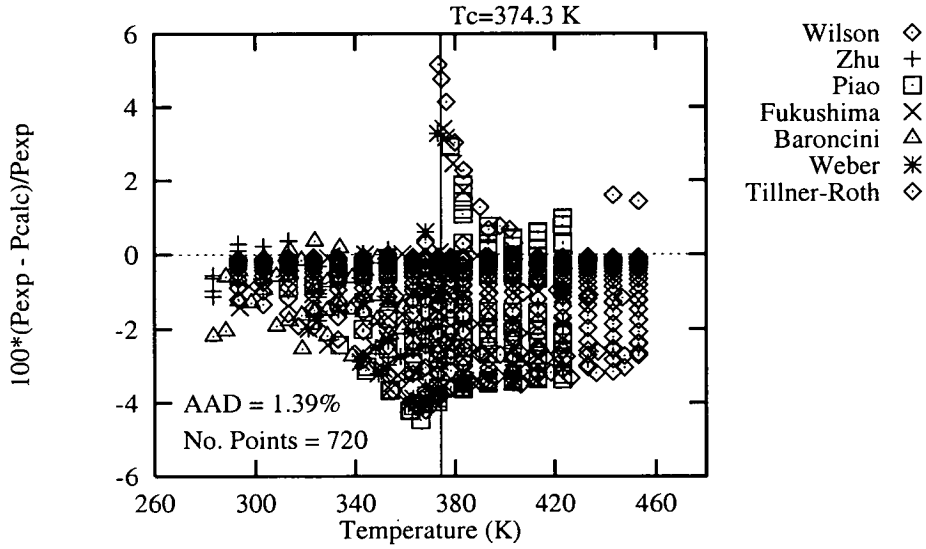

Figure D.36: Deviation of CSD equation from R134a PVT superheated vapour pressure

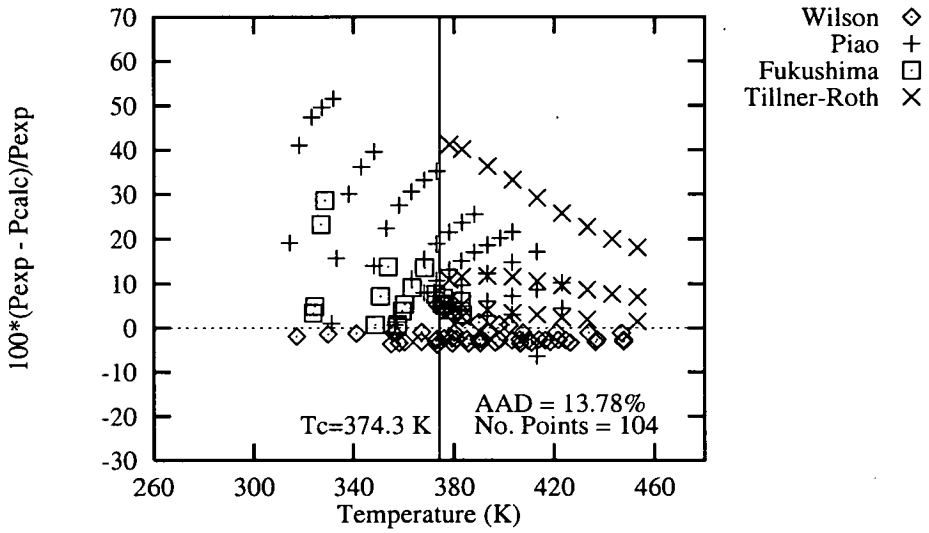

Figure D.37: Deviation of CSD equation from R134a PVT compressed liquid pressure

D.4.4 R152a

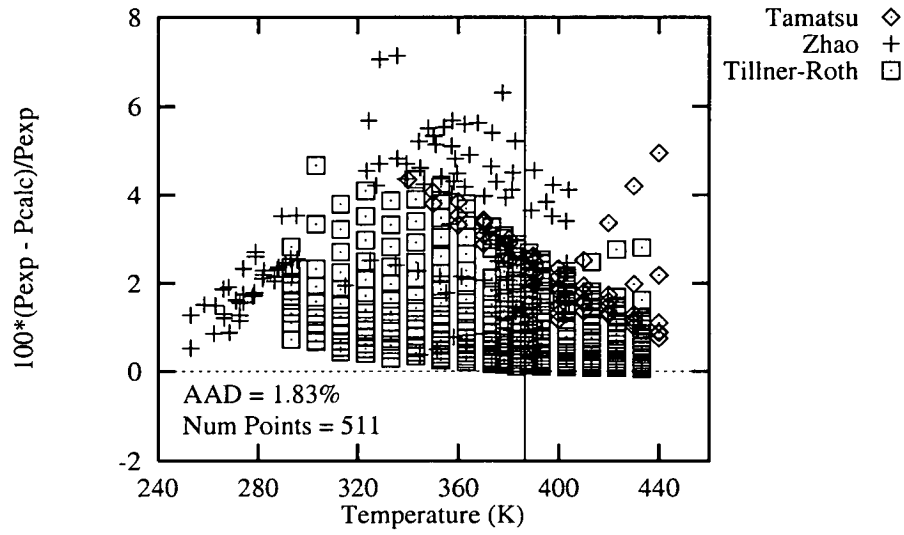

Figure D.38: Deviation of CCOR equation from R152a PVT superheated vapour pressure

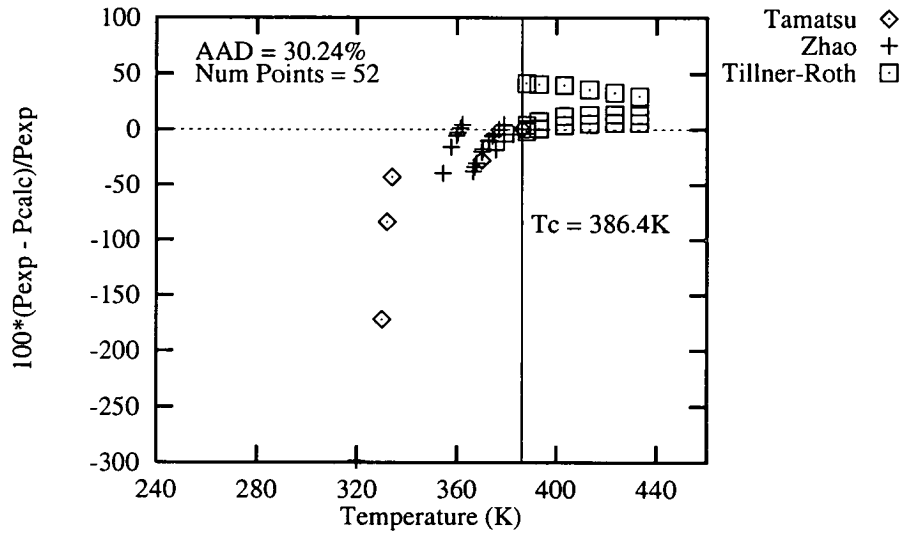

Figure D.39: Deviation of CCOR equation from R152a PVT compressed liquid pressure

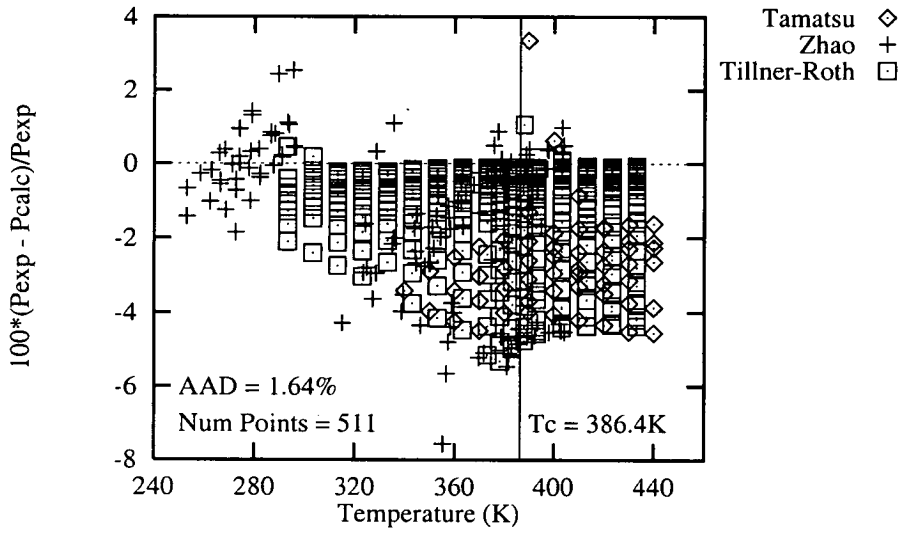

Figure D.40: Deviation of CSD equation from R152a PVT superheated vapour pressure

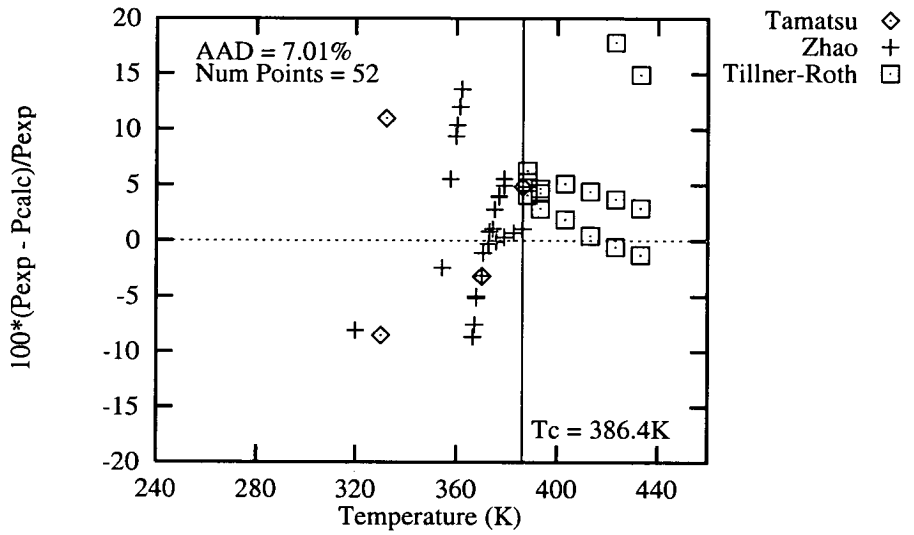

Figure D.41: Deviation of CSD equation from R152a PVT compressed liquid pressure

D.4.5 Error vs. T_r for PVT Behaviour of All Refrigerants

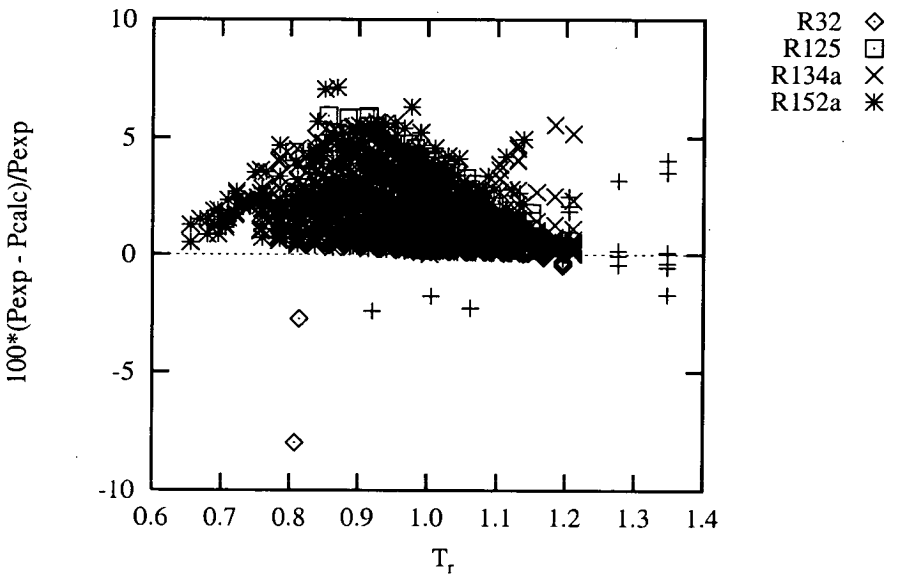

Figure D.42: CCOR error vs. T_r for PVT superheated vapour pressure

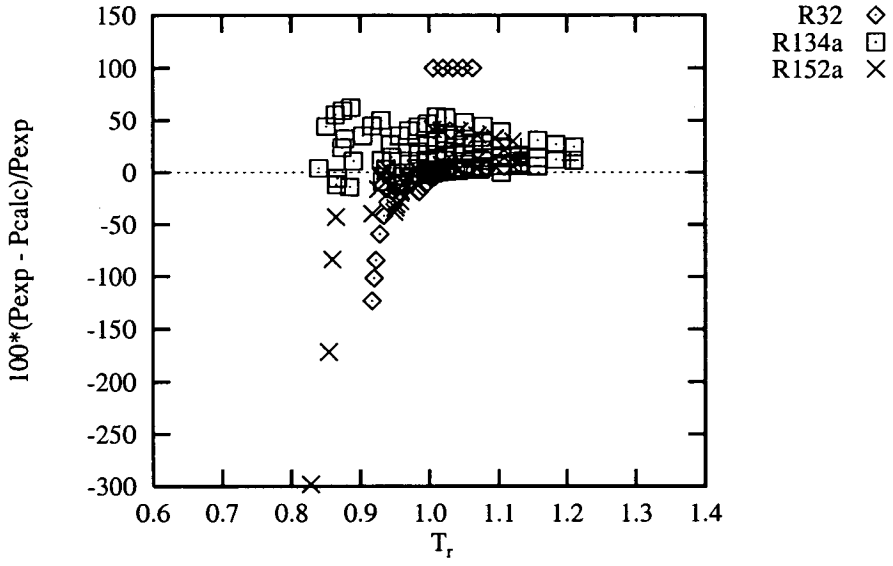

Figure D.43: CCOR error vs. T_r for PVT compressed liquid pressure

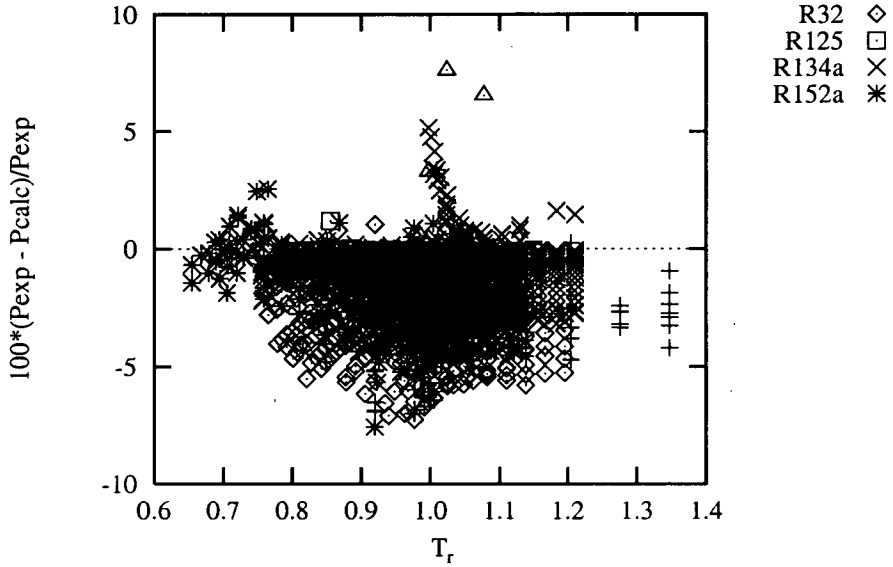

Figure D.44: CSD error vs. T_r for PVT superheated vapour pressure

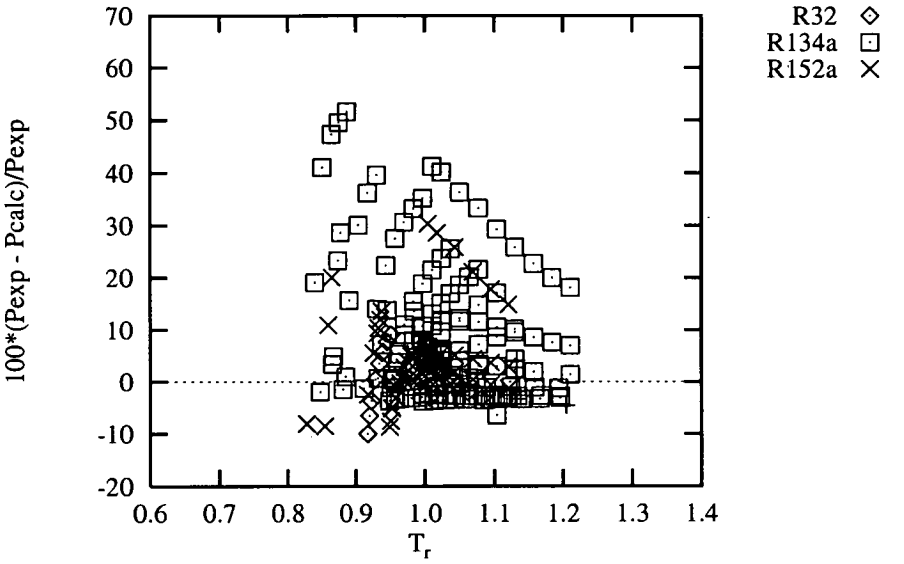

Figure D.45: CSD error vs. T_r for PVT compressed liquid pressure

Appendix E

Tabulated Average Absolute Deviations of CCOR and CSD Thermodynamic Property Comparisons with Pure and Mixed Hydrofluorocarbon Fluids

In this appendix the percentage average absolute deviations (AAD) obtained using the Cubic Chain-of-Rotators and the Carnahan-Starling-DeSantis equations of state for each publication of experimental hydrofluorocarbon refrigerant data is tabulated.The deviations are those found from comparisons detailed in Appendix B and Appendix F. Calculated deviations are given for both pure (Section E.1) and mixed fluids (Section E.2). Each refrigerant and thermodynamic property is tabulated separately. For a given publication of experimental data the year of publication, number of points examined and the CCOR and CSD percentage deviation is given. For pure fluids the deviations are grahpically displayed as functions of temperature in Appendix D.

E.1 Pure Fluids

E.1.1 Vapour Pressure

E.1.1.1 R32

Table E.1: AAD of R32 vapour pressure

Author	Year	No. Points Compared	CCOR AAD %	CSD AAD %
Defibaugh	1994	18	1.48	0.20
Malbrunot	1968	30	2.14	0.31
Sato	1994	21	1.33	0.35
Weber	1993	27	4.05	0.23
Widiatmo	1994b	24	1.56	0.50
Zhu	1993	28	1.49	0.24
Holcomb	1993	25	1.30	0.19
Baroncini	1993	56	1.30	0.19
Overall		229	1.84	0.27

E.1.1.2 R125

Table E.2: AAD of R125 vapour pressure

Author	Year	No. Points Compared	CCOR AAD %	CSD AAD %
Baroncini	1993	58	1.07	0.28
Widiatmo	1994b	20	1.38	0.62
Ye	1995	12	0.91	0.22
Boyes	1995	29	1.27	0.22
Monluc	1991	23	1.03	0.29
Overall		142	1.13	0.31

E.1.1.3 R134a

Table E.3: AAD of R134a vapour pressure

Author	Year	No. Points Compared	CCOR AAD %	CSD AAD %
Fukushima	1990	41	1.15	0.27
Kubota	1989	25	1.11	0.25
Lavrenchenko	1992	28	1.29	1.12
Magee	1992	19	1.33	1.48
Piao	1990	23	1.45	0.17
Weber	1989	22	1.40	0.25
Wilson	1988	32	1.52	0.20
Maezawa	1990	13	1.20	0.41
Morrison	1991	12	0.91	0.29
Niesen	1994	12	1.30	0.23
Baehr	1991	37	1.08	0.40
Baroncini	1990	64	0.83	0.28
Overall		328	1.17	0.42

E.1.1.4 R143a

Table E.4: AAD of R143a vapour pressure

Author	Year	No. Points Compared	CCOR AAD %	CSD AAD %
Widiatmo	1994b	12	1.04	0.45

E.1.1.5 R152a

Table E.5: AAD of R152a vapour pressure

Author	Year	No. Points Compared	CCOR AAD %	CSD AAD %
Tamatsu	1992	15	1.12	0.35
Zhao	1992	168	1.79	0.40
Baehr	1991	55	0.95	0.31
Higashi	1987	44	0.83	0.35
Yada	1988	13	1.14	0.22
Blanke	1992	35	7.10	2.39
Holcomb	1993	33	1.05	0.32
Overall		363	1.94	0.55

E.1.2 Saturated Liquid Density

E.1.2.1 R32

Table E.6: AAD of R32 saturated liquid density

Author	Year	No. Points Compared	CCOR AAD %	CSD AAD %
Defibaugh	1994	21	12.86	0.40
Sato	1994	2	15.23	0.95
Widiatmo	1994b	22	12.51	0.38
Malbrunot	1968	16	14.24	3.87
Holcomb	1993	25	15.46	1.07
Shinsaka	1985	20	12.42	1.40
Kuwabara	1995	13 (17*)	16.69	14.05
Overall		119 (123 *)	13.91	3.04

(* only 13 out of the 17 points of Kuwabara's data was compared with the CCOR equation. The CCOR algorithm would not converge for the remaining four points)

E.1.2.2 R125

Table E.7: AAD of R125 saturated liquid density

Author	Year	No. Points Compared	CCOR AAD %	CSD AAD %
Widiatmo	1994b	25	2.64	0.40

E.1.2.3 R134a

Table E.8: AAD of R134a saturated liquid density

Author	Year	No. Points Compared	CCOR AAD %	CSD AAD %
Maezawa	1990	25	1.17	0.42
Morrison	1991	12	4.89	4.05
Fukushima	1991	7	0.09	0.19
Piao	1990	7	4.47	2.04
Wilson	1988	9	3.18	1.38
Niesen	1994	12	3.30	0.99
Overall		72	2.61	1.37

E.1.2.4 R143a

Table E.9: AAD of R143a saturated liquid density

Author	Year	No. Points Compared	CCOR AAD %	CSD AAD %
Widiatmo	1994b	17	5.99	0.66

E.1.2.5 R152a

Table E.10: AAD of R152a saturated liquid density

Author	Year	No. Points Compared	CCOR AAD %	CSD AAD %
Holcomb	1993	33	10.00	1.22
Sato	1987	27	6.94	0.31
Overall		60	8.62	0.81

E.1.3 Saturated Vapour Density

E.1.3.1 R32

Table E.11: AAD of R32 saturated vapour density

Author	Year	No. Points Compared	CCOR AAD %	CSD AAD %
Defibaugh	1994	28	6.47	7.49
Sato	1994	4	12.34	16.78
Holcomb	1993	25	9.88	17.07
Overall		57	8.38	12.34

E.1.3.2 R134a

Table E.12: AAD of R134a saturated vapour density

Author	Year	No. Points Compared	CCOR AAD %	CSD AAD %
Morrison	1991	9	14.27	13.89
Niesen	1994	12	14.14	7.48
Weber	1989	5	15.75	7.28
Overall		26	14.49	9.66

E.1.3.3 R152a

Table E.13: AAD of R152a saturated vapour density

Author	Year	No. Points Compared	CCOR AAD %	CSD AAD %
Holcomb	1993	33	11.03	12.54

E.1.4 PVT Behaviour

E.1.4.1 R32

Table E.14: AAD of R32 superheated vapour pressure

Author	Year	No. Points Compared	CCOR AAD %	CSD AAD %
Defibaugh	1994	143	1.28	2.88
Malbrunot	1968	79	1.56	4.15
Sato	1994	46	0.82	4.84
Baroncini	1993	93	2.07	3.67
Overall		361	1.49	3.61

Table E.15: AAD of R32 compressed liquid pressure

Author	Year	No. Points Compared	CCOR AAD %	CSD AAD %
Defibaugh	1994	5	2.56	2.75
Malbrunot	1968	7	12.87	2.55
Sato	1994	23	22.88	4.02
Overall		35	17.98	3.55

E.1.4.2 R125

Table E.16: AAD of R125 superheated vapour pressure

Author	Year	No. Points Compared	CCOR AAD %	CSD AAD %
Ye	1995	93	3.51	2.21
Boyes	1995	80	2.77	0.87
Overall		173	3.17	1.59

E.1.4.3 R134a

Table E.17: AAD of R134a superheated vapour pressure

Author	Year	No. Points Compared	CCOR AAD %	CSD AAD %
Fukushima	1991	43	2.57	2.00
Baroncini	1990	41	2.80	1.23
Piao	1990	110	2.50	1.93
Weber	1989	56	3.45	2.80
Wilson	1988	44	1.93	2.53
Zhu	1992	42	1.77	0.59
Tillner-Roth	1992	384	1.44	0.94
Overall		720	1.95	1.39

Table E.18: AAD of R134a compressed liquid pressure

Author	Year	No. Points Compared	CCOR AAD %	CSD AAD %
Fukushima	1991	20	7.99	7.63
Piao	1990	49	21.99	17.74
Wilson	1988	8	1.09	2.76
Tillner-Roth	1992	27	19.23	14.39
Overall		104	16.97	13.78

E.1.4.4 R152a

Table E.19: AAD R152a superheated vapour pressure

Author	Year	No. Points Compared	CCOR AAD %	CSD AAD %
Tamatsu	1992	55	2.13	2.89
Zhao	1992	141	2.83	1.65
Tillner-Roth	1992	315	1.32	1.42
Overall		511	1.83	1.64

Table E.20: AAD R152a compressed liquid pressure

Author	Year	No. Points Compared	CCOR AAD %	CSD AAD %
Tamatsu	1992	5	65.27	9.51
Zhao	1992	27	34.86	4.84
Tillner-Roth	1992	20	15.26	9.32
Overall		52	30.24	7.01

E.1.4.5 Overall Pure Fluid AADs by Property

Table E.21: Overall average pure fluid AADs for all properties investigated

Property	CCOR Points	CSD Points	CCOR AAD %	CSD AAD %
Vapour pressure	1074	1074	1.57	0.42
Saturated vapour density	116	116	10.05	11.80
Saturated liquid density	293	297	8.63	1.83
PVT superheated vapour	1765	1765	1.94	1.94
PVT liquid	191	191	15.13	10.06
Overall	3519	3523		

E.2 Calculated Deviations with Mixtures of Refrigerants

The results of comparing the CCOR and CSD equations of state with refrigerant mixture VLE data are tabulated here. Bubble point data and two-phase mixture (as defined in Section F.3 on page 280) comparison results are displayed in separate tables. The errors associated with predicted bubble pressure and density are expressed as percentage absolute average deviation (Equation B.10 on 211). With two-phase type data the actual compositonal deviation is given (Equation F.8 on 280). It is not expressed as a percentage or ratio. In Section E.2.1 results are given where the interaction constants associated with both equations of state are set to zero. In Section E.2.2 results are given whereby single values of the interaction constants have been optimised from each set of experimental data. Finally in Section E.2.3 interaction constants have been optimised for each data point in an experimental set of equilibrium data. With bubble point type data, the total number of liquid density points is given in brackets underneath or beside the total number of bubble pressure datapoints. Some authors only quote the bubble pressure and not the bubble density. In the rows where the total number of experimental points compared are given are numbers in brackets refer to the total for density. Some bubble point VLE data did not give liquid density measurements. The references for the VLE data are given in Table E.22 and Table E.23.

E.2.1 Interaction Constants Set to Zero

E.2.1.1 CCOR Equation of State

Table E.22: CCOR bubble point pressure and density data AADs with zero interaction constants

Refrigerant Pair	Author	Year	Points Published	Points Modelled	Press. AAD %	Density AAD %
R32/R125	Widiatmo	1993	24	24	2.62	7.90
	Defibaugh	1995	10	9	2.67	0
R32/R134a	Widiatmo	1994a	30	29	2.96	11.43
	Defibaugh	1995	25	20	4.43	0
R32/R152a	Defibaugh	1995	25	21	3.30	0
R134a/R152a	Defibaugh	1995	13	13	5.05	0
R152a/R134	Maezawa	1991c	48	48	3.39	4.37
R22/R152a	Maezawa	1991a	66	66	4.58	6.73
R152a/R142b	Maezawa	1991b	48	44	2.96	5.54
Overall			289 (216)	273 (211)	3.61	6.72

Table E.23: CCOR two phase data composition deviations with interaction constants set to zero

Refrigerant Pair	Author	Year	Points Published	Points Modelled	Liquid Comp. Deviation	Vapour Comp. Deviation
R22/R134a	Arito	1991	14	14	0.0281	0.0237
R22/R152a	Ström	1993	46	46	0.1041	0.1021
R32/R125	Nagel	1995	34	22	0.1618	0.1575
R32/R134a	Nagel	1995	50	38	0.0344	0.0309
R125/R134a	Nagel	1995	31	22	0.0144	0.0108
R134a/R141b	Zheng	1990	38	38	0.0758	0.0513
Overall			213	180	0.0736	0.0658

E.2.1.2 CSD Equation of State

Table E.24: CSD bubble point data pressure and density AADs with the interaction constant set to zero

Refrigerant Pair	Author	Points Published	Points Modelled	Press. AAD %	Density AAD %
R32/R125	Widiatmo	24	24	1.61	0.87
	Defibaugh	10	10	2.38	0
R32/R134a	Widiatmo	30	30	1.04	2.11
	Defibaugh	25	25	2.74	0
R32/R152a	Defibaugh	25	24	1.53	0
R134a/R152a	Defibaugh	13	13	4.89	0
R152a/R134	Maezawa	48	40	12.43	4.03
R22/R152a	Maezawa	66	66	2.37	1.74
R152a/R142b	Maezawa	48	48	17.13	18.79
Overall		289 (216)	280 (203)	6.21	5.84

Table E.25: CSD two phase data composition deviations with the interaction constant set to zero

Refrigerant Pair	Author	Points Published	Points Modelled	Liquid Comp. Deviation	Vapour Comp. Deviation
R22/R134a	Arito	15	15	0.0368	0.0335
R22/R152a	Ström	46	46	0.0950	0.0829
R32/R125	Nagel	34	33	0.2316	0.2108
R32/R134a	Nagel	50	50	0.0299	0.0208
R125/R134a	Nagel	31	31	0.0186	0.0195
R134a/R141b	Zheng	38	38	0.0786	0.0583
Overall		214	213	0.0827	0.0710

E.2.2 Optimisation for Each Set of Experimental Data

E.2.2.1 CCOR Equation of State

Table E.26: CCOR bubble point data pressure and density AADs with single values of k_a and k_c optimised for each experimental VLE data set

Refrigerant Pair	Author	No. Pts.	Optimum k_a	Optimum k_c	Press. AAD %	Density AAD %
R32/R125	Widiatmo	24	0.04444	0.07053	0.46	3.39
	Defibaugh	10	-0.00551	0.00986	0.73	0
R32/R134a	Widiatmo	29	0.07381	0.10611	1.04	3.10
	Defibaugh	22	0.00859	0.00980	1.15	0
R32/R152a	Defibaugh	21	-0.00379	0.00984	0.89	0
R134a/R152a	Defibaugh	12	0.03436	0.00985	0.54	0
R152a/R134	Maezawa	36	0.00338	0.02189	1.80	2.23
R22/R152a	Maezawa	43	0.02207	0.04953	0.96	1.91
R152a/R142b	Maezawa	41	0.06900	0.06890	3.02	1.66
Overall		238 (173)			1.38	2.32

Table E.27: CCOR two phase data composition deviations with single values of k_a and k_c optimised for each experimental VLE data set

Refrigerant Pair	Author	Points Modelled	Optimum k_a	Optimum k_c	Liquid Comp. Deviation	Vapour Comp. Deviation
R22/R134a	Arito	14	0.01267	0.00980	0.0209	0.0219
R22/R152a	Ström	46	-0.01634	0.00982	0.0178	0.0186
R32/R125	Nagel	14	0.00424	0.0150	0.0390	0.0350
R32/R134a	Nagel	39	-0.00365	0.00974	0.0221	0.0192
R125/R134a	Nagel	22	0.01274	0.00992	0.0041	0.0089
R134a/R141b	Zheng	36	0.05675	0.00988	0.0064	0.0229
Overall		170			0.0166	0.0199

E.2.2.2 CSD equation of State

Table E.28: CSD bubble point data pressure and density AADs with a single value of k_a optimised for each experimental VLE data set

Refrigerant Pair	Author	No. Pts.	Optimum k_a	Press. AAD %	Density AAD %
R32/R125	Widiatmo	24	-0.00991	0.61	0.32
	Defibaugh	10	-0.01359	0.89	0
R32/R134a	Widiatmo	30	-0.00679	0.90	1.71
	Defibaugh	25	-0.01069	0.18	0
R32/R152a	Defibaugh	24	-0.00584	0.23	0
R134a/R152a	Defibaugh	13	0.02338	1.35	0
R152a/R134	Maezawa	44	-0.00935	3.68	9.46
R22/R152a	Maezawa	62	-0.01259	0.96	0.99
R152a/R142b	Maezawa	44	0.09469	1.36	0.42
Overall		268 (176)		1.30	3.02

Table E.29: CSD two phase data composition deviations equation a single value of k_a optimised for each experimental VLE data set

Refrigerant Pair	Author	Points Modelled	Optimum k_a	Liquid Comp. Deviation	Vapour Comp. Deviation
R22/R134a	Arito	14	0.00916	0.0112	0.0121
R22/R152a	Ström	46	-0.02026	0.0228	0.0172
R32/R125	Nagel	31	-0.02027	0.1571	0.1515
R32/R134a	Nagel	50	-0.00921	0.0109	0.0123
R125/R134a	Nagel	22	-0.00086	0.0175	0.0129
R134a/R141b	Zheng	38	0.04725	0.0076	0.0279
Overall		201		0.0359	0.0374

E.2.3 Optimisation with Composition and Temperature

E.2.3.1 CCOR Equation of State

Table E.30: CCOR bubble point data pressure and density AADs with k_a and k_c optimised for each experimental VLE data point

Refrigerant Pair	Author	No. Pts.	Press. AAD %	Density AAD %
R32/R125	Widiatmo	24	1.5×10^{-8}	1.2×10^{-8}
	Defibaugh	9	1.3×10^{-8}	0
R32/R134a	Widiatmo	29	1.5×10^{-8}	1.5×10^{-8}
	Defibaugh	20	4.3×10^{-9}	0
R32/R152a	Defibaugh	21	9.9×10^{-9}	0
R134a/R152a	Defibaugh	13	1.8×10^{-5}	0
R152a/R134	Maezawa	44	7.5×10^{-9}	1.2×10^{-8}
R22/R152a	Maezawa	57	1.9×10^{-8}	6.1×10^{-8}
R152a/R142b	Maezawa	41	1.2×10^{-8}	2.8×10^{-8}
Overall		258 (195)	7.7×10^{-9}	1.0×10^{-8}

Table E.31: CCOR two phase data composition deviations with k_a and k_c optimised for each experimental VLE data point)

Refrigerant Pair	Author	Points Modelled	Liquid Comp. Deviation	Vapour Comp. Deviation
R22/R134a	Arito	14	0.0038	0.0054
R22/R152a	Ström	46	0.0030	0.0039
R32/R125	Nagel	17	0.0034	0.0045
R32/R134a	Nagel	39	0.0027	0.0066
R125/R134a	Nagel	22	0.0022	0.0052
R134a/R141b	Zheng	36	0.0013	0.0224
Overall		174	0.0026	0.0087

E.2.3.2 CSD Equation of State

Table E.32: CSD bubble point data pressure and density AADs with k_a optimised for each experimental VLE data point

Refrigerant Pair	Author	No. Pts.	Press. AAD %	Density AAD %
R32/R125	Widiatmo	24	0.16	0.41
	Defibaugh	10	2.5×10^{-5}	0
R32/R134a	Widiatmo	30	0.64	1.67
	Defibaugh	25	7.6×10^{-5}	0
R32/R152a	Defibaugh	24	2.56×10^{-4}	0
R134a/R152a	Defibaugh	13	4.7×10^{-5}	0
R152a/R134	Maezawa	36	0.20	0.63
R22/R152a	Maezawa	57	0.27	0.66
R152a/R142b	Maezawa	44	1.93	8.99
Overall		263 (191)	0.49	2.70

Table E.33: CSD two phase data composition deviations with k_a optimised for each experimental VLE data point

Refrigerant Pair	Author	Points Modelled	Liquid Comp. Deviation	Vapour Comp. Deviation
R22/R134a	Arito	14	0.0015	0.0023
R22/R152a	Ström	46	0.0052	0.0067
R32/R125	Nagel	33	0.0030	0.0037
R32/R134a	Nagel	50	0.0029	0.0043
R125/R134a	Nagel	31	0.0032	0.0046
R134a/R141b	Zheng	38	0.0017	0.0257
Overall		212	0.00315	0.00848

Appendix F

Prediction of Mixture Hydrofluorocarbon Thermodynamic Properties from Sparse Data using the Cubic Chain-of-Rotators Equation of State

F.1 Introduction

The CCOR equation's ability to predict binary vapour-liquid equilibria of hydrofluorocarbons is examined in this appendix. The vapour liquid equilibrium properties for a number of binary mixtures, as calculated by the CCOR equation were compared to experimentally reported values in the literature. At least one component of each mixture was a HFC refrigerant. Average deviations were calculated in a similar fashion to that done in Appendix B for pure fluids. The errors in CCOR prediction were compared to the errors associated with the Carnahan-Starling-DeSantis equation of state, which is theoretically more accurate since it uses experimentally derived parameters. Examination of how well the CCOR equation can predict HFC mixture behaviour, gives an indication if the CCOR is suitable for predicting the behaviour of new refrigerant mixtures.

F.2 Application of CCOR Equation to Mixtures

Applying equations of state to mixtures requires greater subtlety. Composition adds an extra degree of freedom to the problem of property prediction. The most common way to treat mixtures is to infer the properties of the mixture from the pure fluid properties. The molecular interactions of unlike molecules are deduced from the interactions of like molecules. Procedures for doing this are termed *mixing rules.* Usually the parameters of an equation of state (e.g the a parameter in the CCOR equation) are calculated at the prevailing temperature and pressure for each pure component in the mixture. *Cross coefficients* reflect the interactions of unlike molecules and are deduced by some average of the pure parameters. An overall mixture parameter is found by taking an average of the pure parameters and the cross constants. One of the most common mixing rules are those developed by Van der Waals:

$$\Theta_m = \sum_i^n \sum_j^n x_i x_j \Theta_{ij} \qquad \text{(Eq F.1)}$$

Θ_m is the overall mixture parameter; $\Theta_{ii}=\Theta_i$ which is the parameter of pure component i. The cross coefficient (Θ_{ij}) occurs when $i \neq j$ and reflects the interaction of component i on component j. In this case Θ_{ij} is usually taken as some average (not necessarily linear) of Θ_i and Θ_j.

Very often *interaction constants* are introduced into the cross coefficients which attempt to provide a better prediction of mixture properties. These interaction constants are located by finding the values which give the best fit to experimental data. The obvious disadvantage of this, is that with new mixtures experimental VLE data would not exist. In this case the interaction constants are normally set to a value of zero. Attempts have been made to correlate interaction constants with various properties of the pure fluid components of the mixtures [*Pesuit 1978*]. Determination

of interaction constants from the properties of the components in a particular mixture has not proved to be an easy task. The optimal value of the interaction constant depends on the mixing rule used. This restricts the use of optimal values reported in the literature.

The Van der Waals mixing rules are applied to the CCOR so that properties of mixtures can be found [*Kim et al. 1986*]. The mixing rule is applied to the five parameters namely a, b, c, d, and c^R. The cross constants (i.e. where i≠j) of each of the parameters are given by Equations F.2-F.6:

$$a_{ij} = (1 - k_{a_{ij}})(a_{ii}a_{jj})^{1/2} \qquad \text{(Eq F.2)}$$

$$b_{ij} = \frac{b_{ii} + b_{jj}}{2} \qquad \text{(Eq F.3)}$$

$$c_{ij} = (1 - k_{c_{ij}})\left(\frac{c_{ii} + c_{jj}}{2}\right) \qquad \text{(Eq F.4)}$$

$$d_{ij} = (d_{ii}d_{jj})^{1/2} \qquad \text{(Eq F.5)}$$

$$c_{ij}^R = \frac{c_{ii}^R + c_{jj}^R}{2} \qquad \text{(Eq F.6)}$$

Two interaction constants $k_{a_{ij}}$ and $k_{c_{ij}}$ are used in conjunction with the Van der Waals mixing rules in conjunction with the CCOR equation. When experimental data is available optimal values are found by regression. When no data is at hand, they are usually set to zero. Sometimes a slightly different mixing rule for b_{ij} is used namely:

$$b_{ij} = \left(\frac{b_{ii}^{1/3} + b^{1/3}{}_{jj}}{2}\right)^3 \qquad \text{(Eq F.7)}$$

The difference between Equation F.3 and Equation F.7 is very small. The former mixing rule was used in this research. The reader is referred to Low [*1991*] for formulae for the mixture fugacity coefficient and mixture enthalpy departure function.

F.2.1 Mixtures and the CSD Equation of State

Below is the function for the fugacity coefficient of component i in a mixture of n components.

$$\ln\phi_i = \frac{4y-3y^2}{(1-y)^2} + \frac{b_i}{b}\frac{4y-2y^2}{(1-y)^3} - \frac{2}{RTb}\sum_{k=1}^{n} x_i a_{ik} \ln\left(\frac{v}{v+b}\right) \qquad \text{(Eq F.8)}$$
$$- \frac{b_i a}{RTb^2}\ln\left(\frac{v+b}{b}\right) - \frac{1}{RT}\frac{b_i a}{bv+b^2} - \ln z$$

F.3 Properties and Refrigerants Investigated

Published experimental mixture data was found to be more scarce than pure fluid data. It was decided to examine any binary pair where one of the components came from the five refrigerants examined in Appendix B; namely R32, R125, R134a, R143a and R152a. At the start of this research (1992) most of the vapour liquid equilibrium mixture comprised of HFC/HCFC binary mixtures (i.e. one component was a HFC and the other a HCFC). VLE data involving HFCs only began to be published in 1994-5. Thus HCFCs were considered when examining the equations of state with mixtures. It has been found that experimental refrigerant VLE data is published in two manners.

- In the first method bubble point VLE of a particular mixture is described. Bubble pressures and bubble densities are given at different temperatures and compositions. The temperature and composition are varied at regular intervals. The vapour properties are not usually given. This is referred to as "bubble point data" throughout this thesis.

- In the second method, substantial amounts of both phases are presented rather than just the bubble point. Compositions of both phases are given. The temperature is fixed and the pressure varied, which causes the composition of the two phases to vary. The temperature is altered and the process is repeated. Density data are not normally given. This is referred to hereafter as "two-phase data". Experimental bubble point data obviously requires that two phases exist, but for the sake of simplicity the term, "two phase data" describes data where liquid and vapour compositions are tabulated as functions of temperature and pressure.

Both types of experimental data were used to compare the CCOR and CSD equations.

F.4 Results

F.4.1 Introduction

The Cubic Chain-of-Rotators equation of state's ability to predict vapour-liquid equilibria is examined in this section. The literature was surveyed for sources of VLE data where at least one of the components was a Hydrofluorocarbon. Eleven publications were located. There are considerably fewer HFC VLE data compared with the amount of pure fluid data. With the exception of the data of Defibaugh et al. [*1995*] and Nagel et al. [*1995*] the experimental investigations were carried out at relatively high temperatures. Ideally it would have been better if more refrigerant VLE data existed at below ambient temperatures since in this region equations of state would be required to supply thermodynamic data.

About half of the experimental VLE data was of the bubble point variety. Pressure and liquid density are presented as functions of temperature and composition. In carrying out the calculations, temperature and liquid composition were used as the specified variables while pressure and density were calculated and compared to the reported values. For two-phase experimental VLE data the liquid and vapour composition, are

presented as functions of temperature and pressure. With this type of data temperature and pressure were used as the specified variable and a flash calculation was performed to find the liquid and vapour compositions. These predicted compositions were compared to the values reported in the literature. The calculation methods and algorithms outlined in Section B.3 on page 211 are used to compare the predicted values with the calculated ones. As with the pure fluid data, programs were written which read the experimental data from a file. The deviation from the experimental pressure and density is sent to an output result file. The overall percentage absolute average deviation (Equation B.10 on 211) was then calculated and sent to the output file. Composition deviations are expressed as *actual* deviations from the experimental value rather than in percentages i e:

$$Compostiton\ AAD = \frac{\sum_{i=1}^{N_{pts}} |y_{exp} - y_{calc}|}{N_{pts}} \qquad \text{(Eq F.9)}$$

where N_{pts} is the number of points in a given dataset.

In comparing experimental VLE with the predictions of the CCOR initially the interaction constants k_a and k_c described in Equation F.2 and Equation F.4 were set to zero. The results for these predictions are presented in Section F.4.2. In order to examine whether the CCOR equation can predict the behaviour of new mixtures it was necessary to have the values of the interaction constants set to zero. With a new refrigerant it would be unlikely that knowledge of the optimum interaction constants would be available. Normally k_a and k_c are set to zero in such a situation. In Section F.5.2 and Section F.5.3 optimum values for the interaction constants were found. The influence of composition and temperature on the optimum interaction constant were investigated. As with pure fluids the Carnahan-Starling-DeSantis equation of state was applied to the experimental data as a reference equation for the purpose of comparison.

F.4.2 Interaction Constants set to Zero

In this section the CCOR and CSD equations of state were compared with HFC VLE data, with the *interaction constants set at a value of zero.* With new refrigerant mixtures VLE data would not exist, and the interactions constants (k_a & k_c for the CCOR equation; k_a alone for the CSD equation) would be set to zero in such a situation. Comparison results of the CCOR equation are presented graphically. Experimental points are shown as dots whereas predictions by the CCOR are shown as lines. Average absolute deviations for each set of published data are also given. An overall summary of the results is given in Table F.1 and Table F.2 on page 297. In Section E.2.1 of Appendix E the number of points compared and the average error found with each set of published VLE data are given. The results for both equations of state are tabulated. References for also given for each VLE data set.

F.4.2.1 HFC mixtures

R32/R125 System

Three authors have investigated the vapour liquid equilibria of R32/R125: Widiatmo et al. [*1994a*], Defibaugh et al. [*1995*], and Nagel et al. [*1995*]. Widiatmo examined the bubble point behaviour of the liquid phase. Six compositions at four temperatures ranging from 280K to 310K were examined. The compositions considered were 10, 20, 30, 40, 60 and 80 wt.% R125. The liquid density was also measured and tabulated. In Figure F.1 Widiatmo's data is shown with the CCOR predicted bubble point pressure. The liquid density as a function of composition is also shown. The AAD for the pressure was 2.62% which is quite a good prediction of the pressure by the CCOR equation of state.

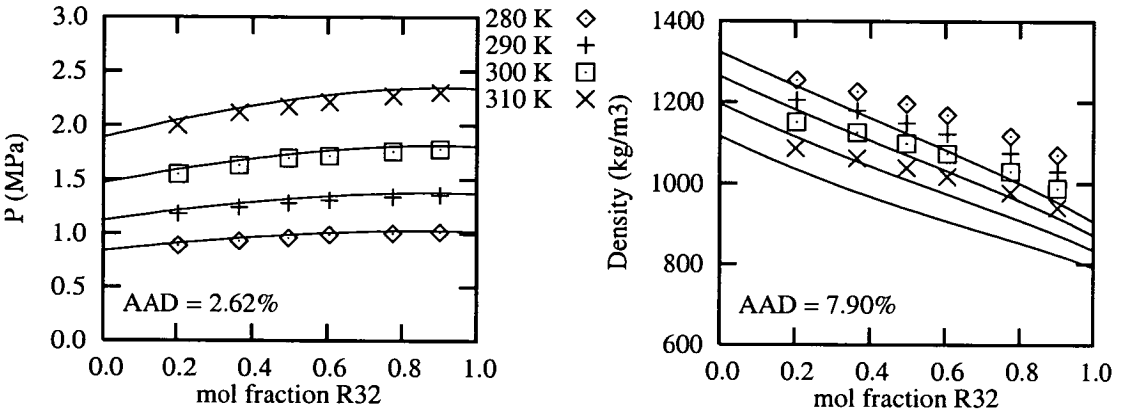

Figure F.1: CCOR calculated and experimental R32/R125 bubble point VLE data of Widiatmo

However, the liquid density deviation is 7.90%. As with pure fluids, the CCOR does not predict the liquid density in this case as accurately as the pressure. The corresponding errors for the CSD equation were 1.61% for bubble pressure and 0.87% for the liquid density. The second set of data investigated was that of Defibaugh who measured the bubble point pressure of an R32/R125 mixture at a composition of 0.763 mole fraction R32. Nine different measurements were recorded over a temperature range of 249-340K. The liquid density was not recorded and so was not considered. The overall AAD for Defibaugh's set of data was 2.67%. This is very similar to the AAD obtained by Widiatmo and indicates a good consistency. The CSD average absolute deviation was 2.38%

Nagel examined four compositions and tabulated pressure, liquid and vapour compositions. The four separate compositions which were examined were 0.25, 0.50, 0.75 and 0.95 mole fraction R32. For each separate composition the temperature was varied from 205K to around 340K. Thirty four data points were published, while only twenty eight of the thirty four points were compared. This was because the VLE algorithm would not converge above a temperature of 333K (T_r = 0.98 for R125).

Where this occurred, the number of actual data points successfully compared to the predicted CCOR values will be given. The CSD equation of state algorithm could achieve VLE convergence at higher temperatures, although there were some cases where it did not reach a solution. With Nagel's data the average composition errors were 0.1618 and 0.1575 mole fraction R32, for liquid and vapour composition respectively. Theses are quite large errors. (The CSD Compositional errors were 0.2316 and 0.2108 mole fraction R32). The experimental data and the predicted bubble and dew point curves are plotted in Figure F.2. From a visual inspection, the experimental and calculated pressures seem to agree quite well.

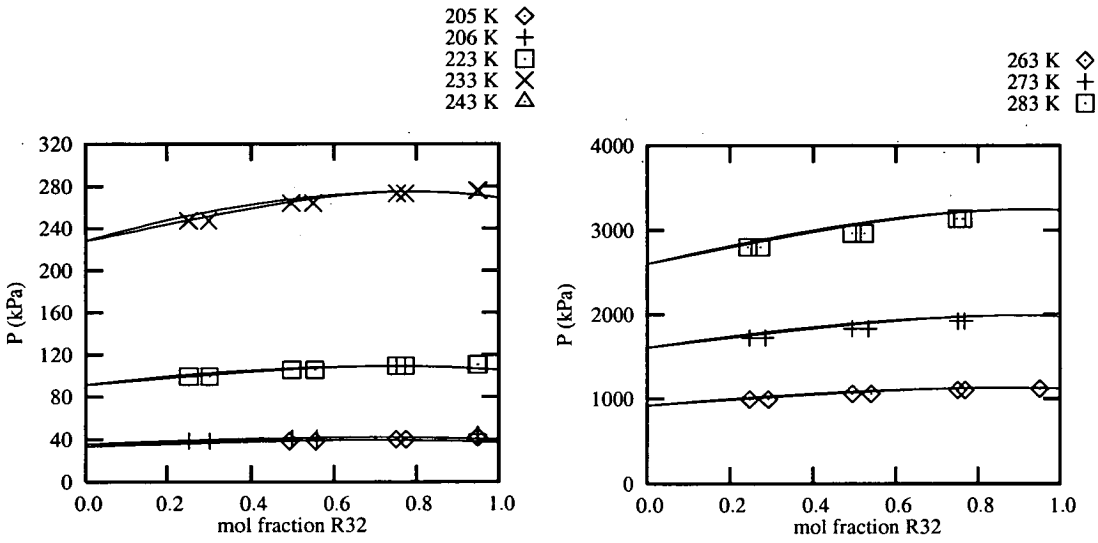

Figure F.2: CCOR calculated and experimental R32/R125 two phase VLE data of Nagel

However, the scale of the graphs masks the errors. Figure F.3 shows the CCOR predicted and the experimental data at 223K. The graph shows that the CCOR equation underpredicts both the liquid and the vapour composition. The error increases as the composition of R32 increases. The CCOR predicts an azeotrope at a composition of 0.73 mole fraction R32, at 223K. An azeotrope does occur at high

R32 compositions and low temperatures. However as can be seen from Figure F.3 the predicted pressure, after the azeotropic composition, decreases to a much greater extent than the actual reported pressure. With temperature and pressure fixed the CCOR flash algorithm could not converge on a solution and calculate the liquid and vapour composition because the experimental pressure lies outside the region for which convergence can be found. This occurred for much of the data with a liquid composition of 0.75 and 0.95 mole fraction of R32. Convergence was achieved for twenty two of the thirty four data points published. The 0.25 and 0.50 compositions made up the majority of points for which convergence was achieved.

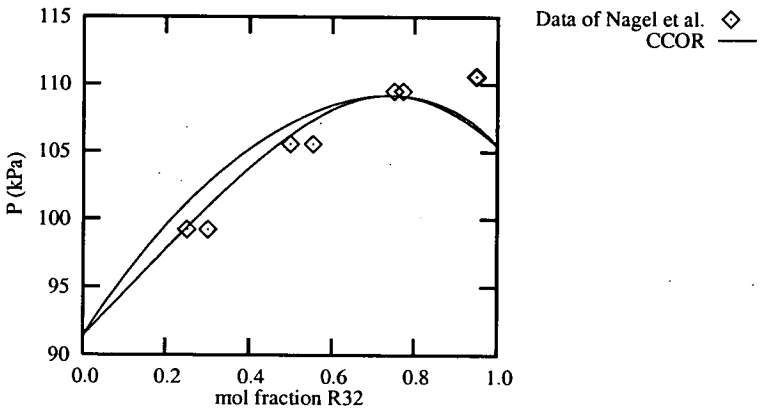

Figure F.3: CCOR calculated and experimental R32/R125 VLE data of Nagel at 223 K

R32/R134a System

As with the R32/R125 mixture the same, three authors examined the R32/R134a system. The data of Defibaugh et al. and Nagel et al. were taken from the same references as given for R32/R125. Widiatmo et al. [*1993*] also published data on this system. As with the previous system, Widiatmo and Defibaugh examined bubble point properties whilst Nagel tabulated VLE data for both liquid and vapour phases.

Widiatmo varied the temperature from 280K to 340K in intervals of 10K. Five compositions were considered: 20, 25, 40, 60 and 80 wt.% R32. Thirty data points were investigated in total. The bubble pressure and density predicted by the CCOR equation is shown in Figure F.4. The pressure AAD was 2.96% while the deviation for the density was 11.43%. The prediction of bubble pressure seems reasonable while the density prediction is not very good. The CSD equation of state showed an improved ability to predict the bubble point VLE of R32/R134a. The pressure error was 1.04% while the liquid density error was found to be 2.11%.

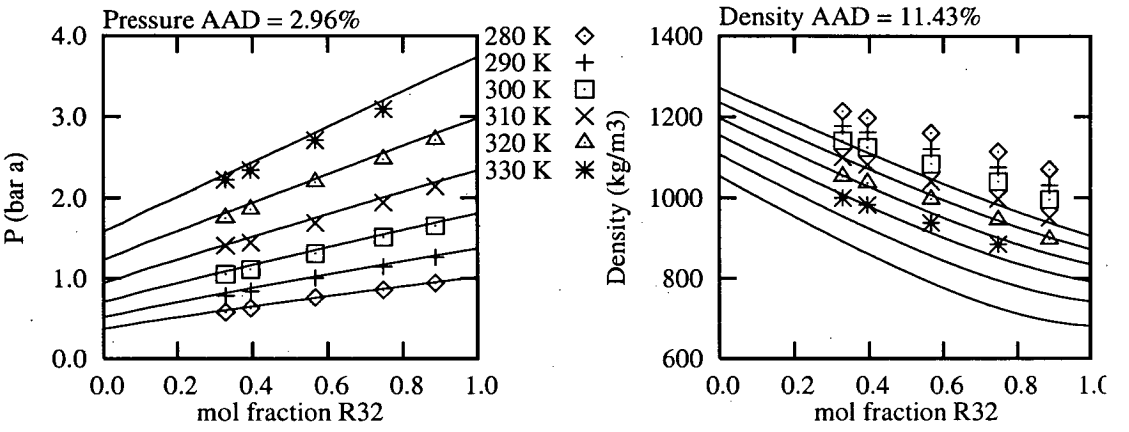

Figure F.4: CCOR calculated and experimental R32/R134a bubble point VLE data of Widiatmo

Two mixtures with compositions of 0.596 and 0.55 mole fraction R32 were investigated by Defibaugh over a temperature range of 252-358K. The AAD of the CCOR equation for the bubble pressure was 4.43%. This agrees with the AAD obtained, when the CCOR equation was compared to the data of Widiatmo. The CSD AAD of Defibaugh's data was found to be 2.74%.

Fifty data points were examined by Nagel. The VLE algorithm converged for 39 of the data points. The liquid phase composition error was 0.034 mole fraction R32. The corresponding average vapour deviation was 0.031 mole fraction. The composition

predictions would seem to be reasonable rather than extremely accurate. The pressure-composition curves for Nagel's data are plotted in Figure F.5. The CSD equation showed slightly smaller errors. The compositonal deviations were 0.0299 mole fraction R32 for the liquid and 0.0208 mole fraction for the vapour phase.

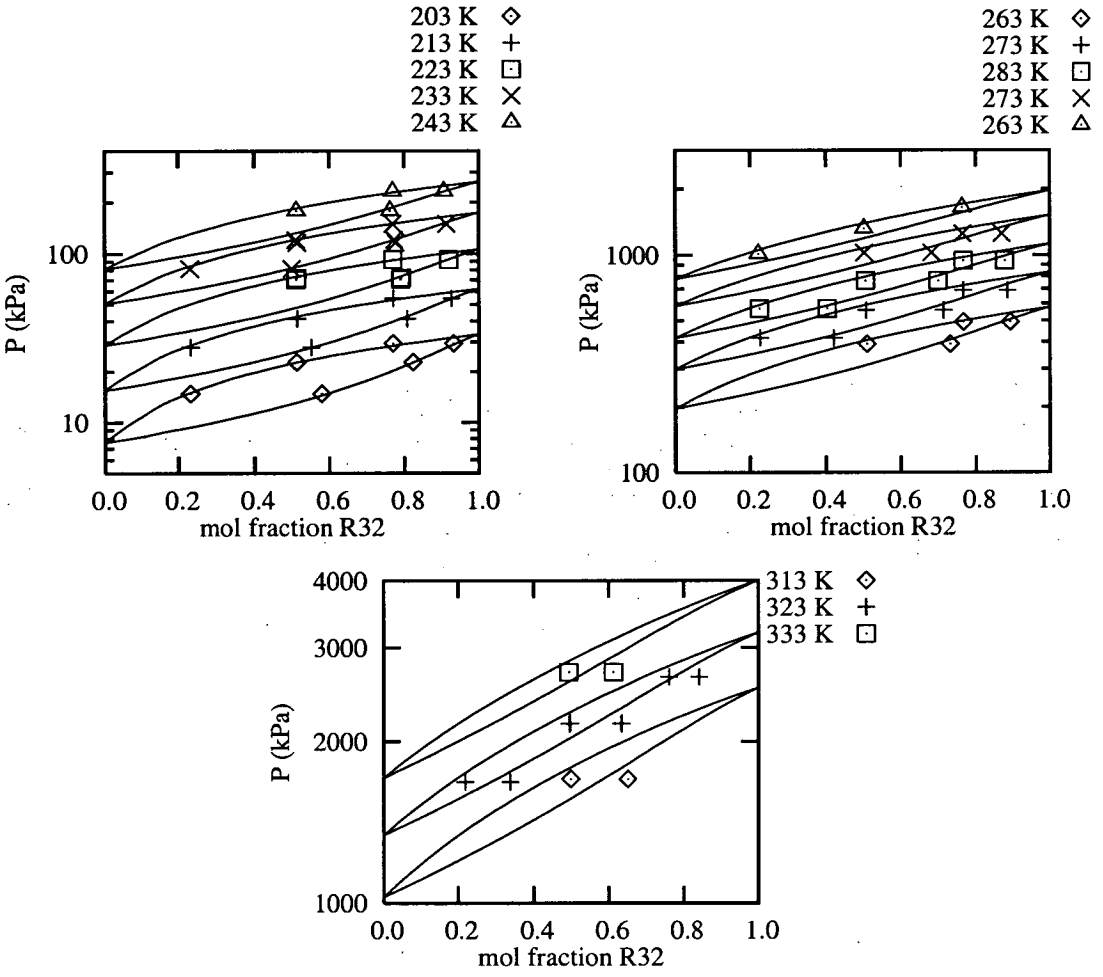

Figure F.5: CCOR calculated and experimental R32/R134a two phase VLE data of Nagel

R32/R152a System

The bubble point pressure of two R32/R152a mixtures were measured by Defibaugh et al. [*1959*]. The compositions considered were 0.498 and 0.5098 mole fraction R32. The temperature was varied from 248K to 358K in steps of 10K. The pressure AAD obtained from the CCOR was 3.30%. Given that the CCOR needs a comparatively small amount of data this would seem to be quite good prediction of the VLE behaviour of this mixture. CSD pressure AAD was of similar magnitude but more accurate. The pressure AAD was 2.74%. No density data was given.

R125/R134a System

Nagel published 31 two phase VLE experimental data points for the system R125/ R134a. Convergence was achieved for all 31 points. The composition errors were 0.014 and 0.022 mole fraction for the liquid and vapour phase respectively. This was felt to be a good prediction of the VLE of this mixture. The CSD liquid and vapour average errors were 0.0186 and 0.0195 mole fraction.

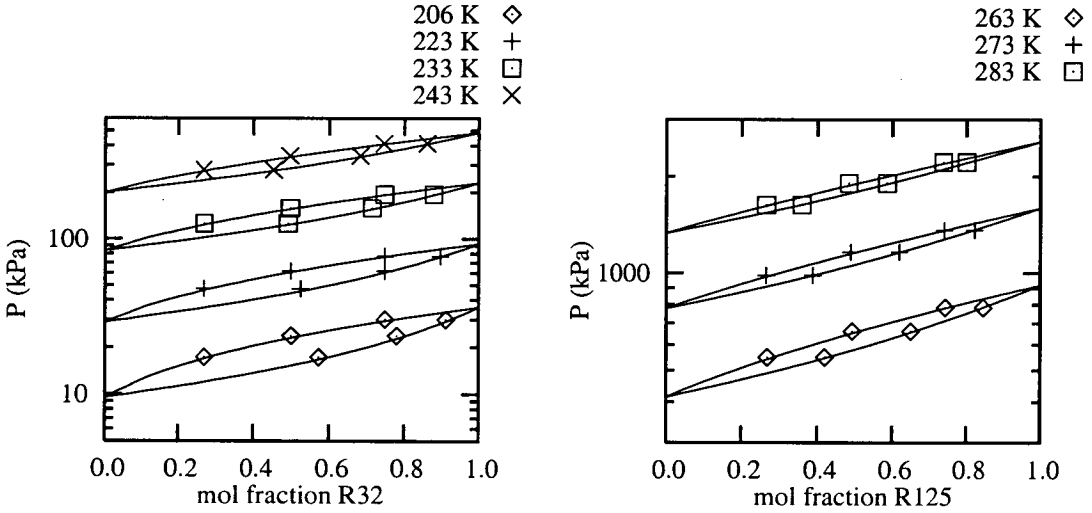

Figure F.6: CCOR calculated and experimental R125/R134a two phase VLE data of Nagel

Experimental and predicted data up to a temperature of 283K are plotted in Figure F.6.

R134a/R152a System

Defibaugh investigated the bubble point pressure of a 0.2231 mole fraction mixture of R134a/R152a over a temperature range of 248-268 K. The CCOR AAD achieved was 5.05% over all of the 13 points. The corresponding error for the CSD equation was 4.89%.

R152a/R134 System

Bubble pressure and density data of the binary pair R152a/R134 was published by Maezawa et al. [1991c] et al. in 1991. Mixtures with compositions of 20, 40, 60 and 80 wt.% R152a were examined over a temperature range of 280K- 380K.

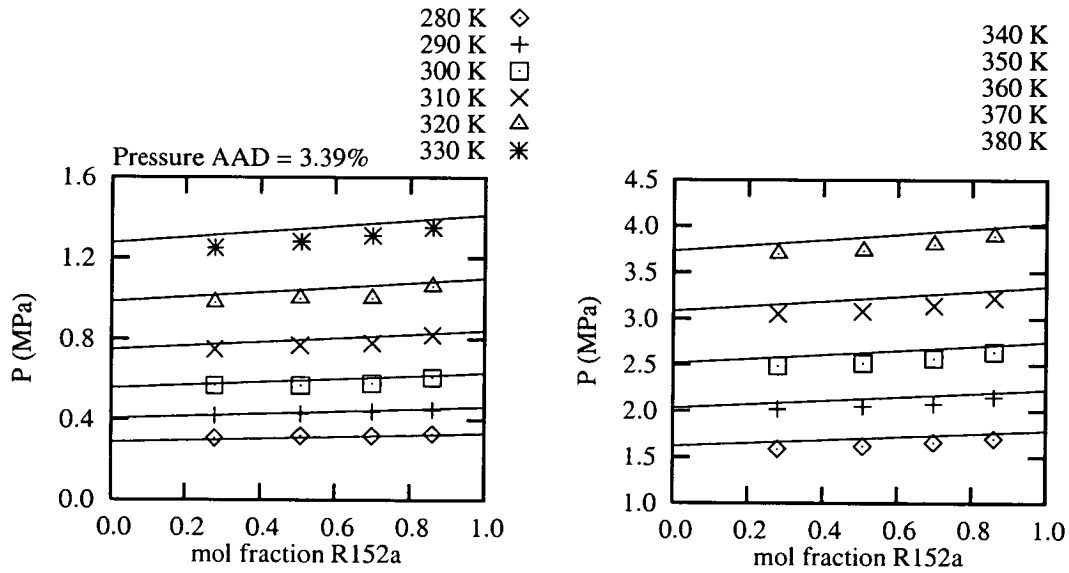

Figure F.7: CCOR calculated and experimental R152a/R134 bubble pressure VLE data of Maezawa

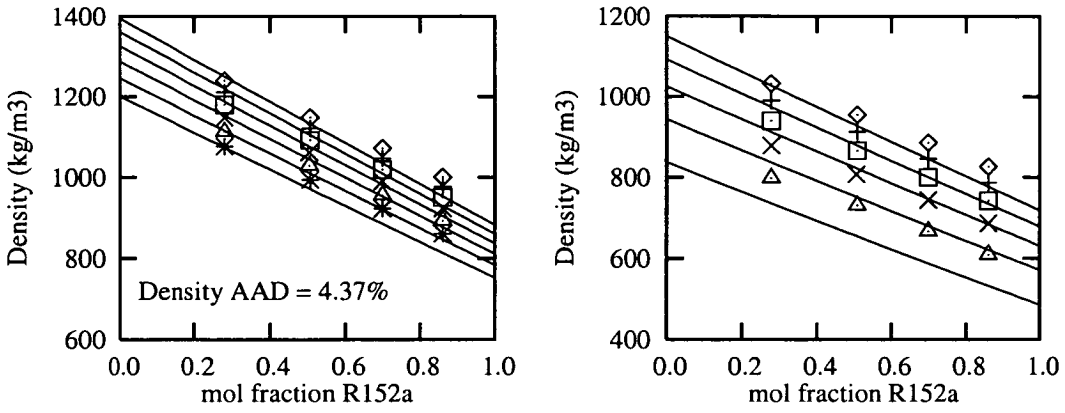

(Same key as in pressure-composition plots)

Figure F.8: CCOR calculated and experimental R152a/R134 bubble point VLE data of Maezawa

Forty eight separate points were tabulated in total. The pressure AAD was 3.39% while the corresponding deviation for the density was 4.37%. The CCOR agreed reasonably well with the measured pressures and densities. The CSD equation exhibited a much larger bubble pressure average error (12.43%). The liquid density error (4.03%) was slightly better than the CCOR error.

F.4.2.2 HFC/HCFC Mixtures

R22/R134a System

The vapour liquid equilibrium compositions of an R22/R134a mixture were measured by Arito et al. [*1991*] et al. The compositions of both phases were measured at 273, 298 and 323K. The average deviations for the compositions are 0.025 mole fraction for the liquid phase and 0.022 for the vapour phase. Six of the total of twenty data points dealt with pure components. These were not used in this analysis. Hence 14 tabulated points were compared with the CCOR equation of state. The CSD

prediction showed a liquid compositonal error of 0.0368 mole fraction whilst the vapour error was 0.0335.

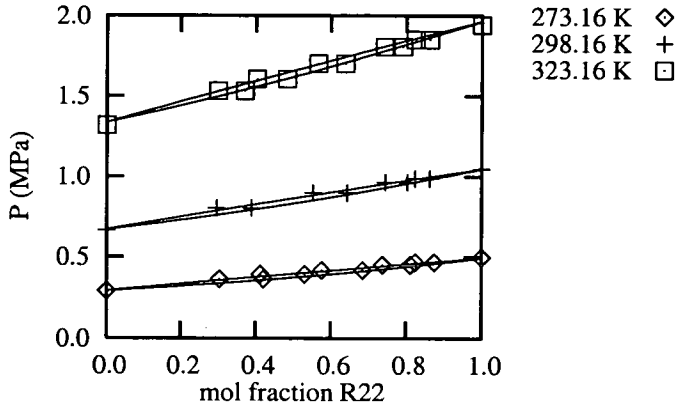

Figure F.9: CCOR calculated and experimental R22/ R134a two phase VLE data of Arita

R22/R152a System

This particular system was investigated by both Maezawa et al. [*1991a*] and Ström et al. [*1993*]. As with previous reported bubble point data Maezawa recorded the pressure and density of 5 compositions: 10, 30, 50, 70 and 90 wt.% R22. Temperature was measured over a range of 280-380K. Sixty six points were reported in total and all were compared against the CCOR equation. The pressure AAD was found to be 4.58% while the density AAD achieved was 6.73%. The experimental and predicted values are shown in Figure F.10. The CSD showed a better ability to predict the VLE of this particular refrigerant pair. The average error for pressure and density were 2.37% and 1.74% respectively.

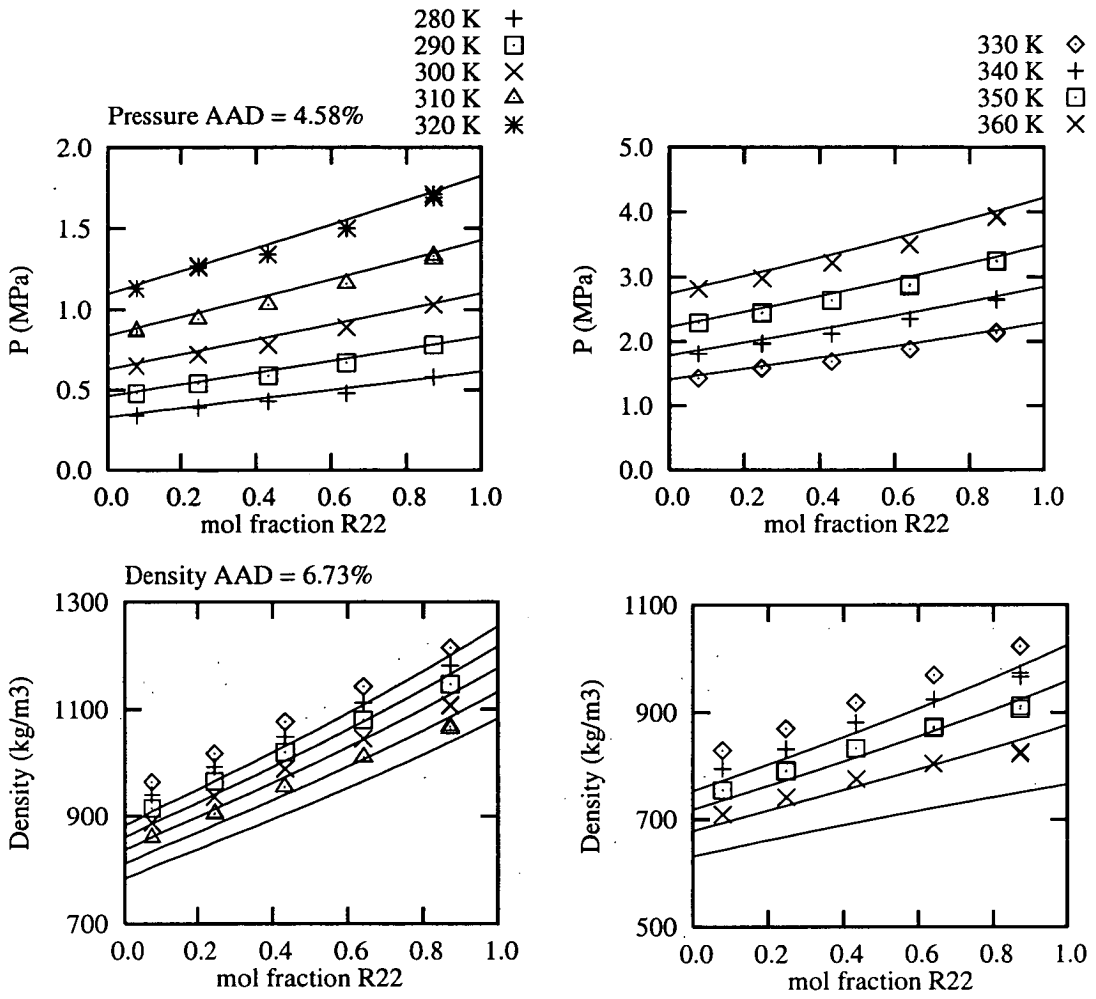

Figure F.10: CCOR calculated and experimental R22/R152a bubble point VLE data of Maezawa

Ström recorded the liquid and vapour compositions of the R22/R152a system at three separate constant pressures: 0.9, 1.47 and 1.8MPa. The average composition errors across all 46 reported data points was 0.104 for the liquid composition and 0.102 for the vapour phase. This seems to be a poor prediction of the phase compositions. There was a certain amount of scatter in the reported data as can be seen from Figure F.11., where all three sets of "constant" pressure data are shown.

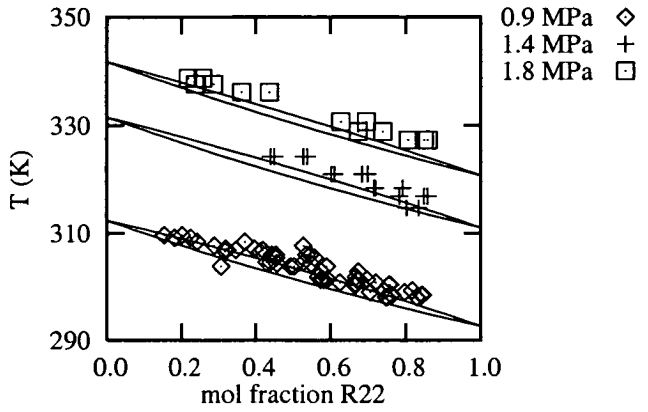

Figure F.11: CCOR calculated and experimental R22/R152a two phase VLE data of Ström

However, the pressure was not kept constant. For example the highest pressure varied from 1.808MPa to 1.889MPa. The CSD errors were similar in magnitude. The liquid average error was found to be 0.095 while the vapour error was 0.0829 mole fraction R22.

R134a/R141b System

Zheng et al. [*1990*] investigated the vapour liquid equilibria of the binary mixture R134a/R141b. The vapour and liquid compositions of thirty eight individual experimental points were recorded. The temperatures at which the compositions were measured were 5°C, 15°C, 30°C, 45°C and 60°C. The CCOR algorithm was successful in supplying calculated compositions for all of the pressures and temperatures. The average composition deviations were 0.076 mole fraction for the liquid phase and 0.051 for the vapour phase. The experimental data and the CCOR predicted pressures are shown in Figure F.12.

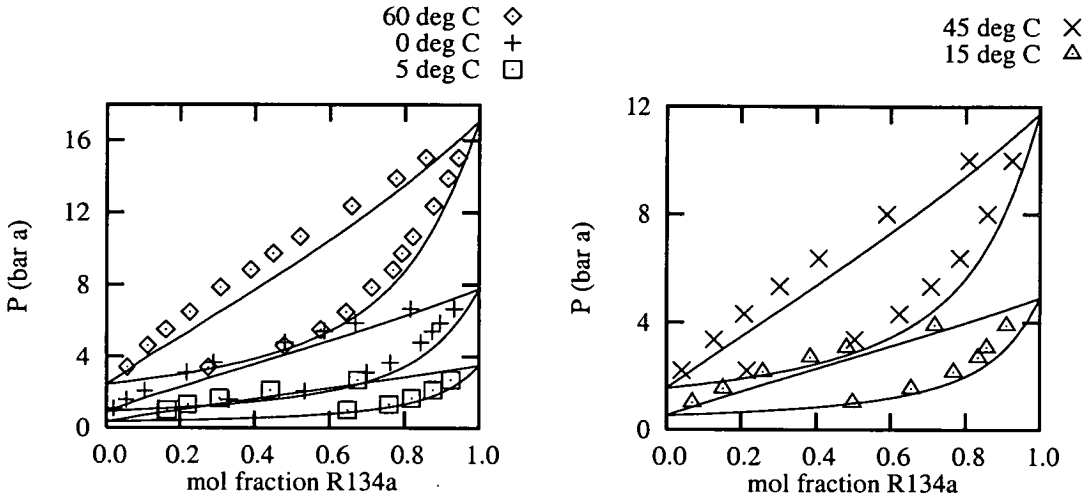

Figure F.12: CCOR calculated and experimental R134a/ R141b two phase VLE data of Zheng

When the CSD equation of state was compared to the experimental data the average errors for the composition were found to be 0.0786 mole fraction for the liquid phase and 0.0583 for the vapour phase.

R152a/R142b System

The bubble point properties of an R152a/R142b mixture were experimentally measured by Maezawa et al. [*1991b*]. The liquid compositions examined were 20, 40, 60 and 80 wt.% while the temperature was varied from 280 K to 400K in intervals of 10K. The CCOR algorithm converged for 44 of the 48 published data points. For temperatures of 390 K and above the VLE algorithm would not converge. The bubble pressure AAD was 2.96% and the density AAD was found to be 5.54%. These deviations are consistent with values obtained for other refrigerant mixtures. Figure F.13 shows the predicted and reported pressures and densities. The CSD

equation demonstrated a much poorer ability to predict the VLE of R152a/R142b. The pressure AAD was 17.13% while the liquid density error was 18.79%.

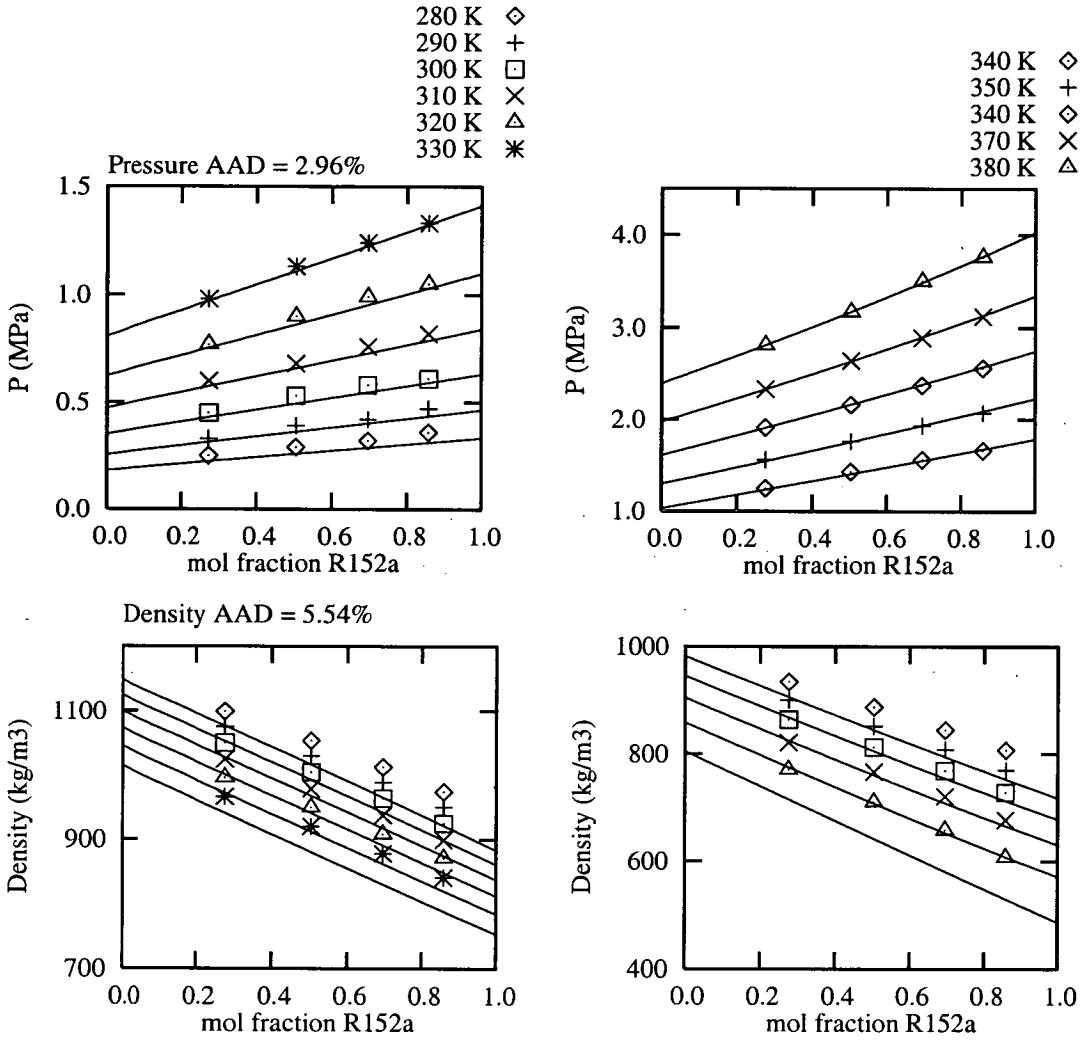

Figure F.13: CCOR calculated and experimental R152a/ R142b bubble point VLE data of Maezawa

F.4.2.3 Summary of Results

The overall average errors calculated in the comparisons of and Section F.4.2.2 are tabulated below. Table F.1 shows the results for bubble point data while in Table F.2 data relating to phase compositions are given. A more detailed analysis is given in Section E.2.1 on page 271 in Appendix E, where the error associated with each refrigerant pair is detailed. The overall grand average deviations have been calculated across all of the binary pairs examined in this study. As mentioned previously not all of the published points were modelled. Some of the data were quite close to the critical temperature of the more volatile component. The algorithm used with both equations of state failed to converge near the critical point of the more volatile component.

Table F.1: Overall AADs for bubble point data with interaction constants set to zero

Equation of State	Pressure Points Published	Pressure Points Modelled	Pressure AAD %	Density Points Published	Density Points Modelled	Density AAD %
CCOR	289	273	3.61	216	211	6.72
CSD	289	280	6.21	216	203	5.84

Table F.2: Overall composition errors for two phase data with interaction constants set to zero

Equation of State	Points Published	Points Modelled	Liquid Deviation (mole fraction)	Vapour Deviation (mole fraction)
CCOR	219	181	0.0734	0.0657
CSD	219	213	0.0827	0.0710

The overall average bubble pressure deviation for the CCOR equation was found to be 3.62% and the average deviation for density was 6.21%. The corresponding overall errors for the CSD equation were 6.21% and 5.84%. Given that the CCOR equation

requires a small amount of data to determine the thermodynamic properties, the average deviation for bubble pressure would seem to be quite good. All of the pressure AADs are in the 2-5% range. No refrigerant had an average AAD far removed from this range. The effectiveness of the CCOR equation can be seen in the fact that it was able to predict bubble pressures to a greater accuracy than the CSD equation from a much smaller amount of information of the components of the mixture. The CSD equation performed better in predicting bubble densities. However the CCOR error is of a similar magnitude as that for the CSD equation. It is interesting to note that the prediction of mixture liquid density by the CCOR equation seems to be superior than the predictions for pure fluids, which have an overall error of 8.6% (Section E.1.4.5 on page 269 of Appendix E). With an average error of 0.0344 mole fraction, prediction of vapour composition was reasonable but not exceptional. An average error in the range 0.0-0.02 would be more acceptable. The liquid error was relatively large (0.0736 mole fraction). There was more scatter in the errors associated with composition prediction. The largest errors were associated with the mixtures R32/R125 and R125/R134a. Overall the CCOR equation provided more accurate predictions of composition than the CSD equation. In summary with the interaction constants set to zero the CCOR equation gave more reliable predictions than the CSD equation even though it required less data to describe a particular mixture.

From the comparison of experimental and predicted VLE data, it seems that the CCOR equation can predict the VLE properties of non-ozone depleting refrigerant mixtures with a reasonable degree of accuracy. The predictions were not exceptionally accurate, but given that only the critical temperature, critical pressure and acentric factor are needed the predictions were quite satisfactory. It would not be recommended to use the CCOR equation to supply high-accuracy thermodynamic data for refrigerant mixtures. It would be more appropriate to use it to provide initial thermodynamic data on a new refrigerant mixture. At the initial examination of a new refrigerant calculated thermodynamic data need not necessarily be exceptional. If

VLE data for a proposed experimental mixture were required, and the data did not need to be extremely accurate then the CCOR equation would be a valid method of providing the initial estimates of the VLE data. The CCOR provides a means of generating reasonably accurate refrigerant VLE data, without requiring a large body of knowledge of the fluids in question.

F.5 Optimisation of Interaction Constants

The comparison of calculated VLE data with experimental data in Section F.4.2 was carried out with the interaction constants of both equations of state set to zero. Following on from this, it was decided to determine the improvement in VLE prediction by the use of optimum interaction constants. With an R22/R11 mixture Low [*1991*] located a non-zero optimum pair of values for the CCOR equation. These improved the VLE prediction of the R22/R11 mixture. Optimum interaction constants were found by minimising the error between experimental and predicted data. An objective function composed of the sum of the square of the error between predicted and experimental data was utilised. The objective function was then minimised. Two different objective functions were used to reflect the two formats in which the refrigerant experimental VLE data was published in the literature. Equation F.10 was the objective function used in conjunction with bubble point data.

$$F_{min} = \sum_{i=1}^{N} w_P \varepsilon_{p_i}^2 + w_\rho \varepsilon_{\rho_i}^2 \qquad \text{(Eq F.10)}$$

$$\varepsilon_{p_i} = \frac{P_{experiment_i} - P_{calculated_i}}{P_{experiment_i}} \qquad \text{(Eq F.11)}$$

$$\varepsilon_{\rho_i} = \frac{\rho_{experiment_i} - \rho_{calculated_i}}{\rho_{experiment_i}} \qquad \text{(Eq F.12)}$$

It is composed of the sum of the square of the pressure and density error. The terms w_p and w_ρ are the relative weighting given to each property. P and ρ refer to the bubble pressure and liquid phase density respectively. N represents the total number of experimental data points used, in the optimisation.

A similar objective function was used when experimental HFC refrigerant data was expressed in the two phase format. The terms x and y represent the liquid and vapour compositions as usual. The minimisation for both objective functions was achieved by using Powell's method as described by Press et al. [*1992*].

$$F_{min} = \sum_{i=1}^{N} w_x \varepsilon_{x_i}^2 + w_y \varepsilon_{y_i}^2 \qquad \text{(Eq F.13)}$$

$$\varepsilon_{x_i} = \frac{x_{experiment_i} - x_{calculated_i}}{x_{experiment_i}} \qquad \text{(Eq F.14)}$$

$$\varepsilon_{y_i} = \frac{y_{experiment_i} - y_{calculated_i}}{y_{experimant_i}} \qquad \text{(Eq F.15)}$$

F.5.1 Effect of the Interaction Constants

Before attempting to locate optimum interaction constants, it is instructive to show how the bubble pressure, bubble density and calculated composition vary with k_a and k_c (regarding the CCOR equation). Figure F.14 shows how the R32/R134a bubble pressure and density vary with k_a. The temperature is 20°C and k_c has been set to zero. As the values of k_a increases, at constant k_c, the bubble point pressure increases and the liquid density decreases. Although not shown here, both the dew point pressure and vapour density are increased as the value of k_a increases.

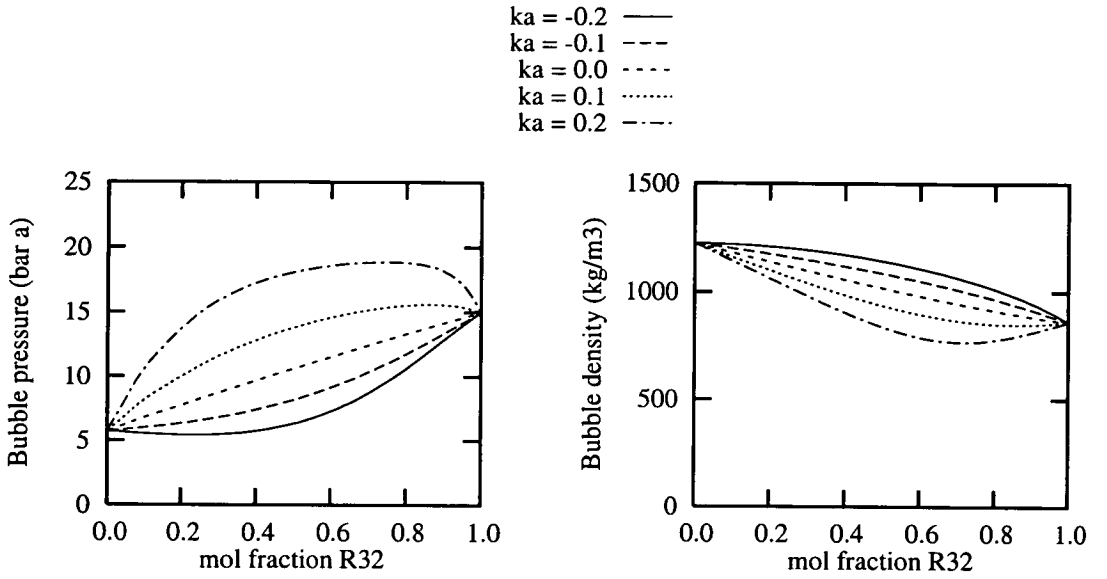

Figure F.14: Variation in R32/R134a bubble pressure and density with k_a (k_c = 0.0)

The k_c interaction constant has the opposite effect (Figure F.15). The bubble pressure decreases and the liquid density increases with increasing k_c.

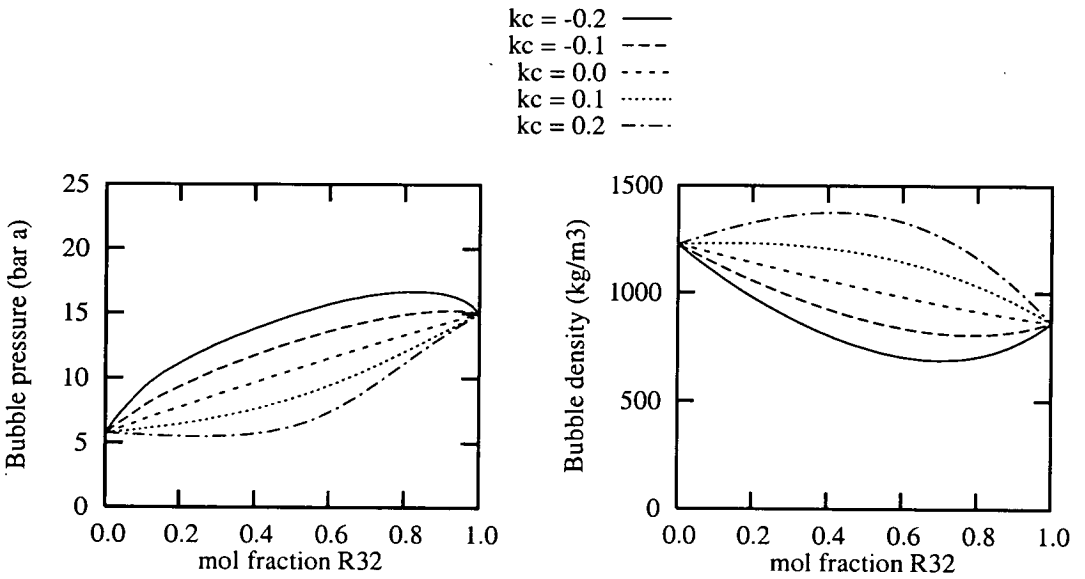

Figure F.15: Variation in R32/R134a bubble pressure and density with k_c (k_a = 0.0)

This is displayed for the R32/R134a pair with k_a set to a value of zero. Increasing values of k_c reduces the dew point pressure and vapour density. Figure F.16 and Figure F.17 show the variation in vapour equilibrium composition with k_a and k_c respectively. Again R32/R134a is the mixture used.

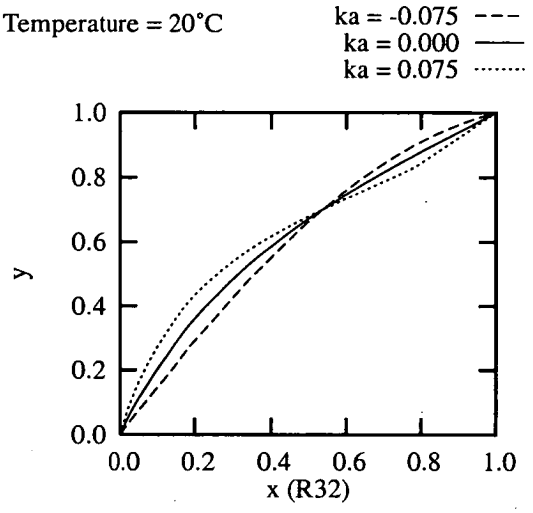

Figure F.16: Variation in composition with k_a (k_c=0.0)

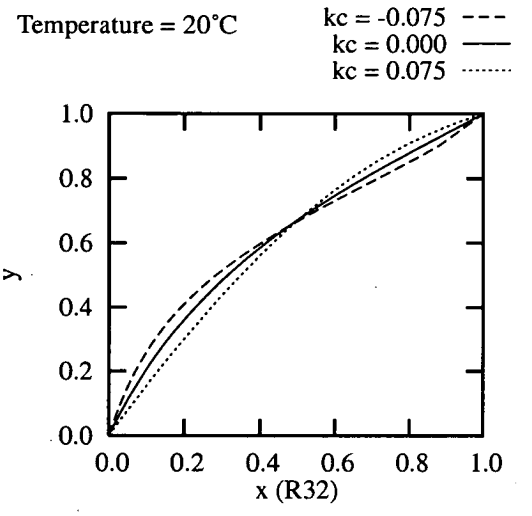

Figure F.17: Variation in composition with k_c (k_a=0.0)

Below a liquid composition of 0.5 mole fraction increasing k_a causes the vapour composition to increases. Above 0.5 liquid mole fraction of R32 the opposite occurs. As k_a gets larger, the vapour composition reduces. From Figure F.17 it can be seen that k_c has the opposite to k_a above and below the equimolar point. Below 0.5 mole fraction the vapour composition is reduced as k_c increases; above the equimolar point the vapour composition increases. The parameters k_a and k_c change the shape of the equilibrium curve in opposite ways. Increasing k_a causes the equilibrium curve to rotate clock wise about a point near the equimolar point while increasing k_c causes a rotation in the opposite direction.

Table F.3 shows the bubble pressure and density overall AAD for the R32/R134a data of Widiatmo et al. [*1994a*], at regular values of k_a and k_c. In each column the pressure AAD is on the right whilst the density AAD is on the left hand side. By inspection it can be seen that the smallest average error occurs when both k_a and k_c are both near a value of 0.1. The error is at a minimum near this point. In fact the optimum value has been located at $k_a = 0.0738$ and $k_c = 0.1061$ (Table E.26 on page 273).

Table F.3: Percentage AADs of CCOR predictions of Widiatmo's R32/R134a VLE data with k_a and k_c varied

k_c	k_a = -0.2		k_a = -0.1		k_a = 0.0		k_a = 0.1		k_a = 0.2	
	Pres.	Den.	Pres.	Den.	Pres.	Den.	Pres.	Den.	Pres.	Den.
-0.2	7.0	21.5	18.2	10.8	28.8	3.3	58.7	24.2	(-)	(-)
-0.1	14.3	29.0	2.1	17.2	15.3	4.7	27.6	9.4	66.6	31.1
0.0	38.0	33.3	13.0	5.1	3.0	11.4	13.0	5.1	27.5	19.8
0.1	48.2	34.4	46.9	28.8	30.0	20.1	7.3	3.5	12.3	14.7
0.2	51.1	33.1	55.0	30.7	52.6	24.4	36.8	12.5	9.9	9.9

Two different types of optimisation were performed. In the first case a single optimum value of k_a and k_c was found for *each set* of published experimental data. Results for this examination are given in Section F.5.2. Using these optimum values calculated VLE data was then compared to the experimental data in a similar manner to that employed in Section F.4. Average absolute deviations were reported for bubble pressure and density. Average compositonal errors were calculated for two phase data according to Equation F.9 on 282. Similarly an optimum interaction constant (k_a) was calculated for the Carnahan-Starling-DeSantis equation of state for each set of data.

In the second case optimum interaction constants were calculated for *each data point* in a published set. The effects of temperature and composition on the interaction constants could be ascertained. Section F.5.3 gives the results of this treatment.

F.5.2 Optimisation of Interaction Constants for Each Set of Experimental VLE Data

The optimisation routine as applied to each *set* of published mixture data i.e. for the CCOR equation an optimum value was calculated for k_a and k_c for each set of data. An improvement in vapour liquid equilibrium prediction was noted. The overall average errors are given in Table F.4 and Table F.5 below:

Table F.4: Bubble point data AADs with interaction constants optimised for each published data set

Equation of State	Pressure Points Published	Pressure Points Modelled	Pressure AAD %	Density Points Published	Density Points Modelled	Density AAD %
CCOR	289	238	1.38	216	173	2.32
CSD	289	268	1.30	216	176	3.02

Errors for each individual dataset are tabulated in Section E.2.2.1 on page 273. The values of the optimum interaction constants, for both equations of state, are also given. Comparing the overall AADs when zero interaction constants were used (Table F.1 and Table F.2) with the deviations when optimum interactions were used, it is apparent that the application of optimised interaction constants improves the fit for both equations of state. The CCOR overall average error for bubble prediction decreased from 3.62% to 1.38%. The improvement for the CSD equation was greater with the corresponding error being reduced from 6.72% to 1.30%.

Table F.5: Two phase data composition deviations with interaction constants optimised for each published data set

Equation of State	Points Published	Points Modelled	Liquid Deviation (mole fraction)	Vapour Deviation (mole fraction)
CCOR	219	170	0.0162	0.0295
CSD	219	201	0.0359	0.0374

The CSD prediction of mixture data for the pairs R152a/R134 and R152a/R142b were substantially improved. The liquid density prediction for the CCOR equation was better than that for the CSD equation. Presumably this is because of the inherent flexibility of the use of two interaction constants with the CCOR equation. Vapour and liquid CCOR composition predictions were more accurate when optimum interaction constants were used. For the liquid phase, the average deviation with k_a and k_c set to zero was 0.070, where as with optimum values the error was found to be 0.01862 mole fraction. With optimised constants, the CCOR equation was found to be predict composition VLE data more accurately than the CSD equation of state. Both equations show an reduction of error of approximately 50% when optimum interaction constants were used.

Optimum values of k_a for the CCOR equation, calculated with bubble point VLE data, had values in the range -0.05 to 0.07. The values for k_c were also in this range (Section E.2.2.1). Optimum values of k_a for the CSD equation tended to be smaller and negative. As an example of the improvement in fit, Figure F.18 shows experimental VLE data for R134a/R141b at 45°C as reported by Zheng et al. [*1990*].

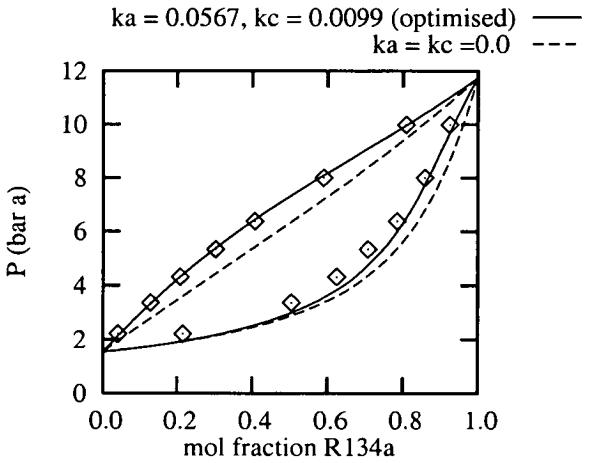

Figure F.18: Optimised and non-optimised R134a/R141b CCOR predictions at 45°C

The CCOR prediction, with k_a and k_c set to zero, is represented by the dashed line. The continuous line denotes predicted bubble and dew pressures calculated using optimum values of k_a and k_c (0.05675 & 0.00988 respectively). The improvement in the fit is apparent from the diagram. The positive value of k_a increases the bubble pressure to closely match the experimental data.

Attempts were made to ascertain if the optimum interaction constants could be correlated with some physical properties of the refrigerants. Morrison and McLinden [*1993*] noted a correlation between the interaction constant and the difference in the ratio of the dipole moment to the cube root of the excluded molecular volume ($\Delta(\mu/b^{1/3})$). Figure F.19 shows the optimum CCOR k_a value plotted against $\Delta(\mu/b^{1/3})$. There does not appear to be any strong relationship for k_a values used with the CCOR equation of state. Attempting a linear regression led to an r^2 value of 0.0052 indicating no apparent linear relationship. Similar attempts were made with k_a of the CSD equation of state. A similar lack of success resulted.

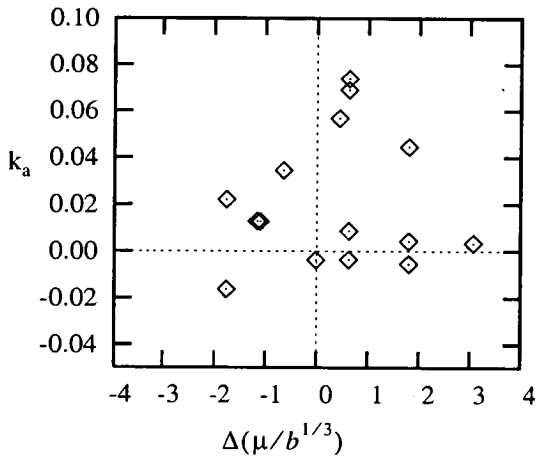

Figure F.19: Optimum k_a values vs. $\Delta(\mu/b^{1/3})$

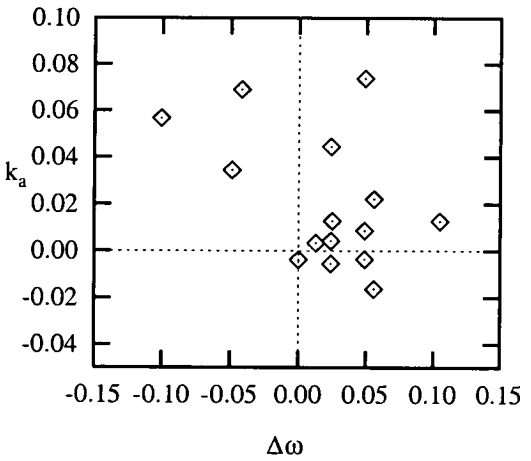

Figure F.20: Optimum k_a vs. acentric factor difference

The optimum k_a values were also plotted against the acentric factor difference. (Figure F.20). The r^2 value in this case was found to be 0.22. This is slightly better than that for the dipole moment factor difference but does not indicate any linear the relationship between acentric factor difference and the optimum value of k_a. For optimum values of k_c the r^2 value was 0.002 showing no relationship between acentric factor difference and the optimum k_c value.

F.5.3 Optimisation of Interactions Constants for Each Experimental VLE Datapoint

In the previous section optimum interaction constant values were found for each dataset (for both equations of state). In this section optimum interaction constants were found for *every point* in a given dataset i.e. in Widiatmo's R32/R134a bubble point data there are 30 individual datapoints and hence 30 values for both k_a and k_c were calculated. Since two interaction constants are associated with the CCOR equation of state, it should be theoretically possible to force the error to zero for each point. The same would not necessarily be possible with the CSD equation since it only has one interaction constant (k_a) associated with the parameter a. In fact with bubble pressure and density data the CCOR error was forced to a very small value. (Typically of the order of 10^{-7}%). The application of two interaction parameters with the CCOR equation added an extra degree of freedom which allows an excellent fit to each datapoint.

Table F.6: Bubble point data AADs with optimum interaction constants optimised for each datapoint.

Equation of State	Pressure Points Published	Pressure Points Modelled	Pressure AAD %	Density Points Published	Density Points Modelled	Density AAD %
CCOR	289	258	0.00	216	195	0.00
CSD	289	263	0.49	216	191	2.70

A residual error remained for the CSD because only one interaction constant was used. Table F.6 shows the overall errors across data describing bubble point VLE behaviour. The average error associated with each dataset can be found in Section E.2.3 on page 275 in Appendix E. The pressure error associate with the CSD is quite small at 0.49%; of a similar magnitude to the pure fluid vapour pressure error.

Table F.7: Two phase data composition deviations with interaction constants optimised for each datapoint

Equation of State	Points Published	Points Modelled	Liquid Deviation (mole fraction)	Vapour Deviation (mole fraction)
CCOR	219	158	0.00530	0.00910
CSD	219	212	0.00315	0.00848

Both equations of state show small non-zero errors for liquid and vapour composition. As can be seen from Figure F.16 and Figure F.17 the CCOR interaction constants have directly opposite effects upon high and low compositions. The effect of independently altering each interaction constant is not the same across the whole of the composition range. In order to force the error to zero, the liquid may require a positive value for k_a while the vapour composition requires a negative value. The optimal fit is located and a non negligible error results. This means that the error was not forced to zero, as in the case of bubble point data when optimising for k_a and k_c for each datapoint.

The interaction constants associated with the CCOR equation, that were calculated to force the error as close to zero as possible, were plotted against the reduced temperature of the more volatile component. The optimised parameters k_a and k_c were plotted against T_r, with composition used as a variable. These plots are shown in Appendix G on page 315 and are discussed below.

F.5.3.1 Bubble Point Data Plots of Optimised k_a and k_c (Excluding Data of Defibaugh)

Plots of the optimum value of k_a and k_c vs. reduced temperature of the m.v.c for bubble point VLE data are considered in this section. The HFC bubble point data of Defibaugh et al. [*1995*] is considered separately (Section F.5.3.2). In her data Defibaugh did not include liquid phase density, thus the value of w_ρ in Equation F.13 was set to zero. As a result, it was decided to consider this separately. Visual inspection of the plots of k_a and k_c vs. T_r for bubble point data (Figure G.1 to Figure G.5), suggest that k_a and k_c have a regular dependence on temperature and composition. Examining the graph of k_a vs. T_r for the R32/R125 pair (Figure G.1) it can be seen that at high composition (0.9 and 0.78 mole fraction R32) both k_a and k_c decrease linearly with increased temperature. At intermediate compositions (0.5 and 0.61 mole fraction R32) k_a and k_c are relatively independent of temperature. At the lowest compositions k_a increase slightly as the temperature increases. There is a remarkable similarity between the pattern for k_a and that for k_c. The values of k_c are slightly larger but the pattern is very similar.

The k_a & k_c vs T_r patterns for R32/R134a (Figure G.2) are quite similar to those found with R32/R125. As composition decreases from high m.v.c. to low the dependence on temperature decreases. At the lower compositions there is a certain amount of overlap between the k_a & k_c vs. T_r plots. The bubble point data for the pairs R22/R152a, R152a/R134 and R152a/R142b were also examined in the same manner and showed similar profiles. However, for each individual composition the profile is not as smooth or as linear as those for R32/R134a or R32/R125. For the other three refrigerant pairs the individual value of k_c for a given composition and temperature tended to be larger than the k_a value although the patterns for k_c are similar to those for k_a. Normally prediction of interaction parameters (based on *whole* sets of data) is hazardous and they tend not to follow such a discernable pattern.

The regular behaviour of k_a and k_c with temperature and composition could point towards a refinement of the interaction parameters. Instead of including a relatively simple (1-k_a) and (1-k_c) term in Equation F.2 and Equation F.4 respectively, it may be possible to replace these with an relationship which is dependent on temperature, composition and some other parameter such as size difference of the molecules or the difference in the dipole moment. This means adjusting or replacing the van Der Waals mixing rules by a more complex set of rules, but which can yield more accurate predictions of thermodynamic properties. Huron and Vidal [*1978*] proposed mixing rules which were based on the Gibbs energy at infinite pressure. These rules are applicable to simple cubic equations of state such as the Redlich-Kwong-Soave or the Peng-Robinson equation. Barolo et al. [*1995*] used a modified UNIFAC group contribution method to calculate activity coefficients at infinite pressure. In this method the properties of a mixture are derived from the subgroups in the molecules. These mixing rules were successfully applied to predict the VLE behaviour of various refrigerants. These mixing rules are more complex than the classical ones.

Developing similar mixing rules for the Cubic Chain-of-Rotators would be no easy task. The RKS and PR equations of state have two parameters whereas the CCOR equation has five. Any proposed mixing rules would need to undergo extensive and rigorous examination. This would mean comparing experimental and calculated thermodynamic properties across a range of substances, such as aromatics, alliphatics and polar substances. However, any putative rules could lead to improvements in the prediction of thermodynamic properties. There is scope for improvement in the prediction of liquid and vapour density. At the very least the phenomena in Figure G.1-Figure G.6 warrants further investigation. This may or may not lead to new mixing rules, but further examination should be carried out.

F.5.3.2 Bubble Point Data Plots of Optimised k_a and k_c From Data of Defibaugh

The bubble point data of Defibaugh et al. [*1995*] is examined separately in this section. Density data was not included and consequently a different objective function was used. Plots of optimised k_a and k_c are shown in Figure G.6-Figure G.9. Only bubble pressures were measured. Liquid density data was not given hence w_ρ in Equation F.13 was set to zero. The range of compositions was much narrower compared to the previous five sets of data. Only one composition was tabulated for R32/R125 and R134a/R152a. Two compositions were given for the two mixtures R32/R134a and R32/R152a (0.50 and 0.55 mole fraction R32 for the former and 0.50 and 0.51 mole fraction R32 for the latter). This made it more difficult to see a relationship between optimised k_a and k_c and the composition. With the mixtures R32/ R125, R32/R134a and R32/R152a k_a decreased with temperature. With the R134a/ R152a mixture k_a seemed independent of temperature. For all four pairs the value of optimised parameter k_c was very small; of the order of -10^{-5} to 10^{-5}. With R32/R125 and R134a/R152a k_c seemed to follow a regular function, with the exception of a few points. For the other two mixtures there did not seem to be an obvious discernable pattern in k_c.

For the mixtures R32/R125, R32/R134a and R32/R152a the bubble pressure was overpredicted when k_a and k_c were set to zero. Thus to achieve an accurate prediction the k_a parameter needed a negative value because this decrease the bubble pressure (Figure F.14 on page 301) hence the values of k_a for these mixtures are negative. Since an increase in k_c decreases the bubble pressure, and since there is no calculated density to be adjusted in the objective function, the k_c parameter is made redundant, hence the very small values obtained. With the R134a/R152a mixture the bubble pressure was underpredicted by the CCOR equation therefore the value of k_a is positive, in order to increase the pressure so it matches the experimental values a close as possible.

F.5.3.3 Two Phase Data Plots of Optimised k_a and k_c

There is far less regularity in the k_a and k_c vs. temperature plots for the two phase type data. A pattern relating k_a and k_c to T_r is far less apparent. The only exception to this seems to be the mixture R32/R134a. The points for k_a and k_c seem to fall along regular loci. With this pair the loci for the different compositions are quite close together, compared to the plots obtained for this pair with bubble point data. For the other pairs (R32/R125, R125/R134a, R22/R134a and R134a/R141b) the values of k_a and k_c seem more random. The relationship with temperature would appear to be stronger than that with composition. In the five plots, the value of k_c is very small, typically in the range -6×10^{-4} to 4×10^{-4} with the exception of two points concerning R32/R125. By varying k_a alone, the minimisation routines find the best fit without any need to substantially adjust k_c away from zero. The experimental VLE for the pair R134a/R141b was not given as a regular function of liquid composition. In Figure G.14 the points represent ranges of composition rather than specific compositions.

F.6 Summary and Conclusions

The following section summarises the work carried out by the author on the prediction of mixture thermodynamic properties. The CCOR equation's ability to predict the binary VLE of HFC and HFC/HCFC mixtures was examined. With zero interaction constants the CCOR equation was able to predict the VLE of most of the mixtures quite well. Bubble pressure, vapour and liquid composition were predicted to a greater degree of accuracy than the CSD equation of state. Bubble density predictions were slightly worse than those of the CSD equation. The CSD equation requires more information on the fluid it describes, yet the comparisons in this study show that it is not as good at predicting refrigerant VLE as the CCOR equation. The CSD equation of state has been used to calculate thermodynamic data in software

packages and in a number of refrigeration cycle simulations in the literature. The size of the errors found in this investigation suggest that the CCOR equation can be used to provide reasonably good estimates of binary VLE from a minimal amount of data. The comparisons carried out in this work indicate that the CCOR equation can provide competent, although not necessarily highly accurate, VLE data. At the initial stages of examining a new refrigerant mixture for its suitability for use in a refrigeration cycle, very accurate data would not be required. The CCOR equation can provide thermodynamic data of sufficient accuracy from sparse data that it could be used in the process of determining whether a new mixture possesses the necessary thermodynamic properties to enable the mixture to be used in a refrigeration cycle.

The ability of the both equations to predict VLE was improved by using interaction constants. Two were used in conjunction with the CCOR equation (k_a and k_c) and one (k_a) was used with the CSD equation. A set of optimum values were located for each set of published experimental data. Using the optimum interaction constants with both equations of state led to a better fit between calculated and experimental VLE data. Both equations showed almost identical reduction in prediction errors (≈50%). Attempts were made to correlate the optimum CCOR k_a interaction constants with the acentric factor difference of the two components in each mixture and also with the dipole moment difference. There did not appear to be any strong link between them.

Optimum values for the CCOR interaction constants k_a and k_c were found for *every* point in a given published set of experimental binary VLE. With experimental data describing bubble point pressure and density, the associated error was negligible. The interaction constants were plotted as functions of temperature. The constants derived from bubble pressure and density seemed to have a regular dependence on temperature and composition. This seemed to indicate that the Van Der Waals mixing rules, used with the CCOR equation, could be refined so that more accurate predictions of VLE data could be made. This would mean that the mixing rules would take account of temperature, composition and characteristic property differences

between the components of the mixture. The mixing rules would be more complex and larger. Replacement of the $(1\text{-}k_a)$ and $(1\text{-}k_c)$ terms in the mixing rules by more complex functions could yield more accurate VLE predictions. Determining these functions would not be an easy task. With bubble point data describing the pressure *only* and with data describing the VLE compositions of both phases the relationship between the interaction constants with temperature and composition seemed to be tenuous at best. Despite this, the apparent regular dependence of optimum values k_a and k_c located for each bubble pressure and density experimental data point upon temperature and composition, leads the author to conclude that there should be further investigation in order to determine if this dependence could be exploited so that more accurate VLE predictions could be made. The apparent regularity may only occur with the CCOR equation of state and these sets of data. Other sources of experimental VLE data should be examined to see if the phenomena reoccurs.

Appendix G

Plots of CCOR Optimised Interaction Constants vs. Temperature and Composition

Appendix G contains plots of optimised CCOR interaction constants (k_a and k_c). These are results obtained from the optimisation described in Section F.5.3 on page 307. The graphs show optimised interaction constants plotted against the reduced temperature of the more volatile component, with composition expressed as a parameter. The constants have been optimised from experimental HFC refrigerant vapour-liquid-equilibrium data. Both k_a and k_c are optimised for each datapoint in a given set of experimental VLE data. All the compositions are expressed in mole fraction.

Section G.1 displays k_a and k_c vs T_r plots for bubble point VLE data. The plots from the data of Defibaugh et al.[*1995*] is displayed separately in Section G.2 since liquid densities were not reported and a different objective function was used to calculate k_a and k_c. Plots from two phase data is displayed in Section G.3. The letter "X" in the legend in each graph signifies mole fraction i.e. "X R32 = 0.20" means the denoted point has a composition of 0.2 mole fraction R32.

G.1 Bubble Point Data Plots of k_a & k_c vs. T_r m.v.c.

R32/R125 (Data of Widiatimo et al. [*1993*])

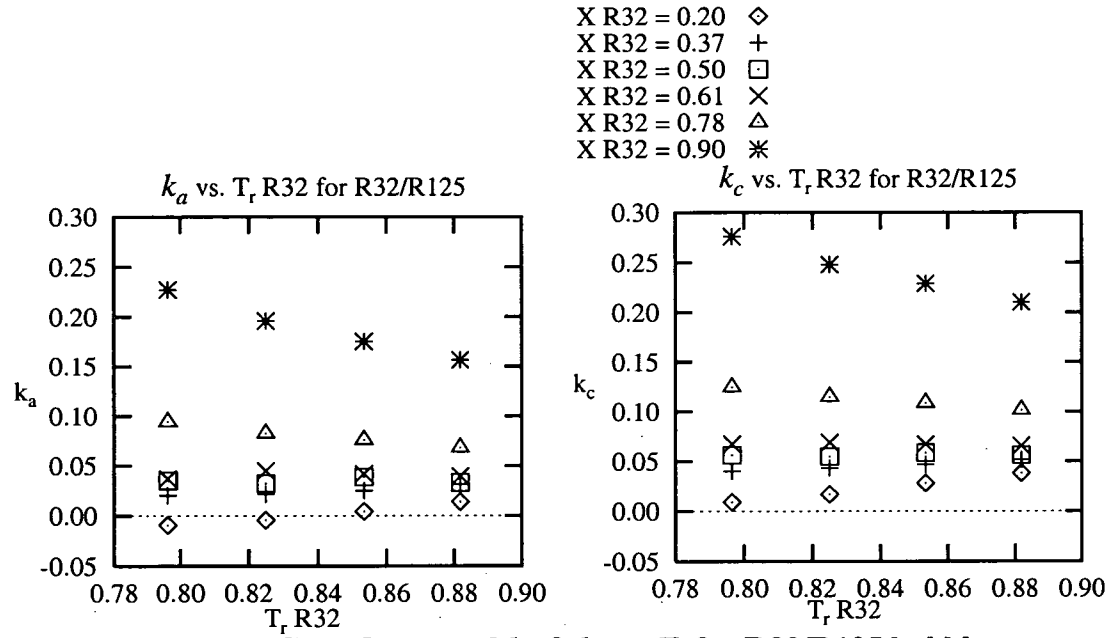

Figure G.1: Optimised k_a & k_c vs. T_r for R32/R125 bubble point VLE data

R32/R134a (Data of Widiatimo et al. [*1994a*])

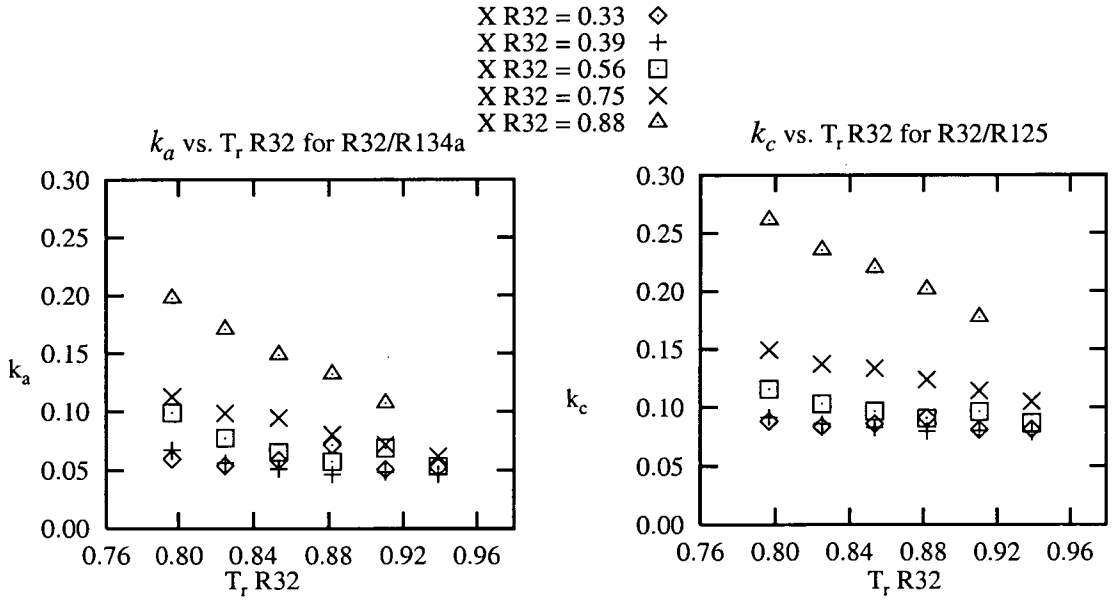

Figure G.2: Optimised k_a & k_c vs. T_r for R32/R134a bubble point VLE data

R22/R152a (Data of Maezawa et al. [*1991a*])

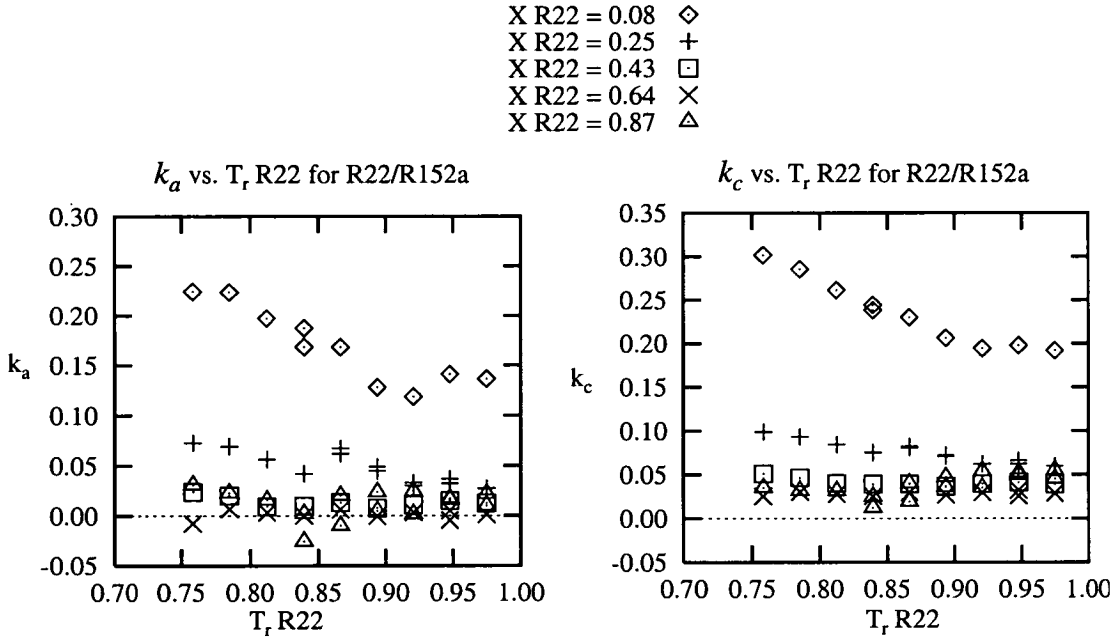

Figure G.3: Optimised k_a & k_c vs. T_r for R22/R152a bubble point VLE data

R152a/R134 (Data of Maezawa et al. [*1991c*])

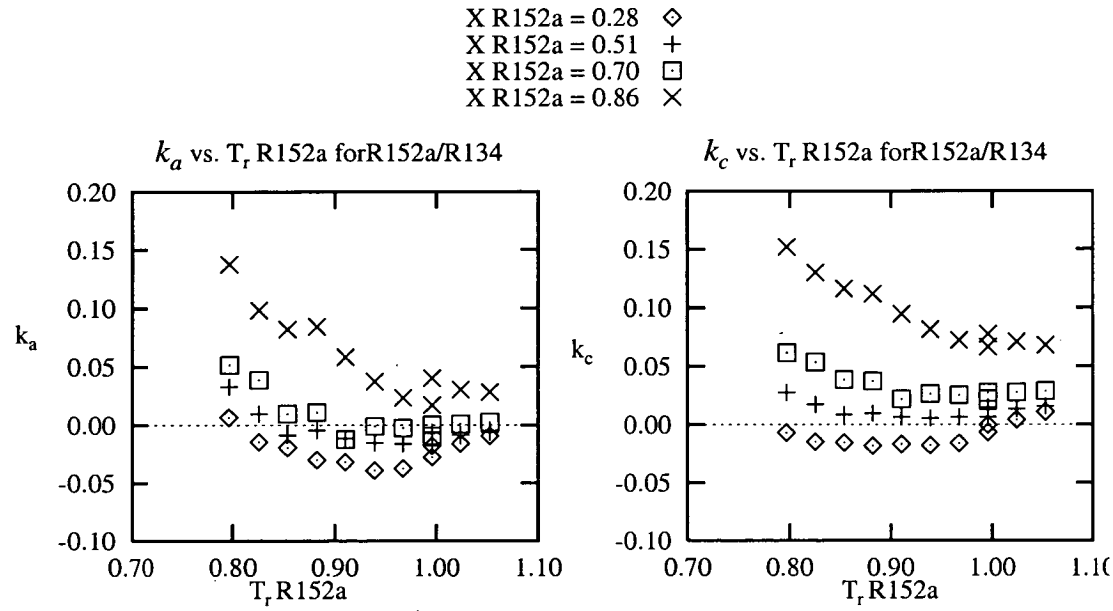

Figure G.4: Optimised k_a & k_c vs. T_r for R152a/R134 bubble point data

R152a/R142b (Data of Maezawa et al. [*1991b*])

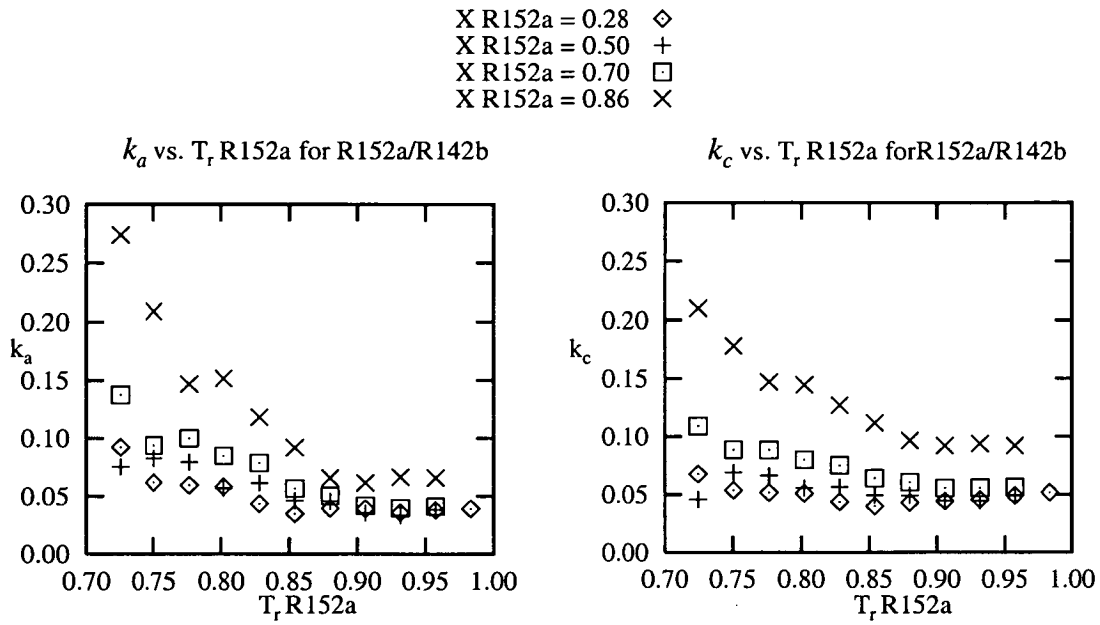

Figure G.5: Optimised k_a & k_c vs. T_r for R152a/R142b bubble point data

G.2 Bubble Point Data Plots of Defibaugh et al.

R32/R125

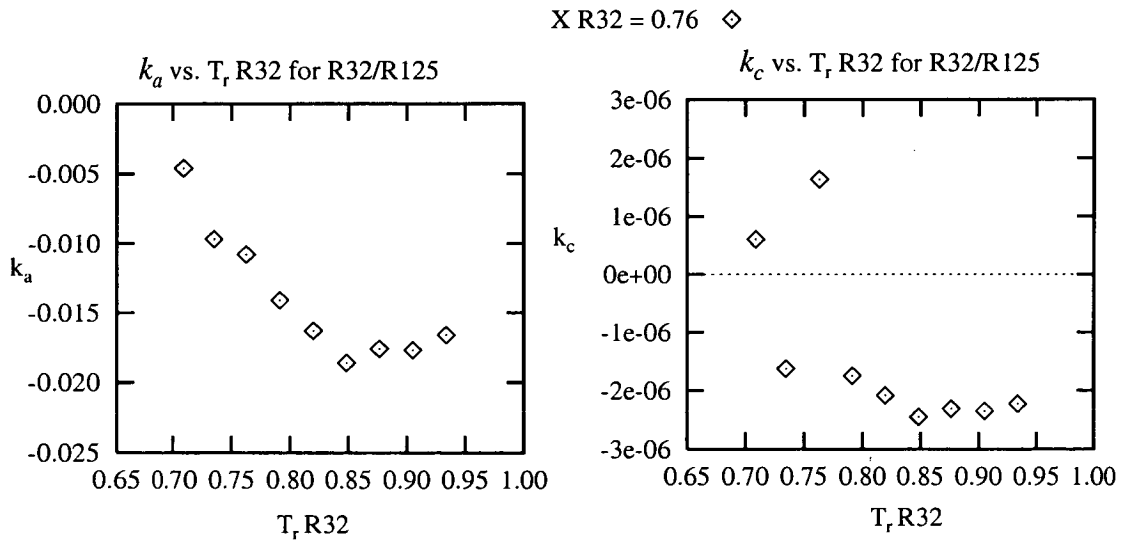

Figure G.6: Optimised k_a & k_c vs. T_r for R32/R125 data of Defibaugh

R32/R134a

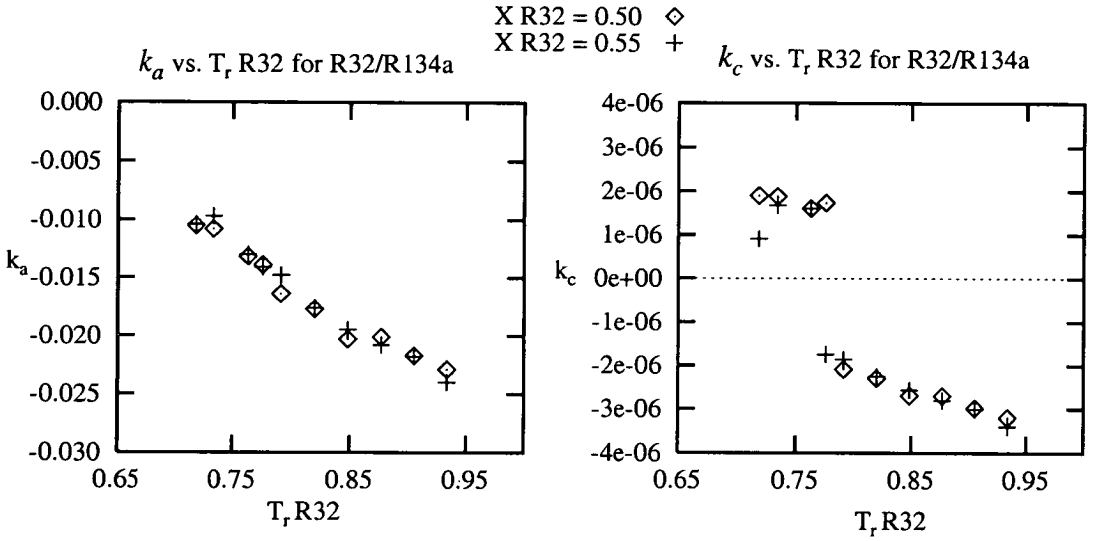

Figure G.7: Optimised k_a & k_c vs. T_r for R32/R134a data of Defibaugh

R32/R152a

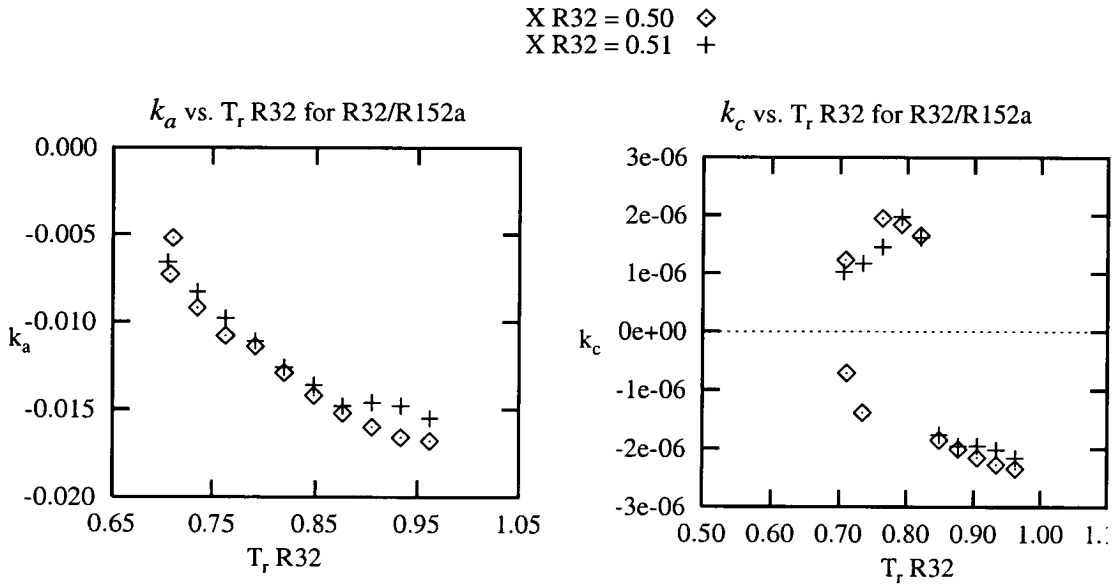

Figure G.8: Optimised k_a & k_c vs. T_r for R32/R152a bubble point VLE data

R134a/R152a

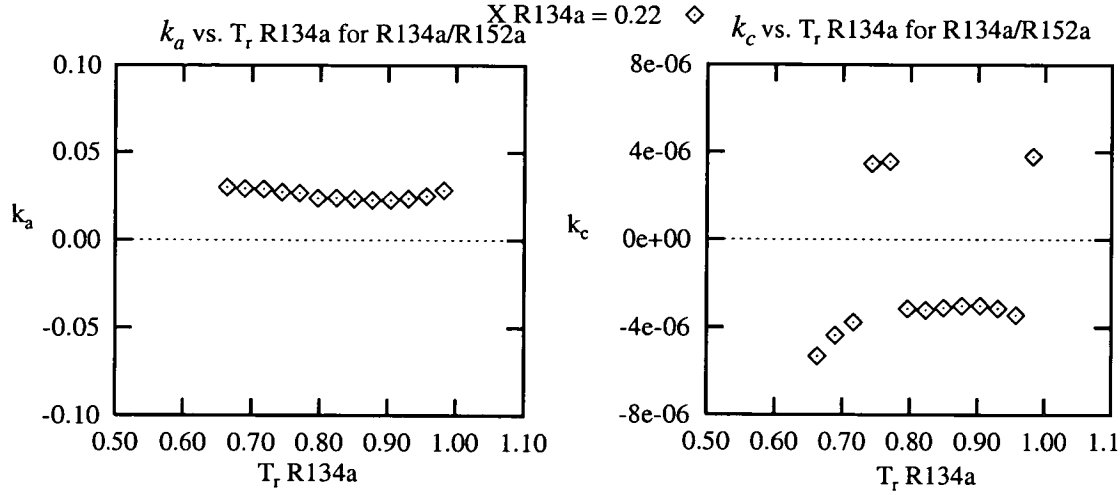

Figure G.9: Optimised k_a & k_c vs. T_r for R134a/R152a two phase VLE data

G.3 Two Phase Plots Data of k_a & k_c vs. T_r m.v.c.

R32/R125 (Data of Nagel et al. [*1995*])

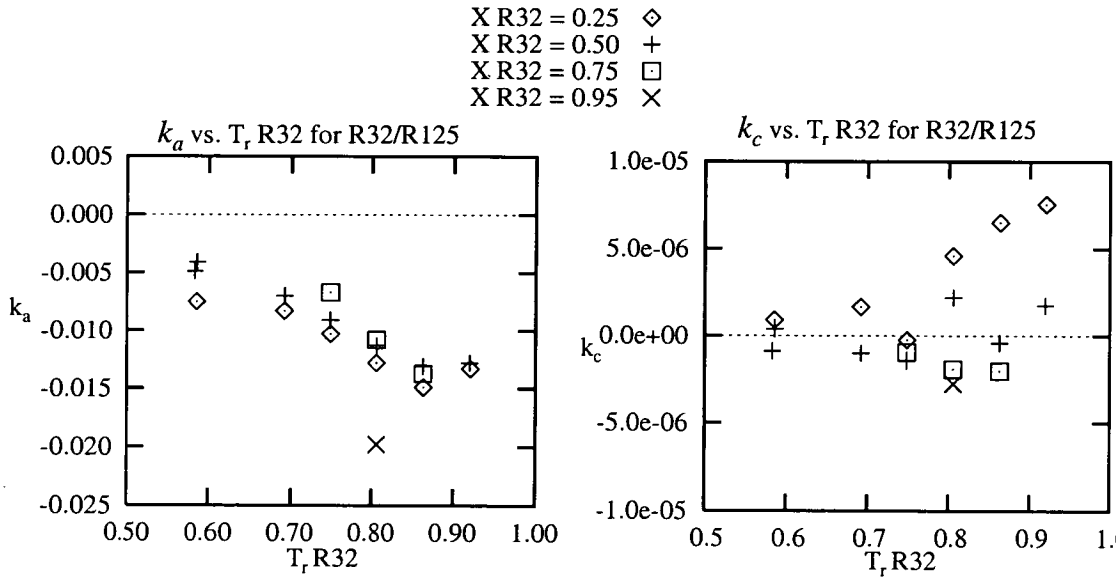

Figure G.10: Optimised k_a & k_c vs. T_r for R32/R125 two phase VLE data

R32/R134a (Data of Nagel et al. [*1995*])

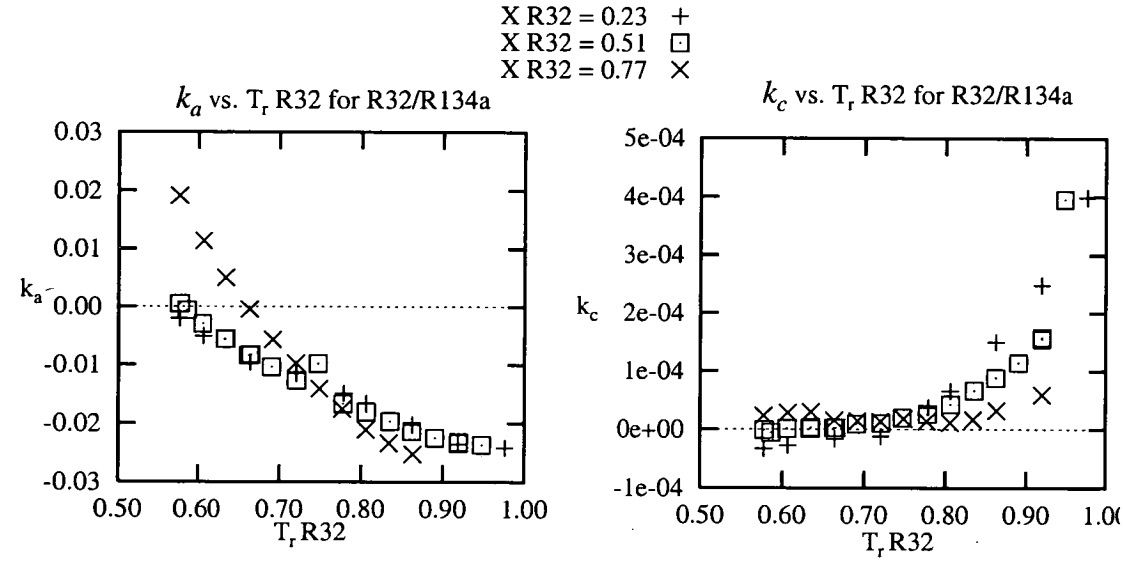

Figure G.11: Optimised k_a & k_c vs. T_r for R32/R134a two phase VLE data

R125/R134a (Data of Nagel et al. [*1995*])

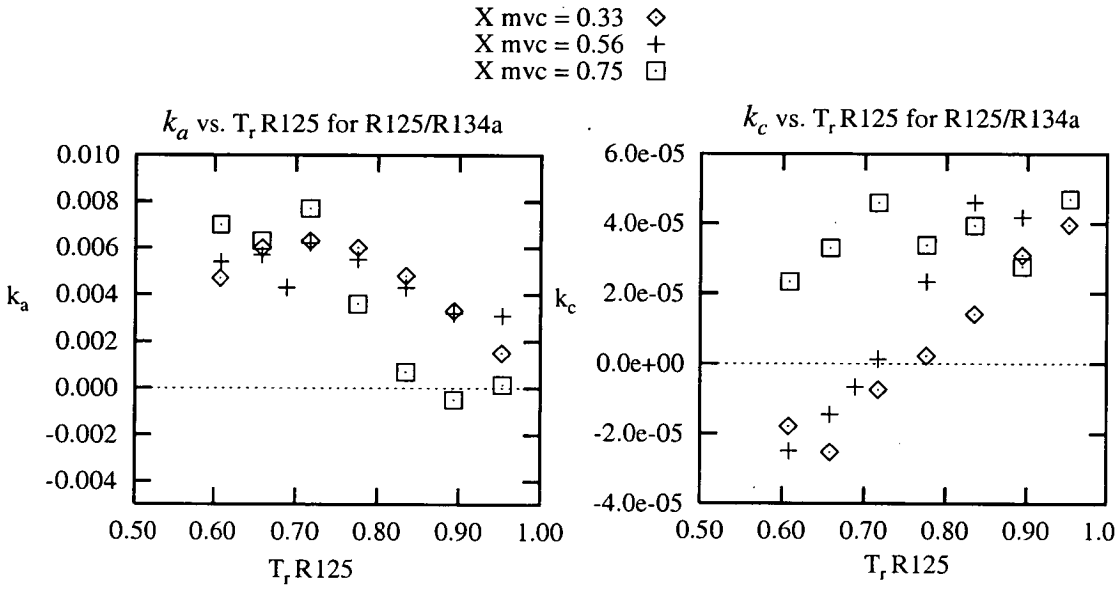

Figure G.12: Optimised k_a & k_c vs. T_r for R125/R134a two phase VLE data

R22/R134a (Data of Arito et al. [*1991*])

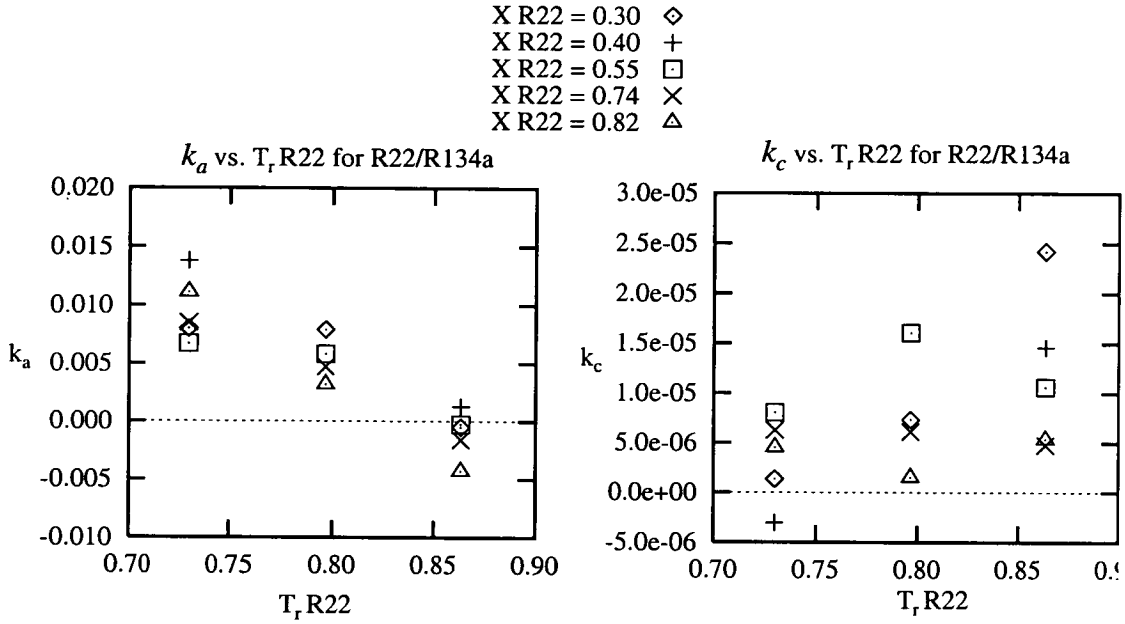

Figure G.13: Optimised k_a & k_c vs. T_r for R22/R134a two phase VLE data

R134a/R141b (Data of Zheng et al. [*1990*])

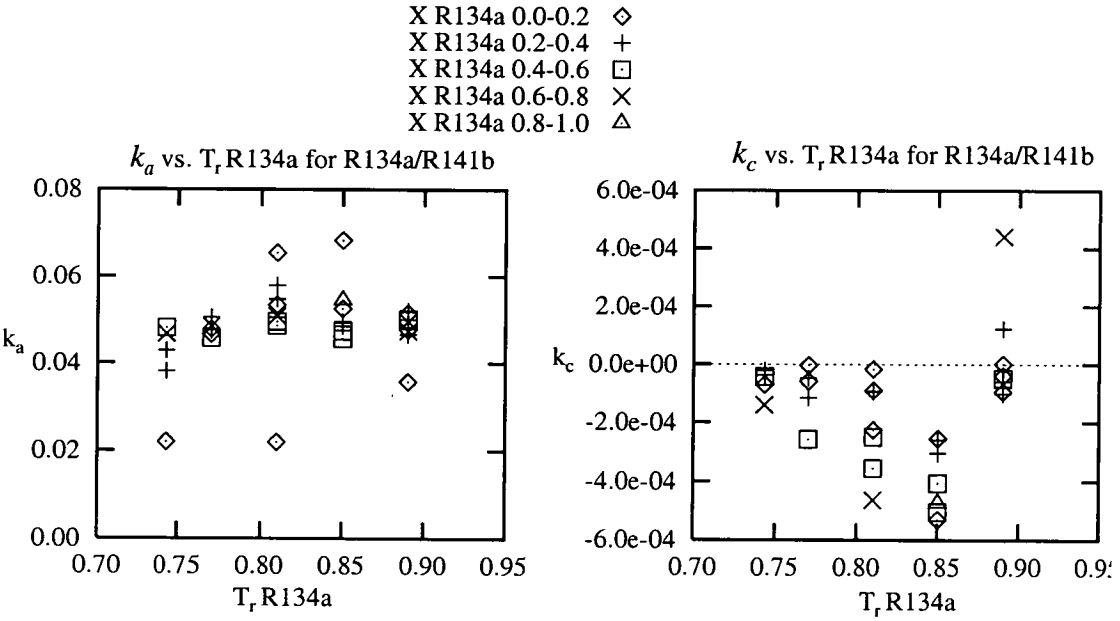

Figure G.14: Optimised k_a & k_c vs. T_r for R134a/R141b two phase VLE data

Appendix H

Simulation Results: Mixture COPs and Mixture COP Changes Relative to Pure Fluid COPs as Functions of Composition

Graphs of COP vs. composition and percentage change in mixture COP relative to the higher pure fluid COP for the simulation described Chapter 5 are presented in Appendix H. These are the results of the model refrigeration cycle discussed in Section 5.7.3 on page 173. The graphs show results from CCORCOMPVARY which simulates a refrigeration over a range of working fluid compositions. Six different pairs were considered: R32/R134a, R32/R152a, R125/R134a, R125/R152a, R143a/ R134a and R143a/R152a. Six different cycle input parameters were examined separately: heat exchanger UA vales, compressor polytropic efficiency, glycol temperature drop, pressure drop, condenser water flow rate and degree of subcooling in the liquid-suction heat exchanger. Four values of each parameter were examined. Simulations were carried out across the composition spectrum for each refrigerant pair; from pure m.v.c. to pure l.v.c in 0.05 weight fraction intervals. Plots of COP vs. weight fraction of the m.v.c for each separate cycle parameter are shown here. Also shown is the percentage change in mixture COP relative to the higher pure fluid COP of a particular mixture, as detailed in Equation 5.18 on page 165. This is referred to as "% COP change" in the figures.

H.1 Heat exchanger UA Values

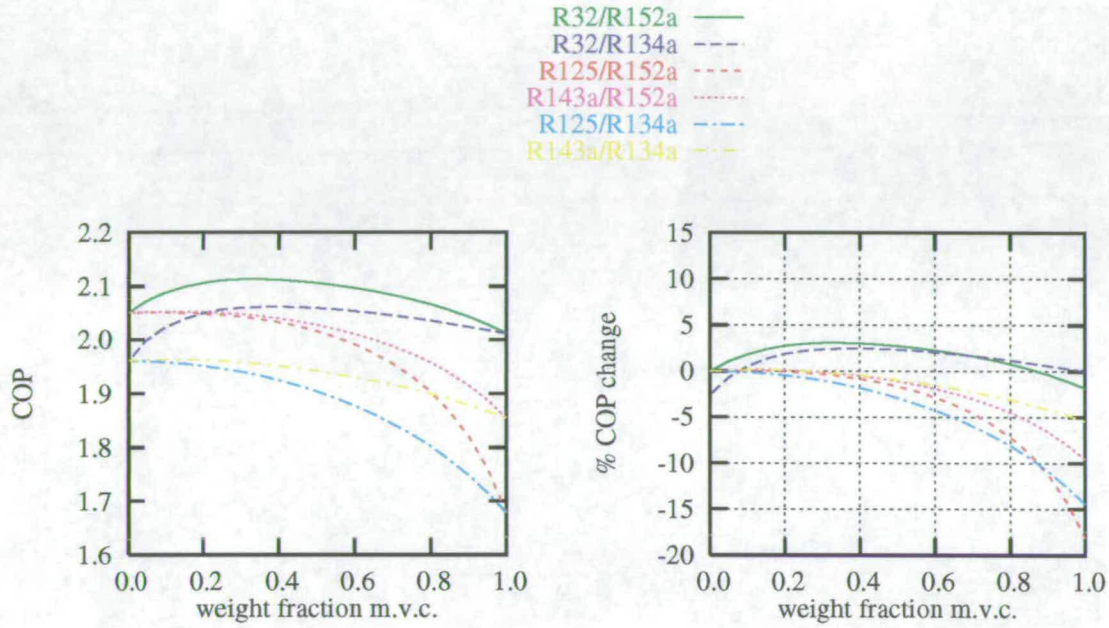

Figure H.1: COP vs. wt. fraction; (UA_e=0.2kWK^{-1}, UA_c=0.26kWK^{-1})

Figure H.2: % COP change (UA_e=0.2kWK^{-1}, UA_c=0.26kWK^{-1})

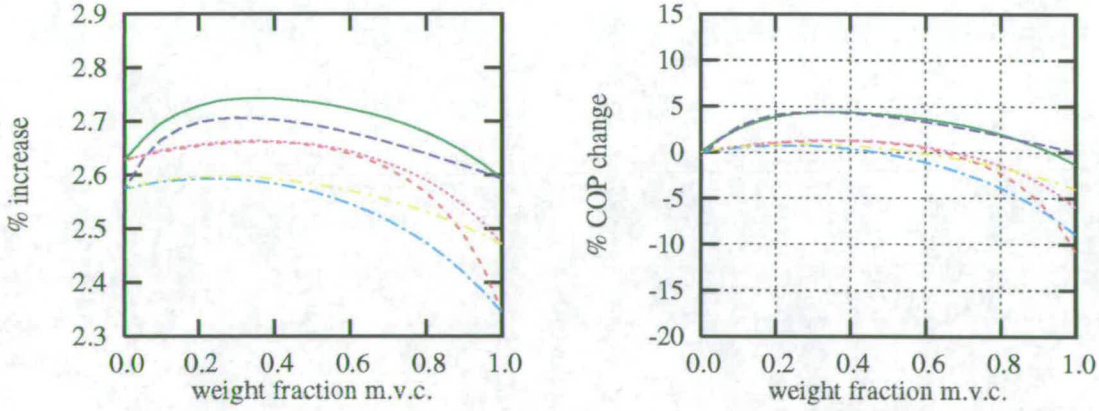

Figure H.3: COP vs. wt. fraction (UA_e=0.3kWK^{-1}, UA_c=0.39kWK^{-1})

Figure H.4: % COP change (UA_e=0.3kWK^{-1}, UA_c=0.39kWK^{-1})

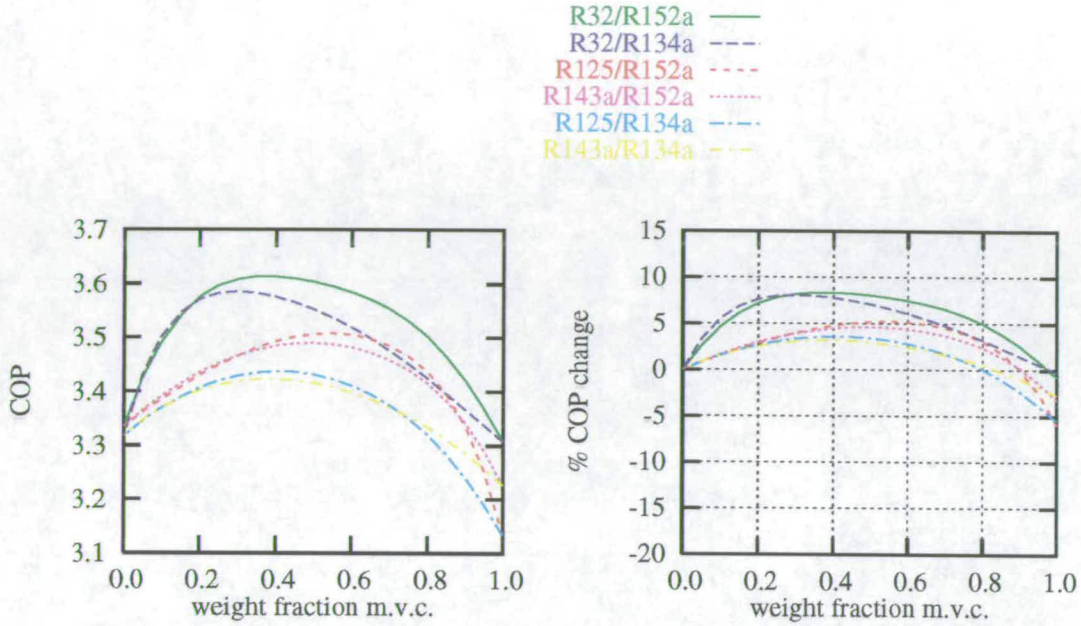

Figure H.5: COP vs. wt. fraction; (UA_e=0.6kWK^{-1}, UA_c=0.78kWK^{-1})

Figure H.6: % COP change; (UA_e=0.6kWK^{-1}, UA_c=0.78kWK^{-1})

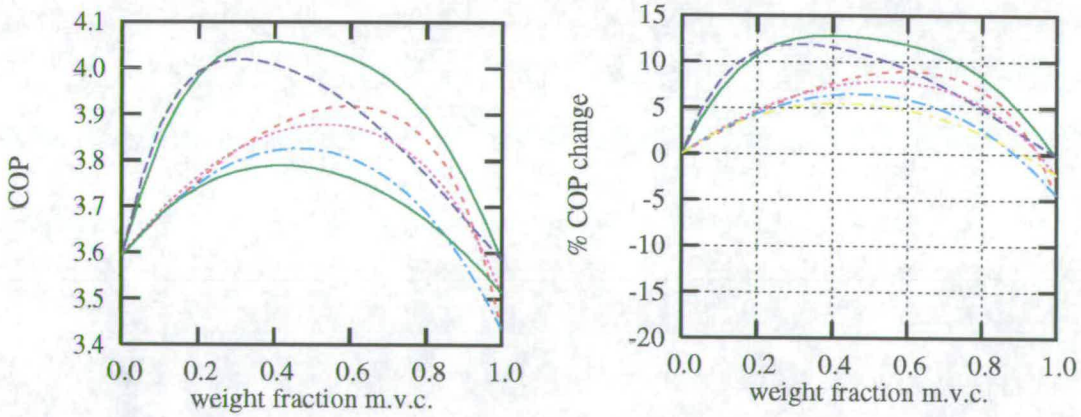

Figure H.7: COP vs. wt. fraction; (UA_e=1.0kWK^{-1}, UA_c=1.3kWK^{-1})

Figure H.8: % COP change; (UA_e=1.0kWK^{-1}, UA_c=1.3kWK^{-1})

H.2 Compressor Efficiency

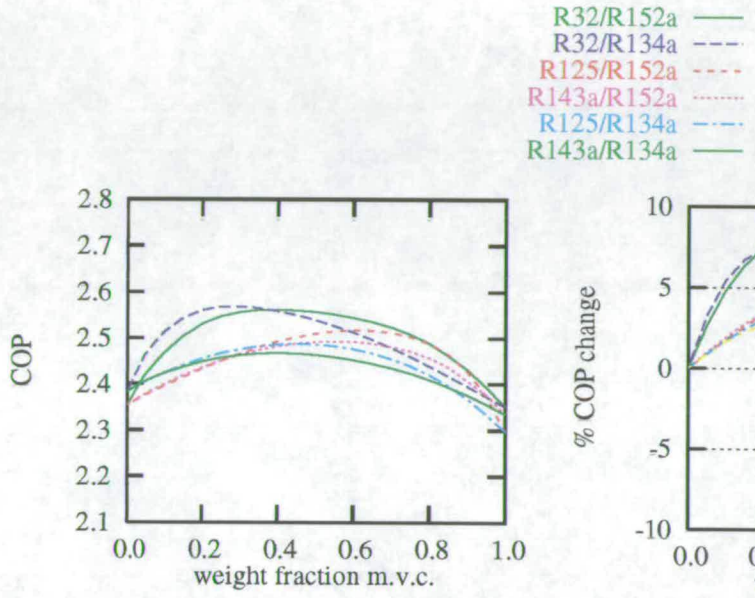

Figure H.9: COP vs. wt. fraction; (Compressor polytropic eff. = 55%)

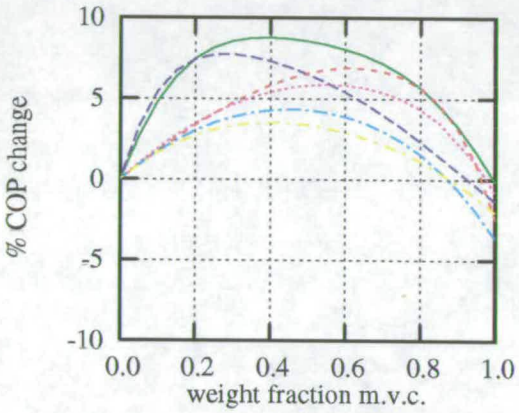

Figure H.10: % COP change; (Compressor polytropic eff. = 55%)

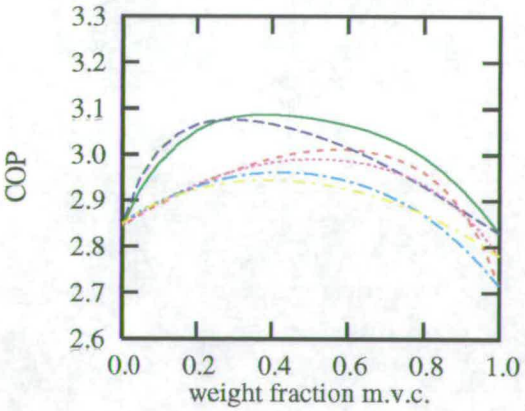

Figure H.11: COP vs. wt. fraction; (Compressor polytropic eff. = 65%)

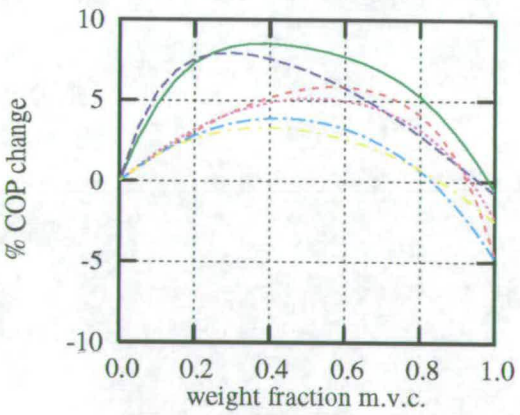

Figure H.12: % COP change; (Compressor polytropic eff. = 65%)

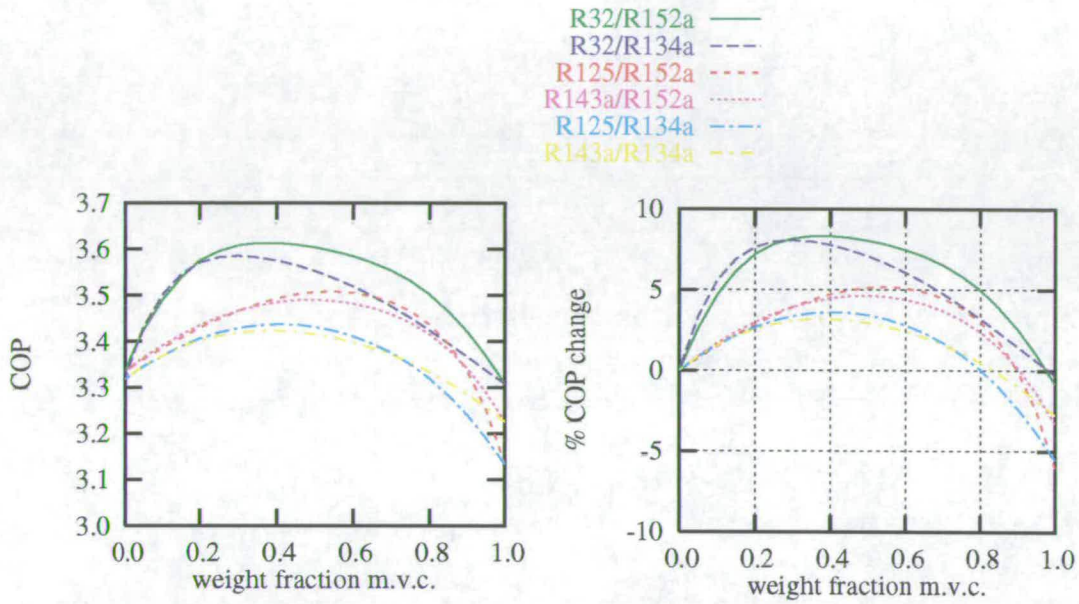

Figure H.13: COP vs. wt. fraction; (Compressor polytropic eff. = 75%)

Figure H.14: % COP change; (Compressor polytropic eff. = 75%)

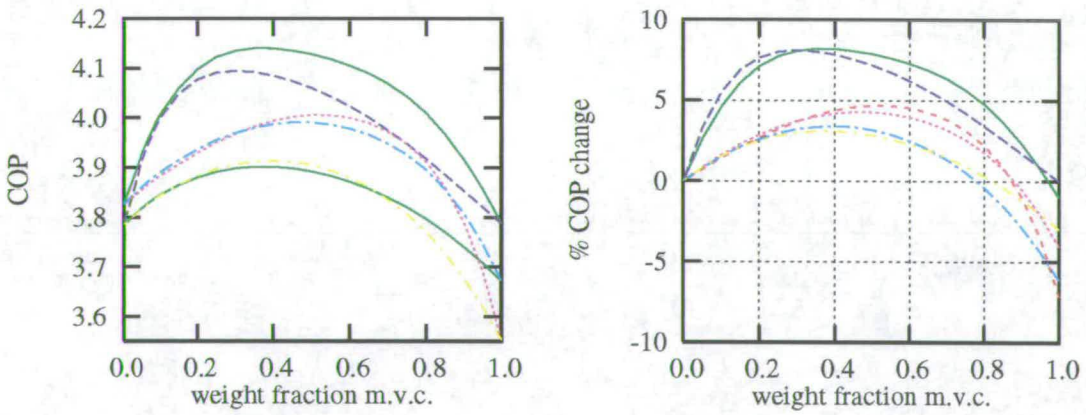

Figure H.15: COP vs. wt. fraction; (Compressor polytropic eff. = 85%)

Figure H.16: % COP change; (Compressor polytropic eff. = 85%)

H.3 Glycol Temperature Change

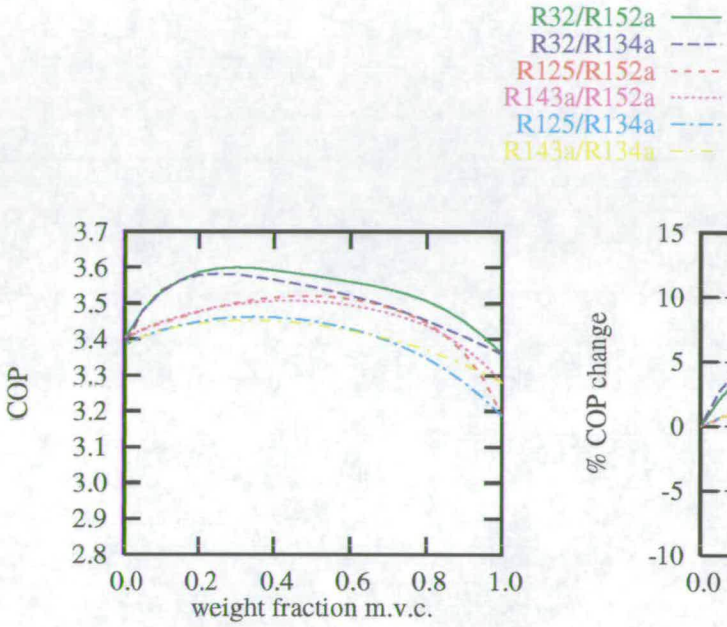

Figure H.17: COP vs. wt. fraction; (Glycol ΔT = 2.5 degrees)

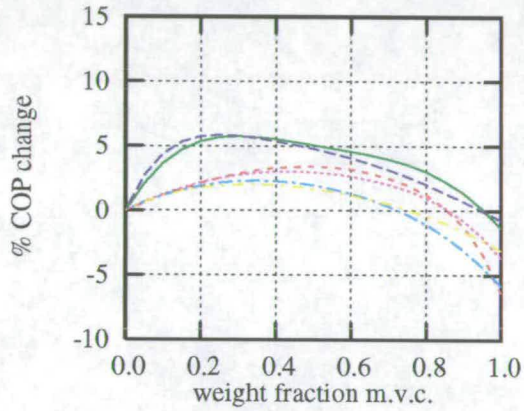

Figure H.18: % COP change (Glycol ΔT = 2.5 degrees)

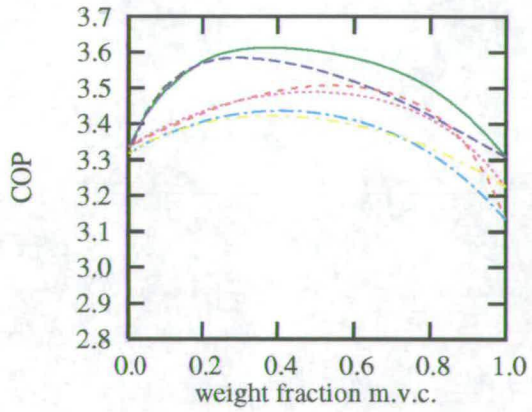

Figure H.19: COP vs. wt. fraction; (Glycol ΔT = 5.0 degrees)

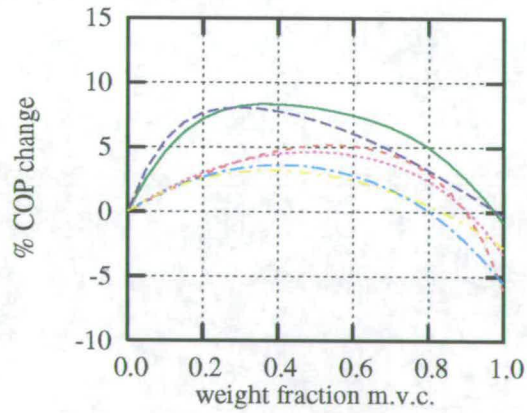

Figure H.20: % COP change Glycol (ΔT = 5.0 degrees)

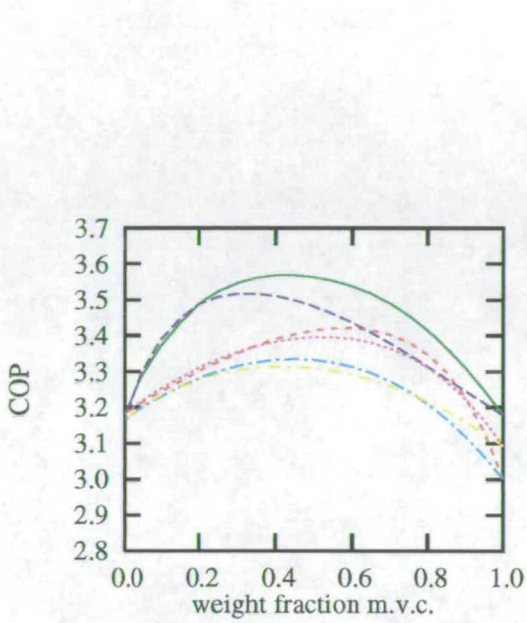

Figure H.21: COP vs. wt. fraction; (Glycol ΔT = 10 degrees)

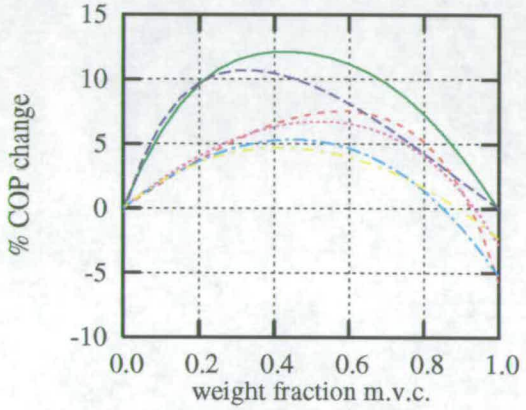

Figure H.22: % COP change (Glycol ΔT = 10 degrees)

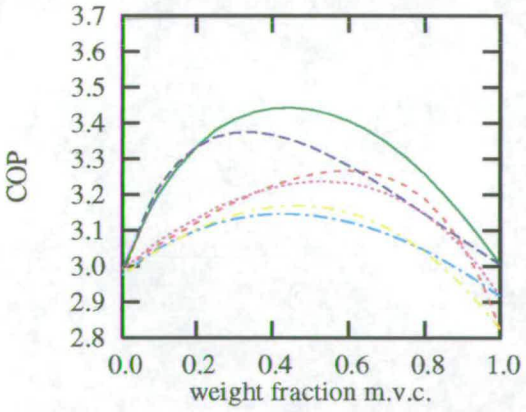

Figure H.23: COP vs. wt. fraction; (Glycol ΔT = 15 degrees)

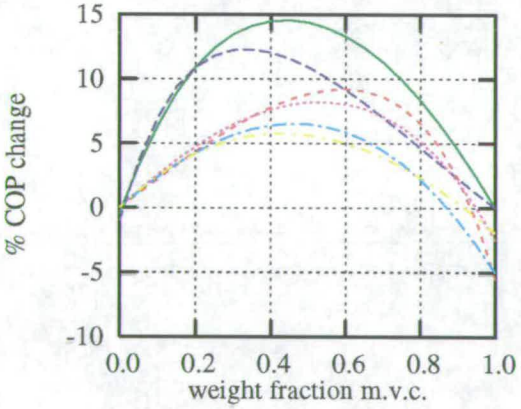

Figure H.24: % COP change (Glycol ΔT = 15 degrees)

H.4 Heat Exchanger Pressure Drop

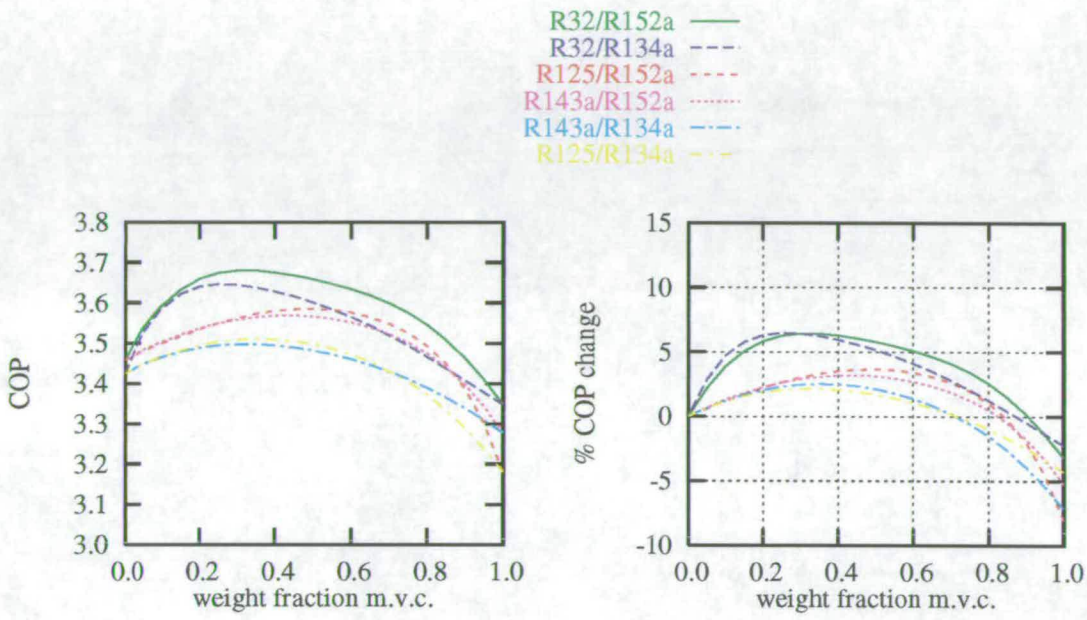

Figure H.25: COP vs. wt. fraction; ($\Delta P_c = \Delta P_e = 5$kPa)

Figure H.26: % COP change; ($\Delta P_c = \Delta P_e = 5$kPa)

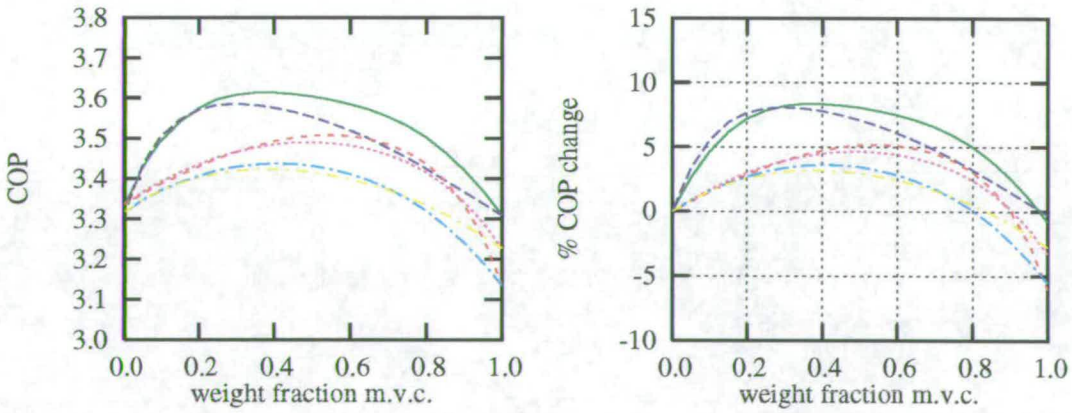

Figure H.27: COP vs. wt. fraction; ($\Delta P_c = \Delta P_e = 15$kPa)

Figure H.28: % COP change; ($\Delta P_c = \Delta P_e = 15$kPa)

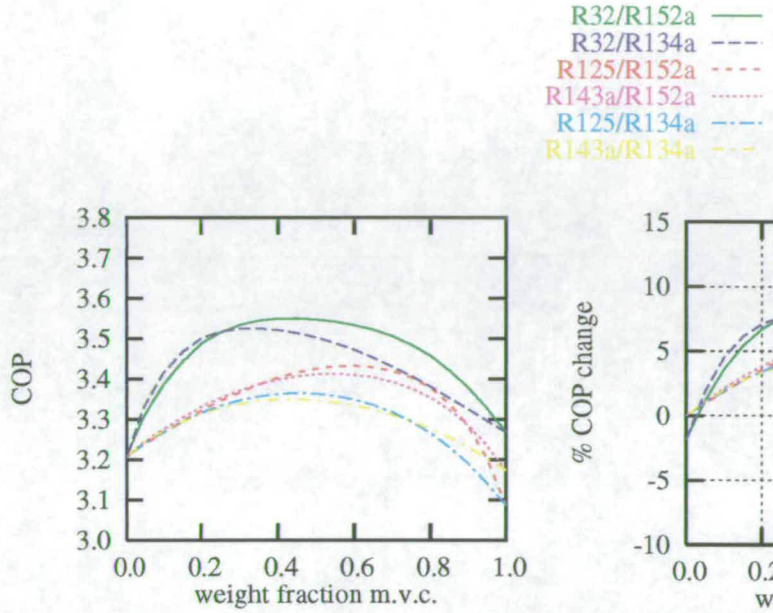

Figure H.29: COP vs. wt. fraction; ($\Delta P_c = \Delta P_e = 25$kPa)

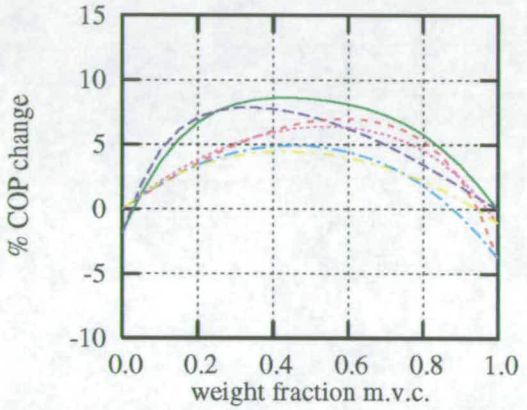

Figure H.30: % COP change; ($\Delta P_c = \Delta P_e = 25$kPa)

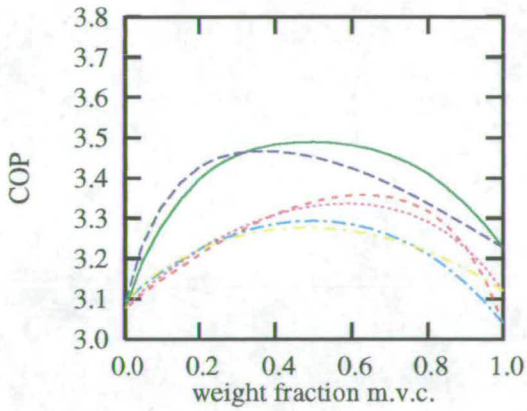

Figure H.31: COP vs. wt. fraction; ($\Delta P_c = \Delta P_e = 35$kPa)

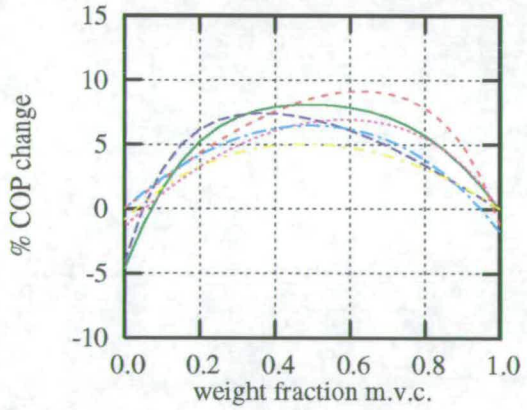

Figure H.32: % COP change; ($\Delta P_c = \Delta P_e = 35$kPa)

H.5 Water Flowrate

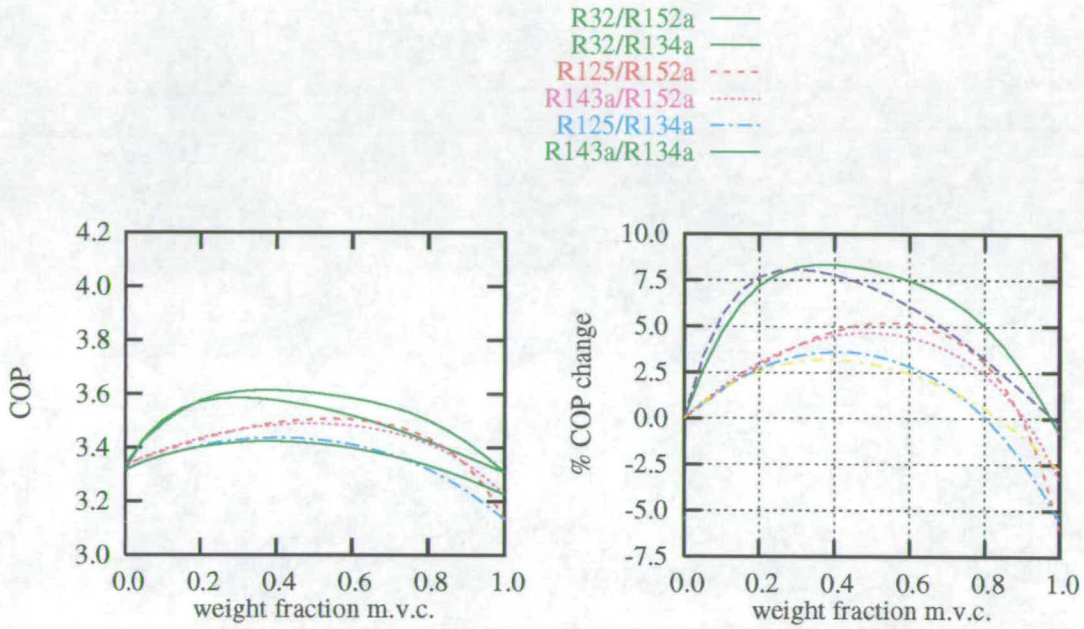

Figure H.33: COP vs. wt. fraction; (water flow = 0.07 kgs^{-1})

Figure H.34: % COP change; (wat flow = 0.07 kgs^{-1})

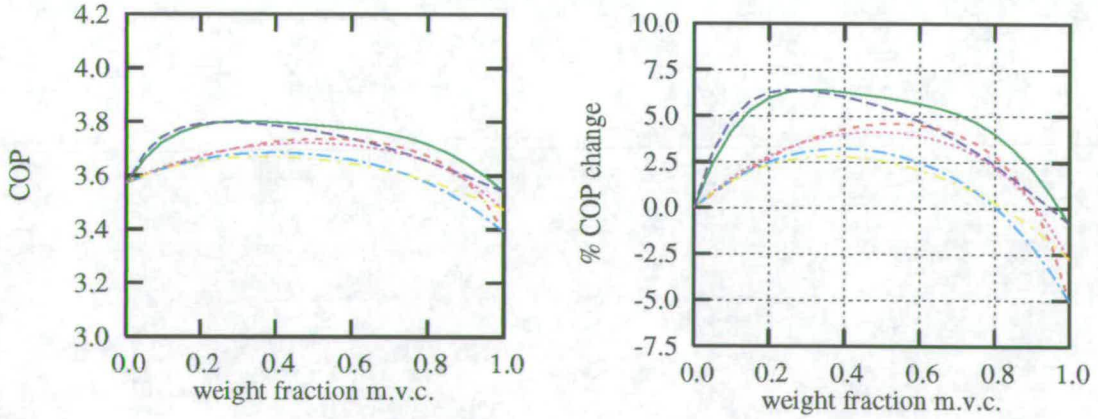

Figure H.35: COP vs. wt. fraction; (water flow = 0.1 kgs^{-1})

Figure H.36: % COP change; (water flow = 0.1 kgs^{-1})

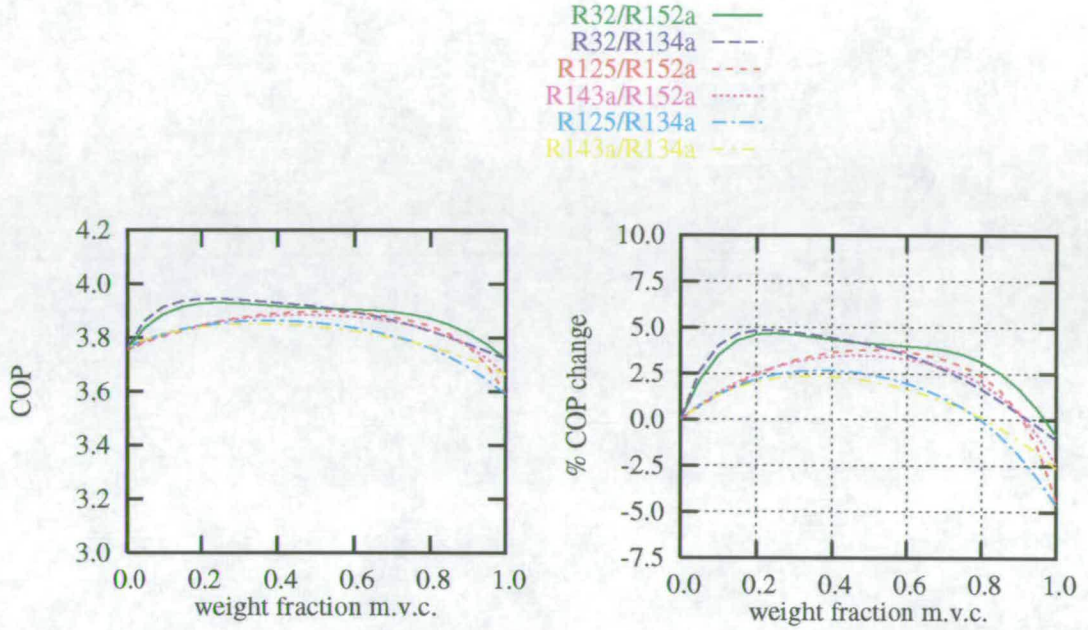

Figure H.37: COP vs. wt. fraction; (water flow = 0.15kgs^{-1})

Figure H.38: % COP change; (water flow = 0.15kgs^{-1})

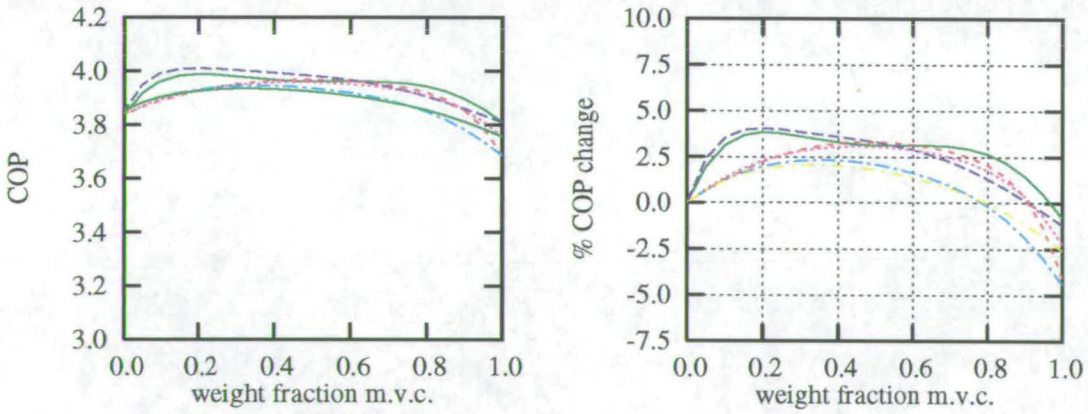

Figure H.39: COP vs. wt. fraction; (water flow = 0.2kgs^{-1})

Figure H.40: % COP change; (water flow = 0.2kgs^{-1})

H.6 Liquid-Suction Heat Exchanger Temperature Drop

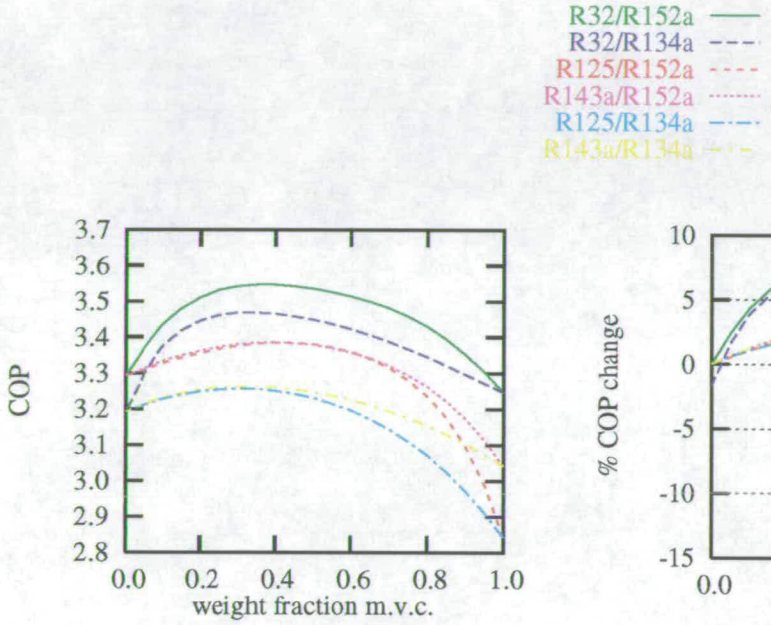

Figure H.41: COP vs. wt. fraction; (ΔT_{lshx}= 0 deg. C)

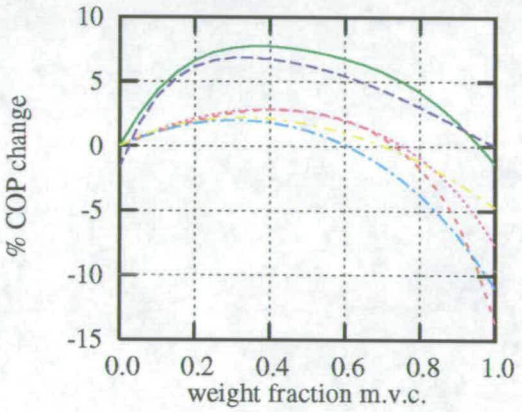

Figure H.42: % COP change vs. wt. fraction; (ΔT_{lshx} = 0 deg. C)

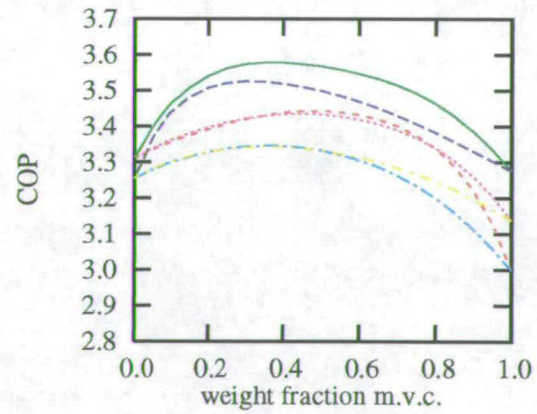

Figure H.43: COP vs. wt. fraction; (ΔT_{lshx} = 5 deg. C)

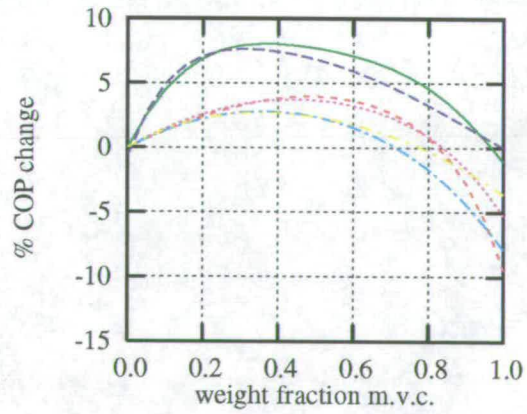

Figure H.44: % COP change vs. wt. fraction; (ΔT_{lshx} = 5 deg. C)

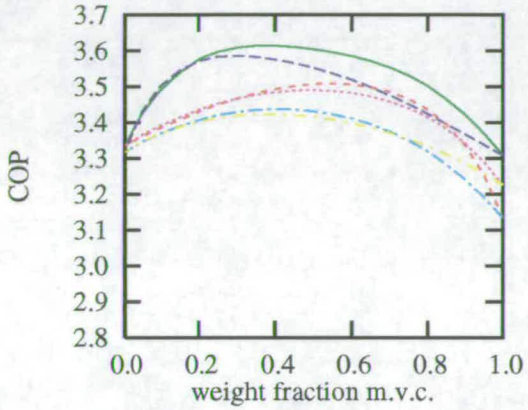

Figure H.45: COP vs. wt. fraction; (ΔT_{lshx} = 10 deg. C)

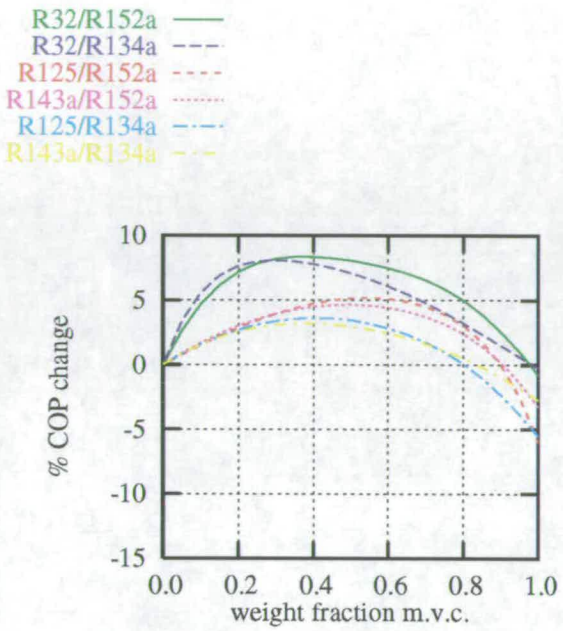

Figure H.46: % COP change vs. wt. fraction; (ΔT_{lshx} =1 0 deg. C)

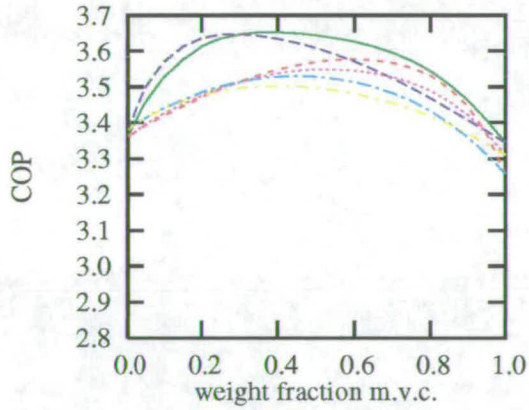

Figure H.47: COP vs. wt. fraction; (ΔT_{lshx} = 15 deg. C)

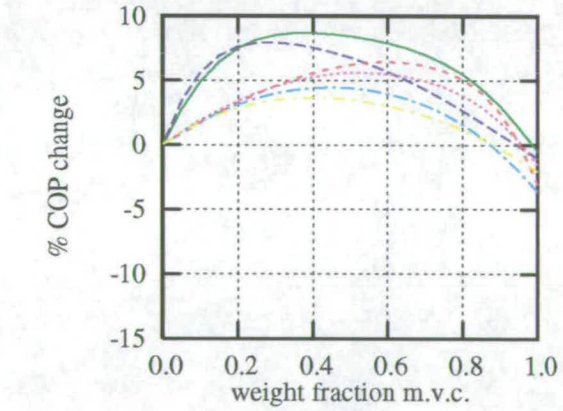

Figure H.48: % COP change vs. wt. fraction; (ΔT_{lshx} = 15 deg. C)

References

Arito, K., Tomizawa, T., Nagakawa, Y., Yoshida, Y., 1991. *Vapour-liquid equilibrium of the non-azeotropic refrigerant mixture formed by chlorofluoromethane and 1,1,1,2-tetrafluoroethane*, Fluid Phase Equilibria, Vol. 63, No. 1-2, pp. 151-156

Arora, C.P., 1967. *Power savings in refrigeration machines using mixed refrigerants*, Proceedings of the 12th International Institute of Refrigeration Congress of Refrigeration, pp. 397-409

Atwood, T., 1985. *The ABCs of NARBS (Nonazeotropic Refrigerant Blends)*, ASHRAE Annual Winter meeting, Honolulu, Vol. 2b, pp. 909-917

Baehr, H.D., Tillner-Roth, R., 1991. *Measurement and correlation of the vapour pressures of 1,1,1,2-tetrafluoroethane (R 134a) and of 1,1-difluoroethane (R 152a)*, Journal of Chemical Thermodynamics, Vol. 23, No. 11, pp. 1063-1068

Barolo, M, Bertucco, A., Scalabrin, G., 1995. *A method for the prediction of vapour-liquid equilibria of refrigerant mixtures at low and moderate pressure*, International Journal of Refrigeration, Vol. 18, No. 8, pp. 550-556

Baroncini, C., Camporese, R., Giuliani, G., Latini, G., Polonara, F., 1993. *Experimental study of the thermodynamic properties of difluoromethane (R32)*, High Temperatures-High Pressures, Vol. 25, pp. 459-464

Baroncini, C., Giuliani, G., Pacetti, M., Polonara, F., 1990. *Experimental study of thermodynamic properties of 1,1,1,2-tetrafluoroethane (R134a)*, "Thermophysical properties of pure substances and mixtures for refrigeration", Proceedings of the meeting of I.I.R. Commission B1, Herzlia, Israel, pp. 83-88

Baroncini, C., Giuliani, G., Latini, G., Polonara, F., Camporese, R., 1993. *Experimental evaluation of thermodynamic properties of refrigerant R125 (CHF_2CF_3)*, "Energy efficiency in refrigeration and global warming impact", Proceedings of I.I.R. Commissions B1/2, Ghent, Belgium, pp. 207-213

Bensafi, A., Haselden, G., 1993. *Wide Boiling Refrigerant Mixtures for Energy Saving*, "Refrigerants beyond the crisis", Institution of Mechanical Engineers Conference, London

Blaise, J.C., Dutto, T., Ambrosino, J.L., 1989. *First industrial application of non-azeotropic mixture*, International Journal of Refrigeration, Vol. 12, No. 5, pp. 255-258

Blanke, W., Weiß, R., 1992. *Isochoric (p,v,T) Measurements of $C_2H_4F_2$ (R152a) in the Liquid State from the Triple Point to 450 K and at Pressures up to 30 MPa*, Fluid Phase Equilibria, Vol. 80, pp.179-190

Blindenbach, W.L., Economou, I.G., Smits, P.J., Peters, C.J., de Swaan Arons, J., 1994. *Modeling of the thermodynamic properties of CFC and HCFC compounds and the vapour -liquid equilibria of CFC and HCFC mixtures and CFC/HCFC-hydrocarbon mixtures with the perturbed anisotropic chain theory (PACT)*, Fluid Phase Equilibria, Vol. 97, pp. 13-28

Boublik, T., Nezbeda, I. 1977. *Equation of State for Hard Dumbbells*, Chemical Physics Letters, Volume 46, p. 315

Boyes, S.J., Weber, L.A., 1995. *Vapour pressures and gas-phase (p, ρ_n, T) values for CF_3CHF_2 (R125)*, Journal of Chemical Thermodynamics, Vol. 27, No.2, pp. 163-174

Carnahan, N.F., Starling, K.E., 1969. *Equation of State for Nonattracting Rigid Spheres*, Journal of Chemical Physics, Vol. 31, No. 2, pp. 635-636

Carr, F., 1949. *Power Savings in Process Refrigeration*, Industrial and Engineering Chemistry, Vol. 41, No. 4, pp. 776-780

Chien, C.H., Greenkorn, R.A., Chao, K.C., 1983. *Chain-of-Rotators Equation of State*, AIChE Journal, Vol. 29, No. 4, pp. 560-571

Defibaugh, D.R., Morrison, G., 1995. *Interaction coefficients for 15 mixtures of flammable and non-flammable components*, International Journal of Refrigeration, Vol. 18, No. 8, pp. 518-523

Defibaugh, D.R., Morrison, G., Weber, L.A., 1994. *Thermodynamic Properties of Difluoromethane*, Journal of Chemical Engineering Data, Vol. 39, No. 2, pp. 333-340

De Santis, R., Gironi, F., Marrelli, L., 1976. *Vapor-Liquid Equilibrium from a Hard-Sphere Equation of State*, Industrial and Engineering Chemistry Fundamentals, Vol. 15, No. 3, pp. 183-189

Didion, D.A., 1994. *Recent developments in the design of new refrigerant mixtures for existing and future systems*, Proceedings of the International Seminar "New technology in refrigeration Progress in the application of new refrigerants", Padova, Italy, pp.173-195

Didion, D.A., Bivens D.B., 1990. *Role of refrigerant mixtures as alternatives to CFCs*, International Journal of Refrigeration, Vol. 13, No. 3, pp. 163-175

Domanski, P., 1986. *Modelling of a Heat Pump Charged With a Non-Azeotropic Refrigerant Mixture*, National Bureau of Standards Technical Note 1218

Domanski, P., Didion, D., 1983. *Computer Modelling of the Vapor Compression Cycle With Constant Flow Expansion Area Device,* National Bureau of Standards Building Science Series 155

Domanski, P.A., Didion, D.A., Doyle, J.P., 1994a, *Evaluation of suction-line/liquid-line heat exchange in the refrigeration cycle,* International Journal of Refrigeration, Vol. 17, No.7, pp. 487-493

Domanski, P.A., McLinden, M.O., 1992. *A simplified cycle simulation model for the performance rating of refrigerants and refrigerant mixtures*, International Journal of Refrigeration, Vol. 15, No. 2, pp. 81-88

Domanski, P.A., Mulroy W.J., Didion, D.A., 1994b. *Glide matching with binary and ternary zeotropic refrigerant mixtures Part 2. A computer simulation,* International Journal of Refrigeration, Vol. 17, No. 4, pp. 226-230

Embler, L.R, Layman P.L., Lepkowski, W., Zurer, P.S., 1986. *Tending the Global Commons*, Chemical and Engineering News, Vol. 64, No. 47, pp. 14-64

Etherington, T.L., 1958. *Variable capacity refrigeration system*, U.S. Patent No. 2,951,349

Fukushima, M., 1991. *Saturated Liquid Densities of HCFC123, HFC134a, CFC11 and CFC12*, Transactions of the Japanese Association of Refrigeration, Vol. 8, No.1 pp. 65-70

Fukushima, M., Watanabe, N., Kamimura, T., 1990. *Measurements of the PVT Properties of HCFC123 and HFC134a*, Transactions of the Japanese Association of Refrigeration, Vol. 7, No. 3, pp. 243-256

Fulkerson, W., Auerbach, S.I., Crane, A.T., Kash, D.E., Perry, A.M., Reister, D.B., 1989. *Energy technology R and D, What could make a difference?*, ORNL-6541, Oak Ridge National Laboratory, USA

Gleason, J.F., Bhartia, P.K., Herman, J.R., McPeters, R., Newman, P., Stolarski, R.S., Flynn, L., Labow, G., Larko, D., Seftor, C., Wellemeyer, C., Komhyr, W.D., Miller, A.J., Planet, W, 1993. *Record low global ozone in 1992*, Science, Vol. 260, No. 5107, pp. 523-526

Guo, T.M., Kim, H., Lin, H.M., Chao, K.C., 1985a, *Cubic Chain-of-Rotators Equation of State. 2. Polar Substances*, Industrial and Engineering Chemistry Process Design and Development, Vol. 24, No. 3, pp. 764-767

Guo, T.M., Lin, H.M., Chao, K.C., 1985b, *Cubic Chain-of-Rotators Equation of State. 3. Mixtures of Polar Substances*, Industrial and Engineering Chemistry Process Design and Development, Vol. 24, No. 3, pp. 768-773

Haselden, G.H., Chen, J., 1994. *A computer simulation program for mixed-refrigerant air conditioning*, International Journal of Refrigeration, Vol. 17, No. 5, pp. 343-350

Hasleden, G.G., Klimek L., 1957-58. *An Experimental Study of the Use of Mixed Refrigerants for Non-isothermal Refrigeration*, Proceedings of the Institute of Refrigeration, London, Vol. 54, pp. 129-154

Higashi, Y., Ashizawa, M., Kabata, Y., Majima, T., Uematsu, M., Watanabe, K., 1987. *Measurements of Vapor pressures, Vapour-Liquid Coexistence Curve and Critical Parameters of Refrigerant 152a*, Japanese Society of Mechanical Engineers International Journal, Vol. 30, No. 265, pp. 1106-1112

Högberg, M., Vamling L., Berntsson, T., 1993. *Calculation methods for comparing the performance of pure and mixed working fluids in heat pump applications*, International Journal of Refrigeration, Vol. 16, No. 6, pp. 403-413

Holcomb, C.D., Niesen V.G., Van Poolen, L.J., Outcalt, S. L., 1993. *Coexisting densities, vapor pressures and critical densities of refrigerants R-32 and R-152a, at 300-385 K*, Fluid Phase Equilibria, Vol. 91, No.1, pp. 145-157

Huron, M.J., Vidal, J., 1979. *New mixing rules in simple equations of state for representing vapour-liquid equilibria of strongly non-ideal mixtures*, Fluid Phase Equilibria, Vol. 3, pp. 255-271

ICI Chemicals and Polymers, *Thermodynamic Properties of KLEA 32 SI Units*

International Institute for Refrigeration, 1992. *Compression Cycles for Environmentally Acceptable Refrigeration, Air Conditioning and Heat Pump Systems*

International Institute for Refrigeration, 1980. *Saving of energy in refrigeration*

Japanese Association of Refrigeration, 1994. *JAR Thermodynamic Tables, 'HFCs and HCFCs version 1.0'*, Volume 1

Jung D.S., Radermacher, R., 1991a. *Performance simulation of single-evaporator domestic refrigerators charged with pure and mixed refrigerants*, International Journal of Refrigeration, Vol. 14, No. 4, pp. 223-232

Jung D.S., Radermacher, R., 1991b. *Performance simulation of a two-evaporator refrigerator-freezer charged with pure and mixed refrigerants,* International Journal of Refrigeration, Vol. 14, No. 4, pp. 254-263

Kanungo, A., Oi, T., Popowicz, A., Ishida, T., 1987. *Vapor-Pressure isotope effects in liquid methylene difluoride*, Journal of Physical Chemistry, Vol. 91, No. 15, pp 4198-4203

Kerr, R.A., 1995. *Studies Say-tentatively-that greenhouse warming is here*, Science, Vol. 268, No. 5217, pp. 1567-1568

Kiernan, V., 1993. *Atmospheric Ozone hits a new low*, New Scientist, Vol. 138, No. 1871, p. 8

Kim, H., Lin, H.M., Chao, K.C., 1986. *Cubic Chain-of-Rotators Equation of State*, Industrial and Engineering Chemistry Fundamentals, Vol. 25, No. 1, pp. 75-84

Kim T.S., Shin J.Y., Kim, M.S., Ro, S.T., 1994. *Cycle analysis and heat transfer characteristics of a heat pump using R22/R142b refrigerant* mixtures, International Journal of Refrigeration, Vol. 17, No. 6, pp. 391-399

Kruse, H., 1981. *The advantages of non-azeotropic refrigerant mixtures for heat pump application*, International Journal of Refrigeration, Vol. 4, No. 3, pp. 119-125

Kubota, H., Yamashita, T., Tanaka, Y., Makita, T., 1989. *Vapor Pressures of New Fluorocarbons*, International Journal of Thermophysics, Vol. 10, No. 3, pp. 629-637

Kuwabara, S., Aoyama, K., Sato, H., Watanabe, K., 1995. *Vapor-liquid Coexistence Curve in the Critical Region and the Critical Temperatures and Densities of Difluoromethane and Pentafluoromethane*, Journal of Chemical Engineering Data, Vol. 40, No. 1, pp. 112-116

Lavrenchenko, G.V., Ruvinskij, G.Ya., Iljushenko, S.V., Kanaev, V.V., 1992. *Thermophysical properties of refrigerant R134a,* International Journal of Refrigeration, Vol. 15, No. 6, pp. 386-392

Lee, M.J., Sun, H.C., 1992. *Thermodynamic Property Predictions for Refrigerant Mixtures*, Industrial Engineering Chemistry Research, Vol. 31, No. 4, pp. 1212-1216

Leet, W.A., Lin, H.M., Chao, K.C., 1986. *Cubic Chain-of-Rotators Equation of State II for Strongly Polar Substances and Their Mixtures*, Industrial and Engineering Chemistry Fundamentals, Vol. 25, No. 4, pp. 695-701

Lin, H.M., Kim, K., Chao, K.C., 1983. *Cubic Chain-of-Rotators equation of state and vle calculations*, Fluid Phase Equilibria, Vol. 13, pp. 143-152

Lorenz, A., Meutzner, K., 1975. *Application of Non-Azeotropic Two-Component Refrigerants in Domestic Refrigerators and Home Freezers*, Proceedings of the 14th International Institute of Refrigeration Congress, Moscow, pp. 1005-1012

Low, R.E., 1991,. *A Variable-Capacity Heat Pump for Renewable Energy Recovery,* PhD Thesis, University of Edinburgh

Lucas, L., 1993. *A new challenge: from the ozone layer to the greenhouse effect*, "Energy efficiency in refrigeration and global warming impact", Proceedings of I.I.R. Commission B1/2, Ghent, Belgium, pp. 31-43

Maezawa, Y., Sato, H., Watanabe, K. 1990. *Saturated Liquid Densities of HCFC 123 and HFC 134a*, Journal of Chemical Engineering Data, Vol. 35, No. 3, pp. 225-228

Maezawa, Y., Sato, H., Watanabe, W., 1991a. *Saturated liquid densities and bubble-point pressures of the binary HCFC 22 + HFC 152a system*, Fluid Phase Equilibria, Vol. 61, No. 3, pp. 263-273

Maezawa, Y., Widiatmo, J.V., Sato, H., Watanabe, W., 1991b. *Saturated Liquid Densities and Bubble-Point Pressures of Binary HFC 152a + HFC 142b System*, International Journal of Thermophysics, Vol. 12, No. 6, pp. 1029-1038

Maezawa, Y., Sato, H., Watanabe, K., Oshima, S., 1991c. *Saturated liquid densities and bubble-point pressures of binary HFC 152a + HFC 134 system*, Proceedings of the ASME/JSME Thermal Engineering Joint Conference, Reno, Vol. 3, pp. 443-449

Magee, J.W., Howley, J.B., 1992. *Vapour pressure measurements on 1,1,1,2-tetrafluoroethane (R134a) from 180 to 350 K*, International Journal of Refrigeration, Vol. 15, No. 6, pp. 362-364

Malbrunot, P.M., Meunier, P.A., Scatena, G.M., Mears, W.H., Murphy, K.P., Sinka, J.V., 1968. *Pressure-Volume-Temperature Behaviour of Difluoromethane*, Journal of Chemical Engineering Data, Vol. 13, No. 1, pp. 16-21

Masuoka, H., Chao, K.C., 1984. *Chain-of-Rotators Equation of State. 2. Polar Fluids*, Industrial and Engineering Chemistry Fundamentals, Vol. 23, No. 1, pp. 24-29

Mattarolo, L., 1990. *Education of young people and training of adults*, "Refrigeration and CFCs", International Colloquium of Brussels, pp. 19-36

McHarness, R.C., Chapman, D.D., 1961. *Refrigerating Capacity and Performance Data for Various Refrigerants, Azeotropes and Mixtures*, ASHRAE Transactions, Vol. 67, pp. 441-464

McLinden, M.O., 1990. *Thermodynamic properties of CFC alternatives: A survey of the available data*, International Journal of Refrigeration, Vol. 13, No. 3, pp. 149-162

McLinden, M.O., Didion, D.A., 1986. *Quest for alternatives*, ASHRAE Journal, Vol. 29, No. 12, pp. 32-42

McLinden M.O., Didion D.A., 1989. *Thermophysical-Property Needs for the Environmentally Acceptable Halocarbon Refrigerants*, International Journal of Thermophysics, Vol. 10, No. 3, pp. 563-576

McLinden M.O., Radermacher, R., 1987. *Methods for comparing the performance of pure and mixed refrigerants in the vapour compression cycle*, International Journal of Refrigeration, Vol. 10, No. 6, pp. 318-325

McLinden, M.O., Huber, M.L., Outcalt, S.L., 1993, Thermophysical Properties of Alternative Refrigerants: Status of the HFCs, Proceedings of the Annual Winter Meeting of The American Society of Mechanical Engineers, Paper No. 93-WA/HT-29

Miyara, A., Koyama, S., Fujii, T., 1992. *Consideration of the performance of a vapour-compression heat-pump cycle using non-azeotropic refrigerant mixtures*, International Journal of Refrigeration, Vol. 15, No. 1, pp. 35-40

Miyara, A., Koyama, S., Fujii, T., 1993. *Performance evaluation of a heat pump cycle using NARMS by a simulation with equations of heat transfer and pressure drop,* International Journal of Refrigeration, Vol. 16, No. 3, pp. 161-168

Molina, M.J., Rowland F.S., 1974. *Stratospheric sink for chlorofluoromethanes, chlorine atom catalysed destruction of ozone*, Nature, Vol. 249, pp. 810-814

Monluc, Y., Sagawa, T., Sato, H., Watanabe, K., 1991. *Thermodynamic Properties of HFC-125*, Proceedings of the Twelfth Japan Symposium on Thermophysical Properties, pp. 65-68

Morrison, G., 1985a. *The Importance of Including the Liquid Phase in Equations of State for Nonazeotropic Refrigerant Mixtures*, ASHRAE Transactions, Vol. 91, Part 1, pp. 260-273

Morrison G., McLinden, M., 1985b. *Two Refrigerant Mixtures and the Hard Sphere Fluid*, ASHRAE Transactions, Vol. 91, pp. 929-943

Morrison, G., McLinden, M.O., 1986a. *Application of A Hard-Sphere Equation of State to Refrigerants and Refrigerant Mixtures*, National Bureau of Standards Technical Note 1226

Morrison, G., McLinden, M.O., 1986b. *Application of the Carnahan-Starling-DeSantis Equation of Sate to Mixtures of Refrigerants*, Proceedings of the Annual Winter Meeting of the American Society of Mechanical Engineers, Anaheim, U.S.A, No. 86-WA/HT-59

Morrison, G, McLinden, M.O., 1993. *Azeotropy in refrigerant mixtures*, International Journal of Refrigeration, Vol. 16, No. 2, pp. 129-138

Morrison, G., Ward, D.K., 1991. *Thermodynamic properties of two alternative refrigerants: 1,1-dichloro-2,2,2-trifluoroethane (R123) and 1,1,1,2-tetrafluoroethane (R134a)*, Fluid Phase Equilibria, Vol. 62, No. 1-2, pp. 65-86

Mulroy, W.J., Domanski, P.A., Didion, D.A., 1994. *Glide matching with binary and ternary zeotropic refrigerant mixtures Part 1. An experimental study*, International Journal of Refrigeration, Vol. 17, No. 4, pp. 220-225

Mulroy, W., Kauffeld, M., McLinden, M., Didion, D., 1988. *An evaluation of two refrigerant mixtures in a breadboard air conditioner*, "Status of CFCs - Refrigeration systems and refrigerant properties", Proceedings of I.I.R Commissions B1, B2, E1, E2, Purdue University, U.S.A., pp. 27-34

Nagel, M, Bier, K., 1995. *Vapour-liquid equilibrium of ternary mixtures of the refrigerants R32, R125 and R134a*, International Journal of Refrigerant, Vol. 18, No. 8, pp. 534-543

National Institute of science and Technology, *NIST Thermodynamic Properties of Refrigerants and Refrigerant Mixtures Database (REFPROP): Version 5.0*, World Wide Web page: http://www.nist.gov/srd/refprop.htm

Niesen, V.G., Van Poolen L.J., Outcalt, S.L., Holcomb, C.D., 1994. *Coexisting densities and vapor pressures of refrigerants R-22, R-134a and R-124 at 300-395 K*, Fluid Phase Equilibria, Vol. 97, pp. 81-95

Pannock, J., Didion, D.A., 1992. *Performance evaluation of chlorine free zeotropic refrigerant mixtures in heat pumps - computer studies and tests*, Proceedings of the 1992 International Refrigeration Conference - Energy Efficiency and New Refrigerants, Vol. 1, Purdue University, U.S.A., pp. 25-34

Parent, D., Larue, P.A., 1989. *Testing and Modelling of a Water-to-Air Heat Pump Operating with a Nonazeotropic Refrigerant Mixture*, ASHRAE Transactions, Vol. 94, No. 2, pp. 405-410

Pearson, S.J., 1993. *What do we require of New Refrigerants?*, "Refrigerants beyond the crisis", Institution of Mechanical Engineers Conference, London

Perry P.H., Glass, D., 1984. *Perry's Chemical Engineers' Handbook*, 6th Edition, McGraw-Hill

Pesuit, D.R., 1978, *Binary Interaction Constants for Mixtures with a Wide Range in Component Properties*, Industrial and Engineering Chemistry Fundamentals, Vol. 17, No. 4, pp. 235-242

Piao, C.C., Sato, H., Watanabe, K., 1990. *An experimental study for PVT properties of CFC alternative refrigerant 1,1,1,2-tetrafluoroethane (R-134a)*, ASHRAE Transactions, Vol. 96, No. 1, pp. 132-140

Press, W.H., Teukolsky, S.A., Vetterling, W.T., Flannery, B.P., 1992. *Numerical Recipes in C The Art of Scientific Computing*, Cambridge University Press, 2nd Edition

Redlich, O., Kwong, 1949. J.N.S.: Chemical Review, Vol. 44, p. 233

Reed, J.W., 1993. *Environmental overview: CFC and HCFC regulatory update*, "Heat Pumps for Energy Efficiency and Environmental Progress" Proceedings of the 4th International Energy Agency Heat Pump Conference, Masstricht, Netherlands, pp. 11-19

Rotameter Manufacturing Co. Ltd., *Calibration Data for 'Metric' Sizes*

Sato, T., Sato, H., Watanabe, W., 1994. *PVT Property Measurements for Difluoromethane*, Journal of Chemical Engineering Data, Vol. 39, No. 4, pp. 851-854

Sato, H., Uematsu, M., Watanabe, K., Okada, M., 1987. *Saturated liquid density of 1,1-difluoroethane(R 152a) and thermodynamic properties along the vapor-liquid coexistence curve*, Fluid Phase Equilibria, Vol. 36, pp. 167-181

Shinsaka, K., Gee, N., Freeman, G.R., 1985. *Densities against temperatures of 17 organic liquids and of solid 2,2dimethylpropane*, Journal of Chemical Thermodynamics, Vol. 17, No. 12, pp. 1111-1119

Singer, F.S., 1994. *The hole truth about CFCs*, Chemistry and Industry, 21st March, p. 240

Smith, J.M., Van Ness, H.C., 1987. *Introduction to Chemical Engineering Thermodynamics*, 4th edition, McGraw Hill

Soave, G., 1972, Chemical Engineering Science, Vol. 27, p. 1197

Stoecker, W.F., Walukas, D.J., 1981. *Conserving energy in domestic refrigerators through the use of refrigerant mixtures*, ASHRAE Transactions, Vol. 87, No. 1, pp. 279-291

Ström, K.H.U, Grén, U.B., 1993. *A study of Vapour-Liquid Equilibria for the Binary Mixtures HCFC22/CFC114, HCFC22,HCFC142b and HCFC22/HFC152a*, The Canadian Journal of Chemical Engineering, Vol. 71, No. 6, pp. 940-947

Tamatsu, T., Sato. T., Watanabe, K., 1992. *An Experimental Study of the Thermodynamic Properties of 1,1-Difluoroethane*, International Journal of Thermophysics, Vol. 13, No. 6, pp. 985-997

Tillner-Roth, R., Baehr, H.D., 1992. *Burnett measurements and correlation of gas-phase (p, ρ, T) of 1,1,1,2-tetrafluoroethane (R-134a) and of 1,1-difluoroethane (R-152a)*, Journal of Chemical Thermodynamics, Vol. 24, No. 4, pp. 413-424

Trepp, Ch., Savoie, P., Kraus, W.E., 1992. *Investigation of the performance behaviour of a compression refrigerating unit with halogen refrigerant mixtures R22/R142b, R22/R114 and R22/R12*, International Journal of Refrigeration, Vol. 15, No. 2, pp. 101-111

United Nations Environmental Program, 1991. *Montreal Protocol 1991 Assessment Report of the Refrigeration, Air Conditioning and Heat Pumps Technical Options Committee*

Vakil, H.B., 1979. *Vapor compression cycle device with multi-component working fluid and method of modulating its capacity*, U.S Patent No. 4,179,898

Vakil, H.B., 1981. *Vapor compression cycle device with multi-component working fluid mixture and method of modulating the thermal transfer capacity thereof*, U.S. Patent No. 4,283,919

Vakil, H.B., 1983. *Means and method for modulating and controlling the capacity of a vapor compression cycle device*, U.S. Patent No. 4,384,460

Weber, L.A., 1989. *Vapor Pressures and Gas-Phase PVT Data for 1,1,1,2-Tetrafluoroethane*, International Journal of Thermophysics, Vol. 10, No. 3, pp. 617-627

Weber, L.A., Goodwin, A.R.H., 1993. *Ebulliometric Measurement of the Vapor Pressure of Difluoromethane*, Journal of Chemical Engineering Data, Vol. 38, No. 2, pp. 254-256

Widiatmo, J.V., Sato, H., Watanabe, K., 1993. *Saturated-liquid densities and bubble-point pressures of the binary system HFC-32 + HFC-125,* High Temperatures-High Pressures, Vol. 25, pp. 677-683

Widiatmo, J.V., Sato, H., Watanabe, K., 1994a. *Measurements of liquid densities of the binary HFC-32 + HFC-134a system*, Fluid Phase Equilibria, Vol. 99, pp. 199-207

Widiatmo, J.V., Sato, H., Watanabe, K., 1994b. *Saturated-Liquid Densities and Vapor Pressures of 1,1,1-Trifluoroethane, Difluoroethane and Pentafluoroethane*, Journal of Chemical Engineering Data, Vol. 39, No. 2, pp. 304-308

Wilson, P., Basu, R., 1988. *Thermodynamic properties of a new stratospherically safe working fluid-refrigerant 134a*, ASHRAE Transactions, Vol. 94, Part 2, pp. 2095-2118

Wuebbles, D.J., 1992. *The role of refrigerants in climate change*, Proceedings from the International Symposium on Refrigeration, Energy and Environment, Trondheim, Norway, pp. 1-19

Yada, N., Uematsu, M., Watanabe, K., 1988. *Study of the PVTx Properties for Binary R 152a + R 114 System*, Transactions of the Japanese Association of Refrigeration, Vol. 5, No. 1, pp. 107-115

Ye, F., Sato, H., Watanabe, K., 1995. *Gas-Phase PVT Properties and Vapor Pressures of Pentafluoroethane (HFC-125) Determined According to the Burnett Method*, Journal of Chemical Engineering Data, Vol. 40, No.1, pp. 148-152

Zhao, Z.Y., Yin, J.M., Tan, L.C., 1992. *Measurements of PVT properties and vapor pressure for HFC152a*, Fluid Phase Equilibria, Vol. 80, pp 191-202

Zheng, X. Y., Kubota, H., Zheng, Q., Makita, T., 1990. *High-Pressure Vapor-Liquid Equilibrium Data of the HFC 134a + HCFC 141b System*, Journal of Chemical Engineering Data, Vol. 35, No. 4, pp. 441-444

Zhu, M.S., Fu, Y.D., Han, L.Z., 1992. *An experimental study of PVT properties of CFC alternative HFC-134a*, Fluid Phase Equilibria, Vol. 80, pp. 149-156

Zhu, M.S., Li. J., Wang, B.X., 1993. *Vapor Pressure of Difluoroethane (HFC-32)*, International Journal of Thermophysics, Vol. 14, No. 6, pp. 1221-1227